Publication 3047

tutive
nships
dels in
eories
Flows

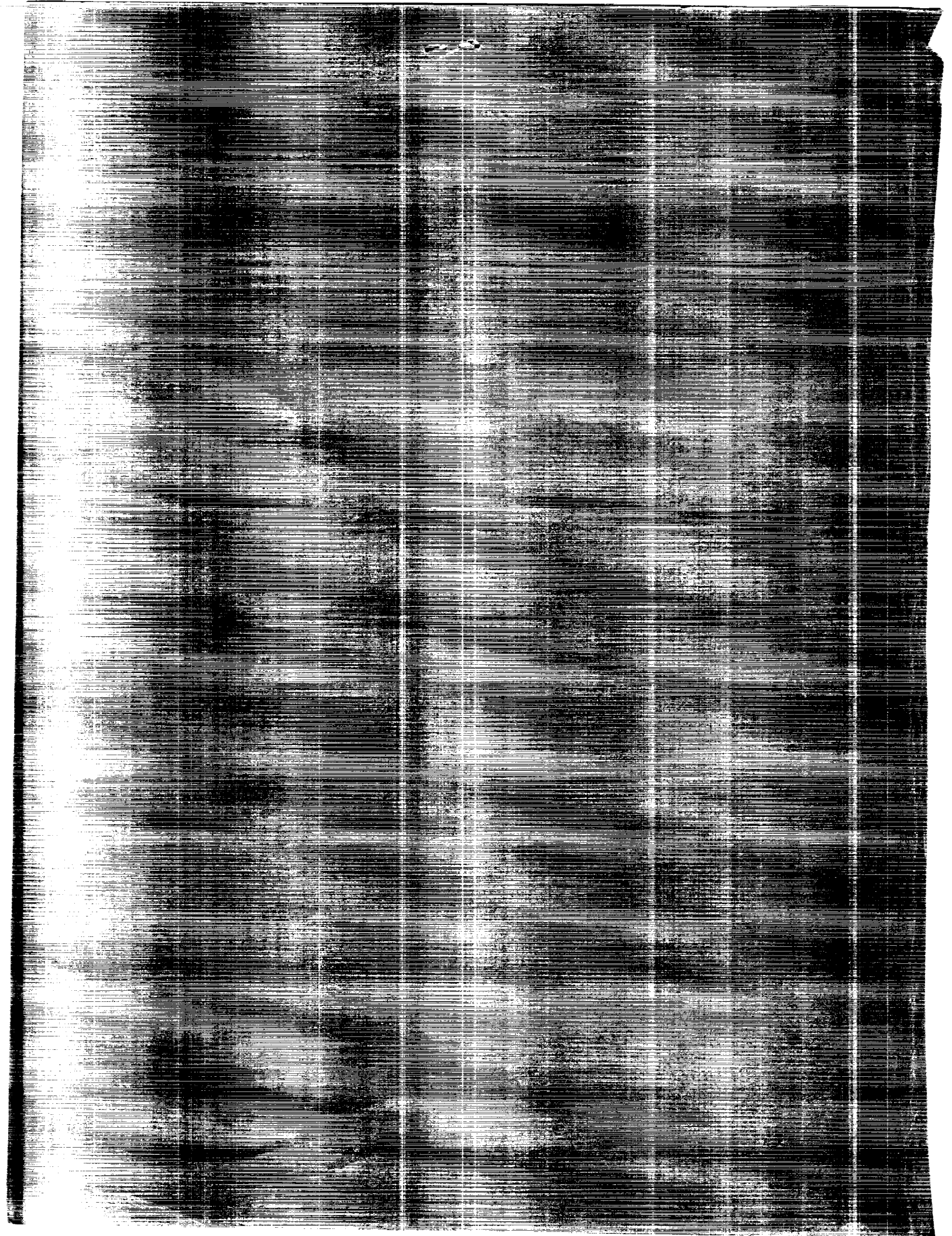

NASA Conference Publication 3047

Constitutive Relationships and Models in Continuum Theories of Multiphase Flows

Edited by
Rand Decker
NASA George C. Marshall Space Flight Center
Marshall Space Flight Center, Alabama

Proceedings of a workshop sponsored by
the National Aeronautics and Space Administration,
Washington, D.C., and the Universities Space Research
Association, Washington, D.C., and held at
George C. Marshall Space Flight Center
Huntsville, Alabama
April 5–7, 1989

National Aeronautics and
Space Administration
Office of Management
Scientific and Technical
Information Division

1989

PREFACE

During the first week of April 1989, a workshop, entitled "Constitutive Relationships and Models in Continuum Theories of Multiphase Flows," was held at NASA's Marshall Space Flight Center. The purpose of this workshop was to open a dialogue on the topic of constitutive relationships for the partial or per phase stresses, including the concept of solid phase "pressure" and the models used for the exchange of mass, momentum, and energy between the phases in a multiphase flow. This volume is the result of the stated objective of the workshop, namely: to provide a state-of-the-art report on constitutive relationships and models in continuum theories of multiphase flows. This written record is intended to be something of a "market place" for those engineers and scientists who are attempting to implement multiphase flow theories for practical calculations. The focus on continuum theories was quite intentional, given the high level of engineering application that the continuum or "two-fluid" theory is seeing. Arguments pertaining to the applicability of the continuum approach versus other multiphase flow schemes, such as the Lagrangian-Eulerian or "tracking" techniques, are not broached. However, it is cautioned that even for certain broad categories of multiphase flows, the applicability of one class of theories over another is debated. Caveat emptor!

The authors are from a variety of backgrounds and have, collectively, a knowledge of the spectrum of typical multiphase flows; i.e., from the dilute to the concentrated in terms of the fraction or concentration of the dispersed phase.

Within the general class of continuum theories, two (perhaps underexplored) formulations for multiphase flows are presented. These are the drift flux approach and the potential flow theory. These formulations provide a very useful and alternative perspective to the problem. However, as with the more familiar mass, momentum (with dissipation), and energy flux formulations, the drift flux and potential flow theories suffer from the problems of "closure" modeling requirements and validating the adjustable parameters.

One author wrote in a summary of this workshop: "We are responsible to agree on the form of the equations, the averaging techniques to be used and the interpretation of the terms in the averaged equations. Without this, we don't even have a common language to discuss the problem." The bulk of the presentations and discussion which resulted during the course of this workshop addressed this objective.

It is recognized from a physical perspective that the interaction of the dispersed phase particles (deformable or otherwise), amongst themselves, either via collision, "lubricated" near collisions, intermingling wakes or wake "drafting," are important processes. Hence, it would be an oversimplification to consider only single particle hydrodynamics when formulating constitutive relationships and momentum/energy exchange models. This requires modeling of paired and multibody interactions with probability distribution functions (PDFs) and the solution of various integrals of products of PDFs over specified field spaces. This is an area where "borrowing" from the evolutionary structure of kinetic gas theory has proven to be useful.

The analysis of dispersed phase stresses, specifically, the concept of solid phase

"pressure," is maturing. There are at least three mechanisms for normal or spherical momentum flux by a rigid dispersed phase: collisional transport, momentum transport due to the kinetic or deviation-about-the-mean motion of the particles, and the transport of hydrodynamic stresses which are present upon the skin of the particle. The first two mechanisms can be recognized as characteristics of the dispersed phase "cloud" or more specifically, as continuous, advectable fields of the dispersed phase. Structures, albeit complex ones, for the the formulation of these stresses are available and are presented in these proceedings. The latter mechanism is of unavoidable importance and requires analyzing the hydrodynamical stress around a single particle and averaging these to achieve a continuous field. Generally, the result is a dissipative (nonrecoverable) spherical stress, ascribed to the dispersed phase, containing, amongst other things, the slip velocity between the dispersed and continuous phases and the continuous phase viscosity. It must be cautioned that it is possible to include these same stresses redundantly in a model for the momentum exchange between the phases.

Within this community, there is a growing consensus that the spin field, not to be confused with the vorticity field, of the dispersed phase is of importance. To date, attempts at modeling higher order interactions between the phases, such as lift forces, requiring some knowledge of the particle spin, have set that value equal to one half the local, continuous phase vorticity. This result is from single particle hydrodynamical analysis in an unbounded, linear shear flow and does not allow for any independent spin motion of the particles due to wall interactions, collisions, or "near" collisions. In addition, it couples the spin inertia of the particles directly to the local vorticity field of the continuous field and does not allow for particle "spin-up" or "spin-down" in the presence of a local shearing flow.

Finally, a suite of experiments which could be used for testing and validating/rejecting various aspects of multiphase flow theory is sorely needed. In a manner similar to the single phase flow community, with their cavity flows and backward facing steps, this community needs to arrive at a consensus for a suite of experiments, so that when we finally all speak the same language, we can all shoot at the same target.

TABLE OF CONTENTS

AGENDA

Constitutive Relationships and Models in Continuum Theories of Multiphase Flows

April 5-7, 1989

NASA/Marshall Space Flight Center
Conference Room P106
Building 4200

Sponsored by: Fluid Dynamics Branch
Space Science Laboratory
and
Universities Space Research Association
Huntsville, Alabama

Wednesday, April 5th:

9:00 am	Welcome to NASA/Marshall Space Flight Center
9:30 am	The Generalized Drift Flux Approach J. A. Boure, Centre d'Etudes Nucleaires de Grenoble
10:15 am	Two-Phase Potential Flow Graham B. Wallis, Dartmouth College
11:00 am	Break
11:30 am	Open Discussion: Workshop Expectations, Goals, and Objectives
12:30 pm	Lunch
2:00 pm	Interpretation of Modeling of the Averaged Equations for a Fluid-Solid Flow Hayley Shen, Clarkson University
2:45 pm	Stress in Dilute Suspensions Stephen L. Passman, Pittsburgh Energy Technology Center
3:30 pm	Break
4:00 pm	Theory of Droplets and its Application in Two-Phase Flows H. H. Chiu, University of Illinois
4:45 pm	Social Announcements, Adjourn

Thursday, April 6th:

9:00 am	Round-Table Discussions
10:30 am	Break
11:00 am	Effect of Particle Velocity Fluctuations on the Inertia Coupling in Two-Phase Flow Donald A. Drew, Cornell University
11:45 am	Kinetic Theory and the Rheology of Concentrated Suspensions James T. Jenkins, Cornell University
12:30 pm	Lunch
2:00 pm	Scaling and Modeling of Turbulent Suspension Flows C. P. Chen, University of Alabama in Huntsville
2:45 pm	The Kinetic Energy Equation in Dilute Suspensions M. C. Roco, California Institute of Technology
3:30 pm	Break
4:00 pm	Round-Table Discussions
5:00 pm	Adjourn

Friday, April 7th:

9:00 am	Administrative Announcements
9:20 am	Round-Table Discussions
11:00 am	Break
11:30 am	Round-Table Discussions (Concluded)
12:30 pm	Closing and Adjourn

THE GENERALIZED DRIFT FLUX APPROACH: IDENTIFICATION OF THE VOID-DRIFT CLOSURE LAW

J. A. Bouré

Commissariat à l'Energie Atomique
Centre d'Etudes Nucléaires de Grenoble
Service d'Etudes Thermohydrauliques
85 X, F 38041, Grenoble Cedex, France

ABSTRACT

The main characteristics and the potential advantages of generalized drift flux models are recalled. In particular it is stressed that the issue on the propagation properties and on the mathematical nature (hyperbolic or not) of the model and the problem of closure are easier to tackle than in two-fluid models.

The problem of identifying the differential void-drift closure law inherent to generalized drift flux models is then addressed. Such a void-drift closure, based on wave properties, is proposed for bubbly flows. It involves a drift relaxation time which is of the order of 0.25 s.

It is observed that, although wave properties provide essential closure validity tests, they do not represent an easily usable source of quantitative information on the closure laws.

I. INTRODUCTION

Generalized drift flux models were recently shown (Bouré, 1988b) to be attractive alternatives for current 1-D two-fluid models. Drift flux models are characterized by the uses of a single momentum balance (the mixture balance instead of two phasic balances) and of a void-drift closure law. In classical drift flux models the void-drift closure law is expressed through an algebraic equation, which amounts to ignoring nonequilibrium drift effects. In generalized drift flux models, the void-drift closure equation is a partial differential equation.

Generalized drift flux models and two-fluid models are compared in the next section and in table 1. The comparison brings out the drawbacks of two-fluid models. However, both kinds of model must be complemented by closure laws. In particular, generalized drift flux models need a void-drift closure law which remains to be specified.

Since generalized drift flux models were introduced to account for the properties of kinematic waves (Bouré, 1988a), it seems logical to use these properties to identify (i.e. to evaluate the coefficients of) the void-drift closure equation. The purpose of the present paper is to discuss the identification problem, assuming that the void-drift closure equation may be approached by a quasi linear differential equation of the first order.

II. A REMINDER ON GENERALIZED DRIFT FLUX MODELS AND TWO-FLUID MODELS

The comparison between generalized drift flux models and two-fluid models is summarized in table 1 which, like must of the substance of this section, is taken from Bouré (1988b). The mass and energy balances are parts of both kinds of models, and they are not discussed further hereafter. It is only noted for completeness that they require a few closure equations, in particular for the mass and energy transfers at the walls and at the interfaces.

The momentum balances contain the two phasic averaged pressures P_G and P_L, the subscripts G and L corresponding to the two phases. For the following discussion, it is convenient to express P_G and P_L in terms of the average pressure P and the pressure difference P_{LG}, with :

$$P \triangleq \alpha P_G + (1 - \alpha) P_L \quad , \qquad P_{LG} \triangleq P_G - P_L \tag{2.1}$$

α being the void fraction. Now, in the set of balance equations, the two phasic momentum balances are equivalent to a subset of two equations, namely the *mixture momentum balance* and the *pressure difference equation*, obtained on eliminating P between the two phasic balances.

The mixture momentum balance may be written :

$$\frac{\partial P}{\partial z} + \alpha \rho_G \left(\frac{\partial W_G}{\partial t} + W_G \frac{\partial W_G}{\partial z}\right) + (1 - \alpha) \rho_L \left(\frac{\partial W_L}{\partial t} + W_L \frac{\partial W_L}{\partial z}\right) \tag{2.2}$$

$$+ \frac{\partial R}{\partial z} + \frac{\partial \tau}{\partial z} + M_{LG} (W_G - W_L) - I_\sigma + F_W + \rho g = 0$$

the terms of the second line representing respectively :

- a term accounting for fluctuation and transverse distribution effects
- a term accounting for longitudinal stress variations
- an interfacial mass transfer term
- a surface tension term (interfacial)
- a friction term (walls)
- a gravity term.

t and z are respectively the time and the space variables, ρ_G and ρ_L are the phase densities, W_G and W_L are the phase average velocities, g is the gravity acceleration, and :

$$\rho \triangleq \alpha \rho_G + (1 - \alpha) \rho_L \tag{2.3}$$

w being the local instantaneous velocity along Oz and $\underline{\underline{\tau}}$ the local instantaneous deviatoric stress tensor, $\overline{}^{k}$ indicating the conditional time or ensemble averaging operator and $\langle\ \rangle$ the space averaging operator, and $\underline{n}_z$ being the unit vector of the Oz axis, R and τ are defined as :

$$R \triangleq \left\langle \alpha\ \rho_G\ \overline{(w_G - W_G)^2}^{G} + (1 - \alpha)\ \rho_L\ \overline{(w_L - W_L)^2}^{L} \right\rangle \qquad (2.4)$$

$$\tau \triangleq - \left\langle \left[\alpha\ \underline{\underline{\tau}}_G^{G} + (1 - \alpha)\ \underline{\underline{\tau}}_L^{L} \right] \cdot \underline{n}_z \right\rangle \cdot \underline{n}_z \qquad (2.5)$$

Independently of the mass transfer, already present in the mass balances, eq. *2.2* requires *four* closure laws for R, τ, I_σ and F_W. Turbulence effects are present through R.

The pressure difference equation may be written :

$$\alpha\ (1 - \alpha) \left[\rho_G \left(\frac{\partial W_G}{\partial t} + W_G \frac{\partial W_G}{\partial z} \right) - \rho_L \left(\frac{\partial W_L}{\partial t} + W_L \frac{\partial W_L}{\partial z} \right) + \frac{\partial P_{LG}}{\partial z} \right]$$

$$+ L_R + L_\tau + M_{LG} \left[(1 - \alpha)\ (W_G - W_{GI}) + \alpha\ (W_L - W_{LI}) \right] \qquad (2.6)$$

$$+ L_I + L_{FW} + L_{FI} - \alpha\ (1 - \alpha)\ \rho_{GL}\ g = 0$$

the terms of the second and third lines representing respectively :

- a term accounting for fluctuation and transverse distribution effects
- a term accounting for longitudinal stress variations
- an interfacial mass transfer term (W_{GI} and W_{LI} are interfacial averages of the phasic velocities)
- an induced inertia ("added mass") term
- two friction terms (respectively wall and interfaces)
- a gravity term, with

$$\rho_{GL} \triangleq \rho_L - \rho_G \qquad (2.7)$$

The above terms are defined in Bouré (1988b). For instance :

$$L_R \triangleq (1-\alpha)\,\frac{\partial}{\partial z}\left\langle \alpha\,\overline{\rho_G (w_G - W_G)^2}^{G}\right\rangle - \alpha\,\frac{\partial}{\partial z}\left\langle (1-\alpha)\,\overline{\rho_L (w_L - W_L)^2}^{L}\right\rangle \qquad (2.8)$$

$$L_\tau \triangleq -(1-\alpha)\,\frac{\partial}{\partial z}\left\langle \alpha\,\bar{\bar{\tau}}_G^{G}\cdot \underline{n}_z\right\rangle \cdot \underline{n}_z + \alpha\,\frac{\partial}{\partial z}\left\langle (1-\alpha)\,\bar{\bar{\tau}}_L^{L}\cdot \underline{n}_z\right\rangle \cdot \underline{n}_z \qquad (2.9)$$

Equation (2.6) requires *seven* closure laws for L_R, L_τ, W_{GI}, W_{LI}, L_I, L_{FW}, L_{FI}. Moreover, retaining eq. (2.6) implies, at least in theory, retaining also the interfacial momentum balance, which requires one supplementary closure law.

In two-fluid models, eqs (2.2) and (2.6) are both implicitly written. A crucial point is that eq. (2.6) is *stiff*. This means that, due to the relative orders of magnitude of its terms, small variations on the closure laws (and in particular on the induced inertia and interfacial friction closure laws) induce large variations on P_{LG} (when P_{LG} is not merely ignored) and/or W_G. Hence the difficulty to adjust the very badly known closure laws of eq. (2.6) to avoid unrealistic values of the light phase velocity.

A second crucial point is that, whenever eq. (2.6) is closed by algebraic laws only, a non-hyperbolic set results : two characteristic velocities are complex conjugate, with the consequence that the model is unconditionally unstable.

In drift flux models, eq. (2.6) is not written, which is acceptable since the value of P_{LG} does not really matter in practice. The two foregoing difficulties are not encountered.

Besides the closure laws already mentioned, current two-fluid models are closed through an assumption on P_{LG} (the set of 6 phasic balance equations involves 7 dependent variables, namely two pressures, two velocities, two enthalpies and the void fraction). Such an assumption imposes an artificial constraint on the pressures and pressure gradients. It disturbs the description of the corresponding propagation phenomena.

Generalized drift flux models are closed through the *direct description of the void-drift dynamic dependency*. Assuming a quasi-linear, partial differential relationship of the first order, and using the convenient variables :

$$W \triangleq \alpha W_G + (1 - \alpha) W_L , \quad \delta \triangleq \alpha (1 - \alpha) (W_G - W_L) = \alpha (W_G - W) \quad (2.10)$$

(center of volume velocity and drift), it may be approached by :

$$\eta \left(\frac{\partial W}{\partial t} + W_2 \frac{\partial W}{\partial z}\right) + (W + W_4 - \Sigma) \frac{\partial \alpha}{\partial t} + (WW_4 - \Pi) \frac{\partial \alpha}{\partial z} + \frac{\partial \delta}{\partial t} + W_4 \frac{\partial \delta}{\partial z} = \frac{1}{\theta} (f - \delta) \quad (2.11)$$

Equation (2.11) requires *seven* closure laws, i.e. the same number as eq. (2.6) but with simpler physical significances and more straightforward consequences : f is the fully-developed drift value, θ a relaxation time, Σ and Π are respectively the sum and product of the two characteristic velocities corresponding to the kinematic waves, η expresses inertia effects, W_2 and W_4 are averaged velocities close to W.

It can be concluded that developing a closure set for eq. (2.11) and using generalized drift flux models appear as less hazardous and hopefully easier than developing a closure set for eq. (2.6) and using current two-fluid models.

III. INFLUENCE OF THE VOID-DRIFT CLOSURE ON THE PROPERTIES OF KINEMATIC WAVES ("Direct problem")

As long as the kinematic wave velocities are small with respect to the sonic velocity, the properties of small harmonic kinematic waves of the form

$$\bar{x} = \bar{x}_0 \; e^{i\,(\omega t - kz)} \tag{3.1}$$

where $\bar{x}_0$ (constant) ω and k are real or complex quantities, result from the approximate dispersion equation (Bouré, 1988b)

$$\omega - C_\alpha\, k + i\,\theta\,(\omega^2 - \Sigma\,\omega k + \Pi\,k^2) = 0 \tag{3.2}$$

where :

$$C_\alpha \triangleq W + f'_\alpha, \qquad \left(f'_\alpha \triangleq \frac{\partial f}{\partial \alpha}\right) \tag{3.3}$$

A first consequence is that the kinematic wave properties, which do not significantly depend on η, W_2, W_4, cannot be used to evaluate these quantities (η is related to the sonic velocity, W_2 and W_4 have only weak influences).

In the exploitable experiments (Tournaire, 1987, Bouré, 1988a) ω is imposed and the kinematic wave velocities V and their spatial amplification coefficients k_i result from the data processing. Eqs. (3.1) and (3.2) must therefore be used with ω real and :

$$k \triangleq k_r + i\,k_i \tag{3.4}$$

from which

$$\bar{x} = \bar{x}_0 \; e^{k_i\, z} \; e^{i\,(\omega t - k_r z)} \tag{3.5}$$

$$V = \frac{\omega}{k_r} \tag{3.6}$$

k_r, which does not depend on the frame of reference, can be used instead of ω, which does, to characterize a wave.

Introducing eqs. (3.4) and (3.6) in the dispersion equation (3.2) and separating the real and imaginary parts lead to :

$$k_r \left[V - C_\alpha + \theta \Sigma V k_i - 2 \theta \Pi k_i \right] = 0 \qquad (3.7)$$

$$- C_\alpha k_i + \theta V^2 k_r^2 - \theta \Sigma V k_r^2 + \theta \Pi \left(k_r^2 - k_i^2 \right) = 0 \qquad (3.8)$$

Equations (3.7) and (3.8) provide the solutions to the direct problem, viz. computing the properties of the kinematic waves of wave number k_r when C_α, θ, Σ and Π are known. There are two solutions corresponding to two modes (noted with the subscripts 3 and 4). In the experiments it was found that modes 3 and 4 are respectively predominant at low void fractions ($0 < \alpha < 0.25$) and at "large" void fractions ($\alpha > 0.30$)

In particular for $k_r = 0$, the two solutions are :

$$k_i = 0 \qquad \text{with } \frac{k_i}{k_r^2} = \frac{\theta \, (C_\alpha - C_3) \, (C_\alpha - C_4)}{C_\alpha}, \qquad V = C_\alpha \qquad (3.9)$$

and

$$k_i = - \frac{C_\alpha}{\theta \, \Pi}, \quad V = C'_\alpha \qquad \text{with } \frac{1}{C'_\alpha} \triangleq \frac{1}{C_3} + \frac{1}{C_4} - \frac{1}{C_\alpha} \qquad (3.10)$$

C_3 and C_4 being defined by :

$$\Sigma \triangleq C_3 + C_4 \qquad \Pi \triangleq C_3 \, C_4 \qquad (3.11)$$

For $k_r \to \infty$, the two solutions are :

$$V = C_3 \qquad k_i = - \frac{C_\alpha - C_3}{\theta \, C_3 \, (C_4 - C_3)} \qquad (3.12)$$

$$V = C_4 \qquad k_i = - \frac{C_4 - C_\alpha}{\theta \, C_4 \, (C_4 - C_3)} \qquad (3.13)$$

In equations (3.7) and (3.8) the three quantities θk_r, k_i are present only through the two products (θk_r) and (θk_i). In actual experimental runs, k_r is never zero and the equations may be written :

$$V - C_\alpha + (C_3 + C_4)\, V\, (\theta k_i) - 2\, C_3\, C_4\, (\theta k_i) = 0 \qquad (3.14)$$

$$- C_\alpha \frac{\theta k_i}{(\theta k_r)^2} + V^2 - (C_3 + C_4)\, V + C_3\, C_4 - C_3\, C_4 \frac{(\theta k_i)^2}{(\theta k_r)^2} = 0 \qquad (3.15)$$

Since in the exploitable experimental data, V does not significantly depend on k_r (no significant dispersion), it is convenient to eliminate V between eqs. (3.14) and (3.15). Eq. (3.14) yields :

$$V = \frac{C_\alpha + 2\, C_3 C_4\, (\theta k_i)}{1 + (C_3 + C_4)\, (\theta k_i)} \qquad (3.16)$$

and eq. (3.15) yields :

$$V = \frac{C_3 + C_4}{2} \pm \sqrt{\frac{(C_4 - C_3)^2}{4} + C_\alpha \frac{\theta k_i}{(\theta k_r)^2} + C_3\, C_4 \frac{(\theta k_i)^2}{(\theta k_r)^2}} \qquad (3.17)$$

The solutions for θk_i are then the real solutions of the equation

$$\frac{2\, C_\alpha - (C_3 + C_4) - (C_4 - C_3)^2\, (\theta k_i)}{1 + (C_3 + C_4)\, \theta k_i} =$$

$$\pm \sqrt{(C_4 - C_3)^2 + 4\, C_\alpha \frac{\theta k_i}{(\theta k_r)^2} + 4\, C_3\, C_4 \frac{(\theta k_i)^2}{(\theta k_r)^2}} \qquad (3.18)$$

Computing directly θk_i as a function of θk_r from eq. (3.18) is not straightforward. It is more convenient to transform eq. (3.18) to express θk_r as a function of θk_i

$$\frac{(\theta\ k_r)^2}{\theta\ k_i} = \frac{[C_\alpha + C_3\ C_4\ \theta\ k_i]\ [1 + (C_3 + C_4)\ \theta\ k_i]^2}{(C_\alpha - C_3)\ (C_\alpha - C_4) - (C_4 - C_3)^2 \theta\ k_i\ [C_\alpha + C_3 C_4\ \theta\ k_i]} \quad (3.19)$$

For a given value of k_i, eq. (3.19) yields zero or one real positive value of k_r.

IV. IDENTIFICATION OF THE VOID-DRIFT CLOSURE EQUATION FROM KINEMATIC WAVE PROPERTIES ("Inverse problem")

The problem posed in this paper is the determination of C_α, θ, Σ and Π, using the experimental data on kinematic waves. It is the inverse of the problem of section 3.

The principle of the method is to write eqs. (3.7) and (3.8), for instance, for several sets of experimental conditions for which k_r, V and k_i are known and to use the resulting equations to compute C_α, θ, Σ and Π.

In the exploitable data, as already noted, V does not depend significantly on k_r. Accordingly, when a single mode is predominant, V may be expected to be close to both C_3 (or C_4) and C_α (or C'_α). This has two consequences :

1. Whenever a single mode is predominant, the experimental correlation for V should be a correlation for C_α as well. This is corroborated by the fact that is satisfies the definition (3.3). In the experimental conditions of Tournaire (1987) (upward vertical flow, low pressure), it leads to (Bouré, 1988a, f and C_α - W in m/s) :

For $0 < \alpha < 0.2$ (mode 3 predominant)

$$\left.\begin{aligned} f &= 0.22\ \alpha\ (1 - \alpha)\ [1 - 1.25\ \alpha\ (1 - \alpha)] \\ C_\alpha - W &= 0.22\ (1 - 2\alpha)\ [1 - 2.5\ \alpha\ (1 - \alpha)] \end{aligned}\right\} \quad (4.1)$$

For $0.3 < \alpha < 0.41$ (mode 4 predominant)

$$\left.\begin{aligned} f &= 0.22\ \alpha - 0.028 \\ C_\alpha - W &= 0.22 \end{aligned}\right\} \qquad (4.2)$$

For $0.2 < \alpha < 0.3$ (the two modes coexist) the values of f and $C_\alpha - W$ may be interpolated between (4.1) and (4.2) with, from the experimental data :

$$C_\alpha - W \simeq 0.08 \qquad (4.3)$$

for $\alpha = 0.25$

2. When mode 3 (respectively mode 4) is predominant, $C_\alpha - C_3$ (respectively $C_4 - C_\alpha$) should be "small".

C_α being known and V eliminated, the problem may now be reformulated, eqs. (3.7) and (3.8) being replaced by eq. (3.18) or (3.19) to be solved for θ, C_3, C_4. Only mode 3 results are exploitable since mode 4 results for k_i are too few in number. In view of the forms of eqs. (3.18) and (3.19), the foregoing problem is far from simple. This is confirmed by fig. 1 in which, as suggested by eq. (3.19), the experimental results for $-k_r^2/k_i$ are plotted as a function of $-k_i$, and which exhibits an important scatter (in the representation of fig. 1, the points corresponding to $|k_i| < 0.1$ are subject to large errors and therefore meaningless. They were not plotted in the figure).

In the domain in which mode 3 is predominant, the conditions :

$$C_3 < C_\alpha < C'_\alpha < C_4 \qquad (4.4)$$

may be expected to hold (see Bouré, 1988a). They entail

$$\frac{C_\alpha - C_3}{\theta\ C_3\ (C_4 - C_3)} < \frac{1}{\theta\ (C_3 + C_4)} < \frac{C_4 - C_\alpha}{\theta\ C_4\ (C_4 - C_3)} < \frac{C_\alpha}{\theta\ C_3\ C_4} \qquad (4.5)$$

Then, as k_i decreases from zero, k_r^2/k_i resulting from eq. (3.19) starts from the value corresponding to eq. (3.9) with a slope which may be of either sign. However, when $|k_i|$ is sufficient, k_r^2/k_i also decreases. It tends towards $-\infty$ for the value corresponding to eq. (3.12). For the values of k_i comprised between those given by eqs. (3.12) and (3.13), there is no physical solution $\left(k_r^2 \leqslant 0\right)$. Finally, for the values of k_i comprised between those given by eqs. (3.13) and (3.10), there is a solution again corresponding to mode 4.

By trial and error, θ, C_3 and C_4 may be adjusted to fit the curve representing eq. (3.19) to mode 3 data. In view of the absence of dispersion C_3 may be expected to be close to C_α.

For $0 < \alpha \leqslant 0.20$: the following set of values is acceptable

$$\left.\begin{array}{l} \theta = 0.25 \text{ s} \\ C_\alpha - C_3 = 0.02 \text{ m/s} \\ C_4 - C_\alpha = 0.08 \text{ m/s} \end{array}\right\} \qquad (4.6)$$

Precise adjustement would need more accurate data for the wave velocities *and* especially for the damping/amplification coefficients. Such data does not exist and cannot be expected to be obtained soon in view of the available instrumentation. For $\alpha > 0.25$, no sufficiently accurate data is available.

Equations (4.1) and (4.6) confirm that, even at low pressure, the relevant velocity differences corresponding to fully developed conditions are fairly small in bubbly flows. They are negligible as soon as W is large enough (say 3 m/s). Accordingly the correlations for $C_\alpha - W$, $C_3 - W$, $C_4 - W$ are probably not crucial. On the other hand, the drift relaxation time θ is an essential parameter of the generalized drift flux model.

V. CONCLUSIONS

After a reminder on the main characteristics and the potential advantages of generalized drift flux models, the problem of the identification of the differential void-drift closure law they imply has been addressed.

Two advantages of generalized drift flux models versus complete two-fluid models are :

1. The correct description of the kinematic wave phenomena and the straightforward control and interpretation of the mathematical nature (hyperbolic or not) of the model set of partial differential equations that they enable.

2. The simplification of the closure problem, involving only closure laws of simple physical significance and easy to assess.

On the other hand, it has been found that the available data on kinematic wave properties is not quite adequate to enable the identification of the void-drift closure law. Such an identification would need a very good accuracy (difficult to reach in practice) on the wave damping or amplification coefficients. Accordingly kinematic wave properties seem to be more useful as a closure validity test than as a source of quantitative information on the closure laws.

However, a void-drift closure, suitable for bubbly flows, has been adjusted on the available kinematic wave data. It involves several velocities which differ only slightly from each other and from the average fluid velocity but whichare necessary to the description of the kinematic wave properties. It also involves a drift relaxation time which is an essential parameter of generalized drift flux models and which was tentatively found to be of the order of 0.25 s for the upward flow of air-water mixtures at low pressure.

Table 1

Simplified comparison of modeling strategies

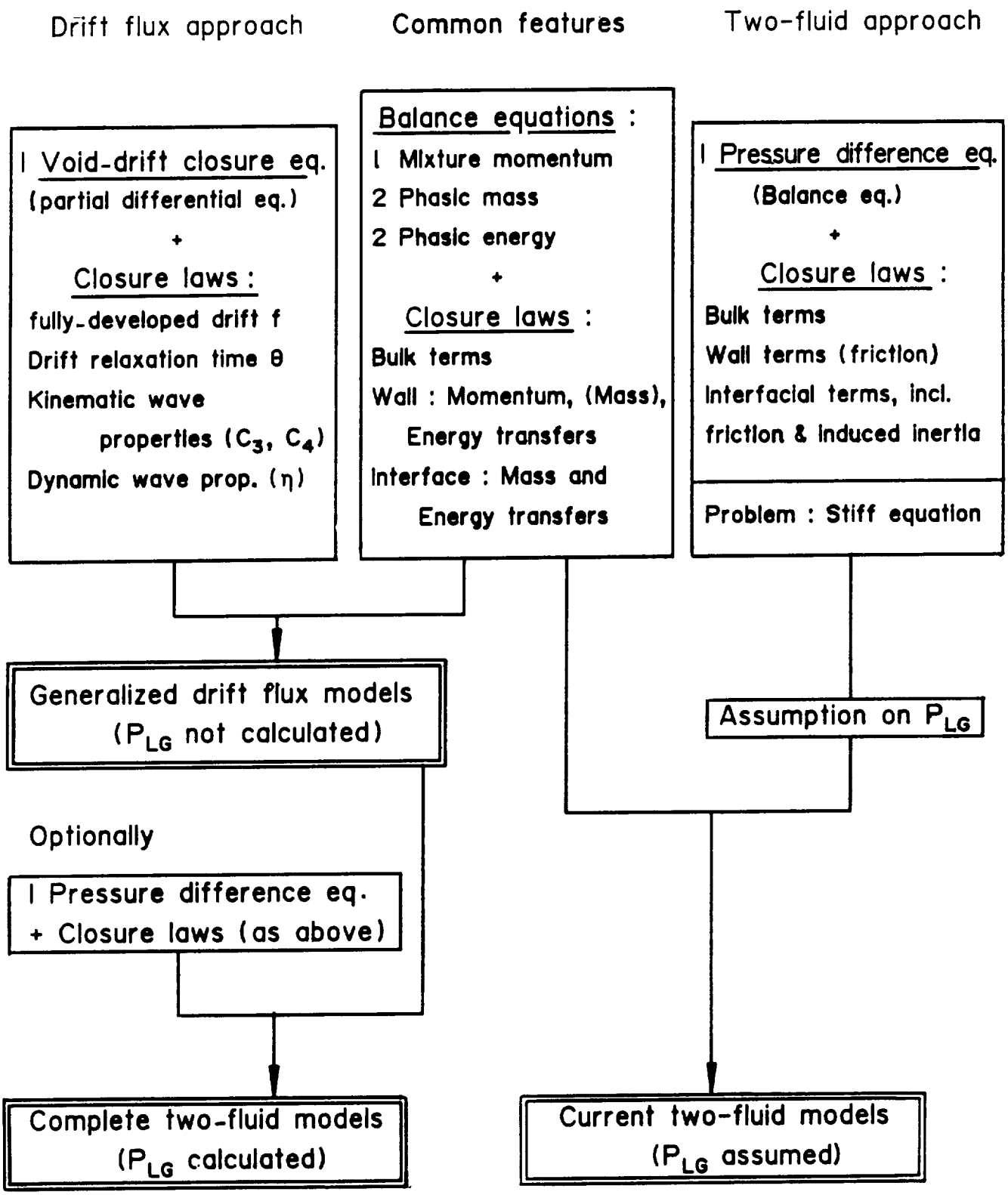

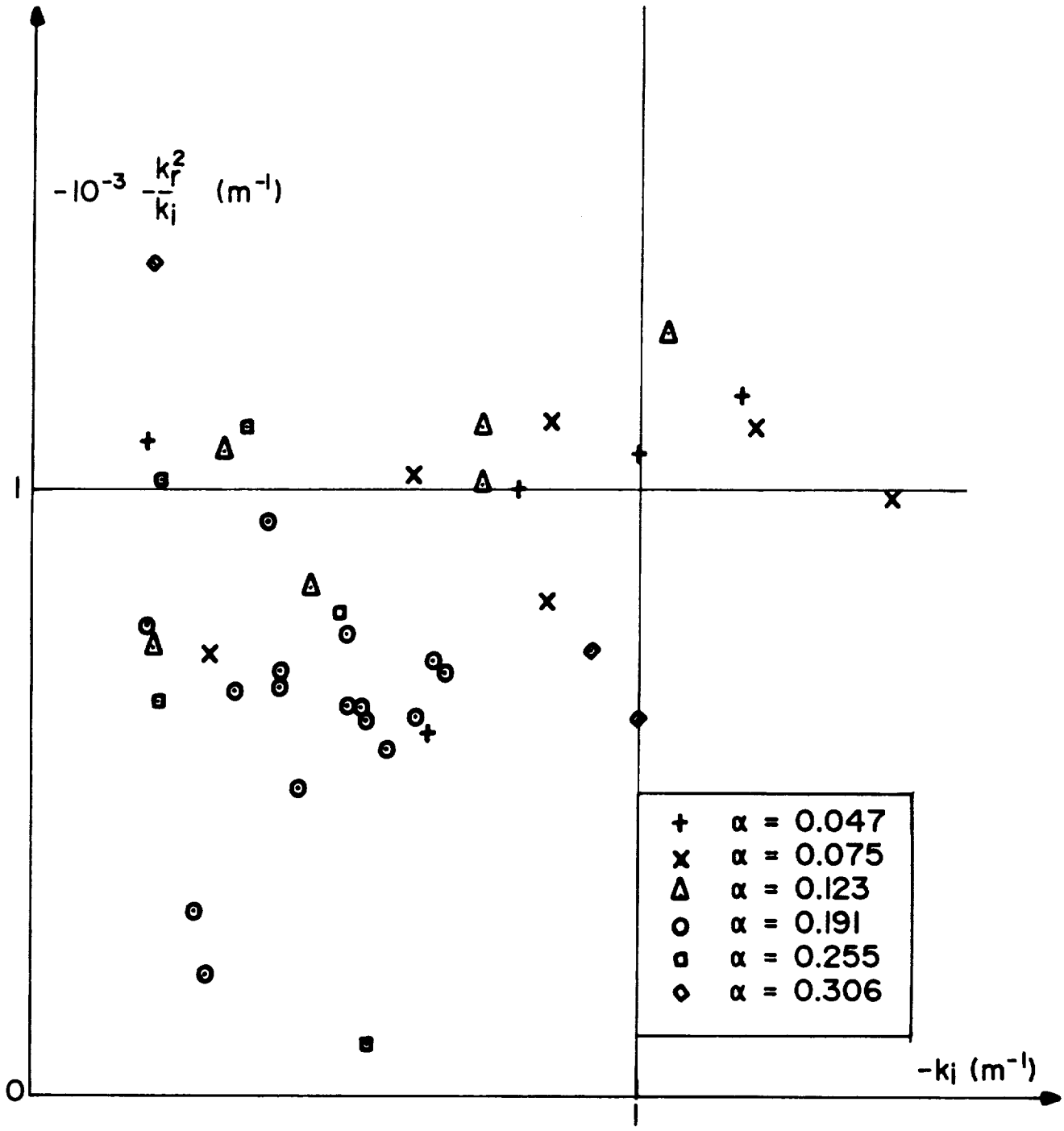

Fig. 1 : Experimental data (Mode 3)

REFERENCES

Bouré, J.A., 1988a, Properties of kinematic waves in two-phase pipe flows. Consequences on the modeling strategy, European Two-Phase Flow Group Meeting, Brussels.

Bouré, J.A., 1988b, An alternative strategy for the development of averaged two-phase flow models, Seminar on Theoretical Aspects of Multiphase Flow Phenomena, Ithaca.

Tournaire, A., 1987, Detection et étude des ondes de taux de vide en écoulement diphasique à bulles jusqu'à la transition bulles-bouchons, Thèse, Université Scientifique, Technologique et Médicale et Institut National Polytechnique de Grenoble.

TWO-PHASE POTENTIAL FLOW

Graham B. Wallis

Thayer School of Engineering
Dartmouth College
Hanover, NH 03755

Prepared for a workshop "Constitutive Relationships and Models in Continuum Theories of Multiphase Flows," Nasa/Marshall Space Flight Center

April 5-7, 1989

NOMENCLATURE

$\mathbf{d}\ell$, $\mathbf{ds}$	Elements of length, area
E	Exertia, $(\alpha_1\beta - 1)$
$\mathbf{f}$	Force per unit volume of a phase
$\mathbf{g}$	Body force per unit mass
$\mathbf{I}$	Unit dyadic
$\mathbf{j}$	Volumetric flux density
k	Kinetic energy density
m	Geurst's added mass coefficient
$\mathbf{m}$	Momentum density
$\mathbf{M}_1^d$	Added mass force
p	Mean pressure in a phase
P	Macroscopic pressure
$\mathbf{P}$	Combined momentum flux and stress tensor
R	Density ratio ρ_1/ρ_2
t	Time
$\mathbf{u}$	Microscopic velocity
$\mathbf{v}$	Average velocity
$\mathbf{w}$	Relative velocity $\mathbf{v}_1 - \mathbf{v}_2$
α	Volumetric fraction of a phase
β	"Resistivity," (1)
η	Macroscopic potential
$\boldsymbol{\pi}$	Specific momentum, (24), (25)
ρ	Density
Φ	Macroscopic potential

Subscripts

0	With particles at rest
1	Phase 1
2	Phase 2

INTRODUCTION

Potential flow theory for a single fluid has been established for many years. Although its limitations for describing real motions are well known, it does provide a self-consistent structure for analysis and often provides a reasonably accurate description of at least part of the flow field of fluids with low viscosity.

As an example of two-phase flow, one can imagine a suspension of particles in a fluid that obeys all the requirements of potential theory at the microscopic level. If the only forces acting on the particles are "conservative," it would appear that their motion might also reasonably be expected to be describable in terms of a suitable potential. Averaging of these potentials would lead to *macroscopic* potentials, true *properties* of the mixture, that should be related in some way to the average motion of the phases. Indeed, previous attempts to determine the inertial coupling terms in the *two-fluid model* have implicitly assumed potential flow at the microscopic level.

A complete two-phase theory of this type will be as *idealized* as was the classical theory of single-phase potential flow. However, it should be useful in the same sorts of ways, both as an approximation in many situations and as a *standard* that must at some level be consistent with other approaches, such as those that attempt to define closure relations for a set of averaged basic equations.

This paper describes some features of two recent approaches along these lines. The first is based on a set of *progressive examples* that can be analyzed using common techniques, such as conservation laws, and taken together appear to lead in the direction of a general theory, the tactic used in [1]. The second is based on *variational methods*, a classical approach to conservative mechanical systems that has a respectable history of application to single phase flows. The latter approach, exemplified by several recent papers by Geurst

[2-5], appears generally to be consistent with the former, at least in those cases for which it has been possible to obtain comparable results.

PROGRESSIVE EXAMPLES

The theory developed in [1] starts with a situation where the particles are at rest. Fluid flows past these particles as though a *porous medium.* At the microscopic level the equipotentials are not "smooth" but they do not differ much from the more gross macroscopic equipotential. Differences between the two levels of equipotential are smeared out over lengths comparable with the particle size. I do not have a rigorous proof, but I believe it is valid to treat these two equipotential surfaces as essentially identical for most purposes. This is not true of the other properties, such as pressure and velocity, that vary more at the microscopic than the macroscopic scale and must be averaged carefully.

Just as in electrical conduction past a matrix of non-conducting particles, the macroscopic fluid flux will be proportional to the macroscopic potential gradient, the "resistivity" being represented by a factor β that depends only on the particle geometry and the void fraction, as long as the arrangement is isotropic. We therefore have

$$\mathbf{j}_0 = -\frac{1}{\beta}\nabla\Phi \tag{1}$$

Since β is unity for unimpeded flow, it will be greater than one when particles are present. A crude description of the situation could be to say that some of the fluid is "held up" or "entrained" by the particles so that only a fraction of the space is available for direct flow.

The average velocity of the fluid is the *relative velocity,*

$$\mathbf{w} = \frac{\mathbf{j}_0}{\alpha_1} = -\frac{1}{\alpha_1\beta}\nabla\Phi \tag{2}$$

The kinetic energy of the fluid in unit volume confined between two equipotentials is, from a standard theorem of potential flow.

$$k_0 = -\frac{1}{2}\rho_1 \int_s \phi \mathbf{u} \cdot \mathbf{ds} = -\frac{1}{2}\rho_1 \nabla\Phi \cdot \mathbf{j}_0 = \frac{1}{2}\rho_1 \alpha_1^2 \beta w^2 \tag{3}$$

The kinetic energy per unit volume of phase 1 is

$$k_1 = \frac{k_0}{\alpha_1} = \frac{1}{2}\rho_1 w^2 (\alpha_1 \beta) \tag{4}$$

If we denote the fluid velocity at the microscopic level by $\mathbf{u}_1$, (2) and (4) are equivalent to

$$\mathbf{w} = < \mathbf{u}_1 > \tag{5}$$

$$w^2 \alpha_1 \beta = < \mathbf{u}_1^2 > \tag{6}$$

Invoking the Schwarz Inequality, it is clear from (5) and (6) that $\alpha_1\beta$ is greater than 1, a proof pointed out to me by my student Chao Luo.

By considering the changes in the fluid kinetic energy resulting from a uniform volume change for every particle it can be shown [1] that the difference is mean pressure between the phases is

$$p_2 - p_1 = \frac{1}{2}\rho_1 w^2 \alpha_1 \frac{d}{d\alpha_1}(\alpha_1\beta - 1) \tag{7}$$

The additional "1" in (7) appears to be gratuitous. It is introduced at this stage because the "exertia," defined [1] as

$$E = (\alpha_1 \beta - 1) \tag{8}$$

turns out to reappear in numerous contexts and to be one version of an *added mass coefficient.*

If we now superimpose a uniform velocity $\mathbf{v}_2$ on the above motion, this is equivalent to superimposing a corresponding potential gradient and we obtain

$$\mathbf{v}_1 + E\mathbf{w} = -\nabla\Phi \tag{9}$$

where the relative velocity is

$$\mathbf{w} = \mathbf{v}_1 - \mathbf{v}_2 \tag{10}$$

The net momentum and kinetic energy densities are then

$$\mathbf{m} = \rho_1 \alpha_1 \mathbf{v}_1 + \rho_2 \alpha_2 \mathbf{v}_2 \tag{11}$$

$$k = \frac{1}{2}\rho_1 \alpha_1 v_1^2 + \frac{1}{2}\rho_2 \alpha_2 v_2^2 + \frac{1}{2}\rho_1 \alpha_1 E w^2 \tag{12}$$

From (11) and (12) we may deduce that the effective *equations of motion* of a uniform suspension accelerating under the influence of a uniform macroscopic pressure gradient and body force fields are

$$\dot{\mathbf{v}}_1 + E\dot{\mathbf{w}} = -\frac{\nabla P}{\rho_1} + \mathbf{g}_1 + \frac{\mathbf{a}_1 \times \mathbf{w}}{\rho_1} \tag{13}$$

$$\dot{\mathbf{v}}_2 - \frac{\rho_1 \alpha_1}{\rho_2 \alpha_2} E\dot{\mathbf{w}} = -\frac{\nabla P}{\rho_2} + \mathbf{g}_2 + \frac{\mathbf{a}_2 \times \mathbf{w}}{\rho_2} \tag{14}$$

$\mathbf{a}_1$ and $\mathbf{a}_2$ are arbitrary vectors subject to the constraint

$$(\alpha_1 \mathbf{a}_1 + \alpha_2 \mathbf{a}_2) \times \mathbf{w} = 0 \tag{15}$$

It would appear that the assembly must be incompressible if it is to be truly "uniform" in a pressure gradient. If $\mathbf{g}_1$ is a conservative force field, comparison between (9) and (13) would seem to indicate that $\nabla \times \mathbf{a}_1 \times \mathbf{w}$ is zero and therefore $\nabla \times \mathbf{a}_2 \times \mathbf{w}$ is as well from (15). Eq. (14) then suggests that if $\mathbf{g}_2$ is conservative, the combination on the left-hand side is the gradient of another "potential" which we could define in a form somewhat resembling (9):

$$\mathbf{v}_2 - \frac{\rho_1 \alpha_1}{\rho_2 \alpha_2} E\mathbf{w} = -\nabla \eta \tag{16}$$

A different argument is used to derive the one-dimensional equivalent of (16) in [1]. In each case, the interpretation of Φ and η could be, in the classical view, in terms of impulsive pressures and body forces necessary to set up the motion. This derivation, made for a uniform suspension, requires further argument, or a leap of faith, if it is to be applied more generally to a dispersion in which $\mathbf{w}$ and α_1, and hence β or E, vary with position.

Eqs. (13) and (14) show that the *exertia* plays the classical role of a *coefficient of apparent mass*, being proportional to various alternative definitions [1] in the literature.

Some other results derived from mechanistic arguments [1] are:

- The combined momentum flux and stress tensor for the suspension:

$$\mathbf{P} = \alpha_1(\rho_1 \mathbf{v}_1\mathbf{v}_1 + p_1\mathbf{I}) + \alpha_2(\rho_2 \mathbf{v}_2\mathbf{v}_2 + p_2\mathbf{I}) + \alpha_1\rho_1 E\mathbf{ww} \tag{17}$$

- Bernoulli's equation for fluid flowing steadily past a stationary particle matrix:

$$p_1 = p_{01} - \frac{1}{2}\rho_1 w^2(1+E) \tag{18}$$

- The force per unit volume on a particle in a stationary lattice:

$$\mathbf{f}_2 = \nabla p_2 = \nabla\left(\frac{1}{2}\rho_1 v_1^2 \alpha_1^2 \frac{d\beta}{d\alpha_1}\right) \tag{19}$$

When these results are used to check several hypothesized forms of the equations of motion in the *two-fluid model* of two-phase flow, there are found to be discrepancies [7], except when Geurst's equations are used.

GEURST'S EQUATIONS

In a series of papers [2-6] Geurst has used variational methods to derive a number of results, starting from the hypothesis that the kinetic energy per unit total volume is

$$k = \frac{1}{2}\rho_1\alpha_1 v_1^2 + \frac{1}{2}\rho_2\alpha_2 v_2^2 + \frac{1}{2}\rho_1 m w^2 \tag{20}$$

which is the same as (12) with the alternative definition

$$m = \alpha_1(\alpha_1\beta - 1) = \alpha_1 E \tag{21}$$

Initially Geurst [2,3] developed a one-dimensional theory, introducing Lagrange multipliers that are the same as the potentials Φ and η in (9) and (16). He went on to derive equations of motion, momentum, fluxes, pressures, etc. that are compatible with the results in Section 2, where there is a clear equivalence.

In three-dimensions the derivation is complicated by the introduction of Clebsch potentials and Lin constraints. Details are not provided in earlier publications [2-4] but they do appear in a recent one [6] in which the equivalents of (9) and (16) are expressed as

$$\boldsymbol{\pi}_1 = \nabla\phi_1 + \psi_1\nabla\chi_1 \tag{22}$$

$$\boldsymbol{\pi}_2 = \nabla\phi_2 + \psi_2\nabla\chi_2 + \frac{n}{\rho_2}\nabla\phi_n \tag{23}$$

where $\boldsymbol{\pi}_1$ and $\boldsymbol{\pi}_2$ are *generalized specific momenta* defined as

$$\boldsymbol{\pi}_1 = \mathbf{v}_1 - \frac{m}{\alpha_1}(\mathbf{v}_2 - \mathbf{v}_1) \tag{24}$$

$$\boldsymbol{\pi}_2 = \mathbf{v}_2 + \frac{\rho_1 m}{\rho_2 \alpha_2}(\mathbf{v}_2 - \mathbf{v}_1) \tag{25}$$

which are identical with the left-hand sides of (9) and (16), in view of (21).

The ϕ's and χ's are five "potentials" or Lagrange multipliers and n is the bubble density. The detailed interpretation of these terms is not important in the present context.

Geurst's equations of motion appear in many equivalent forms. The versions selected in [8] may be written in the present notation as

$$\frac{\partial}{\partial t}(\rho_1\alpha_1\boldsymbol{\pi}_1) + \nabla\cdot(\rho_1\alpha_1\mathbf{v}_1\boldsymbol{\pi}_1) = -\alpha_1\nabla p_2 - \nabla\left[\frac{1}{2}\rho_1(m+\alpha_1 m')w^2\right]$$
$$+\alpha_1\mathbf{f}_1 + \rho_1 m(\mathbf{v}_2-\mathbf{v}_1)\cdot(\nabla\mathbf{v}_2)^T \tag{26}$$

$$\frac{\partial}{\partial t}(\rho_2\alpha_2\boldsymbol{\pi}_2) + \nabla\cdot(\rho_2\alpha_2\mathbf{v}_2\boldsymbol{\pi}_2) = -\alpha_2\nabla p_2 + \alpha_2\mathbf{f}_2 - \rho_1 m(\mathbf{v}_2-\mathbf{v}_1)\cdot(\nabla\mathbf{v}_2)^T \tag{27}$$

which have the form of conservation laws for $\boldsymbol{\pi}_1$ and $\boldsymbol{\pi}_2$. m' denotes $dm/d\alpha_2$.

The two continuity equations are

$$\frac{\partial}{\partial t}(\rho_1\alpha_1) + \nabla\cdot(\rho_1\alpha_1\mathbf{v}_1) = 0 \tag{28}$$

$$\frac{\partial}{\partial t}(\rho_2\alpha_2) + \nabla\cdot(\rho_2\alpha_2\mathbf{v}_2) = 0 \tag{29}$$

If (7) is accepted and (21) is used, we find that the term involving w^2 on the right-hand side of (26) may be rewritten as

$$\frac{1}{2}\rho_1(m+\alpha_1 m')w^2 = \alpha_1(p_1-p_2) \tag{30}$$

Using (28) through (30) it is straightforward to arrange (26) and (27) into the forms

$$\frac{\partial}{\partial t}(\boldsymbol{\pi}_1) + \nabla\left(\mathbf{v}_1\cdot\boldsymbol{\pi}_1 - \frac{v_1^2}{2} - \frac{1}{2}\frac{m}{\alpha_1}(\mathbf{v}_2-\mathbf{v}_1)^2\right) - \mathbf{v}_1\times\nabla\times\boldsymbol{\pi}_1 = -\frac{\nabla p_1}{\rho_1} + \frac{\mathbf{f}_1}{\rho_1} \tag{31}$$

$$\frac{\partial}{\partial t}(\boldsymbol{\pi}_2) + \nabla\left(\mathbf{v}_2\cdot\boldsymbol{\pi}_2 - \frac{v_2^2}{2}\right) - \mathbf{v}_2\times\nabla\times\boldsymbol{\pi}_2 = \frac{-\nabla p_2}{\rho_2} + \frac{\mathbf{f}_2}{\rho_2} \tag{32}$$

Eqs. (31) and (32) are versions of the Bernoulli Equations derived in [8] without identifying $\boldsymbol{\pi}_1$ and $\boldsymbol{\pi}_2$ with gradients of potentials.

Now, if either ρ_1 is constant or ∇p_1 is parallel to $\nabla\rho_1$, and $\nabla \times (\mathbf{f}_1/\rho_1) = 0$, we may take the curl of (31) and obtain

$$\frac{\partial}{\partial t}(\nabla\times\boldsymbol{\pi}_1) - \nabla\times\mathbf{v}_1\times(\nabla\times\boldsymbol{\pi}_1) = 0 \tag{33}$$

which is a conservation law for the *vorticity* of $\boldsymbol{\pi}_1$. If we consider the rate of change of the net vorticity of $\boldsymbol{\pi}_1$ threading a loop moving with the velocity $\mathbf{v}_1$, we obtain

$$\frac{d}{dt}\int \boldsymbol{\pi}_1 \cdot \mathbf{d}\ell = \frac{d}{dt}\int (\nabla\times\boldsymbol{\pi}_1)\cdot \mathbf{d}s$$

$$= \int \frac{\partial}{\partial t}(\nabla\times\boldsymbol{\pi}_1)\cdot\mathbf{ds} + \int (\nabla\times\boldsymbol{\pi}_1)\cdot(\mathbf{v}_1\times\mathbf{d}\ell) \tag{34}$$

The two terms in (34) represent the sum of in-place changes in the flux through the loop and contributions picked up by the motion of boundaries. Changing the order of the scalar triple product in the final term and invoking Stokes' Theorem, we obtain a surface integral of (33) which is identically zero, in other words,

$$\frac{d}{dt}\int \boldsymbol{\pi}_1 \cdot \mathbf{d}\ell = 0 \tag{35}$$

This result was obtained by Geurst [3]. A similar conclusion follows for $(\nabla\times\boldsymbol{\pi}_2)$.

Now, if both phases come from a region in which there is no curl to $\boldsymbol{\pi}_1$ and $\boldsymbol{\pi}_2$ (for example, a stagnation region), conservative body forces act and density gradients (if any) are parallel to pressure gradients, then throughout the flow, in view of (35), it should be true that

$$\nabla \times \boldsymbol{\pi}_1 = 0; \qquad \nabla \times \boldsymbol{\pi}_2 = 0 \tag{36}$$

which implies that both $\boldsymbol{\pi}_1$ and $\boldsymbol{\pi}_2$ are gradients of suitable potentials and only the first term is needed on the right-hand sides of (22) and (23) which reduce to the form of (9) and (16). This development apparently makes more explicit the conditions for the existence of *two-phase potential flow*, requirements which parallel those for the classical single-phase case.

DISCUSSION

The previous sections of this paper have outlined two approaches to *potential two-phase flow*. Each has a justifiable theoretical base and is self-consistent. Moreover, both approaches appear to give the "right" prediction for several well-defined situations [7] while some other formulations fail these tests.

In order for these ideas to blossom further there need to be:

a) Further developments, from the same basic set of assumptions, that encompass more generality.

b) More rigorous derivations that clearly explain the order of approximation involved in treating the flow of discrete entities as a continuum.

c) Reconciliation with alternative approaches, particularly those involving *averaging*.

d) More solutions to specific problems that can be thoroughly investigated for consistency.

e) An understanding of outstanding incompatibilities between these approaches and various other theories, with a clear explanation of what has "gone wrong."

I hope that some of these items can be discussed at this meeting. At this time I only wish to briefly address (d) and (e).

Apart from the "tests" described in [1] and [7] and perturbation techniques leading to the description of wave propagation and stability in bubbly flow [2,3,5], I know of only two complete solutions to Geurst's equations. The first involves steady flow of two incompressible fluids from a common stagnation region. The simple conclusion that is reached is that the void fraction is constant and the velocities of both phases are the gradients of potentials that are proportional to each other and may be borrowed from an equivalent single-phase flow. The velocity ratio, or *slip ratio* is

$$\frac{\mathbf{v}_2}{\mathbf{v}_1} = \left(\frac{3R}{R+2}\right)^{1/2} \tag{37}$$

where

$$R = \rho_1/\rho_2 \tag{38}$$

In the above derivation use was made of Maxwell's [9] approximate expression for the *exertia*,

$$E \approx \frac{\alpha_2}{2} \tag{39}$$

The second solution again uses (39) and leads to a relationship between the velocities in unsteady incompressible flow [8]

$$\left(\rho_2 + \frac{\rho_1}{2}\right)\left(\frac{\partial \mathbf{v}_2}{\partial t} + \frac{\nabla v_2^2}{2}\right) - \frac{3}{2}\rho_1\left(\frac{\partial \mathbf{v}_1}{\partial t} + \frac{\nabla v_1^2}{2}\right) + \mathbf{f}_1 - \mathbf{f}_2 = 0 \tag{40}$$

This has the same form as a relationship which would be obtained by eliminating the pressures from equations of motion that ignored inertial coupling, except that the effective densities are changed. There is opportunity to test (40) by comparison with the one-dimensional transient response of fluidized beds.

Regarding item (e) I will repeat, in a slightly different form, Geurst's equations of motion [4] as presented in [8]

$$\frac{\partial}{\partial t}(\rho_1 \alpha_1 \mathbf{v}_1) + \nabla \cdot (\rho_1 \alpha_1 \mathbf{v}_1 \mathbf{v}_1 + \rho_1 m \mathbf{w}\mathbf{w}) =$$

$$-\alpha_1 \nabla p_1 - (p_1 - p_2)\nabla \alpha_1 + M_1^d + \alpha_1 \mathbf{f}_1 \tag{41}$$

$$\frac{\partial}{\partial t}(\rho_2 \alpha_2 \mathbf{v}_2) + \nabla \cdot (\rho_2 \alpha_2 \mathbf{v}_2 \mathbf{v}_2) = -\alpha_2 \nabla p_2 - M_1^d + \alpha_2 \mathbf{f}_2 \tag{42}$$

with the added mass term expressed as

$$M_1^d = \rho_1 m \left[\left(\frac{\partial}{\partial t} + \mathbf{v}_2 \cdot \nabla \right) \mathbf{v}_2 - \left(\frac{\partial}{\partial t} + \mathbf{v}_1 \cdot \nabla \right) \mathbf{v}_1 + \mathbf{w} \times \nabla \times \mathbf{v}_1 \right]$$

$$+\rho_1 m \nabla \frac{w^2}{2} + \mathbf{w} \left[\frac{\partial}{\partial t}(\rho_1 m) + \nabla \cdot \rho_1 m \mathbf{v}_2 \right] \tag{43}$$

This set of equations contains several more terms than one would find in most similar expressions in the literature. By dint of these extra terms, several "tests" are passed that other formulations fail [7]. Specifically, these tests involve (18) and (19), which reduces for a dilute dispersion to Taylor's expression [10] for the force on a stationary object in an accelerating flow. It would be desirable to devise other "tests" that might help to discriminate further between true and false expressions.

REFERENCES

1. Wallis, G.B., "Inertial Coupling in Two-Phase Flow: Macroscopic Properties of Suspensions in an Inviscid Fluid," *Multiphase Science and Technology*, in press, 1989.

2. Geurst, J.A., "Two-Fluid Hydrodynamics of Bubbly Liquid/Vapour Mixture Including Phase Change," *Philips J. Res.*, **40**, 352-374, 1985.

3. Geurst, J.A., "Virtual Mass in Two-Phase Bubbly Flow," *Physica,* **129A**, 233-261, 1985.

4. Geurst, J.A., "Variational Principles and Two-Fluid Hydrodynamics of Bubbly Liquid/Gas Mixtures," *Physica,* **135A**, 455-486, 1986.

5. Geurst, J.A. and A.J.N. Vreenegoor, "Nonlinear Void-Fraction Waves in Two-Phase Bubbly Flow," *ZAMP,* **39**, 376-386, 1988.

6. Geurst, J.A. "Drift Mass, Multifluid Modelling of Two-Phase Bubbly Flow and Superfluid Hydrodynamics," *Physica*, in press, 1989.

7. Wallis, G.B. "Some Tests of Two-Fluid Models for Two-Phase Flow," U.S.-Japan Seminar on Two-Phase Flow Dynamics, Ohtsu, Japan, July, 1988.

8. Wallis, G.B. "On Geurst's Equations for Inertial Coupling in Two-Phase Flow," Workshop, Institute for Mathematics and Its Applications, University of Minnesota, January, 1989.

9. Maxwell, J.C., *A Treatise on Electricity and Magnetism*, 2nd ed. **1**, Oxford: Clarendon Press, 398, 1881.

10. Taylor, G.I., "The Forces on a Body Placed in a Curved or Converging Stream of Fluid," *Proc. Roy. Soc.,* **A120**, 260-283, 1928.

INTERPRETATION AND MODELING OF THE AVERAGED EQUATIONS FOR A FLUID-SOLID FLOW

Hayley H. Shen and Guann-Jiun Hwang

Department of Civil and Environmental Engineering

Clarkson University, Potsdam, NY 13676

ABSTRACT

In this study, a self-consistent derivation of the conservation laws is given for flows of a fluid-solid mixture. A unified analytical framework for obtaining constitutive relations is provided. This analysis uses a control volume/control surface approach that is widely used in fluid mechanics. All terms in the governing equations and the constitutive relations are written in terms of the mass-weighted averages except solid concentration. It is believed strongly that the mass-weighted average is the natural bridge between micromechanics and constitutive relations. The derived momentum equations contain terms that differ from all existing models except that of Prosperetti and Jones (1984). However, their assumptions are not needed here. Special attention is given to the solid phase pressure. The physical basis of previously assumed form for this pressure (Givler 1987) becomes clear. A number of related phenomena are also discussed. These include the anti-diffusion and anisotropic normal stresses. The energy equations are also different from existing models. But detail discussion on the energy equations is left to future work.

I. INTRODUCTION

Modeling a flowing fluid-solid mixture starts from writing down a set of governing equations. These equations describe the conservation of mass, momentum and energy. In the early stage, the popular approach was to view the mixture as a single phase material. Consequently, the following type of equations were used for mass and momentum conservations (see Zuber 1964, Ishii 1975, 1977).

$$\frac{\partial \langle \rho_m \rangle}{\partial t} + \nabla \cdot \langle \rho_m \rangle \mathbf{u}_m = 0 \tag{1}$$

$$\frac{\partial}{\partial t} \langle \rho_m \rangle \mathbf{u}_m + \nabla \cdot \langle \rho_m \rangle \mathbf{u}_m \mathbf{u}_m = \nabla \cdot \mathbf{T}^m + \langle \rho_m \rangle \mathbf{g} \tag{2}$$

In which, $\langle\ \rangle$ represents the ensemble average, ρ_m is the mixture density, $\mathbf{u}_m$ is the mixture velocity, $\mathbf{T}^m$ is the mixture stress and $\mathbf{g}$ is the body force per unit mass.

Recently, the two-phase flow approach becomes more popular. Using this approach, the conservation equations are formulated for each individual phase separately. This approach allows for direct modeling of a fluid-solid mixture when the two phases have distinctly different dynamics. For mass and momentum, these conservation equations are generically written in the following way (see Ishii 1975, Drew 1976, 1983, McTigue et al. 1986).

$$\partial\langle\rho_s c\rangle/\partial t + \nabla\cdot\langle\rho_s c\mathbf{u}\rangle = 0 \tag{3}$$

$$\partial\langle\rho_f(1-c)\rangle/\partial t + \nabla\cdot\langle\rho_f(1-c)\mathbf{v}\rangle = 0 \tag{4}$$

$$\partial\langle\rho_s c\mathbf{u}\rangle/\partial t + \nabla\cdot\langle\rho_s c\mathbf{u}\mathbf{u}\rangle = \langle\rho_s c\mathbf{g}\rangle + \langle\mathbf{m}\rangle + \nabla\cdot\langle c\mathbf{T_s}\rangle \tag{5}$$

$$\partial\langle\rho_f(1-c)\mathbf{v}\rangle/\partial t + \nabla\cdot\langle\rho_f(1-c)\mathbf{v}\mathbf{v}\rangle = \langle\rho_f(1-c)\mathbf{g}\rangle - \langle\mathbf{m}\rangle + \nabla\cdot\langle(1-c)\mathbf{T_f}\rangle \tag{6}$$

where ρ_s and ρ_f are densities of the solid and fluid phases, $\mathbf{u}$ and $\mathbf{v}$ are the velocities of the solid and fluid phases, $\mathbf{m}$ is the interaction force per unit volume of the mixture, c is the local solid concentration (equals to 1 at a solid point and 0 at a fluid point), $\mathbf{T_s}$ and $\mathbf{T_f}$ are the solid and fluid stress respectively. The above equations do not consider the phase changes at the interface. The energy conservation equations have not been studied as extensively as the mass and momentum conservation equations.

Because the two phases are separated, available information on a single particle's motion and the particle-particle interactions in a fluid environment are incorporated directly. In a mixture model, these informations will first be utilized to obtain the drift flux term in $\mathbf{T}^m$ of Eq. (2). Preference of the two approaches apparently depends on the application. However, since the mixture model can be derived from adding together the two-phase equations, the two-phase approach is considered more fundamental.

Many mathematical models have been derived based on Eqs. (3)-(6). There are two issues in modeling terms appeared in those conservation equations. First, what kind of averaging is used in defining the macro quantities, such as concentration, velocity, velocity divergence, strain-rate, etc. Second, how to obtain the required constitutive relations for

averaged terms like stress, pressure, phase interaction, etc. Neither of these two issues is settled at the moment.

We will refer to the mechanics that governs particle's motion as the "micromechanics". Such micromechanics includes particle-particle and particle-fluid interactions. In order to explicitly formulate constitutive relations, knowledge of micromechanics is essential.

It is understood that the formulation of constitutive relation is extremely complicated, because the micromechanics of fluid-solid interaction is itself not well understood. Another reason for this difficulty is less obvious but more significant. That is, up to the moment, there has not been a set of governing equations in which all terms are interpreted with a consistent averaging method, without such governing equations, and a consistent bookkeeping to account for the micromechanics. It is impossible to correctly formulate the constitutive relations. The authors believe that this is the source of the recent argument about the "solid phase pressure" and related phenomena. A survey of the recent literature shows that different interpretations have been given to the solid phase pressure. It has been suggested to be equal to the (i) fluid phase pressure (Drew 1976), (ii) averaged fluid pressure around the surface of a particle (Givler 1987), or (iii) a more sophisticated version of (ii) with additional consideration of Brownian forces and bulk viscosity (McTigue et al. 1986). All of which are intended to apply to an arbitrary flow of a fluid-solid mixture. Similarly, the phase interaction $\langle \mathbf{m} \rangle$ in Eqs. (5) and (6) has also been modeled in many different ways. Essentially, in all the more recent works this term has been modeled as

$$\langle \mathbf{m} \rangle = n\mathbf{h} + \tilde{p}\nabla\langle c \rangle \tag{7}$$

where n is the averaged number of particles per unit volume of the mixture, $\mathbf{h}$ is the averaged hydrodynamic force per particle. The term $\tilde{p}$ is a source of confusion again. It has been equated to the (i) averaged fluid pressure over the fluid-solid interface (Drew 1983), (ii) fluid phase pressure (McTigue et al. 1986) or (iii) hydrostatic fluid pressure (Ahmadi 1987). Again, all the above are suggested for general flow condition.

Although the existing two-phase flow models appear to be inconsistent, development of the above models has provided a great deal of insights. These insights are essential to the work presented here.

In the following, we will give a step by step derivation of the two-phase flow governing equations based on the mass-weighted average defined as

$$\{\psi\} = \frac{\langle c_k \psi \rangle}{\langle c_k \rangle} \tag{8}$$

where c_k equals to c for the solid phase and $1 - c$ for the fluid phase. This averaging method has been exploited in the theory of compressible turbulence (Van Driest 1951), and applied to granular flow (Ahmadi and Shahinpoor 1983).

The mass-weighted average of any given quantity is the quantity averaged within that phase only. For instance, mass-weighted solid velocity at a point is the average velocity of all observed particles passing that point. This average is the easiest one to measure in most real flows. Moreover, through using this average, a direct bridge between micromechanics and the constitutive relations may be established. Applying this average to the solid phase stress, terms such as the solid phase pressure will have a clear meaning. Thus a unique definition for these quantities in terms of micromechanics is possible. In addition, a number of interesting phenomena that seem to defy the well accepted property of fluids are observed when a fluid-solid mixture is viewed as a composition of two separate continuums.

In the present study, we concentrate on the derivation of governing equations, interpretation of the averaged terms and the development of constitutive relations from micromechanics. Derivation of the actual constitutive relations for various flow conditions is beyond our scope and present ability. A few exceptionally simple cases will however be studied. In order to complete the mathematical modeling, boundary conditions must be derived. Due to the existence of the discrete solid phase, derivation of boundary conditions is equally difficult as constitutive relations. This is also left to future development.

II. GOVERNING EQUATIONS

Consider an arbitrary control volume V as shown in Fig. 1. Its surface S is the control surface. For visual reason this control volume is drawn large compared with the solid particle's size. The derivation is not restricted to this size. The particles are not necessarily spherical or uniform either. However, in order to simplify the notations, we will discuss the case of uniform spherical particles. The essence of the analysis is captured in this simplified case. There has been previous work deriving conservation equations for this type of control volume for a fluid-solid mixture (Soo 1981). Nevertheless, such equations have not been derived in terms of the mass-weighted average nor the interpretation in terms of micromechanics given.

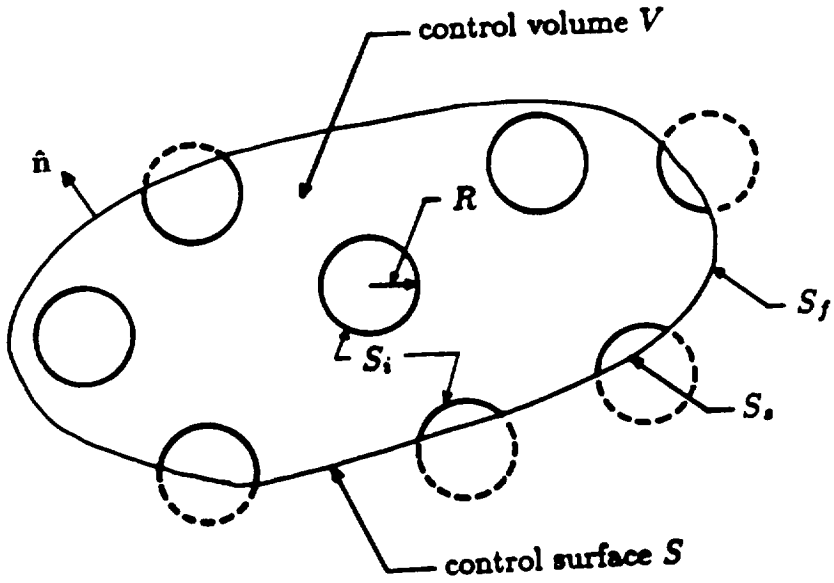

Fig. 1 A control volume V with control surface $S = S_s + S_f$ and internal interface S_i.

In general, the flow situation is such that the condition in any given control volume

from different observations is a random phenomenon. Only an average behavior may be described by a deterministic mathematical model. To allow for cases where flow conditions may vary over a length scale comparable with the particle size, the ensemble average over many realizations of a control volume smaller than the "representative volume" commonly used in fluid mechanics may be necessary.

For one realization, the rate of increase of solid mass in the control volume is

$$\frac{\partial}{\partial t}\int_V \rho_s c\, dV + \int_S \rho_s c\mathbf{u}\cdot\hat{\mathbf{n}}\, dS = 0 \tag{9}$$

where $\hat{\mathbf{n}}$ is the unit outward normal. After ensemble averaging, the resulting integrands are smooth functions. Applying Green's theorem to the second term and removing the integrals, the mass conservation of the solid phase in this control volume is obtained as

$$\frac{\partial\langle\rho^s\rangle}{\partial t} + \nabla\cdot\langle\rho^s\rangle\{\mathbf{u}\} = 0 \tag{10}$$

In the above, $\langle\rho_s c\rangle$ is replaced by $\langle\rho^s\rangle$ and $\langle\rho_s c\mathbf{u}\rangle$ is replaced by $\langle\rho^s\rangle\{\mathbf{u}\}$ where $\{\ \}$ is the mass-weighted average defined in Eq. (8). Similarly, for the fluid phase,

$$\frac{\partial\langle\rho^f\rangle}{\partial t} + \nabla\cdot\langle\rho^f\rangle\{\mathbf{v}\} = 0. \tag{11}$$

The momentum conservation equations require representation of the forcing terms which include the surface and body forces. This conservation for the solid and fluid phases in one realization are, respectively,

$$\frac{\partial}{\partial t}\int_V \rho_s c\mathbf{u}\, dV + \int_S \rho_s c\mathbf{u}\mathbf{u}\cdot\hat{\mathbf{n}}\, dS = \int_S c\mathbf{T}_s\cdot\hat{\mathbf{n}}\, dS + \int_V \rho_s c\mathbf{g}\, dV + \int_V \mathbf{m}\, dV \tag{12}$$

$$\frac{\partial}{\partial t}\int_V \rho_f(1-c)\mathbf{v}\, dV + \int_S \rho_f(1-c)\mathbf{v}\mathbf{v}\cdot\hat{\mathbf{n}}\, dS = \int_S (1-c)\mathbf{T}_f\cdot\hat{\mathbf{n}}\, dS + \int_V \rho_f(1-c)\mathbf{g}\, dV - \int_V \mathbf{m}\, dV \tag{13}$$

Again the ensemble average is first applied to smooth the above integrands. The Green's theorem may then be used to change the surface integral to volume integral. After removing the integral sign, the above equations become

$$\frac{\partial}{\partial t}\langle \rho_s c\mathbf{u}\rangle + \nabla\cdot\langle \rho_s c\mathbf{u}\mathbf{u}\rangle = \nabla\cdot\langle c\mathbf{T_s}\rangle + \langle \rho_s c\mathbf{g}\rangle + \langle \mathbf{m}\rangle \tag{14}$$

$$\frac{\partial}{\partial t}\langle \rho_f (1-c)\mathbf{v}\rangle + \nabla\cdot\langle \rho_f (1-c)\mathbf{v}\mathbf{v}\rangle = \nabla\cdot\langle (1-c)\mathbf{T_f}\rangle + \langle \rho_f (1-c)\mathbf{g}\rangle - \langle \mathbf{m}\rangle \tag{15}$$

Substituting $\mathbf{u}$ by $\{\mathbf{u}\}+\mathbf{u}''$ and $\mathbf{v}$ by $\{\mathbf{v}\}+\mathbf{v}''$ and making use of the mass conservation equations, we obtain the following equations with the Reynolds stresses for both phases. In these equations mass-weighted velocities and stresses appear.

$$\langle \rho^s\rangle(\partial\{\mathbf{u}\}/\partial t + \{\mathbf{u}\}\cdot\nabla\{\mathbf{u}\}) = \nabla\cdot\langle c\rangle\{\mathbf{T_s}\} - \nabla\cdot\langle \rho^s\rangle\{\mathbf{u}''\mathbf{u}''\} + \langle \rho^s\rangle\mathbf{g} + \langle \mathbf{m}\rangle \tag{16}$$

$$\langle \rho^f\rangle(\partial\{\mathbf{v}\}/\partial t + \{\mathbf{v}\}\cdot\nabla\{\mathbf{v}\}) = \nabla\cdot\langle 1-c\rangle\{\mathbf{T_f}\} - \nabla\cdot\langle \rho^f\rangle\{\mathbf{v}''\mathbf{v}''\} + \langle \rho^f\rangle\mathbf{g} - \langle \mathbf{m}\rangle \tag{17}$$

The Reynolds stress in the solid phase is also called the kinetic stress in the granular flow terminology.

In a realization over a period of time, particles cut by the control surface may interact with neighboring particles through collisions. The rate of momentum transfer to the interior of the control volume resulted from these collisions is part of the surface force $\mathbf{T_s}$. Moreover, the hydrodynamic forces acting on particles cut by the control surface also produce surface forces that contribute to $\mathbf{T_s}$. We denote these two stresses as $\mathbf{T^c}$ and $\mathbf{T^p}$ respectively.

Concept for modeling the mass-weighted average of $\mathbf{T^c}$ has been described in the granular flow literature (e.g. Bagnold 1954, Jenkins and Savage 1983, an excellent survey to appear by Campbell 1990). Although most of the work deals with negligible fluid effect, the route to extend to fluid-solid mixture is, though complicated, quite clear (e.g. Ackermann and Shen 1982, Shen et al. 1988). On the other hand, the explanation of the hydrodynamic stress on the solid phase is not readily available. Intuitively, one would

quite comfortably accept that the fluid only acts on each particle in the control volume through the drag, added mass, etc. Hence, it should contribute to the body force only. Consequently the effect of fluid-solid interaction is the hydrodynamic force per particle multiply the number of particles per unit mixture volume. This concept is proved doubtful as demonstrated by the existing various models discussed in Eq. (7). In the following we will rigorously formulate the fluid effect in a two-phase flow.

Consider a surface particle P in Fig. 2. Part of this particle, P^i, is inside the control volume, part of it, P^o is outside of it. The hydrodynamic force acting on P produces a pair of internal forces, $\pm$ $\mathbf{t}$, on the intersection of the particle and the control surface S_s. The total hydrodynamic force acting on this particle, $\mathbf{h}$, can similarly be decomposed into that on the outside of P, $\mathbf{d}^o$, and that on the inside of P, $\mathbf{d}^i$.

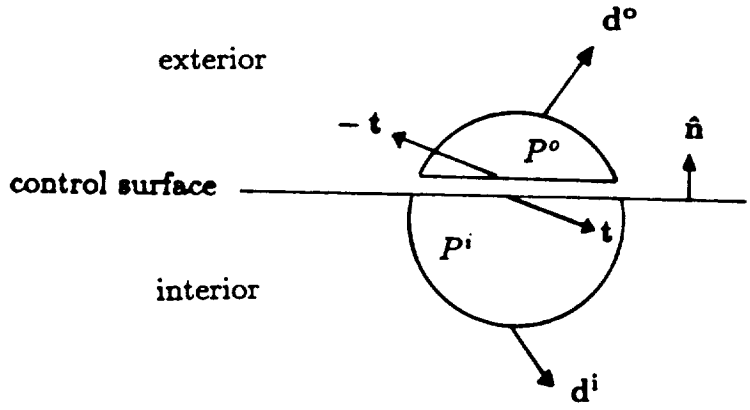

Fig. 2 Decomposing the hydrodynamic force on a surface particle P.
The total hydrodynamic force is $\mathbf{h} = \mathbf{d}^i + \mathbf{d}^o$.

In budgeting the total force acting on the solid portion of V, the interface force $\mathbf{t}$ acting on S_s most naturally belongs to the solid phase stress. In fact it may equally well be classified as part of the body force since after all it acts on P^i which is inside of V. As long as the budgeting of all forces is done in a consistent way, the resulting equation of motion should not depend on the detail of the bookkeeping. Most of the existing

two-phase models appear to fail in using a consistent bookkeeping. That is, force acting on the control surface and that acting on the internal interface are not always carefully distinguished. We choose to call $\mathbf{t}$ the surface force for V and $\mathbf{d^i}$ the body force for V due to fluid-solid interaction.

The internal force $\mathbf{t}$ is the difference between $\mathbf{d^o}$ and the total surface force acting on P^o. The first may be determined if the hydrodynamic force distribution on a particle's surface and the particle's location relative to the control surface are both given.

The second is determined using Newton's second law. That is, the total surface force acting on the partial particle P^o equals to its inertia subtract the body force acting on it. Ensemble average of the inertia and the body force on P^o may also be obtained if the particle's relative position with respect to the control surface is given. For a control volume reasonably away from the boundary of the flow field, the position of particles on the control surface S_s may be assumed to uniformly distribute inside or outside the control volume. Using these arguments it has been shown in Hwang and Shen (1989a) that the ensemble average of the sum of $\mathbf{t}$ in a unit area produces the following stress,

$$\{\mathbf{T^p}\} = \frac{1}{V_o}\left(\int_{A_o} \{\mathbf{\Sigma}\} \cdot \hat{\mathbf{n}}\mathbf{r}\, dA - \int_{V_o} (\nabla \cdot \{\mathbf{\Sigma}\})\mathbf{r}\, dV\right), \tag{18}$$

where A_o and V_o are the surface area and volume of particle P respectively, $\mathbf{\Sigma}$ is the local fluid stress on the particle's surface, and $\mathbf{r}$ is the position vector. The very same equation has been obtained by Batchelor (1970) with a quite different derivation. This term has been named the "particle-presence stress" in Hwang and Shen (1989a), and it contains the "interaction stress" in McTigue et al. (1986). The second term inside the parenthesis in Eq. (18) is related to the particle's rotational inertia (Hwang and Shen 1989a).

Next we discuss the interaction term $\mathbf{m}$ in the solid momentum equation. The most natural way consistent with the above bookkeeping is to define it as the total force acting on the interface of the two phases inside the control volume V. This interface is denoted by S_i in Fig. 1, which consists of the surfaces of whole particles if they are entirely in V,

otherwise only the part of particle's surface that is inside V belongs to S_i. Total force acting on S_i is the sum of all $\mathbf{h}$, the hydrodynamic force on a whole particle, and all $\mathbf{d^i}$, the portion of the hydrodynamic force on P inside of V. As shown in Hwang and Shen (1988), the ensemble average of the total interaction force $\mathbf{m}$ is

$$\langle \mathbf{m} \rangle = \frac{\langle c \rangle}{V_o} \{\mathbf{h}\} + \langle c \rangle \nabla \cdot \{\mathbf{T^f}\} - \nabla \cdot c\{\mathbf{T^p}\} \tag{19}$$

In the above, $\{\mathbf{T^f}\} = \{\mathbf{T_f}\} - \rho_f \{\mathbf{v''v''}\}$ is used to indicate the total fluid stress. Substituting Eq. (19) and $\mathbf{T_s} = \mathbf{T^c} + \mathbf{T^p}$ into Eq. (16) , the solid momentum equation becomes

$$\langle \rho^s \rangle (\partial\{\mathbf{u}\}/\partial t + \{\mathbf{u}\} \cdot \nabla\{\mathbf{u}\}) = \nabla \cdot (\langle c \rangle \{\mathbf{T^c}\}) - \nabla \cdot \langle \rho^s \rangle \{\mathbf{u''u''}\} + \langle \rho^s \rangle \mathbf{g} + \frac{\langle c \rangle}{V_o} \{\mathbf{h}\} + \langle c \rangle \nabla \cdot \{\mathbf{T^f}\} \tag{20}$$

This equation is identical to that derived in Prosperetti and Jones (1984). In that work, a couple of assumptions were made to arrive at Eq. (20). It is shown here that those assumptions are not necessary. Similarly, the fluid momentum equation may be derived as

$$\langle \rho^f \rangle (\partial\{\mathbf{v}\}/\partial t + \{\mathbf{v}\} \cdot \nabla\{\mathbf{v}\}) = (1 - 2\langle c \rangle) \nabla \cdot \{\mathbf{T^f}\} - \{\mathbf{T^f}\} \cdot \nabla \langle c \rangle + \langle \rho^f \rangle \mathbf{g} - \frac{\langle c \rangle}{V_o} \{\mathbf{h}\} + \nabla \cdot (\langle c \rangle \{\mathbf{T^p}\}) \tag{21}$$

As it shows in above equations, the effect of particle-presence stress $\{T^p\}$ appears only in the fluid momentum equation.

Derivation of the energy equations follows the same spirit as the above. Hwang and Shen (1989c) gave the following equations in indicial form for the turbulence energy in the solid and fluid phases respectively,

$$\begin{aligned}
\langle \rho^s \rangle \left(\frac{\partial}{\partial t} \{\frac{\mathbf{u''} \cdot \mathbf{u''}}{2}\} + \{\mathbf{u}\} \cdot \nabla \{\frac{\mathbf{u''} \cdot \mathbf{u''}}{2}\} \right) &= \langle c \rangle \{\mathbf{T^c}\} : \nabla\{\mathbf{u}\} + \langle c \rangle \{\mathbf{T^p}\} : \nabla\{\mathbf{u}\} \\
&- \langle \rho^s \rangle \{\mathbf{u''u''}\} : \nabla\{\mathbf{u}\} + \nabla \cdot \left(\langle c \rangle \{\mathbf{T^c} \cdot \mathbf{u''}\} \right) + \nabla \cdot \left(\langle c \rangle \{\mathbf{T^p} \cdot \mathbf{u''}\} \right) \\
&- \nabla \cdot \left(\langle \rho^s \rangle \{\frac{\mathbf{u''u''}}{2} \cdot \mathbf{u''}\} \right) + \langle \mathbf{m} \cdot \mathbf{u''} \rangle - \langle c \rangle \{\gamma^s\}
\end{aligned} \tag{22}$$

$$\begin{aligned}
\langle \rho^f \rangle \left(\frac{\partial}{\partial t} \{\frac{\mathbf{v''} \cdot \mathbf{v''}}{2}\} + \{\mathbf{v}\} \cdot \nabla \{\frac{\mathbf{v''} \cdot \mathbf{v''}}{2}\} \right) &= -\langle 1 - c \rangle \{p^f\} \nabla \cdot \{\mathbf{v}\} - \langle \rho^f \rangle \{\mathbf{v''v''}\} : \nabla\{\mathbf{v}\} \\
&- \nabla \cdot \left(\langle \rho^f \rangle \{(\frac{\mathbf{v''} \cdot \mathbf{v''}}{2} + \frac{p^{f\prime\prime}}{\rho_f}) \mathbf{v''}\} \right) + \mu \nabla^2 \left(\langle 1 - c \rangle \{\frac{\mathbf{v''} \cdot \mathbf{v''}}{2}\} \right) \\
&- \mu \langle 1 - c \rangle \{\nabla \mathbf{v''} : \nabla \mathbf{v''}\} - \langle \mathbf{m} \cdot \mathbf{v''} \rangle
\end{aligned} \tag{23}$$

where γ^s is the sink of solid turbulence energy from particle-particle interaction (e.g. collisional dissipation), p^f is the fluid pressure, $p^{f\prime\prime} = p^f - \{p^f\}$, and μ is the dynamic viscosity of the fluid.

The interaction force $\mathbf{m}$ does unequal amount of work to the turbulence energy in the fluid and solid phases. This difference, as given in Hwang and Shen (1989c), comes from the slip velocity between the two phases.

The combination of mass, momentum and energy conservation equations given by the six equations: Eqs. (10), (11), (20), (21), (22) and (23) governs the six unknowns c, $\mathbf{u}$, $\mathbf{v}$, $\{\mathbf{u}'' \cdot \mathbf{u}''/2\}$, $\{\mathbf{v}'' \cdot \mathbf{v}''/2\}$ and $\{p^f\}$. To form a closed system, a large number of constitutive relations must be obtained. Most of these constitutive relations require knowledge beyond the current understanding of fluid mechanics around a particle. One example is the term $\{\mathbf{m} \cdot \mathbf{u}''\}$ appeared in Eq. (22). As shown in Eq. (19), $\mathbf{m}$ contains the hydrodynamic force $\mathbf{h}$ acting on a particle. If one considers the drag force part of $\mathbf{h}$, which is in general in terms of $\mathbf{u}'' - \mathbf{v}''$, the term $\{\mathbf{m} \cdot \mathbf{u}''\}$ will produce $\{\mathbf{v}'' \cdot \mathbf{u}''\}$. Namely, the correlation of the fluid and solid turbulence must be formulated as part of the constitutive relations. A number of analyses have indicated that this correlation depends greatly on the particle's size and density (Chao 1964, Xie 1987, Abou-Arab and Roco 1988). Quantitative study of such correlation is far from complete.

Despite the complexity and the lack of necessary knowledge in fluid mechanics, a number of results may be obtained for the constitutive relations appeared in the governing equations. In the next section, we will derive a term associated with the fluid-solid interactions. Namely, the particle-presence stress $\mathbf{T^p}$ including a detailed discussion on the solid phase pressure. A number of interesting observations will be given at the end of the derivation.

III. CONSTITUTIVE MODELING

To simplify the notation, we remove all the average symbols ($\langle\ \rangle$ and $\{\ \}$) and adopt indicial notation from this section on.

In this section, we will discuss the particle-presence stress T^p_{ij}. Detail of this term is given in Eq. (18). The term in Eq. (18) related to the particle's rotational inertia cancels with the rotational contribution in the particle's Reynolds stress in Eq. (16) (Babič 1989). Hence the net particle-presence stress is only the first term on the right side of Eq. (18). This term may be quantified if the distribution of the hydrodynamic stress $\mathbf{\Sigma}$ is known. Before quantifying this stress for special cases, we will provide an interpretation of the solid phase pressure first.

As defined in Continuum Mechanics, pressure means the negative average of the normal stresses. Therefore, in addition to the contributions from the collisional and Reynolds stress, the particle-presence stress will also produce the following solid phase pressure,

$$\begin{aligned} p^p &= -\frac{R^3}{3V_0}\int_0^{2\pi}\int_0^{\pi}\Sigma_{ik}n_k n_i \sin\phi\, d\phi\, d\theta \\ &= -\frac{1}{4\pi}\int_0^{2\pi}\int_0^{\pi}(-p^f\delta_{ik} - \frac{2}{3}\mu e_{ll}\delta_{ik} + 2\mu e_{ik})n_k n_i \sin\phi\, d\phi\, d\theta \\ &= \frac{1}{4\pi}\int_0^{2\pi}\int_0^{\pi} p^f \sin\phi\, d\phi\, d\theta \end{aligned} \tag{24}$$

where ϕ and θ are the polar and azimuthal angles respectively. In the above, a Newtonian fluid is assumed such that

$$\Sigma_{ik} = -p^f\delta_{ik} - \frac{2}{3}\mu e_{ll}\delta_{ik} + 2\mu e_{ik} \tag{25}$$

where e_{ik} is the component of local strain-rate. Moreover, for Eq. (24) to be valid, the fluid flow near the particle must be incompressible and the strain-rate must possess certain symmetry property. Thus the viscous contribution vanishes from Eq. (24). Under these special conditions, it is seen that the solid phase pressure is the numerical average of the

fluid pressure around the particles. This very result has been postulated by Givler (1987) and derived by Prosperetti and Jones (1984) using a couple of assumptions.

We now derive the particle-presence stress in two extreme cases for a very dilute mixture. The two extreme cases are: Stokes regime and inviscid regime. In both cases we assume the fluid is Newtonian and the flow is incompressible.

In case of a shear flow in the Stokes regime, the local strain-rate around a spherical particle in an infinite flow field is (Batchelor 1967)

$$e_{ij}(r_i) = E_{ij}\Big(1 - \frac{R^5}{r^5}\Big) + E_{kl}\Big(\frac{r_i r_k \delta_{jl} + r_j r_k \delta_{il}}{r^2} - \frac{2}{3}\frac{r_k r_l}{r^2}\delta_{ij}\Big)\Big(-\frac{5R^3}{2r^3} + \frac{5R^5}{r^5}\Big)$$
$$+ E_{kl}\frac{r_k r_l}{r^2}\Big(\frac{r_i r_j}{r^2} - \frac{1}{3}\delta_{ij}\Big)\Big(\frac{25R^3}{2r^3} - \frac{35R^5}{2r^5}\Big) \tag{26}$$

where r_i is the ith component of a position vector $\mathbf{r}$, $r = \mid \mathbf{r} \mid$, E_{ij} is the component the undisturbed strain-rate and R is the particle's radius.

The fluid pressure around a spherical particle in a uniform incoming flow U_∞ is (Chester and Breach 1969)

$$p = p^f + \frac{\mu U_\infty}{r}\Big[-\frac{3}{2}(1 + \frac{3}{8}R_e)\cos\phi + \frac{27}{32}R_e\cos^2\phi + O(R_e^2 \log R_e)\Big], \tag{27}$$

where p^f is the undisturbed fluid pressure; U_∞ is equivalent to the relative velocity of the particle to the fluid flow, or $U_\infty = v_r$ where $v_r = \mid \mathbf{v} - \mathbf{u} \mid$; R_e is the particle Reynolds number defined as $2\rho_f R v_r/\mu$; and ϕ is the polar angle of a point on the surface of the particle measured from the direction of U_∞.

Substituting Eqs. (25) and (26) into Eq. (18), the viscous contribution of the particle-presence stress is obtained as

$$T_{ij}^{p\mu} = \frac{5}{2}(2\mu E_{ij}) \tag{28}$$

As discussed in Batchelor (1970), this stress together with the viscous stress in the fluid phase reproduces Einstein's formula for the effective viscosity (1956). The solid phase pressure is shown below after substituting Eq. (27) into Eq. (24),

$$p^p = p^f + \frac{9}{32}\rho_f v_r^2. \tag{29}$$

In the above, we used p^p to indicate the fact that only particle-presence stress $\mathbf{T^p}$ is included in the total solid stress. Neither collisional nor Reynolds pressure is considered.

The above is not the whole story about the particle-presence stress. If one by-passes the solid phase pressure and investigate the normal stresses directly, the following is found.

$$\begin{aligned} T_{11}^{pp} &= -p^f - \frac{81}{160}\rho_f v_r^2 \\ T_{22}^{pp} &= T_{33}^{pp} \\ &= -p^f - \frac{27}{160}\rho_f v_r^2 \end{aligned} \tag{30}$$

The total particle-presence stress is the sum of Eqs. (28) and (30). It is apparent that Eq. (29) can be reproduced by taking the negative average of T_{11}^{pp}, T_{22}^{pp} and T_{33}^{pp}.

Eq. (30) shows that on top of the viscous effect the isotropic fluid pressure induces anisotropic normal stress in the solid phase stress. This anisotropy of the normal stress is the product of the distinctly different dynamics of the two phases involved. If both phases move with exactly same velocity, this phenomenon will disappear.

In case of an inviscid flow, only the fluid pressure contributes to the particle-presence stress. This pressure around the spherical particle is (Lamb 1932),

$$p = p_\infty + \frac{1}{2}\rho_f v_r^2(-\frac{1}{8} + \frac{9}{8}\cos 2\phi). \tag{31}$$

Substituting Eq. (31) into Eq. (25) and neglecting the viscous part, Eq. (18) becomes

$$\begin{aligned} T_{11}^{p} &= -p^f - \frac{1}{20}\rho_f v_r^2 \\ T_{22}^{p} &= T_{33}^{p} \\ &= -p^f + \frac{2}{5}\rho_f v_r^2 \end{aligned} \tag{32}$$

and the solid phase pressure from the hydrodynamic effect alone is the negative average of the above,

$$p^p = p^f - \frac{1}{4}\rho_f v_r^2 \tag{33}$$

The anisotropy of the normal stresses is again observed. Theoretical speaking, without considering Reynolds stress, one may observe the shear force in a two-phase mixture even though the fluid is inviscid.

Comparing the coefficient of the solid phase pressure in the above two extreme cases, one would expect that as the particle Reynolds number increases from nearly zero to nearly infinity, the coefficient in front of the solid phase pressure should vary gradually from $\frac{9}{32}$ to $-\frac{1}{4}$. Explicit determination of this coefficient depends on the knowledge of the hydrodynamic stress distribution around the particle. Unfortunately this information is not available for the entire range of the particle Reynolds number. However, for particle Reynolds number greater than 3000, experimental data shows that the viscous contribution is negligible. In this case, sufficient information exists to empirically determine the pressure distribution, and accordingly the solid phase pressure (Hwang and Shen 1989b).

IV. SOME INTRIGUING POINTS

In deriving the governing equations, a few points have struck the authors as being quite non-trivial. Some of those may have significant implications that is unclear at the moment.

First, the governing equations are for the mass-weighted quantities. All constitutive relations must eventually be written in these quantities to produce a closed system. The kinematic quantities appeared in these governing equations are the mass-weighted velocities. On the other hand, in constitutive relations, we look for mathematical description of the stresses. The average stresses, at least for the viscous component of the fluid stress, is however a function of the average local fluid strain-rate instead of the gradient of the mass-weighted velocity. Namely, this stress is in terms of the mass-weighted strain-rate in stead of the gradient of the mass-weighted velocity. For a fluid-solid mixture with rigid

particles, this relation has been derived as (Hwang and Shen 1989c)

$$\{\frac{\partial v_j}{\partial x_i}\} = \frac{\partial\{v_j\}}{\partial x_i} + \frac{\partial\langle 1-c\rangle}{\partial x_i}\frac{\{v_j\}}{\langle 1-c\rangle} + \frac{1}{\langle 1-c\rangle}\frac{\partial}{\partial x_i}(\langle c\rangle\{u_j\}) - \frac{\langle c\rangle}{\langle 1-c\rangle}\{\Omega^s_{ij}\} \qquad (34)$$

where $\{\Omega^s_{ij}\}$ is the spin tensor (or particle rotation) of the solid phase. In addition to the above two possible definitions for the phase strain-rate, a third strain-rate is also important. This is called the bulk (or mixture) strain-rate defined by

$$\begin{aligned} E_{ij} &= \langle 1-c\rangle\{e^f{}_{ij}\} + \langle c\rangle\{e^s{}_{ij}\} \\ &= \langle 1-c\rangle\{e^f{}_{ij}\} \end{aligned} \qquad (35)$$

where $e^f{}_{ij}$ and $e^s{}_{ij}$ are the local strain-rate for the fluid and solid phase respectively. In case of rigid particles, e^s_{ij}=0. In representing the effective viscous stress in a fluid-solid mixture, the above bulk strain-rate must be used.

In a pure fluid flow, such distinction shown in Eq. (34) or Eq. (35) does not exist. In a two-phase flow, this point becomes essential in many places. In fact, if one interprets the bulk viscous stress using $\partial\{v_j\}/\partial x_i$ instead of $\{\partial v_j/\partial x_i\}$, the coefficient of effective viscosity in Eq. (28), i.e. $\frac{5}{2}$, will become $\frac{3}{2}$ or $\frac{7}{2}$ depends on different interpretations of the mixture strain-rate.

Second, in Givler (1987), a phenomenon called anti-diffusion in the solid phase was mentioned. This term is believed to come from an inconsistent bookkeeping system of the surface and interaction forces in the control volume V. The equation given there for the solid phase was

$$\rho^s(\partial u_i/\partial t + u_j\frac{\partial u_i}{\partial x_j}) = \rho^s g_i + \frac{c}{V_0}h_i - c\frac{\partial p^p}{\partial x_i} - (p^p - p^f)\frac{\partial c}{\partial x_i} \qquad (36)$$

When the potential flow is considered, the $\partial c/\partial x_i$ term has a positive coefficient. This presents a force that moves the solid phase from a low concentration towards high concentration, which is a puzzling phenomenon. However, in the present derivation, it is shown that in the solid momentum equation such $\partial c/\partial x_i$ term does not exist. The

associated diffusive or anti-diffusive forces are thus absent. But, investigating the fluid momentum equation, we do observe such $\partial c/\partial x_i$ term. Through the mass conservation, any diffusion in the fluid phase results an effective anti-diffusion in the solid phase and vice versa. At this point, we have observed a totally opposite trend between Givler (1987) and the present model. Namely, Givler's model would predict a diffusion phenomenon for solid particles in the Stokes regime and anti-diffusion phenomenon in inviscid flow regime. The present model however predicts exactly the opposite. Further verification with detailed experimental data is desirable.

On top of the above, the anisotropy of the solid phase normal stress produced by fluid pressure is a new observation. This may produce interesting thermodynamic properties that are peculiar to a two-phase flow only.

It is natural to ask whether such a great care in deriving governing equations shown here is of importance. In order to see this, two models have been applied to a vertical pipe flow of a fluid-solid mixture (Hwang and Shen 1988). The two models are identical except the phase interaction term m_i. For case (A), m_i is modeled as shown in Eq. (7) with $\tilde{p} = p^p$ and case (B) is the present model given by Eq. (19). The resulting non-dimensional slip velocity $u^* - v^*$ verses the non-dimensional fluid pressure gradient $(\frac{dp}{dx})^*$ is reproduced in Fig. 3 for three different density ratios $\rho_s^* = \frac{\rho_s}{\rho_f}$. Qualitatively different results are obtained from these two models. From the behavior of the neutrally buoyant particles, it is believed that the present model is more reasonable.

V. CONCLUSION

For a two-phase flow, the interpretation of terms in the governing equations is the first step towards deriving constitutive relations using micromechanics. Therefore it has been surprising to us that the work presented here has not been available in the vast amount of two-phase flow literature. On the other hand, this may be explained by the fact that only

recently researchers have started to derive the constitutive relations from micromechanics. Hence the need for such derivation of governing equations is also very recent.

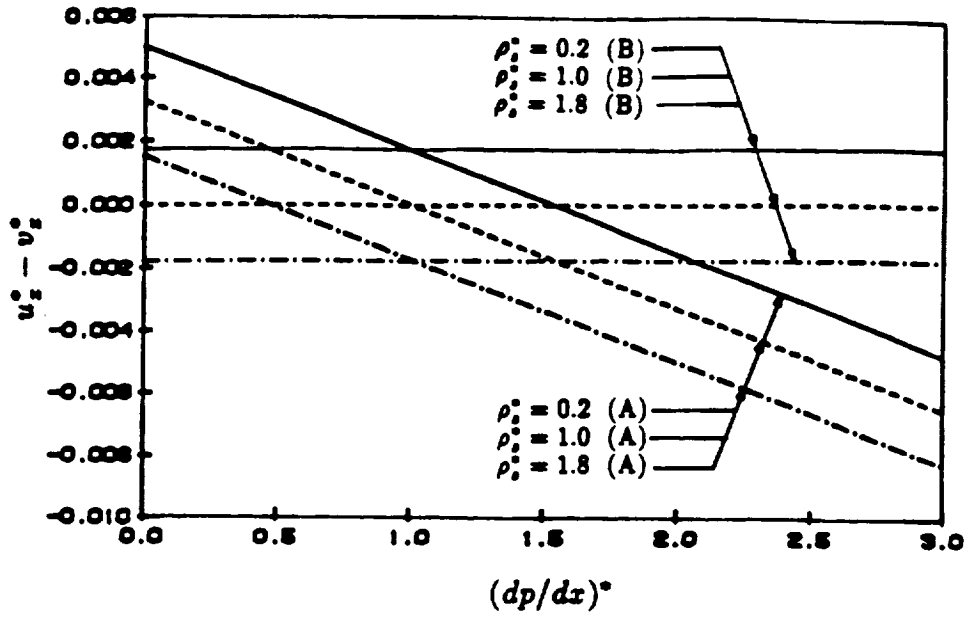

Fig. 3 Effects of ρ_s^* and $(dp/dx)^*$ on slip velocity from model A and model B.

It is shown in this work that the derivation of governing equations for flows of a fluid-solid mixture is not as straightforward as any single phase continuum. This derivation is done with a careful and almost tedious method to account for all transfer quantities between each phase. The resulting equations in terms of mass-weighted average quantities differ from the existing models.

These governing equations provide a foundation to incorporate micromechanics in deriving the constitutive relations. A number of previously well accepted facts about fluid-solid flows emerge naturally from this analysis. In addition, interesting phenomena such as: non-equality of average strain-rate and gradient of the average velocity, anti-diffusion, and anisotropic normal stress have been observed in these equations. Interpretation and

implications of these phenomena is of great interest.

REFERENCES

Abou-Arab, T. W. and Roco, M. C.,"Solid Phase Contribution in the Two-Phase Turbulence Kinetic Energy Equation", *Proc. 3rd Int. Symp. Liquid-Solid Flow*, Chicago, Nov. 28-Dec. 2, 1988, pp. 13–28.

Ackermann, N. L. and Shen, H. H., "Stresses in Rapidly Sheared Fluid-Solid Mixtures", *ASCE, J. Eng. Mech. Div.*, **108**, No. EM1, 1982, pp. 95–113.

Ahmadi, G. and Shahinpoor, M., "Towards a Turbulent Modeling of Rapid Flow of Granular Materials", *Powder Technology*, **35**, 1983, pp. 241–248.

Ahmadi, G., "On the Mechanics of Incompressible Multiphase Suspensions", *Adv. Water Resources*, **10**, 1987, pp. 32–43.

Babič, M., "Contact Stress Tensor in Granular Materials", Department of CEE, Report No. 89-1, Clarkson University, Potsdam, N.Y., 1989.

Bagnold, R. A., "Experiments of Gravity Free Dispersion of Large Solid Spheres in a Newtonian Fluid under Shear", *Proceedings of the Royal Society of London*, Series A, **225**, 1954, pp. 49–63.

Batchelor, G. K., *An Introduction to Fluid Dynamics*, Cambridge University Press, 1967.

Batchelor, G. K., "The Stress System in a Suspension of Force-Free Particles", *J. Fluid Mech.*, **41**, Part 3, 1970, pp. 545–570.

Campbell, C. S., "Rapid Granular Flow", *Annual Review of Fluid Mechanics*, **22**, 1990 (to be published).

Chao, B. T., "Turbulent Transport Behavior of Small Particles in Dilute Suspensions", *Ostereichisches Ingenieur-Archiv.*, **18**(122), 1964, pp. 7–21.

Chester, W. and Breach, D. R., "On the Flow Past a Sphere at Low Reynolds Number",

J. Fluid Mech., **37**, 1969, pp. 751– 760.

Drew, D. A., "Two-Phase Flows: Constitutive Equations for Lift and Brownian Motion and Some Basic Flows", *Arch. Rat. Mech. Anal.*, **62**, 1976, pp. 149–163.

Drew, D. A., "Mathematical Modeling of Two-Phase Flow", *Ann. Rev. Fluid Mech.*, **15**, 1983, pp. 261–291.

Einstein, A., *Investigations on the Theory of the Brownian Movement*, Dover Publications, Inc., New York, N.Y., 1956.

Givler, R. C., "An Interpretation for the Solid Phase Pressure in Slow, Fluid-Particle Flows", *Int. J. Multiphase Flow*, **13**(5), 1987, pp. 717–722.

Hwang, G. J. and Shen, H. H.,"A Consistent Formulation for the Phase Interaction in Flows of a Fluid-Solid Mixture", *Proc. 3rd Int. Symp. Liquid-Solid Flow*, Chicago, Nov. 28-Dec. 2, 1988, pp. 65–73.

Hwang, G. J. and Shen, H. H., "Modeling the Solid Phase Stress in a Fluid-Solid Mixture", *Int. J. Multiphase Flow*, 1989a, in print.

Hwang, G. J. and Shen, H. H., "Modeling Two-Phase Flows of a Fluid and Solid Mixture : Part (III) – Solid-Phase Pressure in a Rapid Flow", Department of CEE, Report in print, Clarkson University, Potsdam, N.Y., 1989b.

Hwang, G. J. and Shen, H. H., "Modeling Two-Phase Flows of a Fluid and Solid Mixture : Part (IV) – Energy Equations and Closure of the System", Department of CEE, Report in print, Clarkson University, Potsdam, N.Y., 1989c.

Ishii, M., "Thermo-Fluid Dynamic Theory of Two-Phase Flow", Eyrolles, Paris, Scientific and Medical Publication of France, N.Y., 1975.

Ishii, M., "One-Dimensional Drift-Flux Model and Constitutive Equations for Relative Motion between Phases in Various Two-Phase Flow Regimes", Argonne National Laboratory Report, ANL-77-47, Argonne, Illinois, 1977.

Jenkins, J. T. and Savage, S. B., "A Theory for the Rapid Flow of Identical, Smooth,

Nearly Elastic, Spherical Particles", *J. Fluid Mech.*, **130**, 1983, pp. 187–202.

Lamb, H., *Hydrodynamics*, 6th ed., Cambridge University Press, 1932.

McTigue, D. F., Givler, R. C., and Nunziato, J. W., "Rheological Effects of Nonuniform Particle Distributions in Dilute Suspensions",*J. of Rheology*, **30**, Issue 5, 1986, pp. 1053–1076.

Prosperetti, A. and Jones, A. V., "Pressure Forces in Disperse Two-phase Flows", *Int. J. Multiphase Flow*, **10**, 1984, pp. 426–440.

Shen, H. H., Hopkins, M. A., and Ackermann, N. L., "Modeling Collisional Stresses in A dense Fluid-Solid Mixture", *Journal of Fluids Engineering*, **110**, March 1988, pp. 85–90.

Soo, S. L., "Effects of Configuration of Phases on Dynamic Relations", *AIChe Symposium Series*, Heat Transfer - Milwaukee, No. 208, **77**, 1981, pp. 152–160.

Van Driest, E. R., "Turbulent Boundary Layer in Compressible Fluids", *J. Aeronaut. Sci.*, **18**, 1951, pp. 145–160.

Xie, D., "Turbulent Kinetic Energy of Particle Phase in Solid-Fluid Suspension Turbulence", *Proc. Int. Symp. Multiphase Flow-China*, 1987, pp. 396–401.

Zuber, N., "On the Dispersed Two-Phase Flow in the Laminar Flow Regime", *Chemical Engineering Science*, **19**, 1964, pp. 897–917.

STRESS IN DILUTE SUSPENSIONS

STEPHEN L. PASSMAN*

Abstract. Generally, two types of theory are used to describe the field equations for suspensions. The so-called "postulated" equations are based on the kinetic theory of mixtures, which logically ought to give reasonable equations for solutions. The basis for the use of such theory for suspensions is tenuous, though it at least gives a logical path for mathematical arguments. It has the disadvantage that it leads to a system of equations which is underdetermined, in a sense that can be made precise. On the other hand, the so-called "averaging" theory starts with a determined system, but the very process of averaging renders the resulting system underdetermined. I suggest yet a third type of theory. Here, the kinetic theory of gases is used to motivate continuum equations for the suspended particles. This entails an interpretation of the stress in the particles that is different from the usual one. Classical theory is used to describe the motion of the suspending medium. The result is a determined system for a dilute suspension. Extension of the theory to more concentrated systems is discussed.

1. Introduction. In theories of multiphase flows, it is natural to postulate or to derive equations of balance similar to those occurring in the theory of dilute mixtures of gases [1,2]. The usual process of doing so, along with reasonable assumptions for the constitutive properties of the materials composing the flow, always leads to a system with more unknowns than equations. Though there is no definitive reason that this is a bad situation, intuition abetted with proved theorems for special types of systems indicates that the normal desirable situation is the same number of equations as unknowns. The resulting quandary for multiphase flows is known as the "closure problem", and methods for "solving" or "closing" it, that is, finding "sufficient" additional equations, has been the focus of considerable research in multiphase flows. Here, we try to shed some light on such problems. Essential to doing so is stating the problems unequivocally. In order to do that, we choose a special but interesting physical situation, then give typical equations of balance and constitutive equations for that physical situation, according to a continuum theory and an averaging theory. The closure problem occurs in both types of theories, though its form is different. However, it is possible to formulate theories in which the closure problem does not occur, and therefore need not be solved. A physical basis for such a system is presented, and a putative set of field equations is suggested.

2. Determined, Underdetermined, and Overdetermined Systems of Equations. Assume we have a system of equations of the form

$$f_i(y_j, D_k y_j) = 0,$$

with $i = 1,\ldots,n$; $j = 1,\ldots,m$; and $k = 1,\ldots,p$. The f_i are n functions of the m variables y_j and their derivatives up to order p. The system is called *determined* if $n = m$,

*Pittsburgh Energy Technology Center, Pittsburgh PA 15236, on temporary assignment from Sandia National Laboratories, Albuquerque NM 87185.

overdetermined if $n > m$, and *underdetermined* if $n < m$. By our definition, all systems of equations are of one of these three types. Ideally, of course, it would be convenient if determined systems always had solutions and they were unique, if overdetermined systems never had solutions, and if underdetermined systems always had families of solutions. That this is not the case can be shown by examples. To begin, consider the underdetermined system

$$x_1^2 + x_2^2 = 0. \tag{1}$$

Naturally, specifying a system of equations is meaningless without specifying their domain, but since this paper is informal, I follow the convention of doing so tacitly, that is, all functions are mappings of all real variables for which they can be defined reasonably into a range defined by the function. Here, the underdetermined algebraic system (1) has the single unique solution

$$x_1 = 0, \quad x_2 = 0.$$

Now consider the determined system

$$\begin{aligned} x_1 + x_2 &= 1, \\ 2x_1 + 2x_2 &= 2. \end{aligned} \tag{2}$$

This system does not have a unique solution, rather it has an infinite one-parameter family of solutions. Finally, consider the overdetermined system

$$\begin{aligned} x_1 + x_2 &= 1, \\ 2x_1 + 2x_2 &= 2, \\ 2x_1 + 4x_2 &= 4. \end{aligned} \tag{3}$$

This system has a unique solution. All of the examples cited involve algebraic equations, not differential equations, but of course examples of the same type can be constructed with differential systems.

It is easy to object to the arguments above because the systems cited are "special" or "pathological". Indeed, I agree with that type of objection, and in a sense that is just the point of this discussion, for to make such arguments, one must use very special properties of the systems. Furthermore, for each system, it would have been possible to rearrange the system using simple manipulations, obtaining very complicated new systems with *exactly the same properties*. Proofs of existence or non-existence, uniqueness or non-uniqueness, then would be much more elaborate exercises, perhaps depending on sophisticated mathematics or luck for ultimate outcome.

A different line of argument is possible. Most often, the equations governing multiphase flow are systems of partial differential equations, so complicated that they are not

easily amenable to existence or uniqueness theorems. Such equations may be relevant to important problems in technology, so important that they must be solved, in no matter in how vague a sense, immediately. More often than not, that means the use of large computer codes. Despite the above examples, we find that an intrinsic part of building such codes is the desire of the numerical analyst for determined systems, that is, *systems determined in exactly the sense defined here.* The idea that the equations obtained by specialists in multiphase flow are "independent" is supported in some vague sense by the fact that they have different physical meanings. For example, some are balance equations for the constituents, some are constitutive equations, and some are constraints.

3. Continuum Theories of Multiphase Flows. Here, we consider a standard type of theory for multiphase flows, as derived from continuum considerations.[1] Intrinsic to such considerations is the assertion that each constituent fills all of a region of space. This is the basic assumption of theories of interpenetrating continua or "solutions" [4]. The theory then is made to model a multiphase medium by the inclusion of volume fractions ϕ_a as basic variables. A typical set of field equations for such a continuum having n constituents is

$$
\begin{aligned}
\Sigma_{a=1}^{n}\phi_a &= 1,\\
\dot{\phi}_a + \phi_a \operatorname{div}\mathbf{v}_a &= 0,\\
\rho_a\dot{\mathbf{v}}_a &= \rho_a\mathbf{b}_a + \mathbf{m}_a + \operatorname{div}\mathbf{T}_a,\\
\Sigma_{a=1}^{n}\mathbf{m}_a &= 0,\\
\{\mathbf{T}_a, \mathbf{m}_a\} &= g(\mathbf{v}_b, \phi_b, \text{ and their derivatives}).
\end{aligned}
\tag{4}
$$

Here for simplicity we consider only pure mechanics, and the symbols have the obvious meanings. The first equation expresses the fact that the material is saturated; the second and third are balances of mass and momentum for each of the constituents. Each constituent is assumed to be incompressible, and the p_a are the reactions to those constraints. The fourth equation is conservation of mass for the mixture, and the last equations express constitutive properties of the constituents, in particular the dependence of the stress on the deformation rate and other properties for each constituent, and appropriate expressions for interactions of the two materials. We note that these last expressions can be somewhat problematical, and in fact debate about their forms has generated a considerable literature. They are not discussed here. Rather, we assume they are known for applications of particular interest.[2] Our intuitive feeling from considering the physics of this situation is that such a system of equations is "complete", but in fact that is not the case. Here and henceforth, for the purpose of counting equations, we assume the multiphase flow consists of two constituents. Though such is not always the case, for the purpose of our arguments here, that case is general. The result is a system of 9 equations in the 10 unknowns

[1] Discussion of the basis of such theories, as well as references to the standard works, are given in [3].

[2] See [5] and [6] for a discussion of these equations.

$\{p_a, \phi_a, \mathbf{v}_a\}$, that is, the system is *underdetermined.* The usual physical motivation for this apparent quandary is plausible: Though Equations (4) express the exchange of momentum between constituents, that is not the only way the constituents interact, for *in addition*, there should be a force balance between the constituents. The most primitive visualization of this is sufficient for arguments here. That is, the solid phase is considered to consist of spherical particles of one size, surrounded by the fluid phase. Then a radial force balance on a single particle gives

$$p_s = p_f. \tag{5}$$

This obvious and elegant closure argument gives a system of equations which is notoriously ill-behaved [7,8], so much so that it must be rejected. More sophisticated arguments are possible, and they sometimes appear to suffice to render the system of equations thus obtained to be at least well-behaved enough to be handled by standard computational techniques. Usually, the arguments adduced are generalizations of those leading to Equation (5) in that they consider a particle in a flow field of a known type at infinity, then use techniques of hydrodynamics to solve or partially solve for the flow field around the spherical particle. Surface tension may be considered also. Of course the resulting pressure on the particle is a function of position on its surface relative to the flow field at infinity, so some sort of integration is required. The result is

$$p_s = p_f + f(\Pi, \sigma), \tag{6}$$

where Π denotes properties of the flow field, and σ denotes properties sufficient to characterize surface tension. I note that since f depends upon the flow field at infinity, adducing it as a constitutive relation valid for all flows has the potential for leading to inaccurate results.[3]

In addition to the mathematical argument against using Equation (5) as a closure relation, there is a physical argument against it, which also is inherited by Equation (6). In doing the arguments leading to these equations, the assumption is that p_s and p_f are pressures "in" the respective materials, and that it is appropriate to write an expression for one in terms of the other. The need for the closure relation comes from arguments about the system (4). In this system, the pressures are derived as reactions to constraints. Therefore [10], they are dependent variables of the system of equations, totally independent of one another. In treating the complete system of equations and boundary conditions.[4] the quantities p_s and p_f thus cannot be related *a priori.* Another way to see this is that in fact Equations (4) are field equations for the *whole continuum*, while the closure relation

[3] A similar difficulty arises in rheology, where it is commonly known [9] that no constitutive equation giving an accurate representation of the physics of shearing flows also represents stretching flows adequately.

[4] Boundary conditions in themselves constitute a difficult problem for multiphase flows. They are not discussed in this paper.

(6) is not. Rather, it is derived from a "micromechanical" argument, then scaled up in a way the nature of which never is made clear, so that the symbols p_s and p_f in Equations (6) are *assumed* to have the same meaning as the same symbols in the closure relation, without proof or explanation.[5]

4. Averaging Theory. The basic ideas behind averaging theories are diametrically opposite from that of the continuum theories, though the objective—finding differential equations for fields, valid throughout a body—is exactly the same. It is perhaps fortuitous, or perhaps a sign that the equations actually represent some sort of physical "truth", that the forms of the equations resulting from the two approaches are so similar. For averaging theories, the region of space occupied by the material is thought of as being occupied by two different types of body, the suspended particles and the suspending medium. Each of the types of body is considered to be distinct in the sense that the join [11] of the bodies constitutes all of the space occupied by the composite body, while the meet is empty. Then each of the types of body is an ordinary continuum, and satisfies exactly the balance and constitutive laws expected of an ordinary continuum, that is,

$$
\begin{aligned}
&\operatorname{div} \mathbf{v}_a = 0, \\
&\rho_a \dot{\mathbf{v}}_a = \rho_a \mathbf{b}_a + \operatorname{div} \mathbf{T}_a, \\
&\{\mathbf{T}_a\} = g(\mathbf{v}_b, \text{ and their derivatives}).
\end{aligned}
\tag{7}
$$

Here, of course, the bodies still are capable of momentum interaction, but unlike the previous situation, the micromechanical model for momentum interaction has a clear meaning. This is eight equations in eight unknowns, and thus is a determined system. Moreover, conditions for the difference of pressure such as Equation (6) now have a correct theoretical status, for now *they are not field equations, rather, they are boundary conditions.* Thus a determined system is obtained, and it is mathematically correct and physically plausible. The difficulty, of course, is that to formulate a boundary-value problem, a reasonable set of boundary and initial values for every particle in the system is needed. Such information normally is not available for any physical problem. Even if it were, finding a solution, with or without a computer as an intermediary, would be a nearly hopeless task. Moreover, even if such a solution were found, most of the information it contained would be of little use, because it would be too detailed. A plausible way to digest such data would be to average it in some sense. The usual approach in averaging theory is, not to go to the considerable trouble of averaging the solutions to (7), but rather to average (7) and then solve the averaged equations. Such an approach is highly appealing intellectually, but is fraught with mathematical difficulty. This paper is not the place to discuss such difficulties in detail. One, of course, is that the term "average" which has been used in a very vague

[5] Of course, the same argument can be made for the expressions in (4) for $\mathbf{m}_a$. There, however, the status of the equations is clear, because the appropriate micromechanical arguments can be used as *motivation* for the continuum theory, which then gives exact relations having the same status as field equations.

way here, must be given a precise meaning. It is fortuitous that, for most of the averaging methods tried so far, the resulting equations have almost the form of the Equations (4) derived from the continuum theory. Unfortunately, for every method of averaging I have seen, though a determined system is averaged, the result of the averaging process is an underdetermined system, that is, the averaging process makes the closure problem reappear. Most readers will be familiar with why this happens without going through the details, for the averaging process always is similar to that used in turbulence theory and some of the extra terms are of the same form as Reynolds stresses. In a broad sense, then, though the continuum theory and the averaging theory start from different places and proceed by different methods, they end in approximately the same place: underdetermined systems of approximately the same form.

5. Sketch of a Theory for Dilute Suspensions. Previously in this paper, much has been made of the fact that most of the equations in the continuum theory have been "postulated". It is possible to interpret that terminology as meaning that they have been made up with no mathematical or physical basis. In fact, that is far from true. The kinetic theory of dilute monatomic gases for identical gas molecules is well-known and is commonly taught in courses for graduate students in science and engineering [1,2,12]. Much less well known is the fact that there is a similar theory for gases where there are a finite number of different types of molecules; in other words, a solution of several gases [13,14]. The resulting balance equations are exactly identical to those for the postulated theory of mixtures.

Here, I use the motivation of the kinetic theory of gases to support a mixture theory in an entirely different way. Most important for the discussion here is the fact that there is an exact definition of the pressure, and it is not the pressure "in" the particles, rather it is a momentum flux — an entirely different concept.[6] Moreover, it is possible to force agreement of the theory with that of a viscous compressible gas, with the viscosity determined in terms of molecular parameters. I consider a dilute solution of particles in an inviscid fluid. Consider only the particles. They are an agglomeration of molecules, exactly like those in the theory of a monatomic gas, except that the scale of the molecules is somewhat larger than in a gas. Thus, precisely the same arguments can be used to motivate a continuum theory for the particle phase of the multiphase flow as is used for a gas. All of the expressions are the same, and *e.g.*, one can accept the viscosity of the particle phase as a phenomenological coefficient, or one can consider it to be determined from molecular quantities, according to one's taste. In either case, unlike in the theories discussed in the previous two sections of this paper, it does have meaning. The equations

[6] In another paper in this volume, O. Walton uses the same definition in his computer molecular dynamics simulations.

for the particle phase then are

$$
\begin{aligned}
\rho_s + \rho_s \operatorname{div} \mathbf{v}_s &= 0, \\
\rho_s \dot{\mathbf{v}}_s &= \rho_s \mathbf{b}_s + \mathbf{m} + \operatorname{div} \mathbf{T}_s, \\
p_s &= \hat{p}_s(\rho_s), \\
\mathbf{T}_s &= \hat{\mathbf{T}}_s(\operatorname{sym} \operatorname{grad} \mathbf{v}_s).
\end{aligned} \tag{8}
$$

This is a system of 5 equations in 5 unknowns, that is, a determined system. Now let the molecules be submerged in an incompressible fluid. Naturally, there will be an interaction between the particles and the fluid, and this interaction can be expressed as a constitutive equation for $\mathbf{m}$, which can be thought of as a part of the body force $\mathbf{b}_f$. Of course, the equations for the fluid phase are the expected ones,

$$
\begin{aligned}
\operatorname{div} \mathbf{v}_f &= 0, \\
\rho_f \dot{\mathbf{v}}_f &= \rho_f \mathbf{b}_f - \mathbf{m} + \operatorname{div} \mathbf{T}_f \\
\mathbf{T}_f &= \hat{\mathbf{T}}_f(\operatorname{sym} \operatorname{grad} \mathbf{v}_f).
\end{aligned} \tag{9}
$$

again, a determined system. Thus, for a theory of this type, no closure problem exists.[7]

Generally in a theory of this type, one expects to see volume fractions appear intrinsically. Since the ideas here are for a very dilute, saturated suspension, the concept is not very important, except, perhaps, in the constitutive equation for $\mathbf{m}$ and in formulas for the "effective viscosity" [5,12]. Of course the idea can be introduced formally by setting

$$\rho_f = \gamma_f \phi_f,$$

with γ_f a constant, and

$$\phi_f + \phi_s = 1.$$

These substitutions introduce the same number of equations as unknowns.

Acknowledgments. Donald Drew, David McTigue, Mehrdad Massoudi, and Kathleen Pericak-Spector have been kind enough to discuss the ideas presented here with me. The work was supported by the United States Department of Energy. I express my deep appreciation to the Institute for Mathematics and its Applications for inviting me to lecture on this subject, and for help in preparation of the manuscript.

[7] In another paper in this volume, J. T. Jenkins and D.F. McTigue present a similar set of ideas for a very concentrated suspension. The kinetic theory is worked out in considerable detail. D. F. McTigue also has presented a similar set of ideas in an unpublished lecture at the meeting of the American Geophysical Union held in December, 1988.

REFERENCES

[1] C. TRUESDELL AND R.G. MUNCASTER, *Fundamentals of Maxwell's Kinetic Theory of a Simple Monotomic Gas*, Academic Press, New York, 1980.

[2] W.G. VINCENTI AND C.H. KRUGER, JR., *Introduction to Physical Gas Dynamics*, Wiley, New York, 1965.

[3] STEPHEN L. PASSMAN, JACE W. NUNZIATO AND EDWARD K. WALSH, *A Theory of Multiphase Mixtures*, in *Appendix 5C of Rational Thermodynamics*, 2nd edition, Springer-Verlag, New York, 1984.

[4] RAY M. BOWEN, *Theory of Mixtures*, in *Continuum Physics*, Vol. III, edited by A.C. Eringen, Academic Press, New York, 1976.

[5] DAVID F. MCTIGUE, RICHARD C. GIVLER AND JACE W. NUNZIATO, *Rheological effects of nonuniform particle distributions in dilute suspensions*, Journal of Rheology, 30, 5 (1986), pp. 1053–1076.

[6] STEPHEN L. PASSMAN, *Forces on the Solid Constituent in a Multiphase Flow*, Journal of Rheology, 30, 5 (1986), pp. 1077–1083.

[7] J. D. RAMSHAW AND J. A. TRAPP, *Characteristics, stability, and short wavelength phenomena in two-phase flow equation systems*, Nuclear Science and Engineering 66 (1978), pp. 93–102.

[8] C. PAUCHON AND S. BANNERJEE, *Interphase momentum interaction effects in the averaged multifield model, Part I: Void propagation in bubbly flows*, International Journal of Multiphase Flow, 12 (1986), pp. 555–573.

[9] C.J.S. PETRIE, *Elongational Flows*, Pitman, London, 1979.

[10] C. TRUESDELL AND W. NOLL, *The Non-Linear Field Theories of Mechanics, Handbuch der Physik III/3*, Springer-Verlag, 1965. A modern discussion is given in P. Podio-Guidugli and M. Gurtin, *The Thermodynamics of Constrained Materials*, Archive for Rational Mechanics and Analysis, 51, (1973), pp. 192–208.

[11] C. TRUESDELL, *A First Course in Rational Continuum Mechanics, Volume 1*, Academic Press, New York, 1977.

[12] J.O. HIRSCHFELDER, C. F. CURTISS AND R. BYRON BIRD, *Molecular Theory of Gases and Liquids*, Wiley, 1954.

[13] J. C. MAXWELL, *On the Dynamical Theory of Gases*, Philosophical Transactions of the Royal Society, London, 157 (1867), pp. 49–88.

[14] C. TRUESDELL, *Sulle Basi di Termomeccanica*, Accademia Nazionale dei Lincei, Rendiconti della Classe di Scienze Fisiche, Mathematiche e Naturali, Series 8, 22 (1957), pp. 33–38, 158–166; (An English translation by the author appears as *On the Foundations of Mechanics and Energetics, Continuum Mechanics II*, Gordon & Breach, New York, 1965, 292–305.

THEORY OF DROPLET: I
RENORMALIZED LAWS OF DROPLET VAPORIZATION IN NON-DILUTE SPRAYS

H.H. CHIU
Department of Mechanical Engineering
The University of Illinois at Chicago
Chicago, Illinois 60680

ABSTRACT

The vaporization of a droplet, interacting with its neighbors in a non-dilute spray environment is examined as well as a vaporization scaling law established on the basis of a recently developed theory of renormalized droplet.[1] The interacting droplet consists of a centrally located droplet and its vapor bubble which is surrounded by a cloud of droplets. The distribution of the droplets and the size of cloud are characterized by a pair-distribution function. The vaporization of a droplet is retarded by the collective thermal quenching, vapor concentration accumulated in outer sphere, and by the limited percolative passages for mass, momentum and energy fluxes. The retardation is scaled by the local collective interaction parameters; group combustion number of renormalized droplet, droplet spacing, renormalization number and the local ambient conditions. The numerical results of a selected case study reveal that the vaporization correction factor falls from unity monotonically as the group combustion number increases, and saturation is likely to occur when the group combustion number reaches 35-40 with interdroplet spacing of 7.5 diameters and the environment temperature of 500 K. The scaling law suggests that dense sprays can be classified into: (1) a "Diffusively Dense" cloud characterized by uniform thermal quenching in the cloud, (2) a "Stratified Dense" cloud characterized by a radial stratification in temperature by the

differential thermal quenching of the cloud, or (3) a "Sharply Dense" cloud marked by fine structure in the quasi-droplet cloud and the corresponding variation in the correction factor due to the variation in the topological structure of the cloud characterized by pair-distribution function of quasi-droplets.

NOMENCLATURE

D	Mass diffusion coefficient
g	Pair - distribution function
G	Group combustion number
L	Latent Heat of vaporization
$\dot{m}$	Vaporization rate
n	Number density
q	Heat of combustion
r	Radial coordinate
R	Radius
s	Droplet separation
T	Temperature
υ	Velocity
W	Molecular weight
α	Schvab-Zeldovich Variable
β	Renormalization number η_{ts}/η_{co}
γ_F	L/q
ε_F	$-(W_F\nu_F)^{-1}$
θ	$r_\ell(\eta)/r_\ell(o)$
ν	Stoichiometric coefficient
η	r/r_ℓ
ρ	Density

Subscript

c	Canonical bubble
co	Canonical bubble of test droplet
F	Fuel
T	Temperature
ℓ	Liquid drop surface
ts	Transition sphere surface

1. Introduction

Increasing theoretical findings [1-13] and experimental evidence [14-18] attest the widely held belief that the short-range collective interaction [2-6, 11-13] among the neighboring droplets and the long-range interaction [1, 7, 9, 10] with the droplets at distance, on a hydrodynamic scale, have profound impact on the state of a droplet, i.e. the states of saturation, vaporization, ignition, combustion and extinction, as well as the droplet interfacial process rates in non-dilute cloud or spray environments. These collective interactions, produced by local hydrodynamic and transport processes in a complex topological environment, serve to control the percolative passage for dispersing mass, momentum energy fluxes and the effective interfacial area for the property exchange processes. These interactions result in the collective thermal quenching, the accumulation of vaporizing species and the tendency for stagnating the microscale local Stefan flow and mean flow through dynamic equilibration between the two phases.

Review of the current theories of collective interactions including: Group Vaporization and Combustion [1, 7, 10] (GVC), Discrete Droplet Model (DDM) [2, 3, 5] and Droplet In Bubble (DIB) [4, 8] reveals two major theoretical deficiencies in the theory of short-range interaction and droplet rate processes at this juncture. These are: (1) the lack of the fundamental concepts and the mechanisms interlinking small scale discrete droplet processes with a large scale quasi-continuum flow of a non-dilute cloud or a spray, and (2) the incomplete understanding of complex interfacial processes, finite rate reaction, turbulence and transport processes that occur in the vicinity of each droplet. The first issue compels the current research of non-dilute sprays to proceed with two rival approaches; GVC, that primarily

deals with the long-range interaction, thus neglecting small scale resolution, and DDM, which focuses attention on the detailed behavior of discrete droplets in well-ordered droplet assemblies, thereby requiring a laborious computational procedure involving a large number of droplets encountered in practical sprays.

The alternative approach, adopting a continuous spray model supplemented by realistic droplet laws, appears the compromised mean of the prediction of non-dilute spray. A recent study of Tishkoff [4] on the numerically correlated vaporization correction factor derived from the DIB model demonstrates the viability of such combined approach to complement modern non-dilute spray calculations formulated on either Eulerian-Eulerian or Eulerian-Lagrangian framework. It must be mentioned, however, that an attempt to deduce an improved droplet vaporization law from the results of existing DDM met with difficulties due to the geniune lack of a self-consistent criterion of "droplet environment" whereupon the gas properties such as the temperature and concentration of vapor species, are inserted in the droplet law for the determination of the vaporization rates. A universal theory of short-range interaction and a set of comprehensive laws of droplet rate processes remain as the major unsolved issues in the contemporary theory of non-dilute sprays which has been the central theme of research [12, 13] conducted. The objectives of this paper are to present the basic concepts, theoretical approaches and the results of Renormalized Droplet (RND) theory to establish vaporization laws for droplets in a stationary non-dilute cloud environment.

The paper begins with the descriptions of droplet models and theories, in section 2, to clarify basic concepts and definitions of "droplet," adopted in modern spray theory. The structure, model and mathematical analysis of RND

are described in Section 3. The results of numerically predicted RND structure, vaporization correction factor and their dependence on collective interactive parameters are presented in Section 4.

2. Droplet Models: Topological Properties and Modeling

2.1 Elemental Model

Three fundamental topological properties that play basic roles in interaction phenomena between the droplet under investigation, termed the "test droplet", and its neighbors, i.e. "field droplets," are; (1) "graininess" or "discreteness" of a droplet, (2) "covolume" or "evacuated volume" of a droplet, and (3) "localization" of a droplet relative to a reference point. Basic droplet models which attempt to capture properties of the droplet to a desired level of accuracy, are classified into three types according to the level of sophistication in the characterization of the topological features, as summarized in Table 1. First, the "natural droplet model" which characterizes a droplet by its true geometrical shape, size and location, simulates all the topological properties described above.

Table 1
Droplet Models

Droplet Properties	Natural Drop Model	Quasi-Droplet Model		
		Non-Uniformly Smeared Drop	Uniformly Sheared Drop	Point Source Model
Graininess	Sharp*	Diffuse**	No	Singular
Covolume	Sharp	No	No	No
Localization	Sharp	Diffuse	No	Singular

*Sharp properties caused by phase discontinuity
**Diffuse properties featured by the absence of phase discontinuity

The natural droplet model provides a sharp droplet configuration required for the predictions of microscale flow structure, and results from a combination of convective and Stefan flows, and interfacial process rates of the test droplet. The solution is given by solving Dirichelt boundary value problems associated with conservation equations and a well defined set of physical boundaries formed by the interface of droplets.

The second type of model, i.e. "quasi-smeared droplet," describes a droplet by a medium spreading through the space. The droplet thus coexists with the host medium without apparent phase discontinuity. The models in this category are further divided into "uniformly" and "non-uniformly" smeared droplets, Fig. 1. In the latter model, the location and spatial extension of droplets are depicted by a joint probability distribution function. The "graininess" and "localization" of droplets are therefore partially characterized by the joint probability function rather than the phase discontinuities as in the case of the natural drop model.

"The uniformly smeared droplet model" which has been adopted in the majority of two-phase flow and spray theories is a special case with a uniform distribution of the joint probability with its numerical value equals to unity throughout the space. In this model, "graininess" and "localization," are

absent. Because of the lack of the basic topological properties, these quasi-droplet models are unable to be used for the determination of the droplet bound flow field and droplet laws. However, when appropriate droplet laws are provided to describe the interfacial processes rates, the flow structure of a farfield can be predicted with an acceptable accuracy by a quasi-two phase approach that is simpler than the Dirichelt boundary value problems.

The third model is a "point source model" which uses a mathematical singularity to characterize the "location" and a "singular graininess" of a droplet in a dilute spray with a large spacing, i.e., the ratio of spacing to the droplet size is much greater than unity. Like a "quasi-droplet model", the "point source model" fails to provide a satisfactory near-field structure required for the prediction of the rates of interfacial processes, but the model offers a simple mathematical theory for the prediction of far field solutions.

2.1.2 Composite Model

Although a specific elemental model has been frequently used in the analysis of single droplet, or many-droplet problems (e.g. natural droplet model in DDM and DIB, uniformly smeared droplet in GVC), the potential advantages of the simultaneous use of two or more than two elemental models has not been fully exploited.

A composite modeling technique permits a strategic selection of a desired elemental model in a certain selected region and an alternative model in another region to enhance the modeling flexibility and the simplicity in analysis. The choice of an elemental model is determined by the type of the flow field data and accuracy required in each region. For example in RND

theory, the test droplet is modeled by a "natural droplet model" to facilitate the determination of the near flow field, which depends on the detailed geometry of the test droplet, and the flow disturbance created by the neighboring field droplets. On the other hand, "field droplets" are modeled by "non-uniformly smeared droplet" which are distributed in the neighborhood of the test droplet. The distribution of these quasi-droplets is described by a joint probability function to simulate localization and graininess of the quasi-droplets. This composite model provides a simple, self-consistent and useful analytical method of treating the interfacial phenomena of a test droplet interacting with its neighbors. The details of the application of composite model in RND is described in the remaining part of this section and the next section.

2.2 Theories of Droplet: Canonical and Renormalized Representation of a Droplet Under Short Range Interaction.

"The Theory of Droplet" concerns itself with interfacial phenomena and the process rates of a test droplet in isolation or under the influence of the collective interaction of field droplets. A representative analytical approach for the former is the single droplet theory, and for the latter case, the approaches are DIB and RND models. Since the latter problem concerns collective interaction between a test droplet and field droplets, the nature of the problems and the theoretical procedures are, in general, similar to that of "many droplet problems". However, an important distinction between the two theories is that the "droplet theory" aims to establish the rate of an interfacial process of a test droplet on the framework of "the minimum-sized many-droplet system" that includes the smallest number, N_{min}, of droplets

i.e., a test droplet and N_{min}-1 field droplets confined in, "the minimum sized region", i.e. R_{min} region. The requirements of "the minimum number of droplets" in "the minimum region" are imposed in RND theory so that the droplet laws, deduced from such a minimum droplet system, can be explicitly formulated in terms of the self-consistently defined "local properties" of a spray flow field. This basic feature of "local representation," is essential in modern spray calculations that use local droplet laws. In contrast to the theory of renormalized droplet, the "cluster" model[8,11] treats a droplet system with an arbitrary number of droplets in a finite region. Thus, the model is appropriate for dealing with a partial or complete domain of a spray by an approach that is different from the conventional spray theory.

2.2.1 Canonical Droplet Theory[4]: CDT

The DIB[4] which consists of a natural droplet and its Wigner-Seitz bubble, has two fundamental properties. Firstly, a high degree of symmetry preserved in the DIB's periodical droplet assembly inhibits the transports of mass, momentum and energy transports among the neighbor droplets. Thus, DIB portrays a thermo-chemically closed adiabatic system with respect to neighbor droplets. Secondly, the strength of the interaction between the droplet and its bubble is determined by the size of the bubble which has the radius equals to half of the droplet spacing. When the droplet separation becomes infinitely large, the predicted vaporization rate approaches to that of an isolated droplet, as expected.

Because of these two unique features of the DIB which may be regarded as a reference model of a short-range interaction, the theory will be termed "canonical droplet theory" (CDT). The theory provides a basis of RND model described in the following subsection.

2.2.2 Renormalized Droplet Theory

Since the canonical theory treats the interfacial processes of a droplet in a hypothetical, well ordered droplet lattice, the validity of the canonical droplet law is questionable when applied to practical sprays with disordered droplet distributions. Needless to say, the adiabaticity and closure of the test droplet relative to its neighbor also break down in practical sprays. Another theoretical deficiency of DIB is the lack of the geometrical compatibility of the "environment" with that of droplet environment in spray theory. In CDT, the edge of a bubble has been adopted as the environment, though such choice is not necessarily the unique alternative, and the gas temperature or species concentration is used for the determination of the vaporization rate and droplet transient heating rate. However, in a spray calculation, the local average gas phase temperature of multi-phase flow is used for the determination of droplet process rates. Clearly, the environment of a canonical droplet does not coincide with that of a spray. Such incompatibility prohibits the encoding of the droplet law, derived by DIB, into a spray calculation unless an explicit link between two environmental properties, i.e., DIB vs smeared droplet model adopted in a conventional multi-phase continuum spray is provided.

The RND theory provides a rigorous theoretical procedure that removes the major shortcomings of the canonical theory and provides encodable droplet laws by the applications of (1) composite droplet modeling technique and (2) the minimum sized many-droplet system, as described in the following section.

3. Renormalized Droplet (RND)

3.1 Structure of Model

The theory of renormalization[12] portrays a test droplet interacting with its neighboring field droplets by a composite "dressed or clothed" droplet model shown in Fig. 2. Two principal structural elements of RND are (1) a Droplet-In-Bubble (DIB) and (2) a cloud of non-uniformly smeared droplets which functions as an external clothing for the DIB. The distribution of the quasi-droplet is described by the pair-distribution function representing the joint probabiltiy of finding a test droplet and its neighbor at a separation s. The pair-distribution function vanishes in the immediate vincinity of the bubble, representing the evacuated volume effect of droplets, and then increases rather rapidly to a value greater than unity at the radial distance comparable to a mean droplet spacing. This first high droplet density region populated by the nearest neighbor droplets is termed the "first coordination shell." The population peaks of the "second and higher order coordination shells" lose their sharpness as they merge with one another and are ultimately lost in a continuous environment where the pair distribution function approaches to unity. The size of the transition sphere, R_{ts}, defined as the radial location where the pair distribution function is 0.99, depends on the droplet size, spacing and arrangement. The ratio of the size of the transition sphere, R_{ts}, to the characteristic hydrodynamic scale, L, is typically much smaller than unity, and thus the sphere degenerates into a point in the limit when R_{ts}/L vanishes. Accordingly, the average properties of the gas over the transition sphere approach to the local properties of the continuum flow as the limit R_{ts}/L goes to zero. This "correspondence hypothesis" and the interlinking transition sphere constitute the two key

factors for the determination of the droplet process rate by the local gas properties of the continuum flow field. In the present analysis, RND is assumed to be spherically symmetric, and non-reacting. Transport properties are constant and the Lewis number is unity.

The criterion of a quasi-steady state is a much more complex issue than that of a single droplet because of the multi-scale and multi-time phenomena linked with mass and energy transport in typical RND. In general, the quasi-steady state assumption is valid when (1) the largest characteristic diffusion and conduction times associated with the transition sphere is much smaller than the life time of any droplet in the cloud, (2) no droplet in the transition sphere is in the state of transient heating, and (3) no gas phase region is experiencing an initial or a terminal transient process. The effects of transient processes, and the validity or the limitation of the quasi-steady theory in a practical spray are discussed in Section 5. Detailed time-dependent analysis of transient processes in RND, which will be presented as Part II in the future, reveal that RND is found in some dense sprays to exhibit only a brief or finite period of quasi-equilibrium state. Additionally, RND exhibits dynamic saturation in time scales comparable to the characteristic diffusion time in the canonical bubble when the local group combustion number exceeds a critical value.

3.2 Mathematical Analysis

Non-dimensional equations governing RND are formulated separately for the inner DIB region and an external quasi-droplet cloud, respectively, as follows.

$$\frac{1}{\eta^2}\frac{d}{d\eta}\left(\eta^2\frac{d\psi_i}{d\eta}\right) = 0 \qquad 1 \leq \eta \leq \eta_{co} \tag{1}$$

and

$$\frac{1}{\eta^2}\frac{d}{d\eta}\left(\eta^2\frac{d\hat{\psi}_i}{d\eta}\right) = G_s g\mu\hat{B}_i \qquad \eta_{co} \leq \eta \leq \eta_{ts} \tag{2}$$

with

$$\psi_m = \rho v \tag{3}$$

$$\begin{pmatrix}\psi_F\\ \psi_T\end{pmatrix} = \psi_m\begin{pmatrix}\alpha_F\\ \alpha_T\end{pmatrix} - \sigma\frac{d}{d\eta}\begin{pmatrix}\alpha_F\\ \alpha_T\end{pmatrix} \tag{4}$$

where $\eta = r/r_\ell(0)$, ρ and v are non-dimensionalized by the gas density, and velocity on the droplet surface, respectively, $Gs = 4\pi n r_{\ell o}^3$, g is a pair distribution function, μ is the vaporization shape factor defined by (12), ψ_i are the fluxes of various properties; mass for i = m, fuel vapor for i=F and thermal energy for i=T, and ^ refers to the properties pertaining to an outer region. The definitions of properties α_i and constants B_i are summarized in Table 2.

Table 2
Schvab-Zeldovichs Variables and Constants

i	α_i	$\hat{\alpha}_i$	$\hat{B}_i$
M	$-(y_f/W_F\nu_F)$	$\int_F^T/W_F\nu_F)$	$\varepsilon_F = -(W_F\nu_F)^{-1}$
T	$\int_{T_b}^{T} C_p dT/q$	$\int_{T_b}^{T}\hat{C}_p\hat{T}dT/q$	$\gamma_F = L/q$

The system of Eqs. (1)-(4) is integrated by a repeated quadrature. The constants of integration are determined from the conditions of the

impermeability of the gaseous species on the droplet surface and the balance of the heat conducted to the droplet with the latent heat of the vaporization. The integration gives the following vaporization laws

$$\dot{m}(0) = \frac{4\pi\rho D r_{\ell}(o) \ \ell n \ (1 + \frac{\alpha_{Tco}}{\gamma_F})}{1 - \zeta_{co}} \tag{5}$$

or

$$\dot{m}(o) = \frac{r\pi\rho D r_{\ell}(o) \ \ell n \ (1 + \frac{\alpha_{Fco} - \alpha_{F\ell}}{\alpha_{F\ell} - \varepsilon_F})}{1 - \zeta_{co}} \tag{6}$$

where

$$\zeta_{co} = \eta_{co}^{-1}$$

These laws, which agree with those obtained by Tishkoff[4], are valid for any value of ζ_{co}, provided the bubble contains no droplet other than the test droplet. This standard law will be termed "canonical vaporization law," the spherical bubble surface will be identified by "canonical environment" and the bubble temperature by "canonical temperature." In contrast to what is described above, an alternative law in which the vaporization rate is determined by the gas temperature on the surface of the transition sphere (see Fig. 2) will be called "renormalized vaporization law," the surface of transition sphere is "renormalized environment" and temperature on the surface is the "renormalized temperature" which is numerically equal to the local gas temperature of the continuum flow field.

Renormalized Droplet Law

Since the continuum theory of sprays predicts the local gas temperature but not the canonical temperature, the canonical vaporization laws (5) and (6) cannot be used in spray calculation as previously described. The alternative proposed in this paper is to use a renormalized vaporization law. The renormalized law is described in this subsection. By adopting a mathematical procedure involving appropriate linear combinations of Eq. (2) governing ψ_m, ψ_F and ψ_T, one obtains two homogeneous equations governing $\hat{\alpha}_T + \gamma_F$ and $\hat{\alpha}_F - \varepsilon_F$. These two equations are integrated and joined with the inner solutions on the surface of the canonical bubble. The resulting solutions are given by

$$\frac{\hat{\alpha}_T + \gamma_F}{\hat{\alpha}_{Tts} + \gamma_F} = \frac{\hat{\alpha}_F - \varepsilon_F}{\hat{\alpha}_{Fts} - \varepsilon_F}$$

$$= \exp\left\{ -\frac{1}{\sigma} \int_{\eta}^{\eta_{ts}} \frac{1}{\eta_2'} \left(1 + G_s \int_{\eta_{co}}^{\xi^2} g\mu\xi^2 d\xi\right) d\eta' \right\} \tag{7}$$

In order to obtain the renormalization laws, one first determines $\hat{\alpha}_{Tco}$ and $\hat{\alpha}_{Fco}$ by replacing the η appearing in the lower limit of the integration of Eq. (7) by η_{co}. Subsequently, by substituting the resulting expressions of $\hat{\alpha}_{Tco}$ and $\hat{\alpha}_{Fco}$ in Eq. (5) and (6) one arrives at the following renormalized vaporization laws:

$$\dot{m}(o) = 4\pi\rho D r_\ell(o) C_v \ln\left(1 + \frac{\hat{\alpha}_{Tts}}{\gamma_F}\right) \tag{8}$$

$$\dot{m}(o) = 4\pi\rho D r_\ell(o) C_v \ln\left(1 + \frac{\hat{\alpha}_{Fts} - \hat{\alpha}_{F\ell}}{\hat{\alpha}_{F\ell} - \varepsilon_F}\right) \tag{9}$$

where C_v is the vaporization correction factor calculated as follows

$$C_v = [\ 1 - \zeta_{ts} + G_s \int_{\eta_{co}}^{\eta_{ts}} \int_{\eta_{co}}^{\eta} K(\eta|\xi)\mu(\xi)d\xi d\eta]^{-1} \tag{10}$$

in which

$$K(\eta|\xi) = \eta^{-2}\ \xi^2 g(\xi) \tag{11}$$

$$\mu = \frac{\dot{m}(\eta)}{\dot{m}(o)} = \frac{4\pi\rho D r_\ell \ell n[1+\frac{\hat{\alpha}_{Tc}(\eta)}{\gamma_F}]}{\dot{m}(o)\ [1-\zeta_c\ (\eta)]} \tag{12}$$

where $\alpha_{F\ell}$ is given by

$$\alpha_{F\ell} = \frac{\hat{\alpha}_{Fts} + \hat{\alpha}_{Tts} + \varepsilon_F}{\hat{\alpha}_{Tts} + \gamma_F} \tag{13}$$

The vaporization laws (8) and (9) remain incomplete until the distribution of μ is provided. The determination of μ requires the knowledge of the canonical temperature $\hat{\alpha}_{Tc}(\eta)$ of a quasi-droplet located at η, see Eq. (12). A theoretical procedure of the determination of $\hat{\alpha}_{Tc}(\eta)$ in terms of the local gas phase temperature, $\hat{\alpha}_T(\eta)$, is described in the following.

Mean Canonical Bubble Temperature of a Field Droplet

In the analytical estimate of a mean canonical temperature one assumes that each field droplet in the transition sphere of RND has a canonical structure, i.e., the temperature and concentration profiles are those given by

canonical model. Consider a canonical field droplet located at the field point, η , measured from the center of the test droplet. Let y be the radial location of an arbitrary point within the bubble of the field droplet measured from the center of the field droplet. Then, according to the result of the DIB model, the temperature distribution in the bubble of the canonical field droplet is given by

$$\alpha_T(\eta,y) = \gamma_F \{\exp[\frac{1}{\sigma(\eta)}(1 - \frac{1}{y})-1]\} \tag{14}$$

where

$$\sigma = 4 \pi \rho D r_\ell(\eta)$$

Additionally, the canonical temperature, $\hat{\alpha}_{Tc}(\eta)$ is obtained by replacing y in Eq. (14) by y_c; i.e., the radius of the bubble. The result is

$$\hat{\alpha}_{Tc(\eta)} \equiv \alpha_T(\eta,y_c) = \gamma_F\{\exp[\frac{1}{\sigma(\eta)}(1 - \frac{1}{y_c})] - 1\} \tag{15}$$

Since the local gas temperature $\hat{\alpha}_T(\eta)$ equals to the volume averaged mean gas temperature in the bubble of a field droplet, one writes

$$\hat{\alpha}_T(\eta) \equiv \frac{1}{V_c} \int_1^{y_c} \alpha_T(\eta,y) y \, dy \tag{16}$$

where V_c is the non-dimensional volume of the bubble given by

$$V_c = \frac{1}{3}(y_c^3 - 1)$$

In order to express $\hat{\alpha}_{Tc}(\eta)$ in terms of $\hat{\alpha}_T(\eta)$, one inroduces the correlation function λ as

$$\lambda(\eta, y_c) = \alpha_{Tc}(\eta, y_c)/\hat{\alpha}_T(\eta) \tag{17}$$

By comparing Eqs. (16) and (17), one identifies $\lambda(\eta, y_c)$ as follows

$$\lambda(\eta, y_c) = \frac{\{\exp[\frac{1}{\sigma(\eta)}(1-\frac{1}{y})-1]-1\} \quad (y_c^3 - 1)}{3\int_1^{yc}\{\exp[\frac{1}{\sigma(\eta)}(1-\frac{1}{y})] - 1\}\, y^2 dy} \tag{18}$$

Thus, the non-dimensional vaporization rate, μ, of a field droplet is given by

$$\mu = \frac{\dot{m}(\eta)}{\dot{m}(o)} = \frac{4\pi\rho Dr_\ell}{\dot{m}(o)} \quad \frac{\ln\left(1+\frac{\lambda\hat{\alpha}_T}{\gamma_F}\right)}{1-\zeta_c(\eta)} \tag{19}$$

where $\zeta_c(\eta) = \zeta_{co}\theta(\eta)g(\eta)^{1/3}$ (20)

By substituting (19) into Eq. (2), for $\hat{\psi}_i = \hat{\psi}_T$, one obtains the following equation.

$$\frac{d^2\phi}{d\eta^2} + \frac{2}{\eta}\frac{d\phi}{d\eta} - G_s\,\theta g\,\frac{\ell n[1-\lambda+\lambda e^{\phi}]}{1-\zeta_c(\eta)} = 0 \tag{21}$$

where

$$\phi = \frac{d\hat{\psi}_m}{d\eta} = \ell n \ (1+ \frac{\hat{\alpha}_T(\eta)}{\gamma_F}) \qquad (22)$$

In the ensuing analysis, λ will be assumed to be unity. This corresponds to droplet vaporization with a high transfer number. The general case, $\lambda \neq 1$, can be solved by an iterative analysis with a guessed value of $\sigma(\eta)$ to calculate approximate ϕ from Eq. (21). The iteration will continue until the vaporization rate prediced from the iterative solution converages to the guessed value of σ. It is expected that the temperature rise in the radial direction is faster when $\lambda>1$. Details of the general case will be reported in the future.

The last step required for determining μ which appears in the scaling law is to determine ϕ as a function of η. With $\lambda=1$, one can show that the expression for ϕ which satisfies $\phi=\phi_{co}$ at $\eta = \eta_{co}$ and $\phi=\phi_{ts}$ at $\eta=\eta_{ts}$ is given by a linear combination of two homogeneous solutions W_1 and W_2, that satisfy the canonical boundary conditions; $W_1(\eta_{co})=1$, $\frac{dw_1}{d\eta}(\eta_{co})=0$ and $\frac{dW_2}{d\eta}(\eta_{co}) = 1$,

$$\phi(\eta) = \phi_{co}\{W_1(\eta) + [\frac{\phi_{ts}}{\phi_{co}} - W_1(\eta_{ts})] \frac{W_2(\eta)}{W_2(\eta_{ts})}\} \qquad (23)$$

where ϕ_{co}, the characteristic value, is determined in terms of ϕ_{ts} as follows.

By equating the vaporization rate in the canonical form (5) and renormalized form (3) and by using the definition of ϕ given by Eq. (22), one obtains

$$\dot{m}(o) = \frac{4\pi\rho Dr_\ell(o)}{1-\zeta_{co}} \phi_{co} = \frac{4\pi\rho Dr_\ell(o) \quad \phi_{ts}}{1-\zeta_{ts} + G_s \int_{\eta_{co}}^{\eta_{ts}} \int_{\eta_{co}}^{\eta} K(\eta|\xi)\mu(\xi)d\xi d\eta} \qquad (24)$$

where $\mu(\xi) = \theta(\xi) \frac{1-\zeta_{co}}{1-\zeta_{c\eta}} \frac{\phi(\xi)}{\phi_{co}}$ (25)

and

$$\theta(\xi) = r_{\ell}(\xi)/r_{\ell o} \tag{26}$$

On substituting the expression of $\phi(\eta)$ given by Eq. (23) into RHS of Eq. (25) and by inserting the resulting expression in the μ-term appears in the denominator of the Eq. (24), one obtains

$$\frac{\phi_{co}}{\phi_{ts}} = \frac{\Omega_{co}}{\Omega_{ts}} = \Lambda(G_s, \eta_{co}, \eta_{ts}) \tag{27}$$

where

$$\Lambda = \frac{1-\zeta_{ts} - G_s \int_{\eta_{co}}^{\eta_{ts}} \int_{\eta_{co}}^{\eta} K(\eta|\xi)\theta(\xi)\frac{1-\zeta_{co}}{1-\zeta_{(\xi)}} \frac{W_2(\xi)}{W_2(\eta_{ts})} d\xi d\eta}{1-\zeta_{ts} + G_s \int_{\eta_{co}}^{\eta_{ts}} \int_{\eta_{co}}^{\eta} K(\eta|\xi)\theta(\xi)\frac{1-\zeta_{co}}{1-\zeta(\xi)} [W_1(\xi) - \frac{W_1(\eta_{ts})}{W_2(\eta_{ts})} W_2(\xi)] d\xi d\eta} \tag{28}$$

Finally, the scaling factor Eq. (10) can be expressed in terms of W_1 and W_2 as follows

$$c_v = \left\{1 - \zeta_{ts} + G_s \int_{\eta_{co}}^{\eta_{ts}} \int_{\eta_{co}}^{\eta} K(\eta|\xi)\theta(\xi) \frac{1-\zeta_{co}}{1-\zeta} [w_1(\xi) + BW_2(\xi)] d\xi d\eta \right\}^{-1}$$

where

$$B = [\frac{1}{\Lambda} - W_1(\eta_{ts})]/W_2(\eta_{ts})$$

4 Numerical Results

A numerical analysis will examine the structure and scaling laws of RND and their dependence on the principal collective interaction parameters of a stationary cloud of n-octane droplets with the following fuel properties; ρ_ℓ=707 Kg/m^3 T_b = 398.7 k, L = 71.7 Kcal/Kg, and W_F= 114.14 Kg/kg-mole.

(1) Pair-Distribution Function and Canonical Bubble

In the absence of experimental data, a pair-distribution function is constructed on the basis of the geometrical distribution of molecules in a dense liquid. The following two parameter function is adopted for the numerical calculation.

$$g(\eta) = 1 + a \exp(-b\eta) \cos(2\pi\eta_{co}), \qquad 2\eta_{co} < \eta \leq \eta_{ts} \qquad (29)$$

where a and b are constants to be determined from the experimental data. In the present analysis a = 1.8, b = 0.65 are chosen. The resulting distribution patterns are shown in Fig. 3. The corresponding signatures of the inverse of the radius of canonical bubbles with η_{co} = 5, 10, and 15 are shown in Fig. 4.

(2) Vaporization Shape Factor

A pronounced increase of μ in the radial direction is observed for a smaller value of droplet spacing, i.e. η_{co} = 7.5 in Fig. 5. The ratio of the vaporization rate of the droplet located at the first coordination shell, for

the case of η_{co} = 7.5, is approximately 5% of the corresponding value of RND with η_{co} = 15. This trend of a higher increasing rate of μ at smaller canonical bubble radii, or droplet spacing, is a common feature for small droplet spacing. This is confirmed for the cases characterized by pair-distribution functions with different values of a and b. The results suggest that "μ -stratification" is a unique feature of RND in non-dilute clouds or spray.

(3) Temperature Distribution

High μ- stratification at smaller droplet spacing, as illustrated in Fig. 5 is due to the steep radial temperature gradients in the transition sphere, shown in Fig. (6). Indeed, the comparison of "μ- T stratifications" suggest that (1) the rapid vaporization in outer layer of the cloud collectively quench the environment and thereby reduce the vaporization of the test droplet and (2) the increase in η_{ts} at a fixed droplet spacing tends to reduce the inward heat transfer rate and thus suppresses the vaporization of the test droplet.

(4) Vaporization Rate - Correction Factor

The correction factors of RNDs for three selected values of η_{co}, Fig. 7, are found to decrease monotonically as the group combustion number of RND increases. Saturation is projected to occur when G_{RN}=30~40 with η_{co}= 7.5. While the group combustion number is a primary factor controlling the magnitude of C_v, Fig. 7 shows a small variation in the correction factor for two RND's which have the same group combustion number but different renormalization number, $\beta = \eta_{ts}/\eta_{co}$.

4 Discussion

Scaling Law with Linear Stratification Model

In order to facilitate the practical application of the scaling law, the correction factor is integrated by adopting the following functional form of g_μ

$$g_\mu = \overline{g_\mu} K_1 \eta$$

where K_1 is a stratification coefficient, and $\overline{g_\mu}$ is the mean value of the weighted vaporization shape factor. The correction factor predicted by the linear stratification model described above, is given by

$$C_v = \{1-\zeta_{ts}+G_{RN}[(1-\frac{1}{\beta})(1+\frac{1}{\beta}-\frac{2}{\beta^2}) + \frac{1}{2} K_1 \eta_{ts}(1-\frac{1}{\beta})(1+\frac{1}{\beta}+\frac{1}{\beta^2}-\frac{1}{\beta^3})]\} \quad (30)$$

where $G_{RN}= \frac{1}{6} G_S \eta_{ts}^2 \overline{g_\mu}$.

SPRAY CLASSIFICATION

Numerical assessment of the scaling law suggests the following structural classification of non-dilute sprays.

1. Diffusively Dense Cloud

In a moderately dense cloud, RND is expected to have a large transition sphere that has no μ- stratification. The reduction in the vaporization is attributed to uniform thermal quenching. The correction factor given below is described by the group combustion alone:

$$C_v = (1 + G_{RN})^{-1} \quad (31)$$

C-2

2. Densely Stratified Cloud

This cloud is featured with a strong stratification in a transition sphere that causes an intense collective quenching and a reduction in the vaporization rate of the test droplet. The renormalization number η_{ts}/η_{co} is larger than unity so that the correction factor is given by

$$C_v = [1 - \zeta_{ts} + G_{RN}(1 + \frac{1}{2} K_1 \eta_{ts})]^{-1} \qquad (32)$$

3. Sharply Dense Cloud - Fine Structure

When the coordination shells contain the largest possible number of the droplet so that the renormalization number is not excessively large compared with unity, the correction factor depends on all the collective parameters: G_{RN}, η_{ts}/η_{co} and η_{ts}. Two sharply dense clouds with the same group combustion number will exhibit structural variation when the renormalization number is different.

5 Conclusion

The present theory portrays a droplet interacting with its neighbors by a minimum sized "dressed" droplet structured with a centrally located droplet and its bubble, e.g. Droplet-in-Bubble, surrounded by a quasi-droplet cloud spreading through a transition sphere. The distribution of quasi-droplets and the size of the cloud are described by a pair distribution function. The introduction of the transition sphere and the correspondence hypothesis postulating the equivalence between the average gas properties on the transition sphere with the gas properties of the continuum flow field, as the limit R_{ts}/L goes to zero, constitutes the fundamental link between the discrete droplet dominated region with that of the surrounding continuum

flow. This feature provides the basis of the theory of short-range interaction and droplet rate processes.

The vaporization scaling law reveals that the droplet vaporization is retarded primarily by the collective thermal quenching and the formation of high vapor concentration in the transition sphere. The retardation is scaled by combined topological-thermochemical parameters: the group combustion number, renormalization number and droplet spacing. The scaling laws suggest that non-dilute clouds or sprays can be classified into: (1) "Diffusively Dense" clouds in which the vaporization reduction is attributed to the effects of uniform thermal quenching that can be scaled by the group combustion number alone; (2) "Densely Stratified" clouds, with marked radial stratification due to the large temperature gradient which exists in the transition sphere; and (3) "Sharply Dense" clouds, with a relatively large canonical bubble, and radial stratification so that the scaling law depends on G_{RN}, η_{ts} and β. Selected case studies show that the correction factor falls monotonically as the group combustion number increases and the saturation is expected to occur when the G_{RN} is of the order of $30 \sim 40$, with the droplet spacing of approximately 7.5 times of the droplet size and environment temperature of 500 K.

Finally, the validity of quasi-steady (Q-S) approximation is examined by comparing the relative magnitude of the characteristic time, $t_{diff.}$, of difusion through the transition sphere and the life time, t_{life}, of RND. By adopting the renormalized vaporization laws, Eqs. (8) and (10), and a standard diffusion time for the transition sphere of RND, one concludes that the Q-S approximation is valid when the following inequality is satisfied

$$\frac{t_{dif.}}{t_{life}} = 2C_v \eta_{ts}^2 \frac{\rho}{\rho_\ell} \ell_n(1 + B) \tag{33}$$

where $B = C_p(T-T_b)/L$.

With $\rho_\ell \sim 10^3 kg/m^3$, $\rho \sim 1\ kg/n^3$, $T-T_b \sim 100^0 K$ $L \sim 10^2 Kcal/kg$, $C_p \sim 0.5$ Kcal/Kg-K the numerical values of $\frac{t_{diff}}{t_{life}}$ is 5×10^{-4}.

Alternatively, by using the asymptotic form of C_v for high G_{RN}, deduced from Eq. (30), i.e., $c_v \sim G_{RN}^{-1} = (\frac{1}{6} G_s \eta_{ts} g\mu)^{-1}$ one transforms Eq. (33) into the following form

$$\overline{g\mu} G_s > > G_s^* \tag{34}$$

where $G_s^* = 12 \frac{\rho}{\rho_\ell} \ln (1 + B)$

Recalling that $G_s = 4\pi\eta r_{\ell o}^3$ is equal to a third of the void fraction, and $\overline{\overline{g\mu}} \sim 0(1)$, one concludes that the Q-S approximation is valid in high G-sprays when the void fraction exceeds a third of the values of G_s^*. For typical values of ρ_ℓ, ρ, $T-T_b$, C_p and L given above, Eq. (34) reduces to

$$n r_{\ell o}^3 > > 4 \times 10^{-4} \tag{35}$$

For example, with SMD=100μ , the Q-S approximation is valid when n is greater than 3200 drops/cc, whereas for SMD=200μ, the corresponding number density is 400 drops/cc.

The criterion (33) or its alternative form can be encoded in a spray numerical code to test the validity of Q-S assumption at each point of a spray

flow field. When the approximation is invalid, an alternative transient droplet laws should be used to determine the interfacial processes. Note that such droplet transient processes should be able to predict the change in the nature of interfacial processes. For example, a vaporizing droplet may reach the state of saturation when the droplet spacing falls below the critical value or when the thermal shielding retards the heat flux to the droplet.

REFERENCES

1. Chiu, H.H. and Liu, T.M.: COMB. SCI. AND TECH., 17, 127, 1(1977).

2. Labowsky, M. and Rosner, D.E., Advances in Chemistry Series No 166 Amer. Chem. Soc., (1978).

3. Twardus, E.M., and Brzustowski, T.A.: Comb. Sci. Tech 17, 215, (1978).

4. Tishkoff, J.M.: Int. J. Heat and Mass Transfer 22, 1407, (1979).

5. Labowsky, M.: Combust. Sci. Tech. 22, 127, (1980).

6. Umemura, A.: Eighteenth Symposium (International) on Combustion, 1335, The Combustion Institute, 1981.

7. Chiu, H.H., Kim, H.Y., and Croke, E.J.: Nineteenth Symposium (International) on Combustion, 971, The Combustion Institute, 1982.

8. Bellan, J. and Cuffel, R.: Combust. Flame 51, 55, (1983).

9. Sirignano, W.A.: Prog. Energy Combust. Sci. 9, 291, (1983).

10. Sichel, M. and Panlaniswamy, S.: Twentieth Symposium (International) on Combustion, 1789, The Combustion Institute, 1984.

11. Chiu, H.H.: "Theory of Bipropellant Combustion, Part I - Conjugate, Normal and Composite Combustion Phenomena:" AIAA-86-0220 Presented at the AIAA 24TH Aerospace Sciences Meeting, Reno, Nevada, 1986.

12. Chiu, H.H.: "Theory of Renormalized Droplets I Law of Droplet Vaporization Rate Under Short-Range Droplet Interaction" Presented at First Annual Conference on Liquid Atomization and Spray Systems ILASS Americas, Madison, Wisconsin, 1987.

13. Jang, S.D. and Chiu, H.H.: "Theory of Renormalized Droplets, II, Nonsteady Vaporization Droplet in Non-Dilute Sprays" AIAA-88-0639, Presented at the AIAA 26TH Aerospace Sciences Meeting, Reno Nevada, 1988.

14. McCreath, C.G. and Chigier, N.A.: Fourteenth Symposium (International) on Combustion, 1355, The Combustion Institute, 1973.

15. Miyasaka, K. and Law, C.K.: Eighteenth Symposium (International) on Combustion, 283, The Combustion Institute, 1981.

16. Yule, A.J. and Bolado: Combust Flame 55, 1, (1984).

17. Xiong, T.Y., Law, C.K. and Miyasaka, K.: Twentieth Symposium (International) on Combustion, 1781, The Combustion Institute, 1984.

18. Roshland, C.P. and Bowman, C.T.: Twentieth Symposium (International) on Combustion, 1979, The Combustion Institute, 1984.

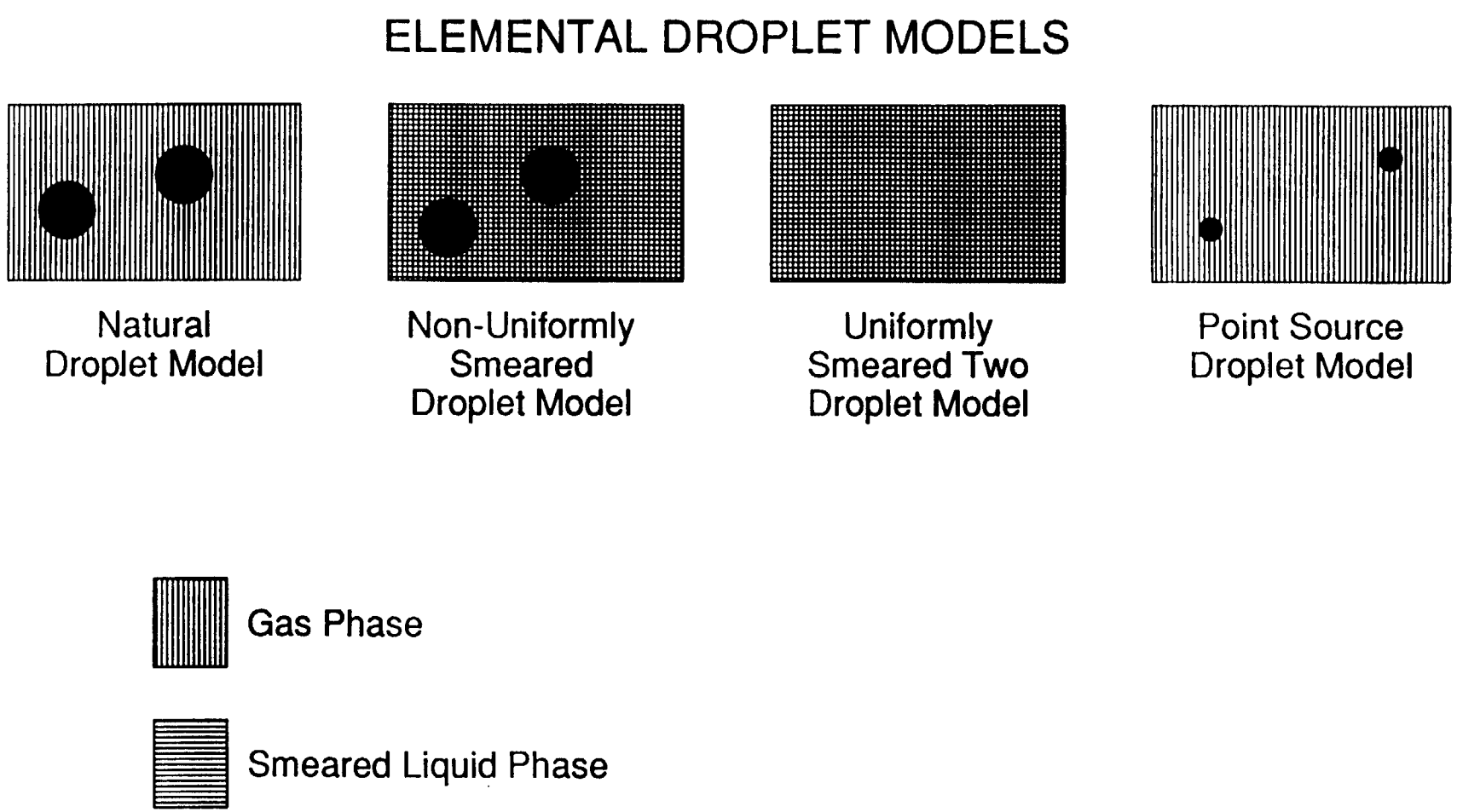

Fig. 1 Droplet Models; Elemental Droplets

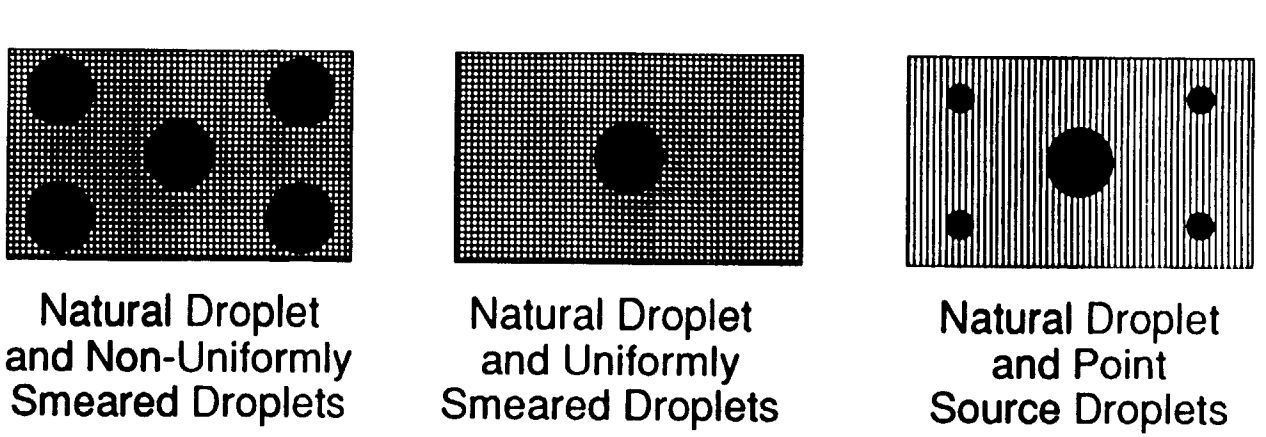

Fig. 1 Droplet Model; Composite Droplet

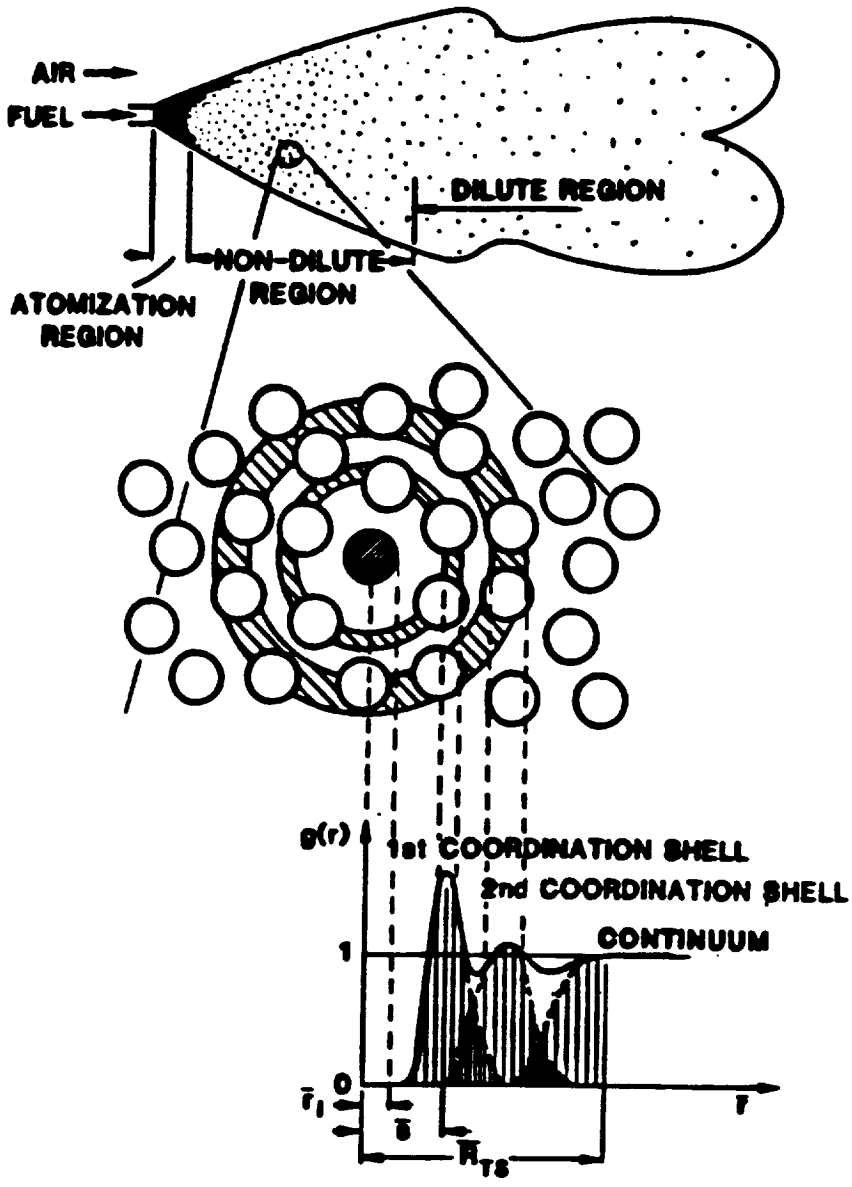

FIG. 2 Structure of renormalized droplet in non-dilute spray and the schematic of quasi-droplet cloud in transition sphere.

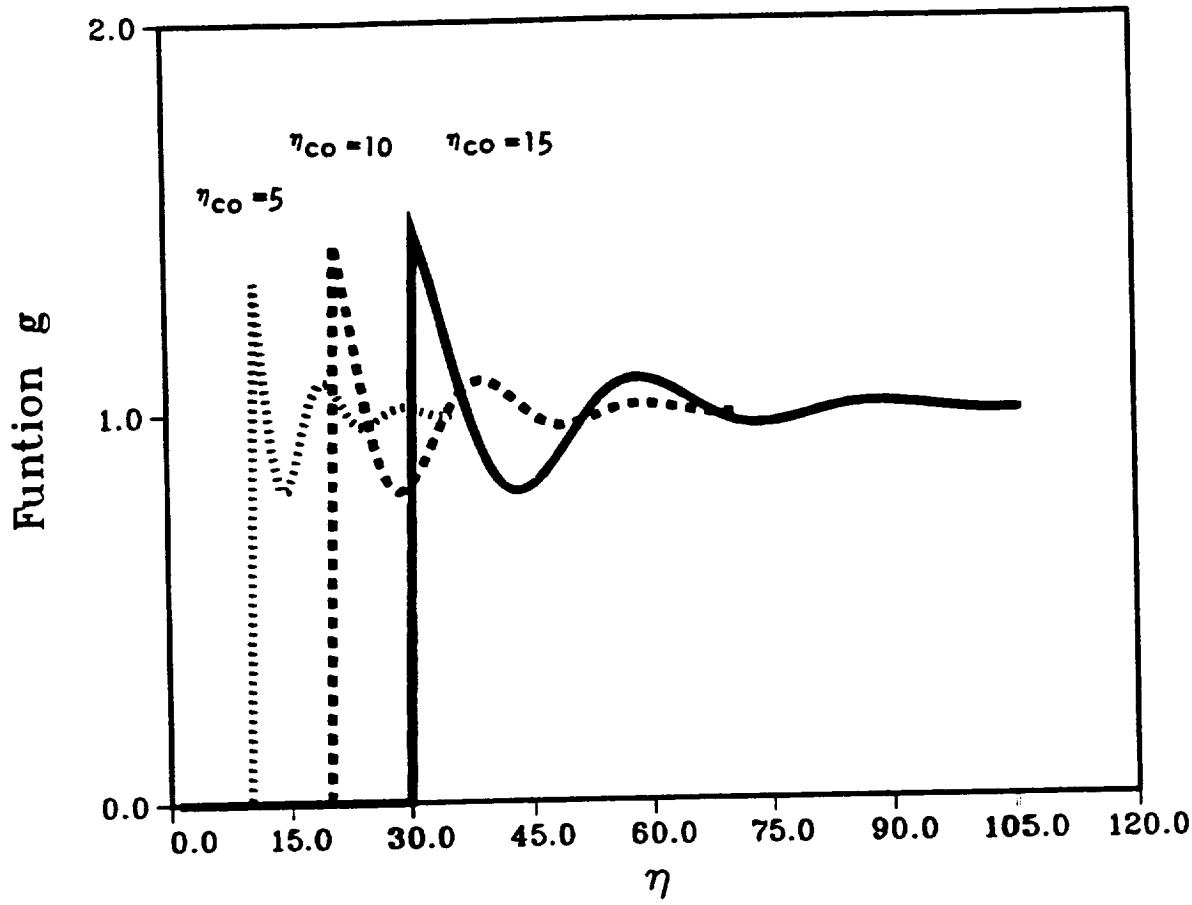

Fig. 3 Pair-distribution function of quasi-droplets in transition sphere for three selected test droplet bubble sizes.

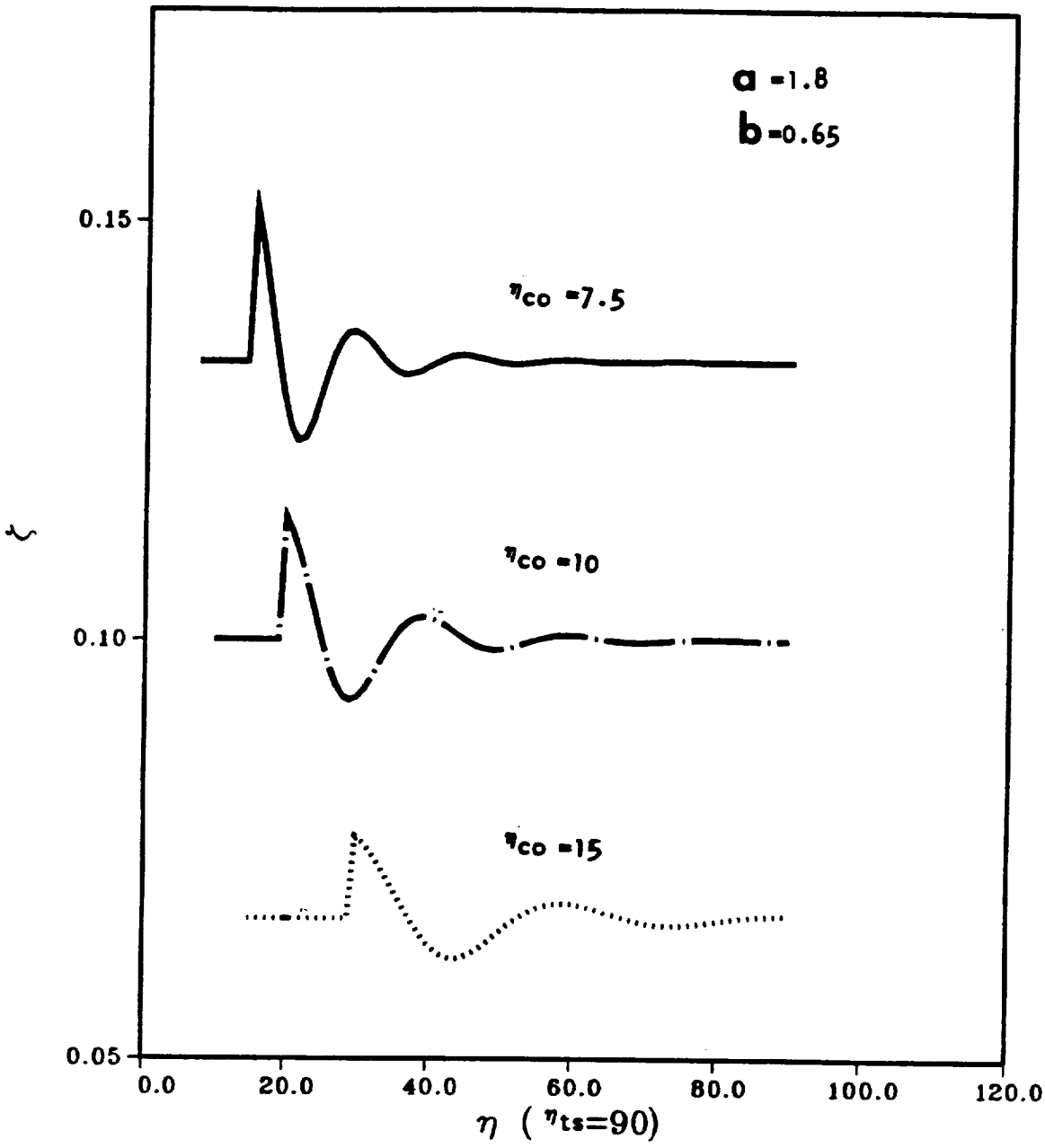

Fig. 4 Signature of the inverse of cannonical bubble radius for three selected test droplet bubble sizes.

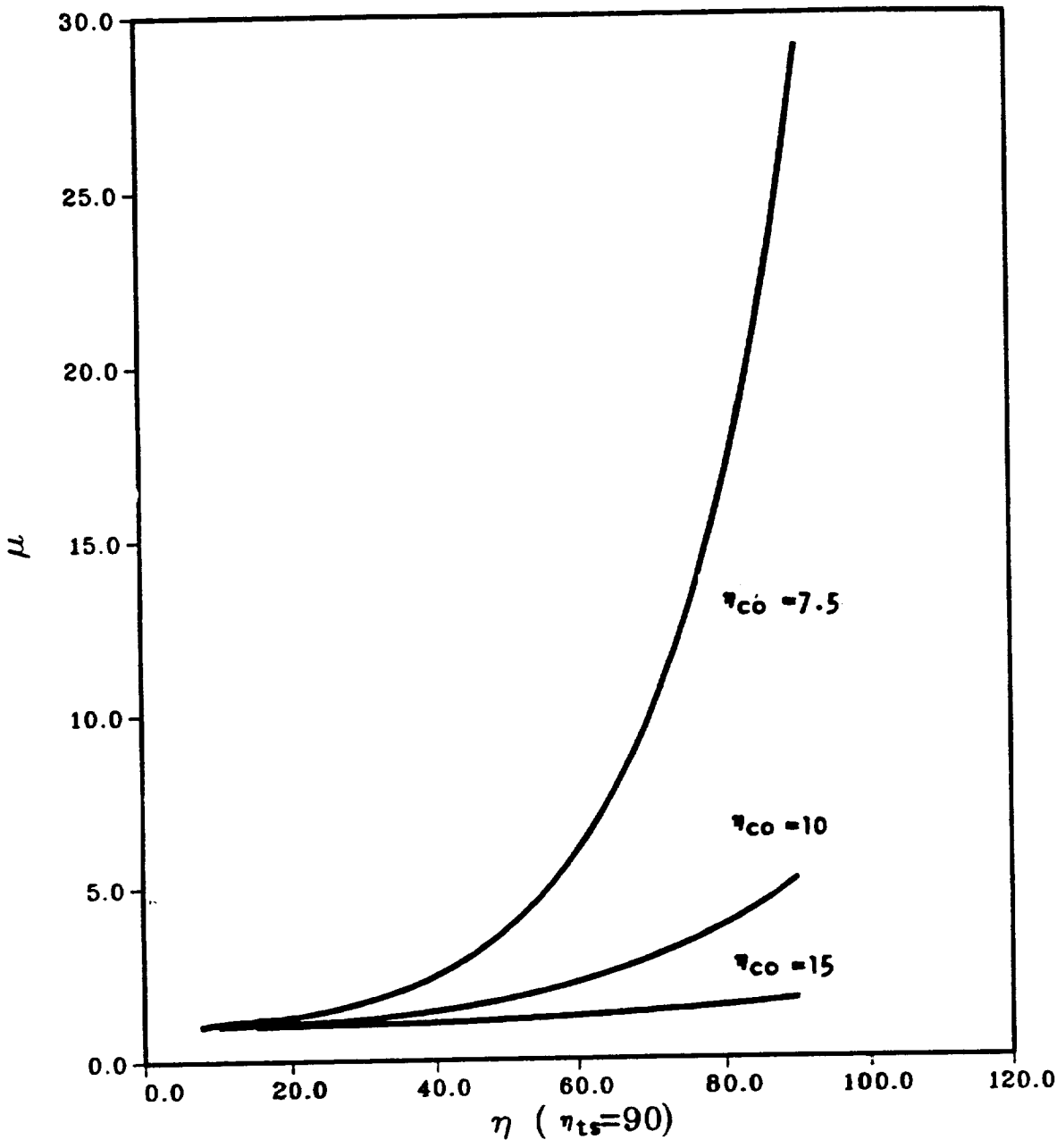

Fig. 5 μ-stratification; Vaporization shape factor distribution in transition sphere for three selected test droplet bubble sizes.

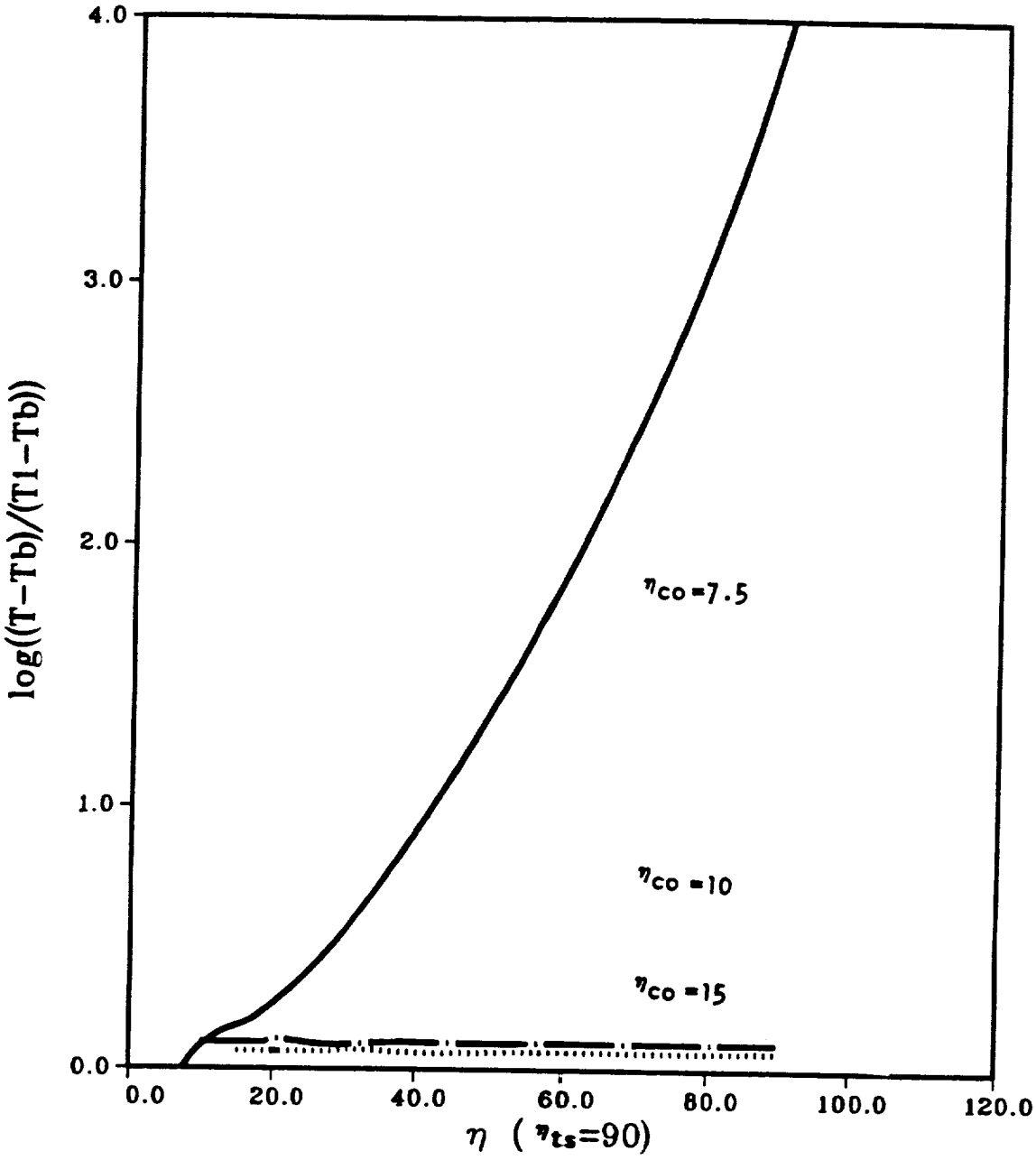

Fig. 6 T-stratification = gas temperature distribution in transition sphere for three selected test droplet bubble sizes.

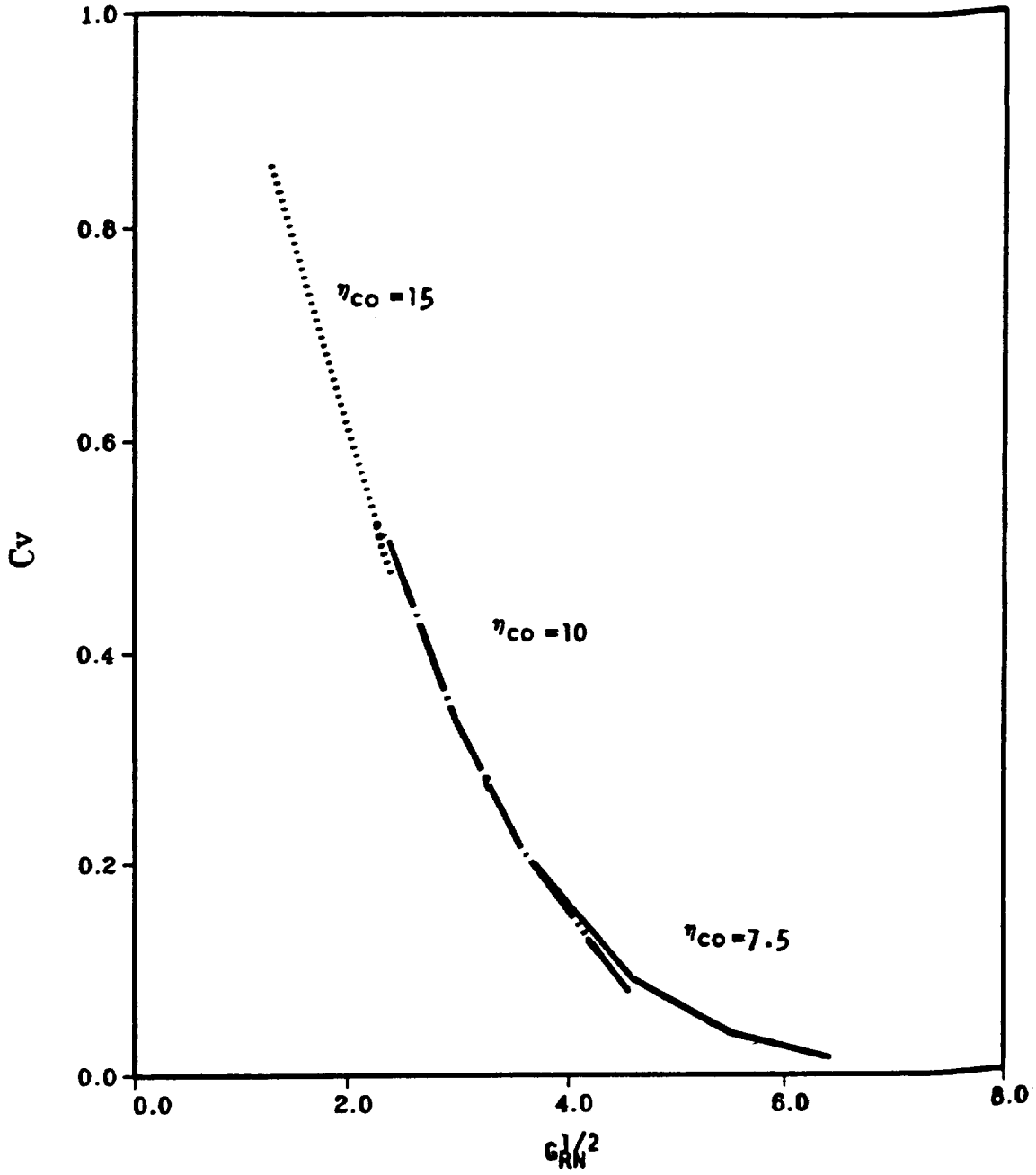

Fig. 7 Correction factor for vaporization rate vs group combustion number for three selected test droplet sizes: Exact Solution.

Effect of Particle Velocity Fluctuations on the Inertia Coupling in Two-Phase Flow

by

Donald A. Drew

Department of Mathematical Sciences

Rensselaer Polytechnic Institute

Troy, NY 12180-3590

Introduction

The fluid dynamics of flows of dispersed materials in a fluid is fundamental to suspensions, bubbly liquids, droplet flows, pneumatic transport, fluidization and erosion. Equations of motion to describe these materials must deal with the interactions between them as well as the deformation of the carrier fluid. Models that treat assemblages of solid particles have been proposed and studied (Jenkins and Savage, 1983) that result in the particles behaving like a gas, with a pressure due to the fluctuations in the velocities that is attributed to collisional motions of the indivual particles. Models for fluid-particle mixtures (Drew 1983) do not include this effect (Passman 1989) The purpose of the present paper is to derive constitutive equations to supplement the equations of motion that include the effects of the particle velocity fluctuations. The particle motions are assumed to be at a sufficiently high Reynolds number that the fluid motion is inviscid, but viscous effects such as boundary layer separation are neglected.

Equations of Motion

The appropriate general average is the ensemble average. The ensemble average is the appropriate generalization of adding the values of the variable for each realization, and dividing by the number of observations. We shall refer to a "process" as the set of possible flows that could occur, given that the initial and boundary conditions are those appropriate to the physical situation that we wish to describe. We refer to a "realization" of the flow as a possible motion that could have happened. Generally, we expect an infinite number of realizations of the flow, consisting of variations of position, attitude, and velocities of the discrete units and the fluid between them.

If f is some field (i.e., a function of position $\mathbf{x}$ and time t) for some particular real-

ization, μ, of the process, then the average of f is

$$\overline{f}(\mathbf{x},t) = \int_M f(\mathbf{x},t;\mu)dm(\mu) \tag{1}$$

where $dm(\mu)$ is the measure (probability) of observing process μ and M is the set of all processes. We refer to M as the ensemble. The ensemble average is the fundamental average that allows the interpretation of the phenomena in terms of the repeatability of experiments. Any one exact experiment or realization will not be repeatable; however, any repetition of the experiment will lead to another member of the ensemble.

In order to apply the averaging procedure to the equations of motion, we shall need some results about the averaging procedure. We shall also give these results for time- and volume averaging.

In order to average to the exact equations, we need expressions for $\overline{\partial f/\partial t}$ and $\overline{\nabla f}$. If f is "well behaved", then it is clear from the definition of the ensemble average that

$$\overline{\frac{\partial f}{\partial t}} = \frac{\partial \overline{f}}{\partial t} \tag{2}$$

and

$$\overline{\nabla f} = \nabla \overline{f} \tag{3}$$

Functions are generally discontinuous at the interface in most multiphase flow. They are well behaved within each phase, however. Thus, consider $\overline{X_k \nabla f}$, where X_k is the phase indicator function for phase k:

$$X_k = \begin{cases} 1, & \text{if } \mathbf{x} \in k; \\ 0, & \text{otherwise.} \end{cases} \tag{4}$$

In the averaging process we will require the result

$$\frac{\partial X_k}{\partial t} + \mathbf{v}_i \cdot \nabla X_k = 0. \tag{5}$$

This relation has a reasonable physical explanation. Note that it is the "material" derivative of X_k following the interface. If we look at a point that is not on the interface, then either $X_k = 1$ or $X_k = 0$. In either case, the partial derivatives are both zero, and hence

the expression (5) is zero. If we consider a point on the interface, if we move with the interface, we see the function X_k as a constant jump. Thus, its material derivative is zero.

The averaged equations are

Mass

$$\frac{\partial \overline{X_k \rho}}{\partial t} + \nabla \cdot \overline{X_k \rho \mathbf{v}} = \overline{\rho(\mathbf{v} - \mathbf{v}_i) \cdot \nabla X_k} \tag{6}$$

Momentum

$$\frac{\partial \overline{X_k \rho \mathbf{v}}}{\partial t} + \nabla \cdot \overline{X_k \rho \mathbf{v}\mathbf{v}} = \nabla \cdot \overline{X_k \mathbf{T}} + \overline{X_k \rho \mathbf{g}} + \overline{(\rho \mathbf{v}(\mathbf{v} - \mathbf{v}_i) - \mathbf{T}) \cdot \nabla X_k}. \tag{7}$$

Next, we define the appropriate average variables describing multiphase mechanics.

First, the geometry of the exact, or microscopic situation is defined in terms of the phase function X_k. The average of X_k is the average fraction of the occurrences of phase k at point $\mathbf{x}$ at time t.

$$\alpha_k = \overline{X_k} \tag{8}$$

The quantity $\partial X_k / \partial n$ is the delta function defining the interface. its average is the interfacial area density.

$$a_i = \overline{\frac{\partial X_k}{\partial n}} \tag{9}$$

All the remaining variables are defined in terms of weighted averages. The main, or "phasic" variables are either phasic weighted variables (weighted with the phase function X_k) or mass-weighted (or Favré) averaged (weighted by $X_k \rho$).

The "conserved" variables are the density

$$\overline{\rho}_k^x = \overline{X_k \rho} / \alpha_k, \tag{10}$$

and the velocity

$$\overline{\mathbf{v}}_k^{x\rho} = \overline{X_k \rho \mathbf{v}} / \alpha_k \overline{\rho}_k^x \tag{11}$$

The averaged stress is defined by

$$\overline{\mathbf{T}}_k^x = \overline{X_k \mathbf{T}}/\alpha_k \tag{12}$$

The average body force is

$$\overline{\mathbf{g}}_k^{x\rho} = \overline{X_k \rho \mathbf{g}}/\alpha_k \overline{\rho}_k^x \tag{13}$$

As discussed above, several terms appear representing the actions of the convective and molecular fluxes at the interface. The convective flux terms are the mass generation rate

$$\Gamma_k = \overline{\rho(\mathbf{v} - \mathbf{v}_i) \cdot \nabla X_k} \tag{14}$$

and the interfacial momentum flux

$$\mathbf{v}_{ki}^m \Gamma_k = \overline{\rho \mathbf{v}(\mathbf{v} - \mathbf{v}_i) \cdot \nabla X_k} \tag{15}$$

The interfacial momentum source is defined by

$$\mathbf{M}_k = -\overline{\mathbf{T} \cdot \nabla X_k} \tag{16}$$

The motion of the interfaces gives rise to velocities that are not "laminar" in general. The velocity fluctuations may be due to turbulence or to the motion in the phases due to the motion of the interfaces. The effect of these velocity fluctuations, whatever their source, on a variable is accounted for by introducing its fluctuating field (denoted by the prime superscript), which is the difference between the complete field and the appropriate mean field. For example,

$$\mathbf{v}_k' = \mathbf{v} - \overline{\mathbf{v}}_k^{x\rho}$$

Then,

$$\begin{aligned} \overline{X_k \rho \mathbf{v}\mathbf{v}} =& \overline{X_k \rho (\overline{\mathbf{v}}_k^{x\rho} + \mathbf{v}_k')(\overline{\mathbf{v}}_k^{x\rho} + \mathbf{v}_k')} \\ =& \overline{X_k \rho} \overline{\mathbf{v}}_k^{x\rho} \overline{\mathbf{v}}_k^{x\rho} + \overline{X_k \rho \mathbf{v}_k' \mathbf{v}_k'} \\ =& \alpha_k \overline{\rho}_k^x \overline{\mathbf{v}}_k^{x\rho} \overline{\mathbf{v}}_k^{x\rho} - \alpha_k \mathbf{T}_k^{Re}. \end{aligned} \tag{17}$$

The Reynolds stress is defined by

$$\mathbf{T}_k^{Re} = -\overline{X_k \rho \mathbf{v}_k' \mathbf{v}_k'}/\alpha_k, \tag{18}$$

The averaged interfacial pressure p_{ki} and shear stress $\boldsymbol{\tau}_{ki}$ are introduced to separate mean field effects from local effects in the interfacial force. The interfacial pressure is defined by

$$p_{ki} = \overline{p \partial X_k/\partial n_k}/a_i \tag{19}$$

and the interfacial shear stress is

$$\boldsymbol{\tau}_{ki} = \overline{\boldsymbol{\tau}_k \partial X_k/\partial n_k}/a_i \tag{20}$$

Thus,

$$\begin{aligned}
\mathbf{M}_k =& -\overline{\mathbf{T} \cdot \nabla X_k} \\
=& \overline{p \nabla X_k} - \overline{\boldsymbol{\tau} \cdot \nabla X_k} \\
=& p_{ki} \overline{\nabla X_k} - \boldsymbol{\tau}_{ki} \cdot \overline{\nabla X_k} - \overline{\mathbf{T}_{ki}' \cdot \nabla X_k} \\
=& p_{ki} \nabla \alpha_k - \boldsymbol{\tau}_{ki} \nabla \alpha_k + \mathbf{M}_k', \qquad (21)
\end{aligned}$$

where we define the interfacial extra momentum source

$$\mathbf{M}_k' = \mathbf{M}_k + p_{ki} \nabla \alpha_k - \boldsymbol{\tau}_{ki} \cdot \nabla \alpha_k \tag{22}$$

and introduce

$$\mathbf{T}_{ki}' = -p_{ki}' \mathbf{I} + \boldsymbol{\tau}_{ki}' = -(p - p_{ki})\mathbf{I} + (\boldsymbol{\tau} - \boldsymbol{\tau}_{ki}).$$

The averaged equations governing each phase are

Mass

$$\frac{\partial \alpha_k \overline{\rho}_k^x}{\partial t} + \nabla \cdot \alpha_k \overline{\rho}_k^x \overline{\mathbf{v}}_k^{x\rho} = \Gamma_k \tag{23}$$

Momentum

$$\frac{\partial \alpha_k \overline{\rho}_k^x \overline{\mathbf{v}}_k^{x\rho}}{\partial t} + \nabla \cdot \alpha_k \overline{\rho}_k^x \overline{\mathbf{v}}_k^{x\rho} \overline{\mathbf{v}}_k^{x\rho} = \nabla \cdot \alpha_k \left(\overline{\mathbf{T}}_k^x + \mathbf{T}_k^{Re} \right) + \alpha_k \overline{\rho}_k \mathbf{g} + \mathbf{M}_k + \mathbf{v}_{ki}^m \Gamma_k \tag{24}$$

The equation of conservation of mass for phase k (23) can be used in the momentum equation (24) to yield the Lagrangian form of the momentum equation:

$$\begin{aligned}\alpha_k\overline{\rho}_k^x\frac{D_k\overline{\mathbf{v}}_k^{x\rho}}{Dt} &= \alpha_k\overline{\rho}_k^x\left(\frac{\partial\overline{\mathbf{v}}_k^{x\rho}}{\partial t}+\overline{\mathbf{v}}_k^{x\rho}\cdot\nabla\overline{\mathbf{v}}_k^{x\rho}\right)\\ &= \nabla\cdot\alpha_k(\overline{\mathbf{T}}_k^x+\mathbf{T}_k^{Re})+\alpha_k\overline{\rho}_k^x\mathbf{g}+\mathbf{M}_k'\\ &\quad +p_{ki}\nabla\alpha_k-\boldsymbol{\tau}_{ki}\cdot\nabla\alpha_k+(\mathbf{v}_{ki}^m-\overline{\mathbf{v}}_k^{x\rho})\Gamma_k.\end{aligned}\tag{25}$$

The jump conditions are derived by multiplying the exact jump condition by $\mathbf{n}_1\cdot\nabla X_1$ and averaging. This process yields the following conditions:

Mass

$$\Gamma_1+\Gamma_2=0\tag{26}$$

Momentum

$$\mathbf{M}_1+\mathbf{M}_2+\mathbf{v}_{1i}^m\Gamma_1+\mathbf{v}_{2i}^m\Gamma_2=\mathbf{m}\tag{27}$$

Constitutive Equations

The exact equations of motion can be solved for the flow of an inviscid, incompressible irrotational fluid around an isolated sphere. We shall use this solution to derive information about constitutive equations for the force on the dispersed phase, the average stress, the Reynolds stress, and the interfacial pressure when the particle phase is allowed to have a random velocity.

The fluid velocity at $\mathbf{x}$ for the irrotational flow of an incompressible inviscid fluid is expressed in terms of the velocity potential by

$$\mathbf{v}(\mathbf{x})=\nabla\phi(\mathbf{x})\tag{28}$$

The continuity equation becomes

$$0=\nabla\cdot\mathbf{v}=\nabla\cdot\nabla\phi=\nabla^2\phi.\tag{28}$$

The pressure at any point $\mathbf{x}$ is given in terms of the velocity by Bernoulli's equation.

$$p-\rho\left(\frac{\partial\phi}{\partial t}+\frac{1}{2}|\nabla\phi|^2\right)=p_0=\text{ constant.}\tag{30}$$

Consider a sphere located at a point $\mathbf{z}$ in a flow field, moving with velocity $\mathbf{v}_p$. The boundary condition at the surface of the sphere is

$$\mathbf{n} \cdot \mathbf{v}_p = \mathbf{n} \cdot \mathbf{v} = \mathbf{n} \cdot \nabla\phi \text{ at } |\mathbf{x} - \mathbf{z}| = a, \tag{31}$$

where a is the radius of the sphere, $\mathbf{n}$ is the normal to the surface of the sphere and $\mathbf{v}_p$ is the velocity of the sphere. The boundary condition far from the sphere is

$$\phi \to \phi_\infty \text{ as } |\mathbf{x} - \mathbf{z}| \to \infty, \tag{32}$$

where

$$\phi_\infty = \mathbf{v}_0(t) \cdot \mathbf{x} + \frac{1}{2}\mathbf{x} \cdot \mathbf{e}_f \cdot \mathbf{x}$$

is the velocity potential that would exist in the fluid if the sphere were not present. Here $\mathbf{v}_0(t)$ is the (unsteady) velocity of the fluid at the origin, and $\mathbf{e}_f$ is the rate of strain tensor for the fluid. We shall assume that $\mathbf{e}_f$ is constant.

A convenient form for the solution of this problem is given by Voinov (1973), and is

$$\begin{aligned} \phi = {} & \mathbf{v}_0(t) \cdot \mathbf{x} + \frac{1}{2}\mathbf{x} \cdot \mathbf{e}_f \cdot \mathbf{x} \\ & + \frac{1}{2}\left(\mathbf{v}_p - \mathbf{v}_0(t) - \mathbf{z} \cdot \mathbf{e}_f\right) \cdot (\mathbf{x} - \mathbf{z}) \left(\frac{a^3}{r^3}\right) \\ & + \frac{1}{3}(\mathbf{x} - \mathbf{z}) \cdot \mathbf{e}_f \cdot (\mathbf{x} - \mathbf{z}) \left(\frac{a^5}{r^5}\right) \end{aligned} \tag{33}$$

If there are many spheres in the flow field, the solution given above (33) will still be a good approximation if the spheres are sufficiently far apart that the flow disturbances due to the individual spheres do not interact. That is, the flow must be sufficiently dilute. Thus, we can think of each sphere as "isolated" in the sense that it only interacts with its neighbors through the averaged fields. We assume that each sphere lies in a "cell," and inside that cell, the velocity is given by eq. (33). We shall approximate the cell to be a sphere of radius R. We choose R so that

$$\frac{4}{3}\pi a^3 / \frac{4}{3}\pi R^3 = \alpha.$$

Averaging

We now introduce a means of evaluating the averaging process. The first aspect of the ensemble average is that the sphere velocity is random, with a distribution function $f^{(1)}(\mathbf{v}_p, \mathbf{x}, t)$. The second aspect is that the sphere and the surrounding cell can lie with the sphere center anywhere within radius R of the space point $\mathbf{x}$. The average is performed by first integrating over the distribution of the velocities that the sphere can have, followed by an integration over the possible positions that the sphere center can have. Note that if $|\mathbf{x}-\mathbf{z}| < a$, the material making up the sphere occupies the field point $\mathbf{x}$ and if $|\mathbf{x}-\mathbf{z}| > a$ the fluid occupies the field point $\mathbf{x}$.

The average of a quantity $g(\mathbf{x}, t; \mathbf{z}, \mathbf{v}_p)$ is performed in two parts, that is first, we perform a conditional average of g for given sphere position $\mathbf{z}$, integrating over the velocity space $\mathbf{v}_p$, followed by the average over the spatial positions the sphere can have. We assume that the distribution of positions is such that

$$\frac{dV}{\frac{4}{3}\pi R^3}\left[1 - \mathbf{x}' \cdot \frac{\nabla \alpha_d(\mathbf{x}, t)}{\alpha_d(\mathbf{x}, t)}\right]$$

is the probability of finding the sphere in a volume dV surrounding the point $\mathbf{z}$, where $\mathbf{x}' = \mathbf{x} - \mathbf{z}$. Thus, for the average over the fluid of a quantity g, we have

$$\overline{g}(\mathbf{x}, t|\mathbf{z}) = \int_{R^3} g(\mathbf{x}, t; \mathbf{z}, \mathbf{v}_p) f^{(1)}(\mathbf{v}_p, \mathbf{z}, t) dV_{\mathbf{v}_p}. \tag{34}$$

Here the notation $\overline{g}(\mathbf{x}, t|\mathbf{z})$ is intended to suggest the conditional average assuming the sphere is located at $\mathbf{z}$. The average of g over the fluid phase is then given by

$$\overline{g}_c^x(\mathbf{x}, t) = \frac{1}{\frac{4}{3}\pi(R^3 - a^3)} \int_a^R \int \int_{\Omega(r)} \overline{g}(\mathbf{x}, t|\mathbf{z}) d\Omega dr, \tag{35}$$

where $\Omega(r)$ is the sphere of radius r centered at $\mathbf{x}$, and the integration is over the $\mathbf{z}$ variable.

It will be convenient to introduce the average particle velocity and the fluctuation particle velocity as

$$\overline{\mathbf{v}}_p(\mathbf{x}, t) = \int_{R^3} \mathbf{v}_p f^{(1)}(\mathbf{v}_p, \mathbf{x}, t)\, dV_{\mathbf{v}_p} \tag{36}$$

$$\mathbf{v}_p'(\mathbf{x}, t) = \mathbf{v}_p - \overline{\mathbf{v}}_p(\mathbf{x}, t) \tag{37}$$

Note that

$$\overline{\mathbf{v}'_p} = 0 \tag{38}$$

The particle kinetic energy per unit particle mass is

$$u_d^{Re}(\mathbf{x},t) = \frac{1}{2}\int_{R^3} |\mathbf{v}'_p|^2 f^{(1)}(\mathbf{v}_p,\mathbf{x},t)\, dV_{\mathbf{v}_p} \tag{39}$$

and the Reynolds stress for the particles is defined by

$$\mathbf{T}_d^{Re}(\mathbf{x},t) = -\rho_d \int_{R^3} \mathbf{v}'_p\mathbf{v}'_p f^{(1)}(\mathbf{v}_p,\mathbf{x},t)\, dV_{\mathbf{v}_p} \tag{40}$$

In order to evaluate the integrals appearing in the averaging process, we must express the $\mathbf{z}$ dependence of the velocities in terms of $\mathbf{x}$ and $\mathbf{x}' = \mathbf{x} - \mathbf{z}$. We have

$$\mathbf{v}_f(\mathbf{z}) = \mathbf{v}_f(\mathbf{x}) - \mathbf{x}' \cdot \mathbf{e}_f$$

and

$$\overline{\mathbf{v}}_p(\mathbf{z}) = \overline{\mathbf{v}}_p(\mathbf{x}) - \mathbf{x}' \cdot \mathbf{e}_p$$

where $\mathbf{e}_p$ is the velocity gradient tensor for the average particle motion. We shall assume that this tensor is constant and symmetric.

We have

$$\begin{aligned}
\mathbf{v}(\mathbf{x},t;\mathbf{z},\mathbf{v}_p) &= \nabla\phi(\mathbf{x},t;\mathbf{z},\mathbf{v}_p) \\
&= \mathbf{v}_f(\mathbf{x}) + \frac{1}{2}(\mathbf{v}_f(\mathbf{x}) - \overline{\mathbf{v}}_p(\mathbf{x}) - \mathbf{v}'_p - \mathbf{x}'\cdot(\mathbf{e}_f - \mathbf{e}_p))\left(\frac{a^3}{r^3}\right) \\
&\quad - \frac{3}{2}(\mathbf{v}_f(\mathbf{x}) - \overline{\mathbf{v}}_p(\mathbf{x}) - \mathbf{v}'_p - \mathbf{x}'\cdot(\mathbf{e}_f - \mathbf{e}_p))\cdot\mathbf{x}'\left(\frac{a^3}{r^5}\right)\mathbf{x}' \\
&\quad + \frac{2}{3}\mathbf{x}'\cdot\mathbf{e}_f\left(\frac{a^5}{r^5}\right) - \frac{5}{3}\mathbf{x}'\cdot\mathbf{e}_f\cdot\mathbf{x}'\left(\frac{a^5}{r^7}\right)\mathbf{x}'
\end{aligned} \tag{41}$$

Note that $\mathbf{v}_f(\mathbf{x})$ is the fluid velocity that would exist at $\mathbf{x}$ if the sphere were not present, and $\mathbf{v}_f(\mathbf{z}) - \mathbf{v}_p$ is the relative velocity between the sphere and the fluid evaluated at the sphere center. It is convenient to have expressions for the integrals of powers of $\mathbf{x}'$ over $\Omega(r)$. For these integrals, we note that

$$\int_{\Omega(r)} \mathbf{x}' \ldots \mathbf{x}' d\Omega = 0 \tag{42a}$$

if the factor $\mathbf{x}'$ appears on odd number of times, and

$$\int_{\Omega(r)} d\Omega = 4\pi r^2 \tag{42b}$$

$$\int_{\Omega(r)} \mathbf{x}'\mathbf{x}' d\Omega = \frac{4}{3}\pi r^4 \mathbf{I} \tag{42c}$$

$$\int_{\Omega(r)} \mathbf{x}'\mathbf{x}'\mathbf{x}'\mathbf{x}' d\Omega = \frac{4}{15}\pi r^6 \mathbf{\Sigma} \tag{42d}$$

where $\mathbf{\Sigma}$ is a fourth order isotropic tensor defined in Cartesian coordinates by

$$\Sigma_{ijkl} = \delta_{ij}\delta_{kl} + \delta_{ik}\delta_{jl} + \delta_{il}\delta_{jk}.$$

We further note that if $\mathbf{v}$ is a vector, and $\mathbf{e}$ is a symmetric second order tensor with $e_{ii} = 0$, then

$$\Sigma_{ijkl} v_j e_{kl} = 2 v_j e_{ji}.$$

Derivation of Averaged Quantities

In order to average eq. (41), we note that the average over the velocity fluctuations gives no contribution, by eq. (38). Then averaging over $\mathbf{z}$ gives

$$\overline{\mathbf{v}}_c^{r\rho}(\mathbf{x}, t) = \mathbf{v}_f(\mathbf{x}, t). \tag{43}$$

Similarly, to obtain the interfacial averaged velocity of the fluid, again the integration over the velocity fluctuations gives no contribution, and we have

$$\overline{\mathbf{v}}_{ci}(\mathbf{x}, t) = \frac{1}{4\pi a^2} \int_{\Omega(a)} \overline{\mathbf{v}}(\mathbf{x}, t|\mathbf{z}) d\Omega.$$

Substituting and performing the integrations lead to the result

$$\overline{\mathbf{v}}_{ci}(\mathbf{x}, t) = \mathbf{v}_f(\mathbf{x}, t). \tag{44}$$

This result is a little surprising at first. The fluid at the surface of the sphere satisfies the condition $\mathbf{n} \cdot \mathbf{v} = \mathbf{n} \cdot \mathbf{v}_p$, but is allowed to slip in the tangential direction. After the passage

of the sphere, the fluid that was momentarily in contact with the surface of the sphere is again moving with the fluid. The result says that even during the time that it is in contact with the surface of the sphere, its average velocity is still equal to the average velocity of the fluid, and not of the sphere.

Now let us compute averaged pressures using this formalism. The exact pressure can be computed by Bernoulli's equation (30). In order to evaluate the derivatives in eq. (30), we note that $\mathbf{x}$ is constant during t derivatives, but $\partial\mathbf{z}/\partial t = \mathbf{v}_p = \overline{\mathbf{v}}_p(\mathbf{z},t) + \mathbf{v}'_p$. Also, when evaluating $\nabla\phi$, both t and $\mathbf{z}$ are held constant. The pressure is given by

$$
\begin{aligned}
(45)\qquad p(\mathbf{x},t;\mathbf{z},\mathbf{v}_p) = p_0 - \rho_c \Bigg(& \frac{\partial \mathbf{v}_0}{\partial t}\cdot\mathbf{x} + \frac{1}{2}\left[\frac{\partial \mathbf{v}_0}{\partial t} - \frac{\partial \overline{\mathbf{v}}_p(\mathbf{x},t)}{\partial t}\right. \\
& \left. + (\overline{\mathbf{v}}_p(\mathbf{x},t)+\mathbf{v}'_p)\cdot\mathbf{e}_f - (\overline{\mathbf{v}}_p(\mathbf{x},t)+\mathbf{v}'_p)\cdot\mathbf{e}_p\right]\cdot\mathbf{x}'\left(\frac{a^3}{r^3}\right) \\
& -\frac{1}{2}(\mathbf{v}_f(\mathbf{x}) - (\overline{\mathbf{v}}_p(\mathbf{z},t)+\mathbf{v}'_p) - \mathbf{x}'\cdot(\mathbf{e}_f-\mathbf{e}_p))\cdot(\overline{\mathbf{v}}_p(\mathbf{z},t)+\mathbf{v}'_p)\left(\frac{a^3}{r^3}\right) \\
& -\frac{3}{2}(\mathbf{v}_f(\mathbf{x}) - (\overline{\mathbf{v}}_p(\mathbf{z},t)+\mathbf{v}'_p) - \mathbf{x}'\cdot(\mathbf{e}_f-\mathbf{e}_p))\cdot\mathbf{x}'\left(\frac{a^3}{r^5}\right)\mathbf{x}'\cdot(\overline{\mathbf{v}}_p(\mathbf{z},t)+\mathbf{v}'_p) \\
& -\frac{2}{3}(\overline{\mathbf{v}}_p(\mathbf{z},t)+\mathbf{v}'_p)\cdot\mathbf{e}_f\cdot\mathbf{x}'\left(\frac{a^5}{r^5}\right) + \frac{5}{3}\mathbf{x}'\cdot\mathbf{e}_f\cdot\mathbf{x}'\mathbf{x}'\cdot(\overline{\mathbf{v}}_p(\mathbf{z},t)+\mathbf{v}'_p)\left(\frac{a^5}{r^5}\right) + \frac{1}{2}\mathbf{v}_f\cdot\mathbf{v}_f \\
& +\frac{1}{8}|\mathbf{v}_f(\mathbf{x}) - (\overline{\mathbf{v}}_p(\mathbf{z},t)+\mathbf{v}'_p) - \mathbf{x}'\cdot(\mathbf{e}_f-\mathbf{e}_p)|^2\left(\frac{a^6}{r^6}\right) \\
& +\frac{1}{2}\mathbf{v}_f\cdot(\mathbf{v}_f(\mathbf{x}) - (\overline{\mathbf{v}}_p(\mathbf{x},t)+\mathbf{v}'_p) - \mathbf{x}'\cdot(\mathbf{e}_f-\mathbf{e}_p))\left(\frac{a^3}{r^3}\right) \\
& +\frac{9}{8}\left((\mathbf{v}_f(\mathbf{x}) - (\overline{\mathbf{v}}_p(\mathbf{x},t)+\mathbf{v}'_p) - \mathbf{x}'\cdot(\mathbf{e}_f-\mathbf{e}_p))\cdot\mathbf{x}'\right)^2\left(\frac{a^6}{r^{10}}\right) \\
& +\frac{2}{3}(\overline{\mathbf{v}}_p(\mathbf{x},t)+\mathbf{v}'_p)\cdot\mathbf{e}_f\cdot\mathbf{x}'\left(\frac{a^5}{r^5}\right) - \frac{5}{3}(\overline{\mathbf{v}}_p(\mathbf{x},t)+\mathbf{v}'_p)\cdot\mathbf{x}'\mathbf{x}'\cdot\mathbf{e}_f\cdot\mathbf{x}'\left(\frac{a^5}{r^7}\right) \\
& \frac{1}{3}(\mathbf{v}_f(\mathbf{x}) - (\overline{\mathbf{v}}_p(\mathbf{x},t)+\mathbf{v}'_p))\cdot\mathbf{e}_f\cdot\mathbf{x}'\left(\frac{a^8}{r^8}\right) \\
& -\frac{5}{6}(\mathbf{v}_f(\mathbf{x}) - (\overline{\mathbf{v}}_p(\mathbf{x},t)+\mathbf{v}'_p))\cdot\mathbf{x}'\mathbf{x}'\cdot\mathbf{e}_f\cdot\mathbf{x}'\left(\frac{a^8}{r^{10}}\right) \\
& +\frac{3}{2}(\mathbf{v}_f(\mathbf{x}) - (\overline{\mathbf{v}}_p(\mathbf{x},t)+\mathbf{v}'_p))\cdot\mathbf{x}'\mathbf{x}'\cdot\mathbf{e}_f\cdot\mathbf{x}'\left(\frac{a^8}{r^{10}}\right)\Bigg)
\end{aligned}
$$

where we have ignored terms of order e_f^2, e_p^2, and $e_f e_p$. Averaging over the velocity fluctuations gives

$$\overline{p}(\mathbf{x},t|\mathbf{z}) = p_0 - \rho_c \left(\frac{\partial \mathbf{v}_0}{\partial t} \cdot \mathbf{x} + \frac{1}{2} \left[\frac{\partial \mathbf{v}_0}{\partial t} - \frac{\partial \overline{\mathbf{v}}_p(\mathbf{x},t)}{\partial t} \right.\right.$$

$$\left. + \overline{\mathbf{v}}_p(\mathbf{x},t) \cdot \mathbf{e}_f - \overline{\mathbf{v}}_p(\mathbf{x},t) \cdot \mathbf{e}_p \right] \cdot \mathbf{x}' \left(\frac{a^3}{r^3} \right)$$

$$- \left[\frac{1}{2} (\mathbf{v}_f(\mathbf{x}) - \overline{\mathbf{v}}_p(\mathbf{z},t) - \mathbf{x}' \cdot (\mathbf{e}_f - \mathbf{e}_p)) \cdot \overline{\mathbf{v}}_p(\mathbf{z},t) - u_d^{Re}(\mathbf{z},t) \right] \left(\frac{a^3}{r^3} \right)$$

$$- \left[\frac{3}{2} (\mathbf{v}_f(\mathbf{x}) - \overline{\mathbf{v}}_p(\mathbf{z},t) - \mathbf{x}' \cdot (\mathbf{e}_f - \mathbf{e}_p)) \cdot \mathbf{x}'\mathbf{x}' \cdot \overline{\mathbf{v}}_p(\mathbf{z},t) + \frac{3}{2} \frac{\mathbf{x}' \cdot \mathbf{T}_d^{Re}(\mathbf{z},t) \cdot \mathbf{x}'}{\rho_d} \right] \left(\frac{a^3}{r^5} \right)$$

$$- \frac{2}{3} \overline{\mathbf{v}}_p(\mathbf{z},t) \cdot \mathbf{e}_f \cdot \mathbf{x}' \left(\frac{a^5}{r^5} \right) + \frac{5}{3} \mathbf{x}' \cdot \mathbf{e}_f \cdot \mathbf{x}'\mathbf{x}' \cdot \overline{\mathbf{v}}_p(\mathbf{z},t) \left(\frac{a^5}{r^5} \right) + \frac{1}{2} \mathbf{v}_f \cdot \mathbf{v}_f$$

$$+ \left[\frac{1}{8} |\mathbf{v}_f(\mathbf{x}) - \overline{\mathbf{v}}_p(\mathbf{z},t) - \mathbf{x}' \cdot (\mathbf{e}_f - \mathbf{e}_p)| + \frac{1}{4} u_d^{Re}(\mathbf{z},t) \right] \left(\frac{a^6}{r^6} \right)$$

$$+ \frac{1}{2} \mathbf{v}_f \cdot (\mathbf{v}_f(\mathbf{x}) - \overline{\mathbf{v}}_p(\mathbf{x},t) - \mathbf{x}' \cdot (\mathbf{e}_f - \mathbf{e}_p)) \left(\frac{a^3}{r^3} \right)$$

$$+ \left[\frac{9}{8} ((\mathbf{v}_f(\mathbf{x}) - \overline{\mathbf{v}}_p(\mathbf{x},t) - \mathbf{x}' \cdot (\mathbf{e}_f - \mathbf{e}_p)) \cdot \mathbf{x}')^2 - \frac{9}{8} \frac{\mathbf{x}' \cdot \mathbf{T}_d^{Re}(\mathbf{z},t) \cdot \mathbf{x}'}{\rho_d} \right] \left(\frac{a^6}{r^{10}} \right)$$

$$+ \frac{2}{3} \overline{\mathbf{v}}_p(\mathbf{x},t) \cdot \mathbf{e}_f \cdot \mathbf{x}' \left(\frac{a^5}{r^5} \right) - \frac{5}{3} \overline{\mathbf{v}}_p(\mathbf{x},t) \cdot \mathbf{x}'\mathbf{x}' \cdot \mathbf{e}_f \cdot \mathbf{x}' \left(\frac{a^5}{r^7} \right)$$

$$\frac{1}{3} (\mathbf{v}_f(\mathbf{x}) - \overline{\mathbf{v}}_p(\mathbf{x},t)) \cdot \mathbf{e}_f \cdot \mathbf{x}' \left(\frac{a^8}{r^8} \right)$$

$$- \frac{5}{6} (\mathbf{v}_f(\mathbf{x}) - \overline{\mathbf{v}}_p(\mathbf{x},t)) \cdot \mathbf{x}'\mathbf{x}' \cdot \mathbf{e}_f \cdot \mathbf{x}' \left(\frac{a^8}{r^{10}} \right)$$

$$\left. + \frac{3}{2} (\mathbf{v}_f(\mathbf{x}) - \overline{\mathbf{v}}_p(\mathbf{x},t)) \cdot \mathbf{x}'\mathbf{x}' \cdot \mathbf{e}_f \cdot \mathbf{x}' \left(\frac{a^8}{r^{10}} \right) \right)$$

The spatial integration is tedious, but results in

$$\overline{p}_c^x = p_0 - \rho_c \frac{\partial \mathbf{v}_f}{\partial t} \cdot \mathbf{x} - \frac{1}{2} \mathbf{v}_f(\mathbf{x}) \cdot \mathbf{v}_f(\mathbf{x}) \tag{46}$$

where we ignore terms of order a/R in addition to those ignored previously. We also obtain

$$\overline{p}_{ci}(\mathbf{x},t) = \overline{p}_c^x - \frac{1}{4} \rho_c |\overline{\mathbf{v}}_c(\mathbf{x},t) - \overline{\mathbf{v}}_d(\mathbf{x},t)|^2 + \frac{1}{2} \rho_c u_d^{Re}. \tag{47}$$

The interfacial force density $\mathbf{M}_d$ is given by $\mathbf{M}_d = \overline{p\nabla X_d}$. Thus,

$$\mathbf{M}_d(\mathbf{x},t) = -\frac{1}{\frac{4}{3}\pi R^3}\int_{\Omega(a)} \mathbf{n}p(\mathbf{x},t|\mathbf{z})\left(1-\frac{\mathbf{x}'\cdot\alpha_d}{\alpha_d}\right)d\Omega. \tag{48}$$

This can be computed by substituting eq. (45) for the pressure, and recognizing that $\mathbf{n} = \mathbf{x}'/a$. We must also expand the terms $u_d^{Re}(\mathbf{z},t) = u_d^{Re}(\mathbf{x},t) - \mathbf{x}'\cdot\nabla u_d^{Re}(\mathbf{x},t)$ and $\mathbf{T}_d^{Re}(\mathbf{z},t) = \mathbf{T}_d^{Re}(\mathbf{x},t) - \mathbf{x}'\cdot\nabla\mathbf{T}_d^{Re}(\mathbf{x},t)$ The result is that

$$\begin{aligned}
\mathbf{M}_d(\mathbf{x},t) &= \overline{p}_c^x\nabla\alpha_d \qquad (49)\\
&+\alpha_d\overline{\rho}_c^x\left(\frac{1}{2}\left[\frac{\partial\overline{\mathbf{v}}_c^{x\rho}(\mathbf{x},t)}{\partial t} - \frac{\partial\overline{\mathbf{v}}_d^{x\rho}(\mathbf{x},t)}{\partial t} + \overline{\mathbf{v}}_c^{x\rho}(\mathbf{x},t)\cdot\nabla\overline{\mathbf{v}}_c^{x\rho}(\mathbf{x},t) - \overline{\mathbf{v}}_d^{x\rho}(\mathbf{x},t)\cdot\nabla\overline{\mathbf{v}}_d^{x\rho}(\mathbf{x},t)\right]\right.\\
&\left.-\frac{7}{20}(\overline{\mathbf{v}}_c^{x\rho}(\mathbf{x},t) - \overline{\mathbf{v}}_d^{x\rho}(\mathbf{x},t))\cdot(\nabla\overline{\mathbf{v}}_c^{x\rho}(\mathbf{x},t) - \nabla\overline{\mathbf{v}}_d^{x\rho}(\mathbf{x},t))\right)\\
&+\overline{\rho}_c^x\left(\frac{2}{5}(\overline{\mathbf{v}}_c^{x\rho}(\mathbf{x},t) - \overline{\mathbf{v}}_d^{x\rho}(\mathbf{x},t))\cdot(\overline{\mathbf{v}}_c^{x\rho}(\mathbf{x},t) - \overline{\mathbf{v}}_d^{x\rho}(\mathbf{x},t))\nabla\alpha_d\right.\\
&\left.+\frac{9}{20}(\overline{\mathbf{v}}_c^{x\rho}(\mathbf{x},t) - \overline{\mathbf{v}}_d^{x\rho}(\mathbf{x},t)(\overline{\mathbf{v}}_c^{x\rho}(\mathbf{x},t) - \overline{\mathbf{v}}_d^{x\rho}(\mathbf{x},t))\cdot\nabla\alpha_d\right)\\
&-\alpha_d\overline{\rho}_c^x\frac{7}{20}\nabla u_d^{Re} - \alpha_d\frac{\overline{\rho}_c^x}{\overline{\rho}_d^x}\frac{9}{20}\nabla\cdot\mathbf{T}_d^{Re} - \nabla\alpha_d\overline{\rho}_c^x\frac{7}{20}u_d^{Re} - \frac{\overline{\rho}_c^x}{\overline{\rho}_d^x}\frac{9}{20}\nabla\alpha_d\cdot\mathbf{T}_d^{Re}
\end{aligned}$$

Note that no drag force is present in eq. (49). This is the result of D'Alembert's paradox, that is, there is no net force on a body moving at a constant velocity through an inviscid fluid at rest.

If a distribution of stresses is applied to the surface of an elastic body, there results a distribution of stresses inside the body. These induced stresses are important in computing constitutive equations for solid-fluid mixtures. The average stress inside the sphere is given by

$$\overline{\mathbf{T}}_d^x(\mathbf{x},t) = \frac{1}{\frac{4}{3}\pi a^3}\int_0^a\int\int_{\Omega(r)}\mathbf{T}(\mathbf{x},t|\mathbf{z})d\Omega$$

where

$$\mathbf{T}(\mathbf{x},t|\mathbf{z}) = \int_{R^3}\mathbf{T}(\mathbf{x},t;\mathbf{z},\mathbf{v}_p)f^{(1)}(\mathbf{v}_p,\mathbf{z},t)\,dV_{\mathbf{v}_p}$$

Here $\mathbf{T}(\mathbf{x},t;\mathbf{z},\mathbf{v}_p)$ is the stress at point $\mathbf{x}$ inside a sphere having its center at $\mathbf{z}$ at time t. We shall assume that the spheres are linearly elastic solids, but we shall assume that the

deformation is sufficiently small that the fluid motion is unaffected by the deformation of the spheres. Then the stress-strain relation is given by

$$\mathbf{T} = \mu_s[\nabla\mathbf{u} + (\nabla\mathbf{u})^{tr}] + \lambda_s \nabla\cdot\mathbf{u}\mathbf{I} \tag{50}$$

This can be written as

$$\mathbf{T} = \boldsymbol{\sigma} + \Theta\mathbf{I} \tag{51}$$

where

$$\Theta = \left(\lambda_s + \frac{2}{3}\mu_s\right)\nabla\cdot\mathbf{u}$$

$$\boldsymbol{\sigma} = \mu_s\left\{[\nabla\mathbf{u} + (\nabla\mathbf{u})^{tr}] - \frac{2}{3}\nabla\cdot\mathbf{u}\mathbf{I}\right\}$$

The spherical part of the stress satisfies (Love, 1932)

$$\nabla^2\Theta(\mathbf{x},t;\mathbf{z},\mathbf{v}_p) = 0 \tag{52a}$$

$$\Theta(\mathbf{x},t;\mathbf{z},\mathbf{v}_p) = -p(\mathbf{x},t;\mathbf{z},\mathbf{v}_p) \text{ on } |\mathbf{x}-\mathbf{z}| = a \tag{52b}$$

Averaging over $\mathbf{v}_p$ gives

$$\nabla^2\Theta(\mathbf{x},t|\mathbf{z}) = 0 \tag{53a}$$

$$\Theta(\mathbf{x},t|\mathbf{z}) = -p(\mathbf{x},t|\mathbf{z}) \text{ on } |\mathbf{x}-\mathbf{z}| = a \tag{53b}$$

Solving and performing the integration over $\mathbf{z}$ gives

$$\overline{\Theta}_d^x(\mathbf{x},t) = -\overline{p}_{ci}(\mathbf{x},t). \tag{54}$$

The solution for $\boldsymbol{\sigma}$ is also given in Love (1932) and can be averaged in $\mathbf{v}_p$ and then integrated in $\mathbf{z}$ to give

$$\begin{aligned}\overline{\boldsymbol{\sigma}}_d^x(\mathbf{x},t) = \overline{\rho}_c^x\Bigg[&-\frac{9}{20}\left((\overline{\mathbf{v}}_c^{x\rho}(\mathbf{x},t) - \overline{\mathbf{v}}_d^{x\rho}(\mathbf{x},t))(\overline{\mathbf{v}}_c^{x\rho}(\mathbf{x},t) - \overline{\mathbf{v}}_d^{x\rho}(\mathbf{x},t)) - \frac{\mathbf{T}_d^{Re}}{\overline{\rho}_d^x}\right)\\ &+ \frac{8}{20}\left(|\overline{\mathbf{v}}_c^{x\rho}(\mathbf{x},t) - \overline{\mathbf{v}}_d^{x\rho}(\mathbf{x},t)|^2 + 2u_d^{Re}\right)\mathbf{I}\Bigg].\end{aligned} \tag{55}$$

We next turn to computations of the Reynolds stress using the velocity fluctuations due to the inviscid flow around a sphere. Using the expression for the velocity (41) and the average fluid velocity (43), we see that

$$\begin{aligned}\mathbf{v}_c'(\mathbf{x},t;\mathbf{z},\mathbf{v}_p) = &\frac{1}{2}(\mathbf{v}_f(\mathbf{z})-\mathbf{v}_p)\left(\frac{a^3}{r^3}\right)\\ &-\frac{3}{2}(\mathbf{v}_f(\mathbf{z})-\mathbf{v}_p)\cdot\mathbf{x}'\left(\frac{a^3}{r^5}\right)\mathbf{x}'\\ &+\frac{2}{3}\mathbf{x}'\cdot\mathbf{e}_f\left(\frac{a^5}{r^5}\right)-\frac{5}{3}\mathbf{x}'\cdot\mathbf{e}_f\cdot\mathbf{x}'\left(\frac{a^5}{r^7}\right)\mathbf{x}'\end{aligned} \tag{56}$$

Averaging over the particle velocity fluctuations yields

$$\begin{aligned}\mathbf{T}_c^{Re}(\mathbf{x},t|\mathbf{z}) = &-\rho_c\overline{\mathbf{v}_c'}(\mathbf{x},t|\mathbf{z})\overline{\mathbf{v}_c'}(\mathbf{x},t|\mathbf{z})\\ &+\rho_c\left[\frac{1}{4}\left(\frac{a^6}{r^6}\right)\frac{\mathbf{T}_d^{Re}}{\rho_d}-\frac{3}{4}\left(\frac{a^6}{r^8}\right)[\mathbf{x}'(\mathbf{x}'\cdot\frac{\mathbf{T}_d^{Re}}{\rho_d})+(\mathbf{x}'\cdot\frac{\mathbf{T}_d^{Re}}{\rho_d})\mathbf{x}']\right.\\ &\left.+\frac{9}{4}\left(\frac{a^6}{r^{10}}\right)\mathbf{x}'\mathbf{x}'(\mathbf{x}'\cdot\frac{\mathbf{T}_d^{Re}}{\rho_d}\cdot\mathbf{x}')\right]\end{aligned}$$

The integration over $\mathbf{z}$ can be performed, yielding

$$\begin{aligned}\mathbf{T}_c^{Re}(\mathbf{x},t) = -\frac{1}{20}\alpha_d\bar{\rho}_c^x\left[\left((\overline{\mathbf{v}}_c^{x\rho}-\overline{\mathbf{v}}_d^{x\rho})(\overline{\mathbf{v}}_c^{x\rho}-\overline{\mathbf{v}}_d^{x\rho})-\frac{\mathbf{T}_d^{Re}}{\bar{\rho}_d^x}\right)\right.\\ \left.+3\left((\overline{\mathbf{v}}_c^{x\rho}-\overline{\mathbf{v}}_d^{x\rho})\cdot(\overline{\mathbf{v}}_c^{x\rho}-\overline{\mathbf{v}}_d^{x\rho})+2u_d^{Re}\right)\mathbf{I}\right].\end{aligned} \tag{57}$$

The fluid fluctuation kinetic energy is $u_c^{Re} = \frac{1}{2}\overline{\mathbf{v}'\cdot\mathbf{v}'}^x$, and can be computed by taking the trace of eq. (57) for $\mathbf{T}_c^{Re}$. The result is

$$u_c^{Re} = \frac{1}{4}\alpha_d|\overline{\mathbf{v}}_c^{x\rho}-\overline{\mathbf{v}}_d^{x\rho}|^2+\frac{1}{2}\alpha_d u_d^{Re}. \tag{58}$$

Conservation of Fluctuation Kinetic Energy

In analogy with statistical mechanics for assemblages of molecules, the theory of averaging as applied to multiphase flows allows the computation of averaged equations for higher moments of velocity and pressure correlations.

We start with the derivation of averaged equations for the fluctuation kinetic energy for each phase. The exact momentum equation is

$$\frac{\partial\rho\mathbf{v}}{\partial t}+\nabla\cdot\rho\mathbf{v}\mathbf{v} = \nabla\cdot\mathbf{T}+\rho\mathbf{g} \tag{59}$$

We shall derive an equation for the evolution of the kinetic energy. The Lagrangian form of the momentum equation is

$$\rho\left(\frac{\partial \mathbf{v}}{\partial t}+\mathbf{v}\cdot\nabla\mathbf{v}\right)=\nabla\cdot\mathbf{T}+\rho\mathbf{g} \tag{60}$$

If we take the dot product of $\mathbf{v}$ with eq. (60), we have

$$\rho\left(\frac{\partial \frac{1}{2}v^2}{\partial t}+\mathbf{v}\cdot\nabla\frac{1}{2}v^2\right)=\mathbf{v}\cdot(\nabla\cdot\mathbf{T})+\rho\mathbf{v}\cdot\mathbf{g} \tag{61}$$

We note that

$$\mathbf{v}\cdot(\nabla\cdot\mathbf{T})=\nabla\cdot(\mathbf{T}\cdot\mathbf{v})-\mathbf{T}:\nabla\mathbf{v}$$

If we also return to the Eulerian form, we have

$$\frac{\partial \frac{1}{2}\rho v^2}{\partial t}+\nabla\cdot\frac{1}{2}\rho v^2\mathbf{v}=\nabla\cdot(\mathbf{T}\cdot\mathbf{v})-\mathbf{T}:\nabla\mathbf{v}+\rho\mathbf{v}\cdot\mathbf{g} \tag{62}$$

If we apply the ensemble average to eq. (62), we have

$$\begin{aligned}\frac{\partial\overline{X_k\frac{1}{2}\rho v^2}}{\partial t}+\nabla\cdot\overline{X_k\frac{1}{2}\rho v^2\mathbf{v}}&=\nabla\cdot\overline{X_k\mathbf{T}\cdot\mathbf{v}}-\overline{X_k\mathbf{T}:\nabla\mathbf{v}}\\&+\overline{X_k\rho\mathbf{v}\cdot\mathbf{g}}-\overline{[\rho\frac{1}{2}v^2(\mathbf{v}-\mathbf{v}_i)+\mathbf{T}\cdot\mathbf{v})\cdot\nabla X_k]}\end{aligned} \tag{63}$$

We define the fluctuation velocity of phase k by

$$\mathbf{v}_k'=\mathbf{v}-\overline{\mathbf{v}}_k^{x\rho} \tag{64}$$

Then

$$v^2=(v_k')^2+2\mathbf{v}_k'\cdot\overline{\mathbf{v}}_k^{x\rho}+(\overline{v}_k^{x\rho})^2 \tag{65}$$

so that, noting that $\overline{X_k\rho\mathbf{v}_k'}=\overline{X_k\rho\mathbf{v}}-\overline{X_k\rho\overline{\mathbf{v}_k^{x\rho}}}=0$, we have

$$\overline{X_k\rho\frac{1}{2}v^2}=\overline{X_k\rho(v_k')^2}+\overline{X_k\rho 2\mathbf{v}_k'\cdot\mathbf{v}_k^{x\rho}}+\overline{X_k\rho(v_k^{x\rho})^2}=\alpha_k\overline{\rho}_k^x u_k^{Re}+\alpha_k\overline{\rho}_k^x\frac{1}{2}v_k^{x\rho}$$

Furthermore,

$$v^2\mathbf{v}=(v_k')^2\mathbf{v}_k'+(v_k')^2\overline{\mathbf{v}}_k^{x\rho}+2\mathbf{v}_k'\cdot\overline{\mathbf{v}}_k^{x\rho}\overline{\mathbf{v}}_k^{x\rho}+2\mathbf{v}_k'\cdot\overline{\mathbf{v}}_k^{x\rho}\mathbf{v}_k'+(\overline{v}_k^{x\rho})^2\mathbf{v}_k'+(\overline{v}_k^{x\rho})^2\overline{\mathbf{v}}_k^{x\rho}$$

so that

$$\begin{aligned}\overline{X_k\rho\frac{1}{2}v^2\mathbf{v}} =&\overline{X_k\rho\frac{1}{2}(v_k')^2\mathbf{v}_k'} + \overline{X_k\rho\frac{1}{2}(v_k')^2}\overline{\mathbf{v}}_k^{x\rho} + \overline{\mathbf{v}}_k^{x\rho}\cdot\overline{X_k\rho\mathbf{v}_k'\mathbf{v}_k'} + \overline{X_k\rho\frac{1}{2}(\overline{v}_k^{x\rho})^2\overline{\mathbf{v}}_k^{x\rho}}\\ =&\alpha_k\mathbf{q}_k^K + \alpha_k\overline{\rho}_k^x u_k^{Re}\overline{\mathbf{v}}_k^{x\rho} - \alpha_k\overline{\mathbf{v}}_k^{x\rho}\cdot\mathbf{T}_k^{Re} + \alpha_k\overline{\rho}_k^x\frac{1}{2}(\overline{v}_k^{x\rho})^2\overline{\mathbf{v}}_k^{x\rho}\end{aligned}$$

Also, note that

$$\mathbf{T}\cdot\mathbf{v} = \mathbf{T}\cdot\overline{\mathbf{v}}_k^{x\rho} + = \mathbf{T}\cdot\mathbf{v}_k'.$$

Note further that

$$\mathbf{T}:\nabla\mathbf{v} = \mathbf{T}:\nabla\overline{\mathbf{v}}_k^{x\rho} + \mathbf{T}:\nabla\mathbf{v}_k'$$

Then we have

$$\overline{X_k\mathbf{T}\cdot\mathbf{v}} = \overline{X_k\mathbf{T}}\cdot\overline{\mathbf{v}}_k^{x\rho} + \overline{X_k\mathbf{T}\cdot\mathbf{v}_k'} = \alpha_k\mathbf{T}_k^x\cdot\overline{\mathbf{v}}_k^{x\rho} - \alpha_k\mathbf{q}_k^T$$

and

$$\overline{X_k\mathbf{T}:\nabla\mathbf{v}} = \overline{X_k\mathbf{T}}:\nabla\overline{\mathbf{v}}_k^{x\rho} + \overline{X_k\mathbf{T}:\nabla\mathbf{v}_k'} = \alpha_k\overline{\mathbf{T}}_k^x:\nabla\overline{\mathbf{v}}_k^{x\rho} + D_k,$$

where $\mathbf{q}_k^T = \mathbf{q}_k^p + \mathbf{q}_k^\tau$ and $D_k = \overline{X_k\mathbf{T}:\nabla\mathbf{v}_k'}$.

Next, in the interfacial terms, we have

$$\overline{\rho\frac{1}{2}v^2(\mathbf{v}-\mathbf{v}_i)\cdot\nabla X_k} = \frac{1}{2}(\overline{v}_k^{x\rho})^2\Gamma_k + \overline{\mathbf{v}}_k^{x\rho}\cdot\mathbf{v}_{ki}^m\Gamma_k + \overline{\rho\frac{1}{2}(v_k')^2(\mathbf{v}-\mathbf{v}_i)\cdot\nabla X_k}$$

and

$$\overline{(\mathbf{T}\cdot\mathbf{v})\cdot\nabla X_k} = \overline{(\mathbf{T}\cdot\overline{\mathbf{v}}_k^{x\rho})\cdot\nabla X_k} + \overline{(\mathbf{T}\cdot\overline{\mathbf{v}}_k')\cdot\nabla X_k} = \mathbf{M}_k\cdot\overline{\mathbf{v}}_k^{x\rho} + W_k$$

The equation for the conservation of fluctuation kinetic energy then becomes

$$\begin{aligned}\frac{\partial}{\partial t}\alpha_k\overline{\rho}_k^x\left(u_k^{Re}+\frac{1}{2}(\overline{v}_k^{x\rho})^2\right) +&\nabla\cdot\alpha_k\overline{\rho}_k^x\left(u_k^{Re}+\frac{1}{2}(\overline{v}_k^{x\rho})^2\right)\mathbf{v}_k^{x\rho} - \nabla\cdot\left(\alpha_k\overline{\mathbf{v}}_k^{x\rho}\cdot\mathbf{T}_k^{Re}\right) =\\ &-\nabla\cdot\alpha_k(\mathbf{q}_k^K+\mathbf{q}_k^T) + \nabla\cdot\alpha_k\overline{\mathbf{T}}_k^x\cdot\overline{\mathbf{v}}_k^{x\rho} + \alpha_k\overline{\rho}_k^x\overline{\mathbf{v}}_k^{x\rho}\cdot\mathbf{g}\\ &-\alpha_k\overline{\mathbf{T}}_k^x:\nabla\overline{\mathbf{v}}_k^{x\rho} - D_k + \frac{1}{2}(\overline{v}_k^{x\rho})^2\Gamma_k + \overline{\mathbf{v}}_k^{x\rho}\cdot\mathbf{v}_{ki}^m\Gamma_k\\ &+\overline{\rho\frac{1}{2}(v_k')^2(\mathbf{v}-\mathbf{v}_i)\cdot\nabla X_k} + \mathbf{M}_k\cdot\overline{\mathbf{v}}_k^{x\rho} + W_k\end{aligned} \tag{66}$$

The equation for the average kinetic energy is

$$\frac{\partial \alpha_k \overline{\rho}_k^x \frac{1}{2}(\overline{v}_k^{x\rho})^2}{\partial t} + \nabla \cdot \alpha_k \rho_k \overline{\mathbf{v}}_k^{x\rho} \frac{1}{2}(\overline{v}_k^{x\rho})^2 =$$

$$\overline{\mathbf{v}}_k^{x\rho} \cdot \nabla \cdot \alpha_k (\overline{\mathbf{T}}_k + \mathbf{T}_k^{Re}) + \mathbf{M}_k \cdot \overline{\mathbf{v}}_k^{x\rho}$$

$$+ \alpha_k \rho_k \mathbf{g} \cdot \overline{\mathbf{v}}_k^{x\rho} + \overline{\mathbf{v}}_k^{x\rho} \cdot \mathbf{v}_{ki}^m \Gamma_k. \tag{67}$$

Subtracting this from eq. (66), we have

$$\frac{\partial \alpha_k \overline{\rho}_k^x u_k^{Re}}{\partial t} + \nabla \cdot \alpha_k \overline{\rho}_k^x u_k^{Re} \overline{\mathbf{v}}_k^{x\rho} = \alpha_k \mathbf{T}_k^{Re} : \nabla \overline{\mathbf{v}}_k^{x\rho} - \nabla \cdot \alpha_k (\mathbf{q}_k^K + \mathbf{q}_k^T)$$

$$+ \frac{1}{2}(\overline{v}_k^{x\rho})^2 \Gamma_k - \overline{\rho \frac{1}{2}(v_k')^2 (\mathbf{v} - \mathbf{v}_i) \cdot \nabla X_k} + W_k - D_k \tag{68}$$

This equation has some interesting interpretations. First, note that the dissipation due to the Reynolds stress $\alpha_k \mathbf{T}_k^{Re} : \nabla \overline{\mathbf{v}}_k^{x\rho}$ acts as a source of fluctuation kinetic energy, while its counterpart for the molecular dissipation $\alpha_k \overline{\mathbf{T}}_k^x : \nabla \overline{\mathbf{v}}_k^{x\rho}$ does not appear in this equation. Dissipation on the macroscopic scale, then, winds up as different things on the microscopic scale. Also, the dissipation due to microscopic velocity fluctuations D_k implies a loss of fluctuation kinetic energy. Thus, loss mechanisms, such as inelastic collisions or viscous dissipation in the velocity fulctuations, cause a loss of fluctuation kinetic energy to heat. Finally, the working of the fluctuations at the interface, W_k appears as a source of fluctuation kinetic energy.

Since this equation is unnecessary for the fluid phase, we shall ignore it for $k = c$. For $k = d$, we note that $D_d = 0$ is consistent with the linear elasticity assumption and the assumption that the particle radius a does not change. Furthermore, if assume no phase change ($\Gamma_k = 0$), and we ignore triple correlations in the particle velocity fluctuations ($\overline{\mathbf{v}_p' \mathbf{v}_p' \mathbf{v}_p'} = 0$), we have

$$\alpha_d \overline{\rho}_d^x \frac{\partial u_d^{Re}}{\partial t} + \alpha_d \overline{\rho}_d^x \cdot \nabla u_d^{Re} \overline{\mathbf{v}}_d^{x\rho} = \alpha_d \mathbf{T}_d^{Re} : \nabla \overline{\mathbf{v}}_d^{x\rho} + W_d \tag{69}$$

Discussion of the Force on a Sphere

The equations of motion for the mixture are

$$\frac{\partial \alpha_d}{\partial t} + \nabla \cdot \alpha_d \overline{\mathbf{v}}_d^{x\rho} = 0 \tag{70}$$

$$\frac{\partial \alpha_c}{\partial t} + \nabla \cdot \alpha_c \overline{\mathbf{v}}_c^{x\rho} = 0 \tag{71}$$

$$\begin{aligned}
\alpha_d \overline{\rho}_d^x \left(\frac{\partial \overline{\mathbf{v}}_d^{x\rho}}{\partial t} + \overline{\mathbf{v}}_d^{x\rho} \cdot \nabla \overline{\mathbf{v}}_c^{x\rho} \right) &= -\alpha_d \nabla (\overline{p}_c^x + \frac{1}{2} \overline{\rho}_c^x u_d^{Re} - \frac{1}{4} \overline{\rho}_c^x |\overline{\mathbf{v}}_c^{x\rho} - \overline{\mathbf{v}}_d^{x\rho}|^2) + \nabla \cdot \alpha_d \mathbf{T}_d^{Re} \\
&+ \nabla \cdot \alpha_d \left\{ \overline{\rho}_c^x \left[-\frac{9}{20} (\overline{\mathbf{v}}_c(\mathbf{x},t) - \overline{\mathbf{v}}_d(\mathbf{x},t))(\overline{\mathbf{v}}_c(\mathbf{x},t) - \overline{\mathbf{v}}_d(\mathbf{x},t)) \right. \right. \\
&\left. \left. + \frac{3}{20} |\overline{\mathbf{v}}_c^{x\rho}(\mathbf{x},t) - \overline{\mathbf{v}}_d^{x\rho}(\mathbf{x},t)|^2 \mathbf{I} \right] \right\} \\
&+ \alpha_d \overline{\rho}_c^x \left(\frac{1}{2} \left[\frac{\partial \overline{\mathbf{v}}_c^{x\rho}(\mathbf{x},t)}{\partial t} - \frac{\partial \overline{\mathbf{v}}_d^{x\rho}(\mathbf{x},t)}{\partial t} + \overline{\mathbf{v}}_c^{x\rho}(\mathbf{x},t) \cdot \nabla \overline{\mathbf{v}}_c^{x\rho}(\mathbf{x},t) - \overline{\mathbf{v}}_d^{x\rho}(\mathbf{x},t) \cdot \nabla \overline{\mathbf{v}}_d^{x\rho}(\mathbf{x},t) \right] \right. \\
&\left. - \frac{7}{20} [\overline{\mathbf{v}}_c^{x\rho}(\mathbf{x},t) - \overline{\mathbf{v}}_d^{x\rho}(\mathbf{x},t)] \cdot [\nabla \overline{\mathbf{v}}_c^{x\rho}(\mathbf{x},t) - \nabla \overline{\mathbf{v}}_d^{x\rho}(\mathbf{x},t)] \right) \\
&+ \overline{\rho}_c^x \left(\frac{2}{5} (\overline{\mathbf{v}}_c^{x\rho}(\mathbf{x},t) - \overline{\mathbf{v}}_d^{x\rho}(\mathbf{x},t)) \cdot (\overline{\mathbf{v}}_c^{x\rho}(\mathbf{x},t) - \overline{\mathbf{v}}_d^{x\rho}(\mathbf{x},t)) \nabla \alpha_d \right. \\
&\left. + \frac{9}{20} (\overline{\mathbf{v}}_c^{x\rho}(\mathbf{x},t) - \overline{\mathbf{v}}_d^{x\rho}(\mathbf{x},t))(\overline{\mathbf{v}}_c^{x\rho}(\mathbf{x},t) - \overline{\mathbf{v}}_d^{x\rho}(\mathbf{x},t)) \cdot \nabla \alpha_d \right) \\
&+ \overline{\rho}_c^x \frac{9}{20} \nabla (\alpha_d u_d^{Re})
\end{aligned} \tag{72}$$

$$\alpha_c \overline{\rho}_c^x \left(\frac{\partial \overline{\mathbf{v}}_c^{x\rho}}{\partial t} + \overline{\mathbf{v}}_c^{x\rho} \cdot \nabla \overline{\mathbf{v}}_c^{x\rho} \right) = -\alpha_c \nabla \overline{p}_c^x \tag{73}$$

$$\begin{aligned}
&+ \nabla \cdot \left\{ -\frac{1}{20} \alpha_d \overline{\rho}_c^x \left[\left((\overline{\mathbf{v}}_c^{x\rho} - \overline{\mathbf{v}}_d^{x\rho})(\overline{\mathbf{v}}_c^{x\rho} - \overline{\mathbf{v}}_d^{x\rho}) - \frac{\mathbf{T}_d^{Re}}{\overline{\rho}_d^x} \right) \right. \right. \\
&\left. \left. + 3 \left((\overline{\mathbf{v}}_c^{x\rho} - \overline{\mathbf{v}}_d^{x\rho}) \cdot (\overline{\mathbf{v}}_c^{x\rho} - \overline{\mathbf{v}}_d^{x\rho}) + 2 u_d^{Re} \right) \mathbf{I} \right] \right\} \\
&+ \left(\frac{1}{4} \overline{\rho}_c^x |\overline{\mathbf{v}}_c^{x\rho}(\mathbf{x},t) + \overline{\mathbf{v}}_d^{x\rho}(\mathbf{x},t)|^2 + \frac{1}{2} \overline{\rho}_c^x u_d^{Re} \right) \nabla \alpha_d \\
&- \alpha_d \overline{\rho}_c^x \left(\frac{1}{2} \left[\frac{\partial \overline{\mathbf{v}}_c^{x\rho}(\mathbf{x},t)}{\partial t} - \frac{\partial \overline{\mathbf{v}}_d^{x\rho}(\mathbf{x},t)}{\partial t} + \overline{\mathbf{v}}_c^{x\rho}(\mathbf{x},t) \cdot \nabla \overline{\mathbf{v}}_c^{x\rho}(\mathbf{x},t) - \overline{\mathbf{v}}_d^{x\rho}(\mathbf{x},t) \cdot \nabla \overline{\mathbf{v}}_d^{x\rho}(\mathbf{x},t) \right] \right. \\
&\left. - \frac{7}{20} [\overline{\mathbf{v}}_c^{x\rho}(\mathbf{x},t) - \overline{\mathbf{v}}_d^{x\rho}(\mathbf{x},t)] \cdot [\nabla \overline{\mathbf{v}}_c^{x\rho}(\mathbf{x},t) - \nabla \overline{\mathbf{v}}_d^{x\rho}(\mathbf{x},t)] \right) \\
&- \overline{\rho}_c^x \left(\frac{2}{5} (\overline{\mathbf{v}}_c^{x\rho}(\mathbf{x},t) - \overline{\mathbf{v}}_d^{x\rho}(\mathbf{x},t)) \cdot (\overline{\mathbf{v}}_c^{x\rho}(\mathbf{x},t) - \overline{\mathbf{v}}_d^{x\rho}(\mathbf{x},t)) \nabla \alpha_d \right.
\end{aligned}$$

$$+\frac{9}{20}(\overline{\mathbf{v}}_c^{x\rho}(\mathbf{x},t)-\overline{\mathbf{v}}_d^{x\rho}(\mathbf{x},t))(\overline{\mathbf{v}}_c^{x\rho}(\mathbf{x},t)-\overline{\mathbf{v}}_d^{x\rho}(\mathbf{x},t))\cdot\nabla\alpha_d\Bigg)$$

$$+\overline{\rho}_c^x\frac{7}{20}\nabla(\alpha_d u_d^{Re})+\frac{\overline{\rho}_c^x}{\overline{\rho}_d^x}\frac{9}{20}\nabla\cdot(\alpha_d\mathbf{T}_d^{Re})$$

It is also possible to calculate the force on a sphere at $\mathbf{z}$ by computing

$$\mathbf{F}_p(\mathbf{z},t)=\int_{\Omega(a)}\mathbf{n}\left(p_0-\overline{\rho}_c^x\left[\frac{1}{2}|\nabla\phi|^2+\frac{\partial\phi}{\partial t}\right]\right)d\Omega,$$

where the integration is over the variable $\mathbf{x}'$, with $\mathbf{x}=\mathbf{z}+\mathbf{x}'$. This results in

$$\mathbf{F}_p(\mathbf{z})=\frac{4}{3}\pi a^3\overline{\rho}_c^x\left(\frac{\partial\mathbf{v}_f}{\partial t}+\mathbf{v}_f\cdot\mathbf{e}_f+\frac{1}{2}\left[\frac{\partial\mathbf{v}_f}{\partial t}-\frac{\partial\mathbf{v}_p}{\partial t}+\mathbf{v}_f\cdot\mathbf{e}_f\right]\right). \tag{74}$$

Note that this force agrees with Taylor's (1928) calculation of the force necessary to hold a sphere at rest in an accelerating stream, obtained by setting $\frac{\partial}{\partial t}=0$ and $\mathbf{v}_p=0$. The force is

$$\frac{3}{2}\left(\frac{4}{3}\pi a^3\right)\overline{\rho}_c^x\mathbf{v}_f\cdot\nabla\mathbf{v}_f \tag{75}$$

If we first take the gradients involved in eq. (72), using $\nabla\cdot\overline{\mathbf{v}}_d^{x\rho}=(1/\alpha_d)(\partial\alpha_d/\partial t+\overline{\mathbf{v}}_d^{x\rho}\cdot\nabla\alpha_d)$ and $\nabla\cdot\overline{\mathbf{v}}_c^{x\rho}=-(1/\alpha_c)(\partial\alpha_d/\partial t+\overline{\mathbf{v}}_c^{x\rho}\cdot\nabla\alpha_d)$, then set $\overline{\mathbf{v}}_d^{x\rho}=0$, $u_d^{Re}=0$, $\alpha_d=$ const., and $\mathbf{T}_d^{Re}=0$; and assume one-dimensional, steady flow, then eq. (72) reduces to eq. (75) in the limit as $\alpha_d\to 0$. Moreover, it is clear that it should. Consider the one-dimensional situation pictured in Fig. 1. The continuum model for the particles between x and $x+\Delta x$ gives the rate of change of the momentum of the particles *and parts of particles* between x and $x+\Delta x$, denoted by $\dot{\mathbf{P}}_d(x,x+\Delta x)$, as the stress force transmitted to the particles by the particle parts outside of the interval, denoted by $(\alpha_d\mathbf{i}\cdot\mathbf{T}_d^x)\,|_x+(\alpha_d(-\mathbf{i})\cdot\mathbf{T}_d^x)\,|_{x+\Delta x}$, plus the force transmitted to the particles through their interface, denoted by $\mathbf{M}_d\Delta x$. Thus,

$$\dot{\mathbf{P}}_d(x,x+\Delta x)=(\alpha_d\mathbf{i}\cdot\mathbf{T}_d^x)\,|_x+(\alpha_d(-\mathbf{i})\cdot\mathbf{T}_d^x)\,|_{x+\Delta x}+\mathbf{M}_d\Delta x \tag{76}$$

The sum of the forces on all particles with their centers in the interval from x to $x+\Delta x$ is equal to the sum of the pressure forces on all the particles involved. This is

denoted by $\Sigma \int p\mathbf{n}dS$. This is equal to the rate of change of the momentum of all the particles, denoted by $\dot{\mathbf{P}}_p$. Thus,

$$\dot{\mathbf{P}}_p = \Sigma \int p\mathbf{n}dS \tag{77}$$

We note that eqs. (76) and (77) differ in the way they treat the particles being cut by the surfaces at x and $x + \Delta x$. The relation is that the

$$\begin{aligned}\dot{\mathbf{P}}_d(x, x+\Delta x) = \dot{\mathbf{P}}_p &+ (\alpha_d \mathbf{i} \cdot \mathbf{T}_d^x)\,|_x + (\alpha_d(-\mathbf{i}) \cdot \mathbf{T}_d^x)\,|_{x+\Delta x} \\ &- \Sigma_{\text{cut,in}} \int p\mathbf{n}dS|_x + \Sigma_{\text{cut,out}} \int p\mathbf{n}dS|_x \\ &- \Sigma_{\text{cut,in}} \int p\mathbf{n}dS|_{x+\Delta x} + \Sigma_{\text{cut,out}} \int p\mathbf{n}dS|_{x+\Delta x}\end{aligned} \tag{78}$$

Here

$$\Sigma_{\text{cut,in}} \int p\mathbf{n}dS|_x$$

is the sum of the pressure forces on the surfaces of the cut particles at x whose centers are inside the interval from x to $x + \Delta x$,

$$\Sigma_{\text{cut,out}} \int p\mathbf{n}dS|_x$$

is the sum of the pressure forces on the surfaces of the cut particles at x whose centers are outside the interval from x to $x + \Delta x$. A similar interpretation is valid for the cut particles at $x + \Delta x$.

The terms on the right hand side of eq. (78) represent the resultants of forces on cut particles. If the approximate equation of motion inside the cut particle is $\nabla \cdot \mathbf{T} = 0$, then the pressure force over the curved side, plus the stress resultant force over the flat side must add up to 0. (Note that if the particles are accelerating, then the forces add up to be the volume of the part of the cut particle, times the acceleration of its center of mass. Presumably, this force is small.)

Conclusion

Consistent forms for the interfacial force, the interfacial pressure, the Reynolds stresses and the particle stress have been derived for the inviscid, irrotational incompressible flow of fluid in a dilute suspension of spheres. The particles are assumed to have a velocity distribution, giving rise to an effective pressure and stress in the particle phase. The velocity fluctuations also contribute in the fluid Reynolds stress and in the (elastic) stress field inside the spheres. The relation of these constitutive equations to the force on an individual sphere is discussed.

Acknowledgement. Stimulating discussions with G. Arnold, J. T. Jenkins, R. T. Lahey, Jr., S. L. Passman and Graham Wallis helped to shape this work. The support of the U. S. Department of Energy and the U. S. Army Research Office through Contract DAAL 03-86-K-0126 and through the Mathematical Sciences Institute at Cornell is gratefully appreciated.

REFERENCES

Arnold, G. 1988 Ph. D. Thesis, Rensselaer Polytechnic Institute, Troy, NY.

Drew, D. A. 1983 Mathematical Modeling of Two-Phase Flow, *Ann. Rev. Fluid Mech.* **15**, 261.

Jenkins, J. T. and Savage, S. B. 1983 A Theory for the Rapid Flow of Identical, Smooth, Nearly Elastic, Spherical Particles, *J. Fluid Mech.* **130**, 187.

Lamb, H. 1932 *Hydrodynamics*, Cambridge University Press.

Love, A. E. H. 1932 *Mathematical Theory of Elasticity*, Cambridge University Press.

Passman, S. L. 1989 Stress in Dilute Suspensions, *Proc. IMA Workshop on Two-Phase Waves in Fluidized Beds, Sedimentation, and Granular Flows*, to appear.

Taylor, G. I. 1928 The Forces on a Body Placed in a Curved or Converging Stream of Fluid, *Proc. Roy. Soc.*, **A120**, 260- 283.

Voinov, O. V. 1973 Force Acting on a Sphere in an Inhomogeneous Flow of an Ideal Incompressible Fluid. *Zh. prikl. Mekh. tekh. Fiz.*, **14**(4), 592-594.

Wallis, G. B. 1989 Inertial Coupling in Two-Phase Flow: Macroscopic Properties of Suspensions in an Inviscid Fluid, to appear.

The Role of Particle Collisions in Pneumatic Transport

by

E. Mastorakos and M. Louge

Sibley School of Mechanical & Aerospace Engineering

and

J.T. Jenkins

Department of Theoretical & Applied Mechanics

Cornell University, Ithaca, NY 14853

ABSTRACT

A model of dilute gas-solid flow in vertical risers is developed in which the particle phase is treated as a granular material, the balance equations for rapid granular flow are modified to incorporate the drag force from the gas, and boundary conditions, based on collisional exchanges of momentum and energy at the wall, are employed. In this model, it is assumed that the particle fluctuations are determined by inter-particle collisions only and that the turbulence of the gas is unaffected by the presence of the particles. The model is developed in the context of, but not limited to, steady, fully developed flow. A numerical solution of the resulting governing equations provides concentration profiles generally observed in dilute pneumatic flow, velocity profiles in good agreement with the measurements of Tsuji, et al. (1984), and an explanation for the enhancement of turbulence that they observed.

INTRODUCTION

Gas-solid flows satisfy the principles of mass and momentum conservation. While the Navier–Stokes equations govern the motion of the gas phase, there is not yet unanimous agreement upon the form of the equations for the particle phase. Treating this phase as a continuum provides a framework in which techniques such as volume averaging may be used. This two–fluid approach results in the derivation of partial differential equations of motion. Depending on the situation, the stress tensor for the particle phase can then be modeled in order to close the system.

For small particles, dilute in a turbulent gas, momentum transfer in the particle phase is due to turbulent diffusion of the particles. In this regime, Elghobashi & Abou–Arab (1983) have rigorously derived a two–fluid k–ε model that relates the Reynolds stress of the particles to gradients of the mean particle velocity using an eddy viscosity that is a

fraction of the eddy viscosity of the gas. This model predicts the reduction of turbulent energy observed in the presence of small particles (e.g., Modaress, et al., 1984). Other models for this regime include the works of Pourahmadi & Humphrey (1983), Chen & Wood (1985) and Berker & Tulig (1986). However, these models do not apply to gas-solid flows with large and heavy particles.

For large particles, the experiments of Soo, et al. (1960) have shown that the intensity of particle velocity fluctuations may exceed that of the fluid, an observation that cannot be explained by treating the particle response to turbulence. Min (1967) attributed this high particle "turbulence" to particle–wall collisions. In this context, Lourenco, et al. (1983) have successfully modeled the air flow in a 10cm wide horizontal duct loaded with 500μm glass particles. By analogy with molecular dynamics, these authors treat particle collisions using a particle velocity distribution function that satisfies the Boltzmann transport equation. They assume that the distribution is determined by particle collisions rather than by the gas turbulence. In other words, the gas affects the mean velocity of the particles but not their random motion. This assumption is justified in Lourenco's model, because the ratio of particle relaxation time to a typical large eddy turbulent timescale is large (Hinze, 1972). Clearly, the success of Lourenco, et al. encourages further studies of the regime dominated by particle collisions.

Another shortcoming of the two–fluid approach is the lack of attention given to the formulation of correct boundary conditions for the particle phase. Unlike the fluid phase, particles can slip at a boundary. For dilute suspensions of small particles, Soo (1969) suggested, without derivation, a set of boundary conditions by analogy with rarefied–gas dynamics. Clearly, for regimes where collisions dominate momentum transfer among the particles, the boundary conditions of the particle phase should be carefully considered.

In this study, a two–fluid model of the vertical flow in a gas-solid riser is proposed. For simplicity, the model assumes that the flow is fully-developed and steady. Particles are assumed to be sufficiently large or heavy so that momentum transfer in the particle phase is due to particle collisions alone. The granular theory used to describe the particles is related to the kinetic theory of gases, but it is not limited to dilute situations or to elastic particles (e.g., Jenkins, 1987). The conservation laws for mass and momentum in the particle phase have familiar forms. An additional balance law governs the measure $w = \sqrt{\langle v'^2 \rangle / 3}$ of the velocity fluctuations v'. The quantity w is the analog of the molecular temperature. For the particle phase, constitutive relations for the stress tensor and the flux of fluctuation energy are those supplied by the kinetic theory (Chapman & Cowling, 1970) and an existing form

for the collisional dissipation of fluctuation energy is employed (Jenkins & Savage, 1983). Finally, boundary conditions for the mean particle velocity and the granular temperature at a solid surface follow from a detailed description of the particle collision dynamics at the surface (Jenkins, 1988). Such rigorous derivation of the constitutive relations and boundary conditions are a major advantage of the granular flow theory against *ad hoc* continuum models for the particle phase.

In this paper, the granular flow equations given, for example, in Jenkins (1987) are modified to include contributions from the gas. In particular, a drag term is added to the momentum equation and viscous dissipation of the particle rms fluctuating velocity is introduced. The resulting equations, constitutive relations and boundary conditions are presented for a dilute, steady, fully developed, upward flow in a vertical pipe with a circular cross-section. A numerical solution of these equations is obtained and compared with the experimental data of Tsuji, et al. (1984).

THE TWO-FLUID MODEL

Balance Laws

The equations of motion for a steady, fully developed, axi–symmetric upward flow of a dilute gas-solid suspension are:

Gas momentum

$$\frac{1}{r}\frac{d}{dr}(r\,\tau) - \varepsilon\frac{dp}{dz} - \varepsilon\rho g - F = 0\,, \qquad (1)$$

where ε is the volume fraction of the gas, r and z are radial and vertical coordinates, τ is the mean gas shear stress, p is the gas pressure, and F is the force per unit volume exerted by the gas on the particles;

Particle momentum

$$\frac{1}{r}\frac{d}{dr}(r\,S) - (1-\varepsilon)\rho_s g - (1-\varepsilon)\frac{dp}{dz} + F = 0 \qquad (2)$$

and

$$\frac{dN}{dr} = 0\,, \qquad (3)$$

where S is the particle shear stress, ρ_s is the density of the particle, g is the gravitational acceleration, and N is the particle pressure;

Particle fluctuation energy

$$-\frac{1}{r}\frac{d}{dr}(r\,q) + S\frac{dv}{dr} - D - D' = 0\,, \qquad (4)$$

where q is the flux of fluctuation energy, v is the mean particle velocity, and D and D' are, respectively, the rates of collisional and viscous dissipation per unit volume.

Constitutive Relations

1) Volume supplies

Equation (1) is the vertical component of the momentum equation for an incompressible gas exerting drag F on the particle phase. The mean drag is equal to the drag force on a single sphere based on the mean velocities, multiplied by the number of particles per unit volume:

$$F = C_d\,|u-v|\,(u-v)\frac{3\rho}{4d}\,(1-\varepsilon)\,f(\varepsilon)\,, \qquad (5)$$

where u is the mean interstitial gas velocity, d is the particle diameter, and the drag coefficient C_d is given in terms of the particle Reynolds number, Re_p, by

$$C_d = \frac{24}{Re_p}\left[1 + 0.15Re_p^{0.687}\right], \qquad (6)$$

with

$$Re_p = \frac{|u-v|\rho d}{\mu}\,, \qquad (7)$$

in which ρ and μ are, respectively, the density and viscosity of the gas. The drag coefficient C_d is taken from Boothroyd (1971) and it is valid for $0 < Re_p < 1000$. The function $f(\varepsilon)$ is an empirical correction to the drag force on a single particle that allows for the presence of other particles. According to Foscolo and Gibilaro (1984), for the same velocity difference, the drag force per particle increases in the presence of other particles according to

$$f(\varepsilon) \approx \varepsilon^2\,\varepsilon^{-3.8}, \qquad (8)$$

where the ε^2 term accounts for the ratio of superficial to interstitial velocities.

Equations (2) and (3) are the vertical and radial components of the balance of particle momentum in this simple flow. The shear stress and particle pressure result from transport of momentum between collisions exactly as in a dilute gas. The vertical balance includes forces due to gravity, gas pressure gradient, and drag.

The first term of equation (4) is the diffusion of particle fluctuation energy. The second term is the energy produced by mean shear, the third is the rate of energy dissipation per unit volume due to inelastic collisions. In the dilute limit of granular flow, the third term is given by

$$D = \frac{24(1-e)\rho_s}{\sqrt{\pi}\ d}\ w^3(1-\varepsilon)^2\ , \qquad (9)$$

where e is the coefficient of restitution for a particle–particle collision; e=1 for elastic particles. This is obtained by considering the kinetic energy lost in each collision, then averaging over all possible collisions (Jenkins & Savage, 1983).

The fourth term, D', is the rate of energy dissipation per unit volume arising from the drag force on the fluctuating particles. To calculate it, we first write the rate at which energy is gained by a particle as the scalar product of its total velocity and the particle drag force. Ignoring the velocity fluctuations in the gas, this is

$$C_d\,|\,\underline{u} - \underline{v} - \underline{C}\,|\,\frac{3\rho}{4d}(1-\varepsilon)\,(\,\underline{u} - \underline{v} - \underline{C}\,)\bullet(\,\underline{v} + \underline{C}\,)\ , \qquad (10)$$

where $\underline{C}$ is the velocity fluctuation of the particle. Then, upon evaluating the second term in the brackets in equation (6) at the mean velocity difference and averaging over all possible $\underline{C}$, we find that the rate of energy loss per unit volume from the fluctuating motion is

$$D' = \frac{9\rho}{4d} C_d\,|\,u\text{-}v\,|\,(1-\varepsilon)\,w^2\ . \qquad (11)$$

2) Fluxes

In most situations of practical interest, the flow Reynolds number is high enough for the gas to be turbulent. For simplicity, the mean gas shear stress is modeled using an eddy viscosity μ_t,

$$\tau = \varepsilon\,(\mu + \mu_t)\,\frac{du}{dr}\ . \qquad (12)$$

In this work, μ_t is approximated using a polynomial fit to the experimental results for turbulent gas flow in a pipe (Hinze, 1975, Sec. 7-13). Thus, we assume that the gas Reynolds stress is unaffected by the presence of particles. We note, however, that several experimental observations have shown that large particles enhance the turbulence, even for conditions as dilute as $(1-\varepsilon) \approx 0.1\%$ (e.g., Tsuji, et al., 1984 and Lee & Durst, 1982). Our view is that any treatment of the gas turbulence should not ignore the details of the particles' motion. In particular, the "pure" turbulent fluctuations in the gas must be distin-

guished from the randomness induced by particle fluctuations and the resulting change of the structure of turbulence must be quantified. Here, for simplicity, we ignore the influence of these induced fluctuations on the eddy viscosity. For a discussion of these effects, see the experiments of Boothroyd (1967), Nouri, et al. (1987), Tsuji, et al. (1984), and Modaress, et al. (1984), and the theoretical discussions of Owen (1969), Elghobashi & Abou–Arab (1983) and Genchev & Karpuzov (1980).

The constitutive relations for the particle shear stress S, the particle pressure N, and the flux of fluctuation energy q for dilute flows of smooth, nearly elastic spheres, are identical to those provided by Chapman & Cowling (1970, Secs. 7.4, 7.41, and 10.21):

$$S = \frac{5\sqrt{\pi}}{96} \rho_s d\, w\, \frac{dv}{dr}, \tag{13}$$

$$N = (1-\varepsilon)\, \rho_s\, w^2, \tag{14}$$

and

$$q = -\frac{25\sqrt{\pi}}{64} \rho_s d\, w^2 \frac{dw}{dr}. \tag{15}$$

The shear stress is Newtonian and the particle viscosity is proportional to the rms fluctuating velocity and the particle diameter. The energy flux is proportional to the gradient of $3w^2/2$, the fluctuation energy per unit mass, and the corresponding coefficient depends linearly upon d and w. In equations (13) through (15), we assume that the particles do not respond to the turbulent fluctuations, so that the particle velocity distribution function is unaffected by the gas fluctuations. From Hinze (1972), this is true if

$$\frac{\Lambda}{d} << \sqrt{\frac{u'\Lambda}{\nu} \frac{\rho_s}{\rho}}, \tag{16}$$

where Λ is the integral lengthscale of turbulence, u' the rms turbulent gas velocity and ν the kinematic viscosity of the gas.

Boundary Conditions

Jenkins (1988) has recently derived boundary conditions for flows of nearly elastic but frictional spheres that interact through collisions with a flat frictional wall. Consideration of the balance of linear momentum, angular momentum, and energy in a single collision and some simple averaging provide the rate per unit area at which momentum and energy are being supplied to the flow by the wall. Boundary conditions are obtained when these are related to the shear stress and energy flux in the flow, evaluated at the wall. When

the mean spin of the particles is assumed to be half the vorticity of the mean particle velocity and fluctuations in the spin are ignored, these conditions are, in the limit of large friction,

$$S = - (2/\pi)^{1/2} (N/7w) [v + (d/4) (dv/dr)] \tag{17}$$

and

$$q = - (2/\pi)^{1/2} N \{ (1/14w) [v + (d/4) (dv/dr)]^2 - (1-e_w+1/7)w \} , \tag{18}$$

where e_w is the coefficient of restitution of the particle-wall collision. Consequently, upon adopting the no-slip condition for the gas velocity at the wall and employing the constitutive relations (13) and (15), the values of u, v and w at the wall must satisfy

$$u = 0 , \tag{19}$$

$$\frac{dv}{dr} = A \frac{v}{d} , \tag{20}$$

and

$$\frac{dw}{dr} = B \frac{w}{d} , \tag{21}$$

where

$$A = - 384\sqrt{2} (1-\varepsilon) / \{ 7[20\pi + 96\sqrt{2} (1-\varepsilon)] \} \tag{22}$$

and

$$B = \frac{32\sqrt{2}}{175\pi} (1-\varepsilon) \{ (\frac{v}{w})^2 [1- (\frac{A}{4})^2] - 14(1- e_w + \frac{1}{7}) \} . \tag{23}$$

The second set of boundary conditions is provided by symmetry. At the centerline,

$$\frac{du}{dr} = \frac{dv}{dr} = \frac{dw}{dr} = 0 . \tag{24}$$

RESULTS AND DISCUSSION

Equations (1), (2), and (4) are solved numerically using a simple iterative finite difference algorithm. To verify the predictions of the model, gas and particle velocity profiles are now compared with detailed measurements in a vertical pipe. Using a laser-döppler-anemometer, Tsuji, et al. (1984) measured gas and particle velocity profiles in a vertical pipe of 30.5 mm ID. In these experiments, polystyrene particles (ρ_s = 1020 kg/m^3, d = 500μm) were suspended in air with ratios of particle-to-gas mass flow rates (loading) as

high as 3.6. Because the integral lengthscale Λ is of the order of the pipe radius, $\Lambda/d \approx 30$ and $[(u'\Lambda/\nu)\,(\rho_s/\rho)]^{1/2} \approx 600$. Therefore, Hinze's criterion (16) is clearly satisfied. Under these conditions, the particles cannot follow the gas turbulence. In the calculation we assume coefficients of restitution of 0.9 and 0.8 for particle–particle and particle–wall collisions, respectively. We input the pressure gradient in the gas and the particle concentration at the wall and adjust these until we agree with the measured gas velocity at the centerline and the measured loading in the experiments.

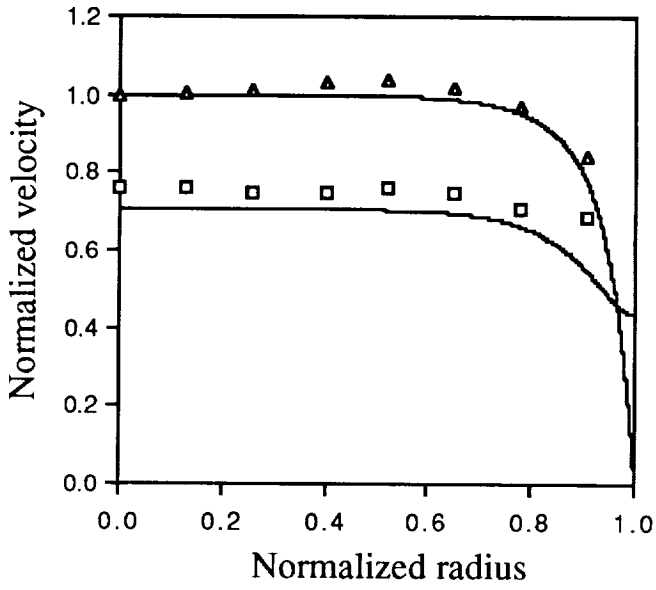

Fig. 1. Calculated gas and particle velocity profiles compared with the data from Tsuji, et al. (1984). The calculated velocities are normalized with the calculated gas velocity at the centerline (7.9 m/s), while the measured velocities (triangles: gas, squares: particles) are normalized with the measured gas velocity at the centerline (8.1 m/s). The ratio of gas–to–particle mass flow rates is 3.6.

Figure 1 shows good agreement between the measured mean velocities and the predictions of the model. At the centerline, the gas velocity is reproduced to within 5%, and the particle slip velocity to within 10%. However, the gas velocity profile near the wall differs from the model predictions. This difference is not altogether surprising, considering the simplicity of the gas equations used. Nevertheless, the overall agreement in the gas phase is good, because the term that dominates the gas momentum equation is not the Reynolds stress, but the difference between the pressure gradient and the particle drag.

The predicted particle velocity at the wall is positive, although not as high as the experimental value. Comparable observations were made by Lee and Durst (1982) in a

similar situation. At first sight, these observation might be surprising; because the gas velocity is zero at the wall, one might expect the particles to fall. In fact, there is a region near the wall where the particles can acquire a velocity higher than that of the gas. This effect results from the shear stress in the particle phase. Particles further from the wall are lifted by the gas and, through the particle shear stress, they lift the particles closer to the wall. Clearly, the details of the momentum exchange in the particle phase are essential for an accurate description of the flow.

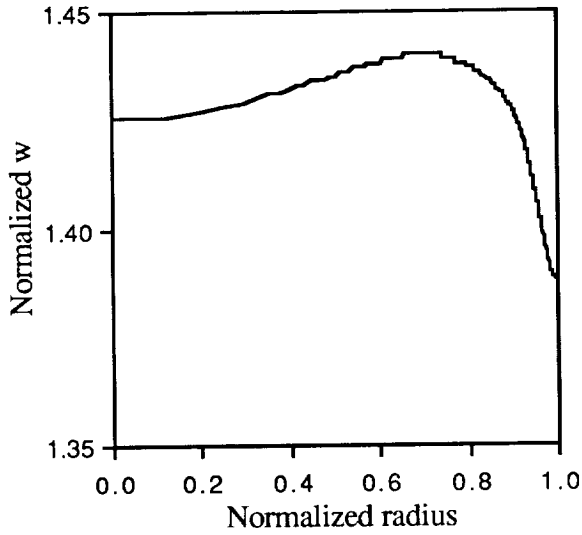

Fig. 2. Particle fluctuation velocity normalized with the calculated gas centerline velocity.

Figure 2 shows the radial distribution of kinetic energy. In this case, w increases away from the wall. There is a slight decrease in energy in the immediate neighborhood of the wall followed by an increase into the interior. In more dense flows the supply or dissipation of energy by the wall is expected to be more important. The particle volume fraction is calculated using equation (14), and it decreases away from the wall (Figure 3). Unfortunately, these predictions cannot be compared with the experiments of Tsuji, et al. (1984), who did not measure the particle velocity fluctuations or the concentration of the particle phase. Nevertheless, the predicted concentration profile agrees qualitatively with other experiments in pneumatic transport (e.g., Boothroyd, 1971 and Kramer & Depew, 1972). Several explanations have been proposed for these larger particle concentrations near the wall. Boothroyd (1971) attributes this to electrostatic forces, while Berker & Tulig (1986) invoke non-gradient turbulent diffusion. In the regime dominated by particle collisions, be-

cause of the constant particle normal stress and the constitutive relation (14), this trend is a direct result of the profile of fluctuation energy.

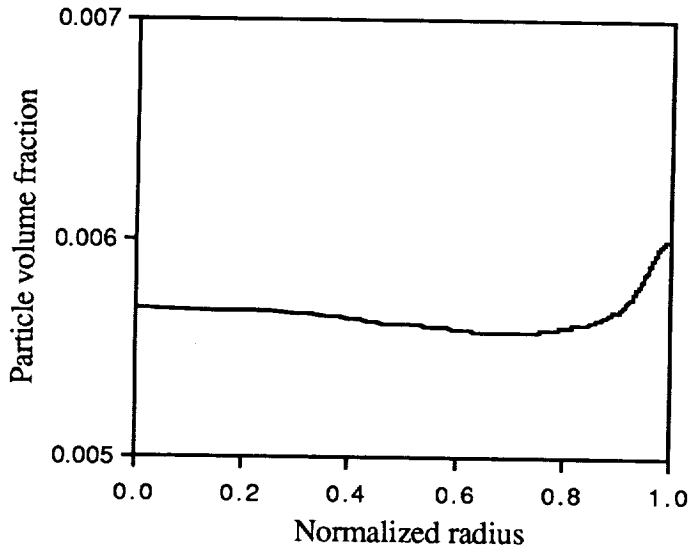

Fig 3. Profile of particle volume fraction.

Finally, we propose that the enhancement of the gas turbulence observed by Tsuji, et al. (1984) in the presence of large particles is due to fluctuations in the gas induced by the random motion of the particles. Turbulent enhancement of the order of our calculated w were measured for the 500μm particles by Tsuji, et al. (1984), and the strength of the turbulence was observed to increase with particle diameter.

ACKNOWLEDGEMENTS

This work was supported in part by a Research Initiation Grant no CBT-8809347 from the National Science Foundation and by grant no DE-FG22-88PC88929 from the US Department of Energy.

REFERENCES

A. Berker & T. J. Tulig, "Hydrodynamics of Gas–Solid Flow in a Catalytic Cracker Riser: Implications for Reactor Selectivity Performance", *Chem Engng Sci* **41**, 821 (1986).

R. G. Boothroyd, "Turbulence Characteristics of the Gaseous Phase in Duct Flow of a Suspension of Fine Particles", *Trans Instn Chem Engrs* **45**, T297 (1967).

R. G. Boothroyd, Flowing Gas–Solid Suspensions, Chapman & Hall, London, 1971.

S. Chapman & T. G. Cowling, The Mathematical Theory of Non-Uniform Gases, Third Ed., Cambridge University Press, 1970.

C. P. Chen & P. E. Wood, "A Turbulence Closure Model for Dilute Gas–Particle Flows", *Can J Chem Engng* **63**, 349 (1985).

S. E. Elghobashi & T. W. Abou–Arab, "A Two–Equation Turbulence Model for Two–Phase Flows", *Phys Fluids* **26**, 931 (1983).

P. U. Foscolo & L. G. Gibilaro, "A Fully Predictive Criterion for the Transition between Particulate and Aggregate Fluidization", *Chem Engng Sci* **39**, 1667 (1984).

Zh. D. Genchev & D. S. Karpuzov, "Effects of the Motion of Dust Particles on Turbulence Transport Equations", *J Fluid Mech* **101**, 833 (1980).

J. O. Hinze, "Turbulent Fluid and Particle Interaction", *Progress in Heat and Mass Transfer* **6**, 433 (1972).

J. O. Hinze, Turbulence, Second Ed., McGraw–Hill, New York, 1975.

J. T. Jenkins, "Rapid Flows of Granular Materials", in Non–Classical Continuum Mechanics, R. Knops & A. Lacey, eds., Cambridge University Press, 1987, pp. 213-225.

J.T. Jenkins, "Boundary Conditions for Granular Flows: Flat Frictional Walls" (in preparation).

J.T. Jenkins and S.B. Savage, "A Theory for the Rapid Flow of Identical, Smooth, Nearly Elastic, Spherical Particles", *J. Fluid Mech.* **130**, 187 (1983).

T. J. Kramer & C. A. Depew, "Experimentally Determined Mean Flow Characteristics of Gas–Solid Suspensions", ASME paper 72–FE–29 (1972).

S. L. Lee & F. Durst, "On the Motion of Particles in Turbulent Duct Flows", *Int J Multiphase Flow* 8, 125 (1982).

L. Lourenco, M. L. Riethmuller & J–A. Essers, "The Kinetic Model for Gas–Particle Flow and its Numerical Implementation", in the Proceedings of the International Conference on the Physical Modelling of Multiphase Flow, Coventry, England, April 1983, p. 501.

K. Min, "Intensity of Particle Motion in Solid–Gas Suspension Flow", *J Appl Phys* **38** (2), 564 (1967).

D. Modaress, H. Tan & S. Elghobashi, "Two–Component LDA Measurements in a Two–Phase Turbulent Jet", *AIAA Journal* **22**, 624 (1984).

J. M. Nouri, J. H. Whitelaw & M. Yianneskis, "Particle Motion and Turbulence in Dense Two–Phase Flows", *Int J Multiphase Flows* **13**, 729 (1987).

P. R. Owen, "Pneumatic Transport", *J Fluid Mech* **39**, 407 (1969).

F. Pourahmadi & J. A. C. Humphrey, " Modeling Solid–Fluid Turbulent Flows with Application to Predicting Erosive Wear", *Physico-Chemical Hydrodynamics* **4**, 191 (1983).

S. L. Soo, H. K. Ihrig, Jr., and A. F. El Kouh," Experimental Determination of Statistical Properties of Two–Phase Turbulent Motion", Trans. ASME, *J. Basic Eng.* **82D**, 609 (1960).

S. L. Soo, "Pipe Flow of Suspensions", *Appl Sci Res* **21**, 68 (1969).

Y. Tsuji, Y. Morikawa & H. Shiomi, "LDV Measurements of an Air–Solid Two–Phase Flow in a Vertical Pipe", *J Fluid Mech* **139**, 417 (1984).

Scaling and Modeling of Turbulent Suspension Flows

C. P. Chen
Department of Mechanical Engineering
University of Alabama in Huntsville
Huntsville, AL 35899

Introduction

The challenge of the study of gas-solid turbulent flows arises because of the complexity of physical interactions between the two phases. Research needs are also not universal for different situations. Depending on the particle loading ratios, particle sizes and particle-particle collision frequencies, the flow of gas-particle mixture law can be classified as dense flows or dilute flows. The characteristic dimensions of the distribution of particles in turbulent flows may determine whether the two-phase mixture can be regarded as a continuum or not [1,2]. In a dilute suspension flow in which particle motion is controlled by the aerodynamic forces on the particle, Crowe [3] has suggested a criterion for treating the particle cloud as a continuum. In this case, the Stokes number (St) which is defined $St = v_r t_* / \lambda_c$, where v_r is the slip velocity between two phases, t_* is the particle relaxation time and λ_c the distance traveled between collisions, should be less than 0.1 and depending on the magnitude of flow Reynolds number, boundary conditions for particulate phase have to be modified.

In this paper, scaling factors determining various aspects of particle-fluid interactions and the development of physical models to predict gas-solid turbulent suspension flow fields will be discussed based on two-fluid, continua formulation.

Scaling Rules

The motions of particles in a turbulent flow field are determined by relative density, particle size, inertia, free fall velocity, as well as the correlation between particles and underlying flow turbulence. On the other hand, the particulate phase may influence the turbulence energy spectrum of the gas phase in wave number ranges corresponding to the size of spacing of dispersed-phase dimensions [4]. To investigate the various modes of interaction, the relaxation time t_* of particles has to be compared with various characteristic times of the underlying flow field. t_*, in its simplest definition $\equiv \frac{1}{18} \frac{\rho_s}{\rho} \frac{d_p^2}{\nu}$, is a measure of how quickly a particle of density ρ_s and diameter d_p can respond to changes in the ambient fluid velocity, ν is the kinematic viscosity of the fluid. In the continuum mixture theory, t_* can be redefined based on a particle Reynolds number weighted by the concentration of

solids [5]. If t_* is small compared with a time scale corresponding to some particular flow structure, then the particle will follow the motion of that structure; if not, the particle will tend to be uncoupled from these motion.

Hinze [4] pointed out that the dynamic behavior of a discrete particle will not be determined by the eddies of size much smaller than that of the particles. The effect of these smaller eddies will tend to average out over the particle surface. In the case of turbulent flows, this requires that the particle size be smaller than the important dynamic scales of turbulence before the time scale ratio becomes a useful measure of the particle-fluid interaction.

Let us consider the dynamically smallest eddies in the turbulent flow. These eddies can be characterized by the Kolmogorov microscale η, and the characteristic time scale τ is of order $(\nu/\epsilon)^{1/2}$. The ratio of the particle relaxation time to this time then becomes $\frac{t_*}{\tau} \sim \frac{d_p^2}{\eta^2}\frac{\rho_s}{\rho}$. So for the typical suspension problem we are interested in, i.e., $\rho_s/\rho \geq O(10^2)$, the particles have to be at least one order of magnitude smaller than the Kolmogorov length scale in order to be subjected to the motion of the smallest eddies.

Direct interaction between particles which results from particle-particle collisions can be estimated from the ratio of t_* and the time scale between particle collisions t_c which is given [4] $\sim O(\frac{1}{v_r d_p^2 n})$ for particles of uniform size d_p. v_r is the relative velocity between particles and n is the particle number density. For the case $t_*/t_c \ll 1$, the particle has time to respond to the local velocity field before the next collision so its motion is dominated by the supporting flow forces and the collision which leads to direct interaction between particles can be neglected. Then a solid particle is subjected to a variety of time-varying forces by the ambient fluid flow. For particles with $\rho_s/\rho > 10^2$, the governing forces due to inertia effect (drag) and crossing trajectory effect have been singled out [6,7,8]. To describe the behavior of particles in a turbulent flow, the simplified Basset, Boussinesq and Oseen (BBO) equation has to be solved. This equation in principle cannot be solved unless the relation of the Lagrangian and Eulerian correlations of the random fluid field is known rigorously. However, the particle trajectory can be determined similar to a random walk computation [9] in which a dispersed-phase element is assumed to interact with an typical turbulent eddy as long as the relative displacement of the element with respect to the eddy does not exceed the characteristic eddy size, l_e, and the time of interaction does not exceed the characteristic eddy time, t_e. The selections of l_e and t_e are cleanly arbitrary since turbulent flows composed a spectrum of length scales and time scales.

To gain some insight of the scaling rule for turbulent dispersion, the fundamental dispersion results of Snyder and Lumley [6] are used to compare with the stochastic predictions. The experiments involved the dispersion of individual particles which were isokinetically injected into a grid-generated turbulent flow. The mean flow are uniform in the test region and the detailed turbulent structure were measured downstream of the

injection point. Since the grid-generated turbulent field is homogeneous decaying and is approximately isotropic with fluctuating intensity decreasing in the direction of the mean flow. Typically, grid turbulence is also characterized by self-similar spectral distribution in which a local set of characteristic eddy time scale can be identified. Following Gosman and Ioannides, the eddy time scale is evaluated from the expression $t_e = l_e(\frac{2k}{3})^{-\frac{1}{2}}$ and $l_e = C_\mu^{\frac{3}{4}} k^{\frac{3}{2}}/\epsilon$, where k is the turbulent kinetic energy $(= \frac{1}{2}\overline{u_i' u_i'})$ and ϵ is the isotropic turbulent kinetic energy dissipation rate and $C_\mu = 0.09$. The ratios of t_* over eddy time scales for the three types of mono-dispersed particles used in Snyder and Lumley's experimental setup are plotted on Figure 1. Mean-squared radial dispersion of the particles is plotted as a function of the residence time in the flow for three types of particles.

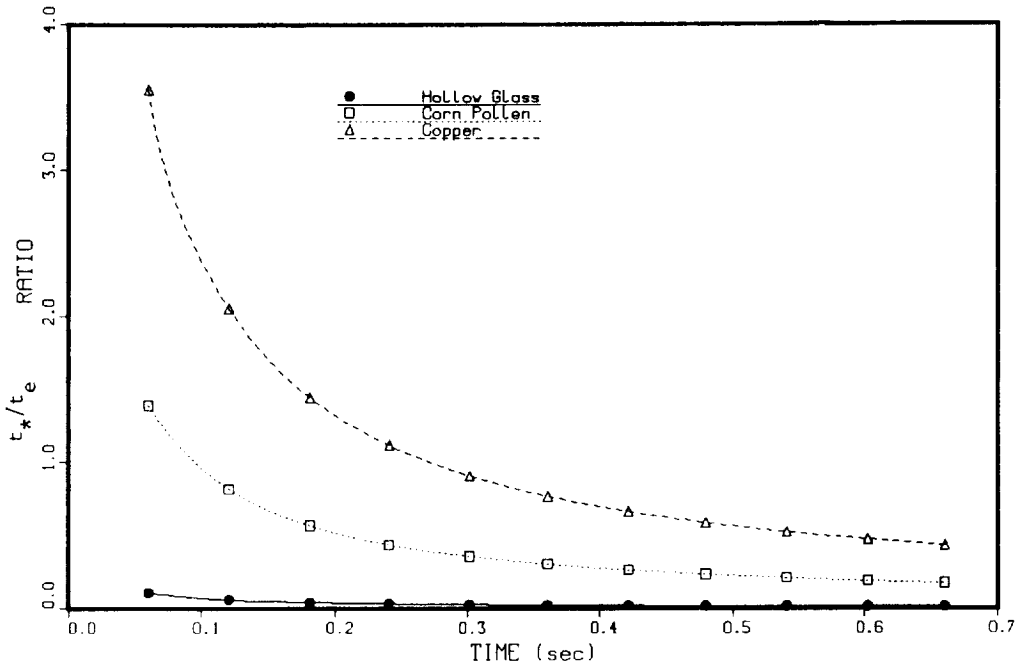

Figure 1. Time scale ratio of various particles in a uniform grid generated turbulent flow

The results are obtained by averaging over 2000 particles following a 4th-order Runge-Kutta integration of the simplified BBO equation (only inertia term retained) using 10 percent of interaction time as integration time step. The agreement between the stochastic model predictions and the measurements for the case of corn pollen (with material density $1000kg/m^3$ and $87\mu m$ diameter) are much better compared to the other two cases of hollow glass particles and copper particles. This is not surprising in viewing the scaling rules involved (see Figure 1): the corn pollen particles are most closely associated with the turbulent time scales responsible for dispersion. For light particle such as glass particles, the turbulent eddies responsible for the dispersion should be of higher frequency (smaller time scales), probably Kolmogorov time scales. The net results is that the numerical model underpredicts the dispersion. On the other hand, copper particles should interact

with eddies associated with larger time scales. Using the integral time scale (t_e) results in overpredicting the turbulent dispersion by inertia effects.

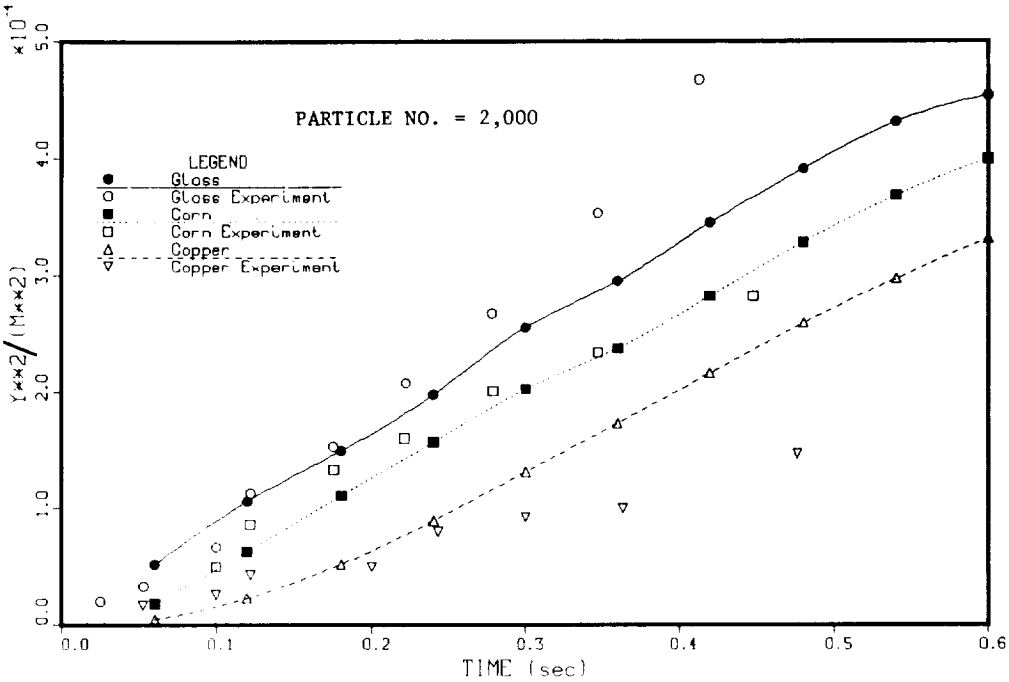

Figure 2. Predicted and Measured particle dispersion in a uniform grid generated turbulent flow

The numerical models used for the calculation in this study do not account for the crossing trajectory effect due to the particle free fall. For the particles studied, especially heavy particles, inertia and crossing trajectories are inseparable at the very downstream of the decay. According to the scaling rule, gravity has an influence on the two-phase flow when $u_t \cong u'$, where u_t is the terminal velocity ($= gt_*$) and u' is the characteristic velocity scale of turbulence. In the grid turbulence $\frac{u'^2}{U_M^2} \propto (\frac{x}{M})^{-1}$, thus we expect the free-fall effects to be insignificant in the decay of the grid turbulence if $\frac{x}{M} \ll O(\frac{U_M}{gt_*})^{1/2}$. Here, U_M is the mean longitudinal velocity along x-axis and M is the mesh size. Only for the smaller particles with $t_* \leq 10$ msec this condition can be satisfied. However, the above calculations indicate the close relationship between the scale parameters and the particle-fluid interactions.

Two-Phase Turbulence Modeling

In most turbulent multiphase flows of practical interest there exists a spectrum of dispersed phase time and length scales. Despite the abundant use of single time and length scale models (such as the $k - \epsilon$ model), the underlying carrying gas turbulence is also dominated by a variety of time scales. A two-phase two-scale turbulence model

based on continuum approach has since been developed [10] according to the scaling rule described above. The modification of particles on the turbulence, the so called modulation effect, has been taken into account for large eddies by mean slip between two phase and small eddies caused by the particle slip velocity on the fluctuation level.

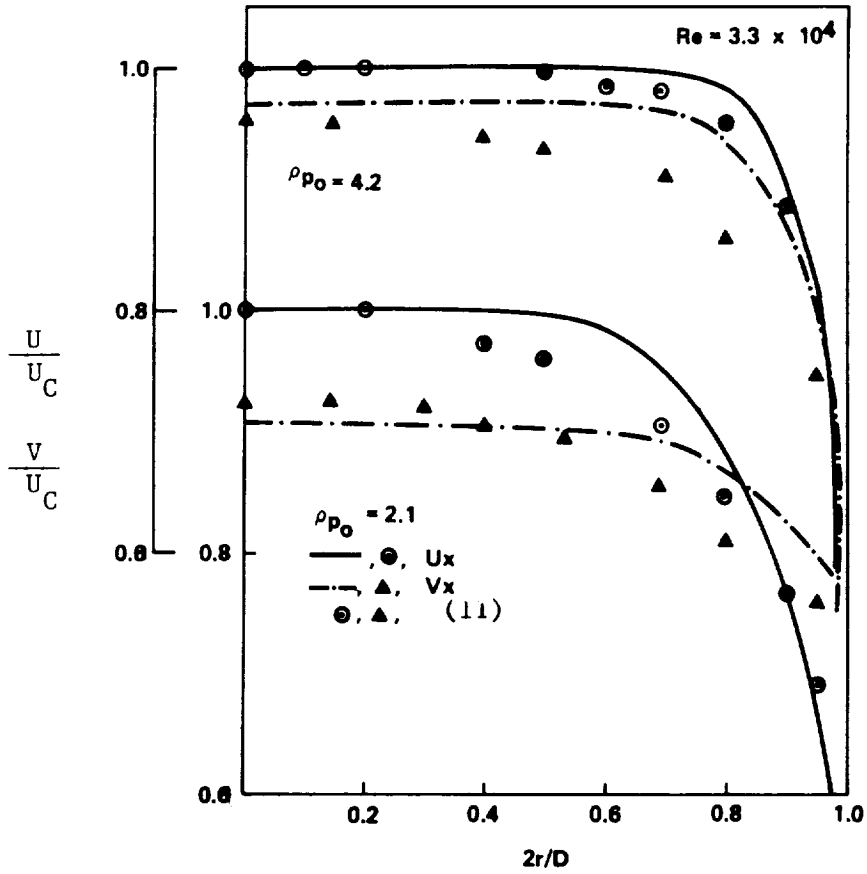

Figure 3. Mean axial velocity profiles across the pipe of gas phase and particulate phase

The turbulent transport equations are summarized here:

$$\frac{\partial}{\partial x_i}(U_i k_p) = \frac{\partial}{\partial x_i}(\frac{\nu_t}{\sigma_{k_p}}\frac{\partial k_p}{\partial x_i}) + P_k - \epsilon_p - \frac{\overline{\rho_p' u_i'}}{\rho t_*}(1 + 0.79\sqrt{Re_p} + 0.013 Re_p)(U_i - V_i) \quad (1)$$

$$\frac{\partial}{\partial x_i}(U_i k_t) = \frac{\partial}{\partial x_i}(\frac{\nu_t}{\sigma_{k_t}}\frac{\partial k_t}{\partial x_i}) + \epsilon_p - \epsilon_t - \frac{2k}{t_*}\frac{\overline{\rho_p}}{\rho}(1 - exp[-\frac{1}{2}\frac{t_*}{\tau}]) \quad (2)$$

$$\frac{\partial}{\partial x_i}(U_i \epsilon_p) = \frac{\partial}{\partial x_i}(\frac{\nu_t}{\sigma_{\epsilon_p}}\frac{\partial \epsilon_p}{\partial x_i}) + \frac{\epsilon_p}{k_p}(C_{p1} P_k - C_{p2}\epsilon_p) \quad (3)$$

$$\frac{\partial}{\partial x_i}(U_i \epsilon_t) = \frac{\partial}{\partial x_i}(\frac{\nu_t}{\sigma_{\epsilon_t}}\frac{\partial \epsilon_t}{\partial x_i}) + \frac{\epsilon_p}{k_p}(C_{t1}\epsilon_p - C_{t2}\epsilon_t) - 2\frac{\overline{\rho_p}}{\rho}\frac{\epsilon_t}{t_*} \quad (4)$$

Here, the k_p and k_t are turbulent kinetic energy of the large-scale energetic eddies and the small-scale transfer eddies and ϵ_p is the energy transfer rate from the large eddies to the transfer eddies. This model composed of two set of scales for gas-phase turbulence. The model is valid for the situation $\tau_p(=\frac{k_p}{\epsilon_p}) \geq t_* \gg \tau$ (Kolmogorov time scale) and particle loading ratio (ρ_p/ρ) of order of 1. This model has been applied to a gas-solid suspension pipe flow by Tsuji et al [11]. In Figure 3, the comparisons are made for two particle loadings with $d_p = 200\mu m$. The predicted velocity profiles are flatter than the experimental data and the relative velocities between two phases decrease with increasing particle loadings. The distance of the sign change of the slip velocity shifts toward the wall for larger particle loadings. The flattening effect by the particles on the fluid velocity distributions can be observed in the Figure 4. Besides this flattening effect, the point of maximum gas phase velocity even deviates from the pipe axis as the loading increases. Such a concave profile indicate counter-diffusion type of momentum transport and cannot be predicted by the current model. It is interesting to note that such profiles were not found in other LDV measurements for similar configuration [12,13], this phenomena should await further experimental confirmation.

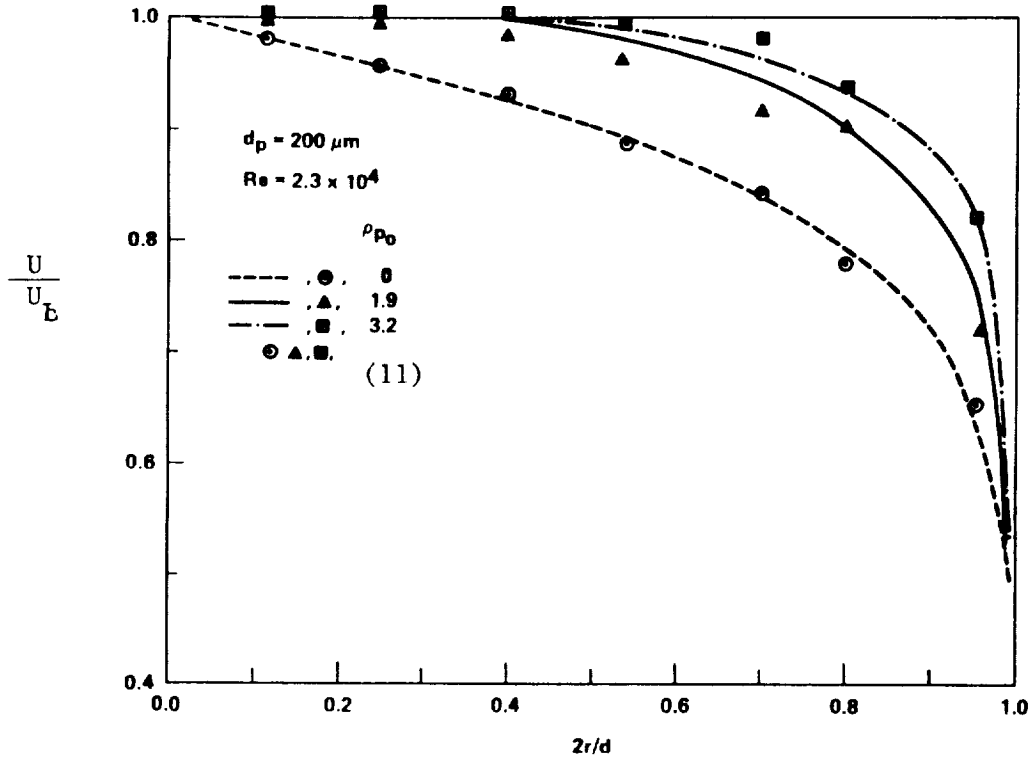

Figure 4. Effect of particle loadings on gas phase velocity profiles

The modulation effect of particles on the turbulence is shown in Figure 5 for longitudinal turbulence intensity profiles for $200\mu m$ particles. Cases with particle size greater than $200\mu m$ were not computed due to model limitation based on the scaling rules. It is

known that fluid turbulence is greatly influenced by the particles and the mode of influence differs with particle size. For larger particles ($\geq 300\mu m$), the turbulence intensities of the fluid are increased due to the presence of particles while suppression of the turbulence properties is observed for smaller particles. It is seen in Figure 5 that for a particle loading of 0.9 the turbulence intensities are reduced by 30 % in the core region. However, the intensity in the core region increases again as the particle loading increases from 0.9 to 3.2 and the intensity in the wall region is monotonously damped. This phenomenon can be explained by the competitive mechanism between modulation due to mean motion and fluctuation motion. The small scale modulation effect always acts as a sink term in the k_t equation while the large eddy motion modulation effect can be extra production or dissipation depending on the signs of $(U_i - V_i)$ and the distribution of mean particle density profiles. The cross-over of the intensity profiles is closely related to the cross-over of mean velocity profiles of gas phase and particulate phase. The relative magnitude of the modulation effects is reasonably well represented by the model.

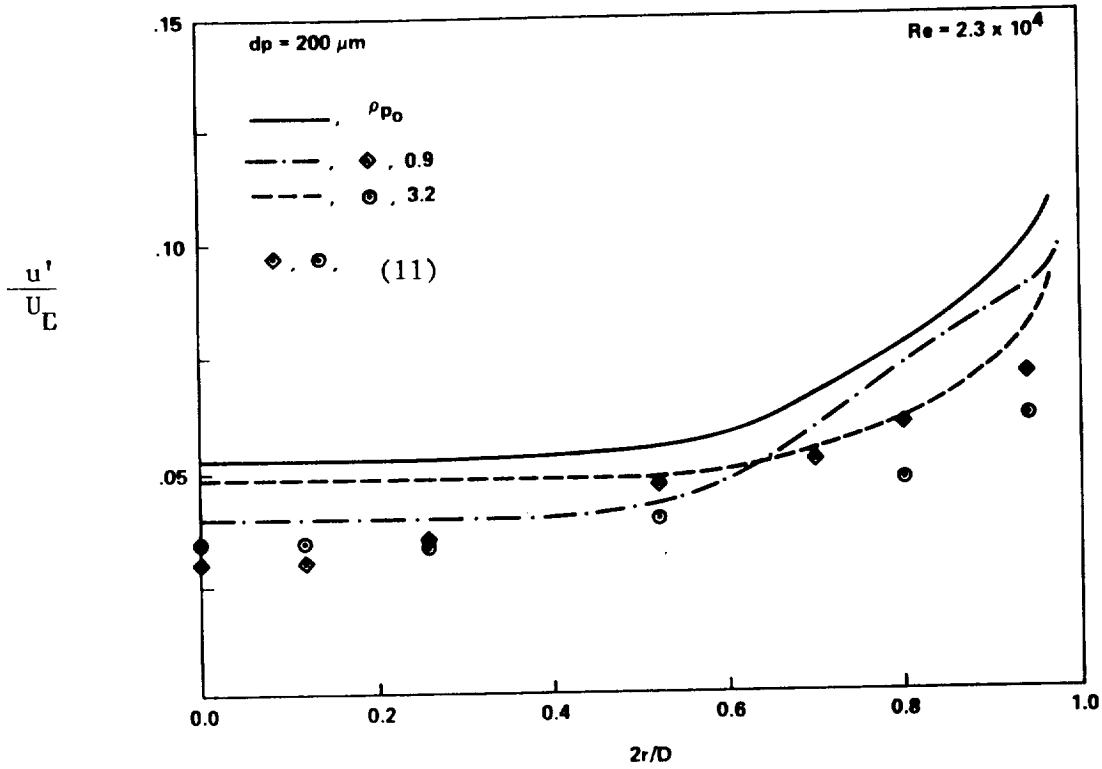

Figure 5. Modulation Of particles on gas phase turbulence intensities

Summary

The modes of particle-fluid is discussed based on the length and time scale ratio, which depends on the properties of the particles and the characteristics of the flow turbulence. For particle size smaller than or comparable with the Kolmogorov length scale and con-

centration low enough for neglecting direct particle-particle interaction, scaling rules can be established in various parameter ranges. The various particle-fluid interaction will give rise to additional mechanisms which will affect the fluid mechanics of the conveying gas phase. These extra mechanisms are incorporated into turbulence modeling method based on the scaling rules. A multiple-scale two-phase turbulence model has been developed, which gives reasonable predictions for dilute suspension flow. Much works is yet to be done to account for the poly-dispersed effects and the extension to dense suspension flows.

Acknowledgements

This work was partially supported by NASA-Marshall Space Flight Center (NAS8-36718).

Reference

1. Lumley, J.L., "Two-Phase and Non-Newtonian Flows," Chapter 7 in Turbulence, ed. P. Bradshaw, Springer-Verlag, 1978.
2. Soo, S. L., Fluid Dynamics of Multiphase System, Blaisdell Pub., 1967.
3. Crowe, C. T., "Two-Fluid versus Trajectory Models," Gas-Solid Flows, ASME FED 35, 91, 1986.
4. Hinze, J. O., Prog. Heat Mass Transfer, 6, 433,1972.
5. Givler, R. C. and Mikatarian, R. R., J. of Fluid Eng. 109, 325, 1987.
6. Snyder, W. H. and Lumley, J. L., J. Fluid Mech. 48, 41, 1971.
7. Calabrese, R. V. and Middleman, S., AIChE. J. 25, 1025, 1979.
8. Wells, M. R. and Stock, D. E., J. Fluid Mech. 136, 31, 1983.
9. Gosman, A. D. and Ioannides, E., AIAA Paper 81-0323, 1981.
10. Chen, C. P., "Numerical Analysis of Confined Recirculating Gas-Solid Turbulent Flows," Gas-Solid Flows, ASME FED 35, 117, 1986.
11. Tsuji, Y. et. al., J. Fluid Mech. 139, 417, 1984. 109, 325, 1987.
12. Steimke, J. L. and Dukler, A. E., Int. J. Multiphase Flows, 9, 751, 1983.
13. Lee, S. L. and Durst, F., Int. J. Multiphase Flows, 8, 125, 1982.

N90-10394

TURBULENCE KINETIC ENERGY EQUATION FOR DILUTE SUSPENSIONS

T.W. Abou-Arab and M.C. Roco*
Department of Mechanical Engineering
University of Kentucky
Lexington, KY 40506, USA

ABSTRACT

This paper presents a multiphase turbulence closure employing one transport equation, namely the turbulence kinetic energy equation. The proposed form of this equation is different from the earlier formulations in some aspects. The power spectrum of the carrier fluid is divided into two regions, which interact in different ways and at different rates with the suspended particles as a function of the particle-eddy size ratio and density ratio. The length scale is described algebraically. A mass/time averaging procedure for the momentum and kinetic energy equations is adopted. The resulting turbulence correlations are modeled under less restrictive assumptions comparative to the previous work. The closures for the momentum and kinetic energy equations are given. Comparisons of the predictions with experimental results on liquid-solid jet and gas-solid pipe flow show satisfactory agreement.

NOMENCLATURE

a	amplitude ratio
$\underline{b}$	body force
$C_1, C_{\phi 1}, C_{\phi 2}, C_{\phi 3}, C_{\phi 4}, C_{\phi 5}, C_D, C_\mu$	= constants
d	particle diameter
D	turbulent diffusion coefficient for solid phase
$E(\kappa)$	energy spectrum
f	flow variable
$(\underline{I}_K)_{-K}$	interaction term
$\underline{J}_\phi$	flux vector for a variable ϕ
k	kinetic energy of turbulence
ℓ	length scale
N_S	Stokes number
$K(\underline{r},t)$	phase distribution function, Eq. (1)
p	pressure
$\underline{r}$	position vector
Re	Reynolds number based on the most energetic eddy size
$t, \Delta T, \Delta t$	time and averaging time intervals corresponding to the turbulence production and transfer range, respectively
u, v	Eulerian and Lagrangian velocities, respectively
$V, \Delta v$	volume and averaging volume, respectively
x_i, x_j, x_n	Cartesian coordinates
y	distance from the wall
α	concentration of volume
ϵ	dissipation rate of turbulence kinetic energy
η	Kolmogorov length scale
κ	wave number
μ	dynamic viscosity
ρ	density
σ	turbulent Schmidt/Prandtl number
τ	shear stress

Subscripts

i,j,n	denote Cartesian coordinates (= 1,2,3)
e	eddy
k	turbulence kinetic energy
K	flow component K
KP	phase K in the production range
KT	phase K in the transfer range
ℓ	laminar
L,S	denote liquid and solid, respectively
P	production range
t	turbulent
T	transfer range
Tot	total
Σ	average over area
ϵ	dissipation rate of turbulence kinetic energy

Superscripts

$\bar{f}$	mass average of f
f^t	turbulence fluctuation of f
f'	fluctuation of f at low wave number (production range)
f''	fluctuation of f at intermediate wave number (transfer range)
P	production
T	transfer
$\bar{f}^K, f_K$	volume/time and mass/time averages of f over K
$\langle f_K \rangle$	intrinsic space average of f over K

(*) - For further correspondence;
On sabbatical leave at Caltech 104-44, CA 91125, until May 30, 1989.

1. INTRODUCTION

Multiphase flows are widely applied in engineering processes from chemical, petroleum, mining and other industries. Various theoretical and experimental techniques for the investigation of those flows are available. Some of them are a straightforward extension from the single phase flow models by introducing some ad hoc modifications. Other investigations originate from the gas-solid flow (Soo, 1983) or fluidized bed models (Wang et al., 1988).

Increasing concern for the prediction of turbulent multiphase flows have been noticed during the last twenty years (Danon et al. (1974), Al-Taweel and Landau (1977), Genchev and Karpuzov (1980) , Melville and Bray (1979), Crowe and Sharma (1978), Michaelides and Farmer (1983), and Shuen et al. (1983)). Two equation turbulence models have been proposed for dilute particulate flows by Elghobashi et al. (1982, 1983, 1984) and Crowder et al. (1984). Algebraic and one equation turbulence models have been suggested also for dense liquid-solid flows (Roco et al., 1983, 1985, 1986) in which the particle-particle interactions play an important role besides the fluid-fluid and fluid-solid interactions. Most of these studies as well as other earlier investigations have some limitations. In the above mentioned studies the response of solids to the turbulent fluctuations of the carrier fluid is obtained under restrictions similar to those refered by Hinze (1975, p. 460), which limit their use. In addition to that, empirical constants and empirical functions are usually introduced in these models.

The purpose of the present paper is

i) To propose a specific mass/time averaging approach for multiphase turbulent flows. Even if the approach is developed for incompressible flow, its application for other multiphase flows is foreseen; From the liquid-solid interaction forces only the drag force is considered in this paper.

ii) To improve the one-equation turbulence model reported in [28] by including the modulation of turbulence by particles as a function of particle size and density.

iii) To test the proposed model with other models and experimental data for various two-phase flows, without adopting any adjusting empirical coefficients.

2. MIXED AVERAGING APPROACH

The continuum transport equations for multiphase flows can be obtained by assuming a continuum medium with averaged field quatities by using either time, local volume, local mass or spectral averaging (see Buyevich (1971), Soo (1967), Vernier and Delhaye (1968), Hetsroni (1982)). The averaging for multiphase flow systems may be performed in various ways. Mass averaging technique was applied by Abou-Arab (1985) for turbulent incompressible and compressible flows. To express the spatial nonuniformities and interactions between the flow components Roco and Shook (1985) have developed a specific volume/time averaging technique for turbulent multicomponent systems, in which the size of the averaging volume Δv is related to the turbulence scale. Since the Eulerian description of the flow is more convenient than the Lagrangian description and there are more comprehensive mathematical schemes for such formulation, they transformed the volume/time averaging into double time averaging. For any flow function f and any component K in the mixture, at a position $\underline{r}$ and time t

$$\bar{f}^K(\underline{r},t) = \frac{1}{\Delta T}\int_{t-\Delta T/2}^{t+\Delta T/2} \langle f_K \rangle \, dt \qquad (1)$$

where

ΔT = time averaging interval corresponding to the turbulence production range ($\Delta T \to \infty$).

$$\langle f_K \rangle = \frac{1}{\Delta t}\int_{t-\Delta t/2}^{t+\Delta t/2} f(\underline{r},\tau)\, K(\underline{r},\tau)\, R(\tau-t)\, d\tau \qquad (2a)$$

= intrinsic averaging of f over Δt and the flow component K.

Δt = Eulerian time scale for the most energetic eddies $= \int_0^\infty R(\tau-t)d\tau$ (corresponding to the Taylor's length scale). Note that $\Delta t \ll \Delta T$, but much larger than particle residence time at $\underline{r}$.

$$K(\underline{r},\tau) = \begin{cases} 1 & \text{if the considered flow component resides at point } \underline{r} \text{ and time } \tau \\ 0 & \text{otherwise} \end{cases} \qquad (2b)$$

= phase distribution function

$$R(\tau-t) = \frac{\overline{V''(t)V''(t-\tau)}}{\overline{V''^2(t)}} \qquad (2c)$$

= auto-correlation coefficient of the velocity fluctuations of the most energetic eddies (Taylor's scale)

The time averaging over Δt corresponds to the averaging over local volume Δv. The dimension of Δv is given by the turbulence mixing length, and Δt = (length scale of Δv)/(mean velocity) [29]. By integrating over a flow component K its interfaces with other flow components become boundary of integration, and the interaction terms are derived in a straighforward manner in the differential formulation. According to (1), any instantaneous value differs from the mean value by a turbulence fluctuation with two components f'_K and f''_K:

$$f_K = \bar{f}_K + f^t = \bar{f}_K + f'_K + f''_K \qquad (3)$$

where

$$f''_K = f_K - \langle f_K \rangle \qquad (4)$$

= spatial nonuniformities within Δv (or temporal nonuniformities within Δt)

$$f'_K = \langle f_K \rangle - \bar{f}^K \qquad (5)$$

= temporal nonuniformities of $\langle f_K \rangle$ within ΔT.

Since the averaging domain (Δv or Δt) has the dimensions of the mixing length or Eulerian time scale, respectively, the turbulence fluctuation f_K'' corresponds to the turbulence transfer range. The temporal nonuniformities f_K' reflect the turbulence fluctuations in the production range.

By averaging with formula (1) the point instantaneous conservation equations, one obtains the double time averaged equations. The formulation is equivalent to the volume/time averaging. The momentum and kinetic energy equations are given in Appendix A.

The local mass average of f over a flow component K is denoted $\bar{f}_K$. It is obtained by applying (1), in which the phase distribution function $K(\underline{r},\tau)$ is weighted by the specific mass ρ_K.

In this paper we model the phase interaction by using spectral analysis and suggest a closure of the mass averaged equations for linear momentum and kinetic energy. The averaged equations are initially written with all the terms, and then simplified formulations for various flow conditions are suggested.

3. ENERGY SPECTRUM AND SOLIDS - EDDY INTERACTION

It is well accepted that turbulence is characterized by fluctuating motions defined by an energy spectrum (Tennekes and Lumely (1972)). Single time scale models, which are normally used for the prediction of turbulent flows, seems simplistic because different turbulent interactions are associated with different parts of the energy spectrum (Hanjalic' et al. (1979)). A typical energy spectrum can be divided into three regions. The first region is the production region of large eddies and low wave number. The third region is the dissipation region with small eddies and high wave number, in which the total kinetic energy produced at the lower wave number is dissipated. The intermediate range of wave numbers represents the Taylor's transfer range. The total kinetic energy k of turbulence may be divided into production range (k_p) and transfer range (k_T) because there is negligible kinetic energy in the dissipation range:

$$k \simeq k_p + k_T \qquad (6)$$

where

$$k_p = \frac{1}{2}\overline{u_i'^2}, \qquad (7a)$$

$$k_T = \frac{1}{2}\overline{u_i''^2} \qquad (7b)$$

u_i', u_i'' = fluctuating velocities in the production and transfer range, respectively.

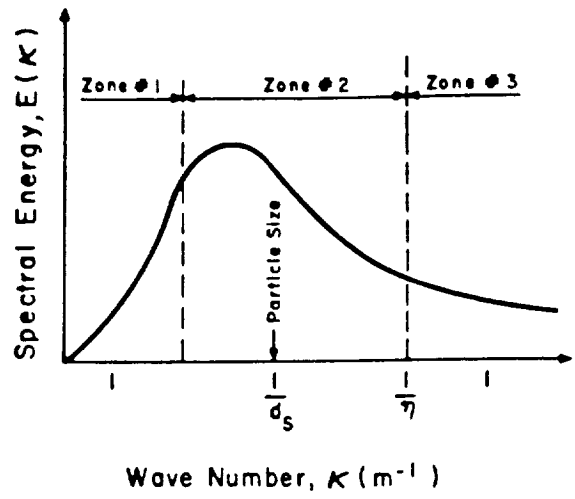

Figure 1. Schematic showing the relative particle size to different eddy sizes in the energy spectrum.

This partitioning of the energy spectrum was shown to be important for swirling flows (Chen (1986)), and hetrogeneous mixture flows such as two-phase jet (Al-Taweel and Landau (1977)).

By using spectral analysis in conjunction with mass/time averaging some additional turbulent correlations will result in the mixture flow equations comparative to homogenous flows. These correlations can be classified into five categories:

i) Eddy-eddy interaction
ii) Eddy-mean flow interaction
iii) Eddy-particle interaction
iv) Particle-mean flow interaction
v) Particle-particle interaction (for dense suspension flow).

These correlations have to be modeled. Since the suspended particles may be of different sizes and different materials, their response to the carrier fluid fluctuations will vary as a function of the mean and fluctuating properties of the flow. The present work will consider a two-way interaction mechanism between solid particles and fluid vorticies in dilute suspensions. This interaction mechanism depends on the ratio between the particle size d_S and the turbulent vortex (eddy) size l_e. These length scales are compared with the turbulence dissipation micro-scale (η).

To determine the particle-eddy interaction the energy spectrum for multiphase flow system is divided into three typical zones (Figure 1):

1. "Large vortex zone" (#1), where the turbulence energy is extracted from the mean flow by low frequency eddies. Here, the eddy length scale ℓ_{el} is larger than the particle size d_S:

$$l_{e1} > d_S > \eta \qquad (8a)$$

2. "Medium vortex zone" (#2), where the solid particles are about the same size with the vortex size, i.e.

$$l_{e2} \approx d_S > \eta \qquad (8b)$$

3. "Small vortex zone" (#3), which would correspond to the Kolmogorov's length scale, i.e.

$$d_S > l_{e3} \approx \eta \qquad (8c)$$

In zone #1 the solid particles generally follow the motion within a vortex, and have an energy dissipation effect. The particle response to the turbulent fluctuations (turbulence modulation) is fully determined (see Hinze, 1975). In the small vortex zone #3 the solid particles can not significantly affect the turbulence microstructure. For the intermediate zone #2 a linear variation of the particle response is considered. This partitioning allows for the particles-nonuniform size eddies interaction to be efficiently modeled.

The present closure formulation originates from the idea of subgrid scale modeling. If this idea is to be accepted, any flow quantity u, v, α, k, ..., etc. may be separated into three parts according to (3), where f_K' and f_K'' define the fluctuations in the production and transfer ranges of the energy spectrum, respectively. By starting from the particle equation of motion in its general form, the relation between the particle motion and different fluid eddies can be determined, and from here the fluctuation components f_K' and f_K'' (see section 6).

4. COMPOSED AVERAGED EQUATIONS

4.1 Mean Flow Governing Equations

The mass/time averaged momentum equation (Appendix A, Eq. A2) with $f_K^t = f_K' + f_K''$ yields:

$$\rho_K \frac{\partial}{\partial t}(\bar{\alpha}_K\bar{u}_{Ki} + \overline{\alpha_K'u_K'} + \overline{\alpha_K''u_K''} + \overline{\alpha' u_{Ki}''} + \overline{\alpha'' u_{Ki}'})$$

Time rate change of the mean flow convection

$$+\rho_K \frac{\partial}{\partial x_j}[\bar{\alpha}_K\bar{u}_{Ki}\bar{u}_{Kj}]$$

Mean flow convection

$$+ \rho_K \frac{\partial}{\partial x_j}[\bar{\alpha}_K\overline{u_{Ki}'u_{Kj}'} + \bar{\alpha}_K\overline{u_{Ki}''u_{Kj}''}]$$

Inertial effect

$$+\rho_K \frac{\partial}{\partial x_j}([\overline{\alpha_K'u_{Ki}'u_{Kj}'} + \overline{\alpha_K''u_{Ki}''u_{Kj}''}] + \bar{u}_{Kj}[\overline{\alpha_K'u_{Ki}'} + \overline{\alpha_K''u_{Ki}''}]$$

Collisional/Inertial Effects

$$+ \bar{u}_{Ki}[\overline{\alpha_K'u_{Kj}'} + \overline{\alpha_K''u_{Kj}''}] + \bar{\alpha}_K[\overline{u_{Ki}'u_{Kj}'} + \overline{u_{Ki}''u_{Kj}''}]$$

$$+ \bar{u}_{Ki}\overline{\alpha_K'u_{Kj}''} + \bar{u}_{Kj}\overline{\alpha_K'u_{Ki}''} + \overline{\alpha_K'u_{Ki}''u_{Kj}'} + \overline{\alpha_K'u_{Ki}''u_{Kj}''}$$

$$+ \overline{\alpha_K''u_{Ki}'}\bar{u}_{Kj} + \overline{\alpha_K''u_{Ki}''}\bar{u}_{Kj} + \overline{\alpha_K''u_{Kj}'u_{Ki}'} + \overline{\alpha_K''u_{Ki}''u_{Kj}''})$$

$$= \rho_K[\bar{\alpha}_K\bar{b}_{Ki} + \overline{\alpha_K'b_{Ki}'} + \overline{\alpha_K''b_{Ki}''} + \overline{\alpha' b_{Ki}''} + \overline{\alpha'' b_{Ki}'}]$$

Body force

$$- \frac{\partial}{\partial x_i}[\bar{\alpha}_K\bar{p}_K + \overline{\alpha_K'p_K'} + \overline{\alpha_K''p_K''} + \overline{\alpha' p_K''} + \overline{\alpha'' p_K'}]$$

Pressure effect

$$+ [\bar{p}_K\frac{\partial\bar{\alpha}_K}{\partial x_i} + \overline{p_K'\frac{\partial\alpha_K'}{\partial x_i}} + \overline{p_K''\frac{\partial\alpha_K''}{\partial x_i}} + \overline{p_K''\frac{\partial\alpha_K'}{\partial x_i}} + \ldots]$$

$$+ \frac{\partial}{\partial x_j}[\bar{\alpha}_K\bar{\tau}_K + \overline{\alpha_K'\tau_{K\Sigma ji}'} + \overline{\alpha_K''\tau_{K\Sigma ji}''}$$

Frictional effect

$$+ \overline{\alpha' K''\tau_{K\Sigma ji}''} + \overline{\alpha'' K'\tau_{K\Sigma ji}'}] + (\overline{I_{Ki}})_K \qquad (9)$$

Phase interaction

where K is a flow component, b_{Ki} is the body force in the i-th direction, and $(I_{Ki})_{-K}$ is the projection in the i-th direction of the interaction vector $(\underline{I}_K)_{-K}$

Equation (9) contains correlations which are related to the production and transfer wave number ranges of the turbulence spectrum. It contains also mixed correlations.

4.2 The Kinetic Energy Equation

Similar to the mean flow governing equation the mass/time averaging form of the turbulent kinetic energy equation can be derived for a flow component K. The exact form of this equation for steady state turbulent flow is given in Appendix A (Eq. A5). It contains more than one hundred correlations which are related to the eddies in the production and transfer ranges as well as some mixed correlations. However, only some of these are predominant in a given flow situation as a function of relative particle-vortex size and density ratio.

4.3 Some Modeling Principles and Assumptions

By analysing the derived mean momentum and kinetic energy conservation equations, it can be easily recognized that some modeling assumptions must be made, based on the physical interpretation and the nature of each term. Previous experimental and theoretical findings can help in modeling "collectively" similar terms with minimum number of empirical constants. Secondly, carrying out an order of magnitude analysis for different correlations which appear in the governing equations some terms may be neglected. Thirdly, the micromechanics which control the ability of the flow variables to correlate with each other and the factors affecting the magnitude of these correlations should be considered. With the previous remarks in mind, one can assume for the sake of simplicity that:

1) The correlations between the large eddies from the production range and the small eddies from the transfer range (mixed correlations e.g. $\overline{u'u''}$) can be neglected as they originate differently and they are related to different ranges of the power spectrum. Similar assumptions are accepted in the classical single fluid turbulence theory.

2) The void fraction fluctuations occur mainly at low frequencies i.e.

$$\alpha = \bar{\alpha} + \alpha' + \alpha'' \tag{10}$$

$$\text{with} \quad \alpha' \gg \alpha'' \tag{11}$$

This is a simplifying assumption which is acceptable for such complicated problems. If the particles are of small diameter their concentration is relatively uniform distributed in the Taylor length scale. High void fractions are mostly associated with large size and high density particulate flows. These large size particles are mainly fluctuating at low frequencies due to its high inertia, hence they in turn correlate weakly at high frequencies.

3) The correlations of higher order than three, for instance $\overline{\alpha' u' \partial p'/\partial x_i}$, $\overline{u_i' u_j' \frac{\partial p'}{\partial x_j}}$ ... etc., are neglected. These are at least an order magnitude smaller than those of the third order (see Hanjalic' and Launder (1972)).

4) Pressure diffusion contribution to the total turbulent diffusion in the kinetic energy equation will be neglected because of its relatively small magnitude (Hanjalic' and Launder (1972)).

5) The Boussinesq gradient type approximation is adopted for modeling of different fluxes and triple correlations, with assumptions similar to Elghobashi and Abou-Arab (1983) and Roco and Mahadevan (1986)

6) The following constitutive relations are employed for the shear stress of carrier fluid:

$$-\rho\overline{u_i' u_j'} = \mu_{LP}\left(\frac{\partial \bar{u}_i}{\partial x_j} + \frac{\partial \bar{u}_j}{\partial x_i}\right) - \frac{2}{3} k_{LP}\delta_{ij} - \frac{2}{3}\mu_{LP}\delta_{ij}\bar{u}_{n,n} \tag{12}$$

$$-\rho\overline{u_i'' u_j''} = \mu_{LT}\left(\frac{\partial \bar{u}_i}{\partial x_j} + \frac{\partial \bar{u}_j}{\partial x_i}\right) - \frac{2}{3} k_{LT}\delta_{ij} - \frac{2}{3}\mu_{LT}\delta_{ij}\bar{u}_{n,n} \tag{13}$$

while the total shear stress $-\rho\,\overline{u_i^t u_j^t}$ can be given by

$$\rho\,\overline{u_i^t u_j^t} = \rho\,\overline{u_i' u_j'} + \rho\,\overline{u_i'' u_j''}\,. \tag{14}$$

where

$$\mu_{LP} = C_{\mu P}\,\rho_L k_{LP}^{1/2}\, l_P, \tag{15}$$

$$\mu_{LT} = C_{\mu T}\,\rho_L k_{LT}^{1/2}\, l_T \quad , \text{ and} \tag{16}$$

$$\mu_{Lt} = \mu_{LP}^{P} + \mu_{LT}^{T} = C_\mu \rho_L k_L^{1/2}\, l_L \tag{17}$$

Similar relations can be written for the viscosity of the dispersed phase μ_{St} (see Roco and Balakrishnan (1985)). However, in the present work we choose to define the eddy viscosity of solids as follows:

$$\nu_{St} = \nu_{Lt} / \sigma \tag{18}$$

where

$$\sigma = \sigma_{\alpha S} / \sigma_S \tag{19}$$

and

$$\sigma_{\alpha S} = \nu_{Lt}/D_S \tag{20}$$

$$\sigma_S = \nu_{St}/D_S \tag{21}$$

Appropriate expressions for $\sigma_{\alpha S}$ are cited in many articles such as Peskin (1971), Picart et al. (1986), and Hetsroni (1982). σ_S is a Schmidt number and its value is about 1.5 (Abou-Ellail and Abou-Arab (1985)).

7) In the present approach for dilute particulate flows the turbulence kinetic energy equation is written only for the carrier flow. The solid phase turbulence kinetic energy and turbulence correlations are evaluated from the available solution of the linearized equation of motion of a solid particle after its transformation from the real time to the frequency domain.

8) Terms which are of similar nature i.e. convection, diffusion, dissipation, etc. can be modeled collectively. The length-, velocity- and time-scale which are appropriate for the description of their rate of change must be identified from the physical interpretation of these terms.

9) The response function which shows the ability of solid particles to follow the eddies is obtained from the equation of motion of particles for different local dimensionless parameter, d_S/l_e and ρ_S/ρ_L.

10) To establish the degree of generality of the proposed model validation tests were carried out for air-laden and water-laden jet, and air-solid pipe flow.

5. CLOSURE FOR THE MEAN FLOW EQUATIONS

With the modeling assumptions given in the previous section, the steady state mean flow momentum equations for any flow component, reads

$$\rho_K \frac{\partial}{\partial x_j}\left(\bar{\alpha}_K \bar{u}_{Ki} \bar{u}_{Kj}\right) + \frac{\partial}{\partial x_j}\rho_K\left(\bar{\alpha}_K \overline{u_{Ki}' u_{Kj}'} + \bar{\alpha}_K \overline{u_{Ki}'' u_{Kj}''}\right) +$$

$$+\frac{\partial}{\partial x_j}\{\rho_K[(\overline{\alpha'_K u'_{Ki} u'_{Kj}} + \overline{\alpha''_K u''_{Ki} u''_{Kj}}) + \bar{u}_{Ki}(\overline{\alpha'_K u'_{Kj}} + \overline{\alpha''_K u''_{Kj}})$$

$$+ \bar{u}_{Kj}(\overline{\alpha'_K u'_{Ki}} + \overline{\alpha''_K u''_{Ki}})] + (\overline{\alpha'_K \tau'_{K\Sigma ji}} + \overline{\alpha''_K \tau''_{K\Sigma ji}})\}$$

$$= \rho_K(\bar{\alpha}_K \bar{b}_{Ki} + \overline{\alpha'_K b'_{Ki}} + \overline{\alpha''_K b''_{Ki}}) - \frac{\partial}{\partial x_i}(\bar{\alpha}_K \bar{p}_K + \overline{\alpha'_K p'_K} + \overline{\alpha''_K p''_K})$$

$$+ (\bar{p}_K \frac{\partial \bar{\alpha}_K}{\partial x_i} + \overline{p'_K \frac{\partial \alpha'_K}{\partial x_i}} + \overline{p''_K \frac{\partial \alpha''_K}{\partial x_i}})$$

$$+ \frac{\partial}{\partial x_j}(\bar{\alpha}_K \bar{\tau}_{K\Sigma ji}) + (\overline{I_{Ki}})_{-K} \qquad (22)$$

In Eq. (22) there are 16 correlations, half of them in the production "large eddy" range of the spectrum. The terms are modeled following the criteria: i) Physically correct behavior, ii) Minimum number of empirical functions and constants, and iii) Comparisons against experimental data over a wide range of conditions are required to check the validity of the model.

The turbulent stresses caused by the large and small size energetic eddies, $-\rho_L \overline{u'_i u'_j}$ and $-\rho_L \overline{u''_i u''_j}$. are defined by Eqs. (12) and (13). The correlation between u''_i and u''_j is weak when $i \neq j$. This finding will be explained in the next section.

The collisional effect correlations are modeled after Launder (1976):

$$\overline{\alpha'_K u'_{Ki} u'_{Kj}} = - C^P_{\phi 5} \left(\frac{k_{KP}}{\epsilon_{KP}}\right)\left(\overline{u'_{Ki} u'_{Kl}} \frac{\partial}{\partial x_l} \overline{u'_{Kj} \alpha'_K}\right.$$

$$\left. + \overline{u'_{Kj} u'_{Kl}} \frac{\partial}{\partial x_l} \overline{u'_{Ki} \alpha'_K}\right) \qquad (23)$$

where $C^P_{\phi 5}$ is a constant of a value of about 0.1. Similarly

$$\overline{\alpha''_K u''_{Ki} u''_{Kj}} = - C^T_{\phi 5} \left(\frac{k_{KT}}{\epsilon_{KT}}\right)\left(\overline{u''_{Ki} u''_{Kl}} \frac{\partial}{\partial x_l} \overline{u''_{Kj} \alpha''_K}\right.$$

$$\left. + \overline{u''_{Kj} u''_{Kl}} \frac{\partial}{\partial x_l} \overline{u''_{Ki} \alpha''_K}\right) \qquad (24)$$

where $C^T_{\phi 5}$ must be optimized by comparison with experimental data. The fluxes in (23) and (24) can also be collectively modeled as:

$$\overline{\alpha'_K u'_{Ki} u'_{Kj}} + \overline{\alpha''_K u''_{Ki} u''_{Kj}} =$$

$$- C_{\phi 5} \frac{k_K}{\epsilon_K}\left(\overline{u^t_{Ki} u^t_{Kl}} \cdot \frac{\partial}{\partial x_l} \overline{u^t_{Kj} \alpha^t_K}\right.$$

$$\left. + \overline{u^t_{Kj} u^t_{Kl}} \cdot \frac{\partial}{\partial x_l} \overline{u^t_{Ki} \alpha^t_K}\right) \qquad (25)$$

The diffusion fluxes namely $\overline{\alpha'_K u'_{Ki}}$, $\overline{\alpha''_K u''_{Ki}}$ .... etc. are modeled using Boussinesq approximation as:

$$- \overline{\alpha'_K u'_{Ki}} = \frac{\nu_{KP}}{\sigma^P_{\alpha K}} \frac{\partial \bar{\alpha}_K}{\partial x_i} \qquad (26)$$

while

$$- \overline{\alpha''_K u''_{Ki}} = \frac{\nu_{KT}}{\sigma^T_{\alpha K}} \frac{\partial \bar{\alpha}_K}{\partial x_i} \qquad (27)$$

Similar expression can be written for $\overline{\alpha'_K u'_{Kj}}$ and $\overline{\alpha''_K u''_{Kj}}$.... etc. However, according to our assumptions, especially those concerning the void fraction fluctuation at high frequency α'', the fluxes in Eqs. (26) and (27) can be modeled collectively as:

$$- \overline{\alpha^t_K u^t_{Ki}} = \frac{\nu_{Kt}}{\sigma_{\alpha K}} \frac{\partial \bar{\alpha}_K}{\partial x_i} \qquad (28)$$

The solution of the two transport equations (for k_P and k_T) would require also a description for the length scales. This point will be explained in more details in the next section.

The fourth group of terms with the void fraction-shear stress turbulent correlations contains the laminar viscosity as a multiplier, and will be neglected due to its smaller order of magnitude.

The pressure effect contribution to the mean flow equation consists of two groups. Each contains three terms. The first of these terms is the mean pressure-void fraction. The second and the third terms are the pressure-void fraction correlations which can be modeled after Elghobashi and Abou-Arab (1983) by

$$- (\overline{\alpha'_K p'_K} + \overline{\alpha''_K p''_K}) = \psi_1 + \psi_2 \qquad (29)$$

where

$$\psi_1 = - C_{\phi 3} \rho_K k_K^{1/2} \cdot \overline{u^t_{Km} \alpha^t_K}$$

and

$$\psi_2 = - C_{\phi 4} \rho_K k^{1/2} \cdot u^t_{Km} \alpha^t_K$$

The values of the constants $C_{\phi 3}$ and $C_{\phi 4}$ are about unity.

The second correlation in the second group of terms can be also modeled following Launder (1976). The final form is

$$\overline{p'_K \frac{\partial \alpha'_K}{\partial x_i}} + \overline{p''_K \frac{\partial \alpha''_K}{\partial x_i}} = \rho_K \left(\frac{\epsilon}{k}\right)_K [C_{\phi 1} \cdot \overline{u^t_{Ki} \alpha^t_K}$$

$$+ C_{\phi 2}\left(\frac{\overline{u^t_{Ki} u^t_{Kl}}}{k_K} - \frac{2}{3}\delta_{il}\right)\cdot\overline{u^t_{Kl}\alpha^t_K}\Big] + \rho_K\left(0.8\,\overline{u^t_{Kl}\alpha^t_K}\cdot\frac{\partial \bar{u}_{Ki}}{\partial x_i} - 0.2\,\overline{u^t_{Kl}\alpha^t_K}\cdot\frac{\partial \bar{u}_{Kl}}{\partial x_i}\right) \quad (30)$$

The values of the constants $C_{\phi 1}$ and $C_{\phi 2}$ are 4.3 and -3.2, respectively. The modeling of these correlations suffers from the embodied assumptions concerning the velocity and length scale description. It would require a large number of transport equations to model accurately each of the above correlations.

The interaction term $(\overline{I_{Ki}})_{-K}$ for K = L (liquid) and -K = S (solid) is modeled for dilute suspensions with particle Reynolds numbers less than unity:

$$\overline{(I_{Li})_S} = -(18\mu_L/d_S^2)\left[(\bar{u}_{Li} - \bar{u}_{Si})\,\bar{\alpha}_S + \left(\frac{\nu_{LP}}{\sigma^P_{\alpha S}} + \frac{\nu_{LT}}{\sigma^T_{\alpha S}}\right)\frac{\partial \bar{\alpha}_L}{\partial x_i} + \left(\frac{\nu_{LP}}{\sigma\sigma^P_{\alpha S}} + \frac{\nu_{LT}}{\sigma\sigma^T_{\alpha S}}\right)\frac{\partial \bar{\alpha}_S}{\partial x_i}\right] \quad (31)$$

where the first term is the drag interaction for particles in the Stokes range. The second and third terms are the turbulent fluxes due to the relative motion between the particles and fluid. The gradient transport model with the exchange coefficients ν_{LP} and ν_{LT} corresponding to the production and transfer ranges is adopted for these fluxes ($\overline{\alpha'_L u'_{Li}}$, $\overline{\alpha''_L u''_{Li}}$, $\overline{\alpha'_S u'_{Si}}$, and $\overline{\alpha''_S u''_{Si}}$).

If only single velocity scale is chosen for the whole energy spectrum, k_L, there will be only one momentum exchange coefficient ν_{Lt} instead of ν_{LP} and ν_{LT}

$$\nu_{Lt} = \frac{\nu_{LP}}{\sigma\sigma^P_{\alpha S}} + \frac{\nu_{LT}}{\sigma\sigma^T_{\alpha S}} \quad (32)$$

6. CLOSURE FOR THE KINETIC ENERGY EQUATION

In the present work, the turbulence kinetic energy for the liquid phase "k_L" (turbulence velocity scale) is obtained from an exact transport equation (Eq. A5 in Appendix A), and the length scale "l" is described algebraically. The kinetic energy equation A5 contains a large number of turbulence correlations. In order to obtain an engineering turbulence model, it is sufficient to consider the principles and the assumptions given in Section 4.3. By engineering turbulence model, it is meant, a physically correct model with minimum number of empirical coefficients.

The first group of terms in the k-equation (Group #1) is the convection of the total specific kinetic energy, where

$$\frac{\partial k_L}{\partial x_j} = \frac{\partial k_{LP}}{\partial x_j} + \frac{\partial k_{LT}}{\partial x_j} \quad (33)$$

Diffusion transport of k is composed of two main parts. The first part (Group #2) is the velocity diffusion and it contains the 3rd order velocity correlations, while the second part (Group #3) is the pressure diffusion with the pressure-velocity correlations. The modeling of the velocity diffusion part is obtained as follows:

$$\rho_L\bar{\alpha}_L\,\overline{u'_{Lj}u'_{Li}u'_{Li}} = -\rho_L\bar{\alpha}_L\frac{\nu_{LP}}{\sigma^P_k}\frac{\partial k_{LP}}{\partial x_j} \quad (34)$$

and

$$\rho_L\bar{\alpha}_L\,\overline{u''_{Lj}u''_{Li}u''_{Li}} = -\rho_L\bar{\alpha}_L\frac{\nu_{LT}}{\sigma^T_k}\frac{\partial k_{LT}}{\partial x_j} \quad (35)$$

where σ^P_k and σ^T_k are the turbulent Prandtl/Schmidt numbers for the kinetic energy in the production and transfer ranges. To reduce the number of empirical constants and the number of governing equations the above two correlations are modeled collectively as follows

$$-\rho_L\overline{u^t_{Lj}u^t_{Li}u^t_{Li}} = -\rho_L\bar{\alpha}_L\frac{\nu_{Lt}}{\sigma_k}\frac{\partial k_L}{\partial x_j} \quad (36)$$

where σ_k is of order of unity.

The presure diffusion term is negligible relative to the velocity diffusion (Hanjalic' and Launder (1972)).

Mixed and higher order correlations (Groups #3 and #5) can be neglected according to the modeling assumptions stated and discussed in section 4.3 of the present paper.

The production terms are divided into two groups. The first group (Group #6) is common for single and multiphase incompressible flows, $\rho_L\bar{\alpha}_L\,\overline{u'_{Li}u'_{Lj}}\cdot\frac{\partial \bar{u}_{Li}}{\partial x_j} + \rho_L\bar{\alpha}_L\,\overline{u''_{Li}u''_{Lj}}\cdot\frac{\partial \bar{u}_{Li}}{\partial x_j}$, and can be modeled collectively as follows:

$$\rho_L\bar{\alpha}_L\,\overline{u^t_{Li}u^t_{Lj}}\cdot\frac{\partial \bar{u}_{Li}}{\partial x_j} = \bar{\alpha}_L\mu_{Lt}\left(\frac{\partial \bar{u}_{Li}}{\partial x_j}\right)^2 \quad (37)$$

The physics of turbulence and the consideration of the spectral energy transfer assume that the production is only due to the interaction between the mean flow and the large eddy. Since the $\overline{u''_{Li}u''_{Lj}}$ correlation is for medium size eddies which have almost no direct interaction with the mean flow, it results that the

contribution of these small eddies to the turbulence production via the mean field is smaller than that of the large eddies. This means also that $\overline{u''_{Li}u''_{Lj}}$ correlation is weak if $i \neq j$, i.e. it is only of significant value if the turbulent normal stress components ($\overline{u''^2_{Li}}$, i = 1, 2, 3) are considered. According to Hanjalic' et al. (1979) multiple scale model the turbulent viscosity is defined as follows:

$$\mu_{Lt}/\rho_L = C_\mu \, k_L \, (k_{LP}/\epsilon_{LP}) \qquad (38)$$

$$\text{where } k_L = k_{LP} + k_{LT} \qquad (39a)$$

$$\text{and } C_\mu = 0.09 \qquad (39b)$$

This equation can be rewritten as

$$\mu_{Lt}/\rho_L = C_\mu \left(\frac{k^2_{LP}}{\epsilon_{LP}} + \frac{k_{LT}\, k_{LP}}{\epsilon_{LP}}\right)$$

$$= C_{\mu P} k^{0.5}_{LP} l_{LP} + C_{\mu T} k^{0.5}_{LT} l_{LT} = (\mu_{LP} + \mu_{LT})/\rho_L \qquad (40)$$

where $C_{\mu P}$ and $C_{\mu T}$ are two additional constants and l_{LP} and l_{LT} are also two additional length scales for the large and medium size eddies. The length scale can be related with the following relations (from Eqs. (38) and (40))

$$l_{LT} = C_l \, l_{LP} \, (k_{LT}/k_{LP}) \qquad (41)$$

Since the ratio k_{LT}/k_{LP} is of the order of unity and $l_{LP} > l_{LT}$, the constant C_l should be smaller than unity. Thus if the multiple time scale model is not recommended (due to its large number of additional constants) an alternative approach is to consider a multiple velocity scale model. In this model only two differential equations for k_{LP} and k_{LT} have to be solved. The length scales can be obtained by using the previous relation Eq. (41) and any expression for the length scale of the large eddies l_{LP}, for example that used by Roco and Shook (1983) for cylindrical pipes.

The modeling of the additional production terms (Group #7) is achieved as follows:

$$-\overline{\alpha'_L u'_{Li}} \frac{\partial \bar{p}_L}{\partial x_i} = \frac{\nu_{LP}}{\sigma^P_{\alpha S}} \frac{\partial \bar{\alpha}_L}{\partial x_i} \frac{\partial \bar{p}_L}{\partial x_i} \qquad (42)$$

$$-\overline{\alpha''_L u''_{Li}} \frac{\partial \bar{p}_L}{\partial x_i} = \frac{\nu_{LT}}{\sigma^T_{\alpha S}} \frac{\partial \bar{\alpha}_L}{\partial x_i} \frac{\partial \bar{p}_L}{\partial x_i} \qquad (43)$$

and both collectively as

$$-\left(\overline{\alpha'_L u'_{Li}} + \overline{\alpha''_L u''_{Li}}\right) \frac{\partial \bar{p}_L}{\partial x_i} = \frac{\nu_{Lt}}{\sigma_{\alpha S}} \frac{\partial \bar{p}_L}{\partial x_i} \frac{\partial \bar{\alpha}_L}{\partial x_i} \qquad (44)$$

Terms like $\overline{\alpha'_L u'_{Li}} \frac{\partial \bar{u}_{Li}}{\partial x_i}$ and $\overline{\alpha''_L u''_{Li}} \frac{\partial \bar{u}_{Li}}{\partial x_i}$ are modeled in a similar manner to that of the above terms i.e.

$$-\left(\overline{\alpha'_L u'_{Lj}} + \overline{\alpha''_L u''_{Lj}}\right) \frac{\partial \bar{u}_{Li}}{\partial x_i} = \frac{\nu_{Lt}}{\sigma_{\alpha S}} \frac{\partial \bar{u}_{Li}}{\partial x_i} \frac{\partial \bar{\alpha}_L}{\partial x_j} \qquad (45)$$

The extra production terms (Group #7) can be written in the following form

$$\text{Extra production} = \frac{\nu_{Lt}}{\sigma_{\alpha S}} \frac{\partial \bar{\alpha}_L}{\partial x_i} \left(\frac{\partial \bar{p}_L}{\partial x_i} + \bar{u}_{Lj} \frac{\partial \bar{u}_{Li}}{\partial x_j}\right)$$

$$+ \frac{\nu_{Lt}}{\sigma_{\alpha S}} \frac{\partial \bar{\alpha}_L}{\partial x_j} \left(\bar{u}_{Li} \frac{\partial \bar{u}_{Li}}{\partial x_j}\right) \qquad (46)$$

The terms $\rho_L \bar{\alpha}_L \mu_L \overline{\frac{\partial u'_{Li}}{\partial x_i} \frac{\partial u_{Li}}{\partial x_i}}$ and $\rho_L \bar{\alpha}_L \nu_L \overline{\frac{\partial u''_{Li}}{\partial x_j} \frac{\partial u''_{Li}}{\partial x_j}}$ in Group #8 represents the dissipation rate from large eddies ϵ_{LP} and transfer eddies ϵ_{LT}. Since viscous dissipation is mainly confined to small scale eddies and to simplify the mathematical form of the multiple time scale turbulence models, Hanjalic' et al. (1979) have assumed that there is an equilibrium spectrum energy transfer between the dissipation and transfer region i.e., $\epsilon_{total} = \epsilon_L$, where ϵ_L is the dissipation rate in the single scale scheme. Thus

$$\rho_L \bar{\alpha}_L \nu_L \overline{\frac{\partial u'_{Li}}{\partial x_j} \frac{\partial u_{Li}}{\partial x_j}} = -\rho_L \bar{\alpha}_L \epsilon_{LP} = \bar{\alpha}_L \mu_{LT} \left(\frac{\partial \bar{u}_{Li}}{\partial x_j}\right)^2 \qquad (47)$$

and

$$\rho_L \bar{\alpha}_L \nu_L \overline{\frac{\partial u''_{Li}}{\partial x_j} \frac{\partial u''_{Li}}{\partial x_j}} = -\rho_L \bar{\alpha}_L \epsilon_{LT} \qquad (48)$$

where

$$\epsilon_{LP} = C_{DP} \, k^{1.5}_{LP}/l_{LP} \qquad \text{and}$$

$$\epsilon_{LT} = C_{DT} \, k^{1.5}_{LT}/l_{LT}$$

In equation (47) a spectral cascading between the production and transfer eddies is considered (Hanjalic' et al. (1979)). This equation gives an additional relation between the spectrum scales.

The correlations between the fluctuating velocity component and the fluctuating friction forces (interaction terms in Groups #8 and #10) are due to fluid-fluid and fluid-solid drag force in dilute flows. The friction interaction terms due to molecular collision (fluid-fluid interaction, Group #8) are given above by Eq. (47) and (48). The form of the correlation between the fluctuating drag force and the velocity fluctuations depends on the expression adopted for the drag force. The viscous drag correlation (VDC) in Group #10 for Stokes flow over particles in dilute suspensions reads

$$VDC = -\frac{18\mu_L}{d_S^2}(\bar{u}_{Li} - \bar{u}_{Si})\cdot A_1$$

$$-\frac{18\mu_L}{d_S^2}(\bar{\alpha}_S\cdot A_2 + A_3) \qquad (49a)$$

where:

$$A_1 = \overline{\alpha_S' u_i'} + \overline{\alpha_S'' u_i''} \qquad (49b)$$

$$A_2 = \overline{u_{Li}'(u_{Li}' - u_{Si}')} + \overline{u_{Li}''(u_{Li}'' - u_{Si}'')} \qquad (49c)$$

$$A_3 = \overline{\alpha_S' u_{Li}'(u_{Li}' - u_{Si}')} + \overline{\alpha_S'' u_{Li}''(u_{Li}'' - u_{Si}'')} \qquad (49d)$$

The first correlation group A_1 (Eq. 49a) can be approximated using the gradient type assumption. The second correlation in this expression (49b) is that due to the relative slip fluctuating motion $\overline{u_{Li}'(u_{Li}' - u_{Si}')}$ and $\overline{u_{Li}''(u_{Li}'' - u_{Si}'')}$. These can be modeled using similar approach to that of Elghobashi and Abou-Arab (1983) but with some modifications which allow for different particle-eddy interaction according to their relative size. These modifications are based on the spectral analysis carried out by Dingguo (1987) for the response of the particles to the turbulent fluctuations of the carrier fluid. For very large eddies $\kappa << \kappa_S$.

$$u_S' = (v_S')_\kappa = (v_L')_\kappa\, a \cdot \exp[-i(\kappa\bar{u}_L t - \beta)] \qquad (50)$$

where κ is the wave number; κ_S is the Basset-Boussinesq-Ossen wave number defined as $1/d_S$; $(v_S')_\kappa$ and $(v_L')_\kappa$ are the solid and liquid velocity components with the wave number κ; a is the amplitude ratio of oscillations

$$a = [(1 + q_2)^2 + q_1^2]^{0.5} \qquad (51a)$$

and β is the phase angle of oscillation

$$\beta = tg^{-1}[q_2/(1 + q_1)] \qquad (51b)$$

The expressions of q_1 and q_2 are

$$q_1 = \frac{(1 + \frac{9N_S}{\sqrt{2}(s+0.5)})(\frac{1-s}{s+0.5})}{\frac{81}{(s+0.5)^2}(2N_S^2 + \frac{N_S}{\sqrt{2}})^2 + (1 + \frac{9N_S}{\sqrt{2}(s+0.5)})^2} \qquad (52a)$$

$$q_2 = \frac{\frac{9(1-s)}{(s+0.5)^2}(2N_S^2 + \frac{N_S}{2})}{\frac{81}{(s+0.5)^2}(2N_S^2 + \frac{N_S}{\sqrt{2}})^2 + (1 + \frac{9N_S}{\sqrt{2}(s+0.5)})^2} \qquad (52b)$$

with the following dimensionless parameters:

$$s = \rho_S/\rho_L$$

$$N_S = \sqrt{\frac{\nu_L}{u_L \kappa d_S^2}} = \frac{\kappa}{\kappa_T}\sqrt{\frac{\kappa Re}{\kappa_T}}$$

where

κ_T = is the wavenumber of the most energetic eddies,

Re = Reynolds number based on l_T, and

N_S = Stokes number.

For small eddies with wave numbers $\kappa >> \kappa_S$, the particle response can be described by

$$u_S' = (v_S')_\kappa = (v_L')_\kappa (\frac{\kappa_S}{\kappa})^3 \frac{\rho_L}{\rho_S} \qquad (53)$$

For the intermediate size eddies $\kappa \simeq \kappa_S$ one can use (50) with

$$a = \frac{1}{s} \quad \text{and} \qquad (54a)$$

$$\beta = \tan^{-1}(s) \qquad (54b)$$

If the fluctuating slip velocity w_i' is defined as

$$w_i' = u_{Si}' - u_{Li}' \qquad (55)$$

then the ratio of the mean square $\overline{w_i'^2}$ and $\overline{u_{Li}'^2}$ becomes

$$\overline{w_i'^2}/\overline{u_{Li}'^2} = (\overline{u_{Si}'^2} - 2\overline{u_{Li}'u_{Si}'} + \overline{u_{Li}'^2}) / \overline{u_{Li}'^2} \qquad (56)$$

with

$$\overline{u_{Li}'u_{Si}'} = \frac{1}{2}\overline{u_{Li}'^2}(1 + \overline{u_{Si}'^2}/\overline{u_{Li}'^2} - \overline{w_i'^2}/\overline{u_{Li}'^2})$$

$$= \frac{1}{2}\overline{u_{Li}'^2}(1 + \Gamma_{SL} - \Gamma_{RL}) \qquad (57)$$

The values of Γ_{SL} and Γ_{RL} can be obtained by using the preceding solution (Eq. 50):

$$\Gamma_{SL} = [\int_0^{\kappa_S} a^2 E_L(\kappa)d\kappa + \int_{\kappa_S}^{\infty}(\frac{\kappa_S}{\kappa})^6 s^{-2} E_L(\kappa)d\kappa]/\int_0^{\infty} E_L(\kappa)d\kappa \qquad (58)$$

or

$$\Gamma_{SL} = \frac{2h}{\pi(h+1)}\tan^{-1}(\kappa_S/\kappa_T) \qquad (59)$$

where

$$h = \frac{A}{\kappa_T u_L} = \frac{18}{(s+0.5)}(\kappa_S/\kappa_T)^2/Re,\ A = \frac{18\nu_L}{(s+0.5)d_s^2}$$

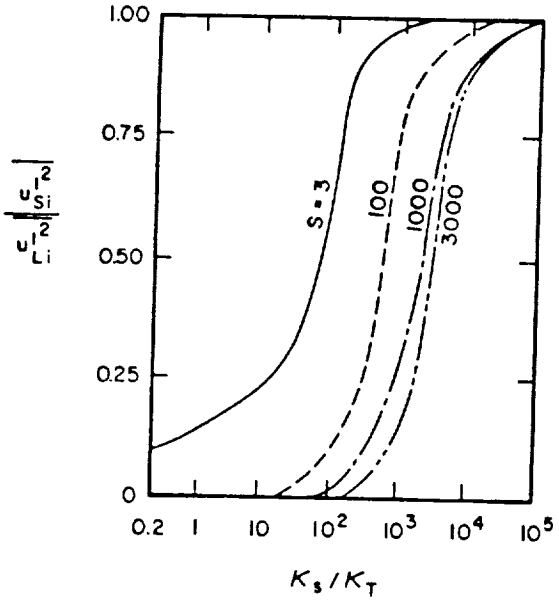

Figure 2. The effect of eddy-particle size ratio (κ_S/κ_T) on the particle response to the eddy fluctuations ($\overline{u_{Si}^2}/\overline{u_{Li}^2}$)

and

$$\Gamma_{RL} = \left[\int_0^{\kappa_S} (a^2-1)\, E_L(\kappa)\, d\kappa + \int_{\kappa_S}^{\infty} \left(\left(\frac{\kappa_S}{\kappa}\right)^3 s^{-1}-1\right)^2 E_L(\kappa) d\kappa\right] \Big/ \int_0^{\infty} E(\kappa)\, d\kappa \quad (60)$$

where $a_1 = (f_1^2 + f_2^2)^{0.5}$ and $E_L(\kappa)$ is the liquid energy spectrum function for which any arbitrary form can be adopted, for instance

$$E_L(\kappa) = \frac{2}{\pi} \frac{\overline{u_{Li}^2}}{\kappa_T} \frac{1}{1+(\kappa/\kappa_T)^2} \quad (61)$$

Figure 2 illustrates the effect of eddy-particle size ratio expressed as κ_S/κ_T on the ratio $\Gamma_{SL} = \overline{u_{Si}^2}/\overline{u_{Li}^2}$ which indicates the particle response to the eddying motion. It can be noticed that high values of κ_S/κ_T (i.e. small particle or large eddy) the particles follows quite well the eddy motion.

Substituting the expressions for Γ_{SL} and Γ_{RL} (Eqs. (58) or (59), and Eq. (60)) into Eq. (57), the correlation A_2 can be obtained

$$A_2 = \frac{1}{2} \overline{u_{Li}^2} (1 - \Gamma_{SL} + \Gamma_{RL}) \quad (62)$$

The above analysis applies equally well to the large eddies as to small eddies. The energy spectrum function $E_L(\kappa)$ for a two-phase flow is given by Al-Taweel and Landau (1977). However, since its form is not essential (Dingguo (1987)) it is sufficient to adopt any simple form as that given above by Eq. (61). It is clear from the above analysis that the particle response to the carrier fluid fluctuations is a function of the density ratio ρ_S/ρ_L, size of interacting eddy relative to particle size κ_S/κ and Reynolds number based on the size of the most energetic eddies of the flow. An analogous expression to that given by Eq. (62) is that based on the Chao's solution (see Chao (1964)). This solution can be considered as a substitution of Dingguo's solution only for $\kappa \ll \kappa_S$ i.e. for fine particles.

The last term to be modeled in the VCD group, A_3, is separated into four correlations:

$$A_3 = -\frac{18\mu_L}{d_S^2}\left[\underbrace{(\overline{\alpha_S' u_{Li}' u_{Li}'}}_{T1} + \underbrace{\overline{\alpha_S'' u_{Li}'' u_{Li}''}}_{T2} - \underbrace{(\overline{\alpha_S' u_{Li}' u_{Si}'}}_{T3} + \underbrace{\overline{\alpha_S'' u_{Li}'' u_{Si}''}}_{T4})\right] \quad (63)$$

where the triple correlations T3 and T4 are modeled in a similar manner to that used for the calculation of T1 and T2 by using Eqs. (23) and (24), thus

$$T1 = \overline{\alpha_S' u_{Li}' u_{Li}'} = -C_{\phi 5}^P (k_{LP}/\epsilon_{LP}) (\overline{2u_{Li}' u_{Ll}'} \frac{\partial \overline{u_{Li}' \alpha_S'}}{\partial x_l})_P.$$

$$T2 = \overline{\alpha_S'' u_{Li}'' u_{Li}''} = -C_{\phi 5}^T (k_{LT}/\epsilon_{LT}) (\overline{2u_{Li}'' u_{Ll}''} \frac{\partial \overline{u_{Li}'' \alpha_S''}}{\partial x_l})_T.$$

$$T3 = -C_{\phi 5}^P (k_{LP}/\epsilon_{LP})(\overline{u_{Li}' u_{Si}'} \frac{\partial \overline{u_{Sl}' \alpha_S'}}{\partial x_l} + \overline{u_{Si}' u_{Ll}'} \frac{\partial \overline{u_{Ll}' \alpha_S'}}{\partial x_l})_P$$

$$T4 = -C_{\phi 5}^T (k_{LT}/\epsilon_{LT})(\overline{u_{Li}'' u_{Sl}''} \frac{\partial \overline{u_{Sl}'' \alpha_S''}}{\partial x_l} + \overline{u_{Si}'' u_{Ll}''} \frac{\partial \overline{u_{Ll}'' \alpha_S''}}{\partial x_l})_T \quad (64)$$

These correlations can also be collectively modeled using single velocity and length-scale, and total k_L and ϵ_L. The first two and the last two terms yield, respectively:

$$T1 + T2 = C_{\phi 5} \frac{2k_L}{\epsilon_L} (\overline{u_{Li}^t u_{Ll}^t} \frac{\partial \overline{u_{Li}^t \alpha_S^t}}{\partial x_l}) \quad (65a)$$

$$T3 + T4 = C_{\phi 5} \frac{2k_L}{\epsilon_L} (\overline{u_{Li}^t u_{Si}^t} \frac{\partial \overline{u_{Sl}^t \alpha_S^t}}{\partial x_l}$$

$$+ \overline{u^t_{Si} u^t_{Li}} \; \overline{\frac{\partial u^t_{Ll} \alpha^t_s}{\partial x_l}} \;) \qquad (65b)$$

The terms in Group #9 of Eq. A5 are of diffusive and dissipative nature. The diffusion terms as they appeared in Group #9 are multiplied by the molecular viscosity and therefore will be neglected due to their relatively small magnitude. Other higher order correlations and mixed correlations in this group are also neglected according to the modeling principles stated previoulsy in section 4.3 and as they are also multiplied by the molecular viscosity.

By substituting all previously modeled terms into the exact form of the turbulence kinetic energy equation, and rearranging these terms, one obtains the simplified modeled form given in Appendix B (Eq. B2).

Since the present model is based on an exact equation, namely the turbulence kinetic energy equation, and the modeled form of this equation has no adjusting coefficients it is expected that the model will generally produce good results and have less limitations compared to other models. The only modeling assumption is that of the Boussinesq gradient type, which generally is accepted. The correlations that requires questionable semi-empirical modeling assumptions and introduction of empirical constant are (i) fewer in number (for $\overline{\alpha'_L u'_{Li} u'_{Lj}}$ and $\overline{\alpha'_L u'_{Si} u'_{Lj}}$), and (ii) for terms having an order of magnitude smaller (by ratio $\alpha'/\bar{\alpha}$) compared to other main terms in the k-equation. The only significant new correlation used in the present closure is that due to the relative motion between the phases. This is modeled with less restrictions and taking into consideration the effect of the particle diameter-eddy size ratio on the particle response to the eddying motion. The limitation of the present one-equation k model closure is the algebraic formulation for the length scale. Since there are many factors affecting this length scale and since it is even difficult in many practical applications to give a unique and accurate description of the length scale, the use of a transport equation for the length scale in the two-equation model of Elghobashi and Abou-Arab (1983) is expected to give better results with fine particles ($d_S < \eta$). However, it should be noticed that the former model and any other similar models contain some empirical constants specific for various flow conditions, and they require the solution for an additional transport equation. It can be expected that the present model combined with an appropriate length scale equation e.g. dissipation rate equation will simulate better most of the important features of multiphase turbulent flows, particularly the fluid particle interaction. In that case the number of closure transport equations will increase to three (if two velocity scale, k_p and k_T, and one length scale transport equations) or four transport equations (if two velocity scales and two length scale, l_p and l_T, are adopted).

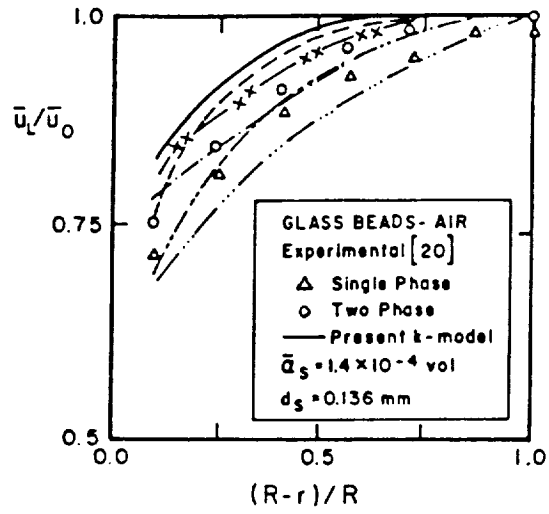

Figure 3. Computed and measured [20] mean velocity distribution of air in air-solid pipe flow (—·· single-phase, —— 2 Eqs. k-ε model [12], --- 1 Eq. k-model [27], -xx- 1 Eq. k-model [12], ----- 1 Eq. ν_t-model [26]).

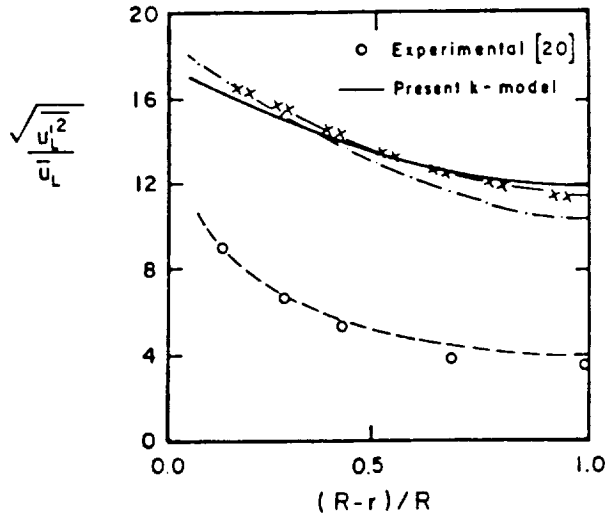

Figure 4. Predicted radial distribution of the turbulence intensity of air in air-solid pipe flow using different turbulence models (keynote as in Fig. 3).

7. SAMPLE OF RESULTS

Figures 3 to 6 compare the present predictions with LDA-measurements for single and two-phase turbulent pipe flow (see Maeda et al (1980)) and turbulent round water jet laden with uniform-size solid particles (see Parthasarathy and Faeth (1987)). Both flows are oriented vertically downward. These flows are axisymmetrical. The concentration profiles are given as input data based on experimental results.

In these flow situations the average eddy size ℓ_e was varying from about one d_S to few hundreds

d_S. The corresponding representative eddy size in the transfer range was only a fraction of particle diameter d_S in the pipe flow case. In the jet flow case the mean size of large eddies and the Kolmogrov length scale were also varied in a wide range. These scales are field variables, and they depend upon the flow configuration, location in the flow domain and particle dimensions.

Two-phase flow solutions were obtained by solving the flow governing equations in their modeled form which are described in the previous section and given in Appendix B. The numerical procedure used for these predictions is based on a developed version of the Genmix-Code of Spalding (1977). However, since the main objective of this paper is to give a complete description of a developed turbulence closure for multiphase flows and due to the space limitation the details of this numerical approach will not be given here. The CPU Time for the two considered flow cases was about 4 minutes on a VAX 760 Mini-Computer and 2 minutes on IBM 3084.

Case I: Gas-Solid Vertical Pipe Flow:

Figure 3 shows a comparison between the experimental data and the present predictions using five different models of turbulence namely 1. One-equation k-model of Roco and Mahadevan (1986), 2. One-equation ν_t-model of Roco and Balakrishnan (1985), 3. The k-equation as given in the two-equation k-ϵ model of Elghobashi and Abou-Arab (1983), 4. The two-equation model of Elghobashi and Abou-Arab (1983), and 5. The present one-equation k-model. The figure displays the mean axial velocity distribution in the fully developed zone of the pipe flow for single and two-phase cases. The differences between the predictions of all one-equation turbulence models and experiments is mainly caused by the general algebraic expression adopted for the turbulence length scale which was not optimized or adjusted. In the present computation the concentration profiles are assumed based on previous experimental data. The inlet concentration distribution is taken to be similar to that given by the best curve fit after the experimental data of Soo (1967). Figure 4 compares the calculated turbulence intensity defined as $\sqrt{\overline{u_L'^2}(=\frac{2}{3}k_L)} \;/\; \bar{u}_L$ with its measured values. The near wall treatment is based on a modified form for the law of wall (see Abou-Ellail and Abou-Arab (1984), Lee and Chung (1987)) and the particle slip condition at the pipe wall.

The present model as compared with the one equation models of Refs. [12] and [27] predicts slightly higher values for the mean flow quantities. However, it must be mentioned that the last k-models contain empirical constants in the dissipation term of the k equation. Concerning the fluctuating flow quantities the present model gives slightly better results for the turbulence intensity in the near wall region than other one-equation models. The expression for the turbulence length scale was not optimized. It is also expected that the current model will give better predictions for coarse ($d_S > \eta$) and heavy

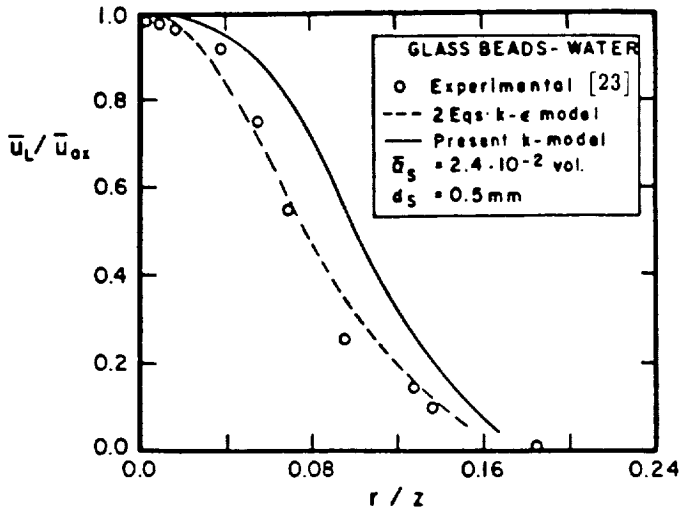

Figure 5. Computed and measured [23] mean velocity distribution in water-solid jet flow.

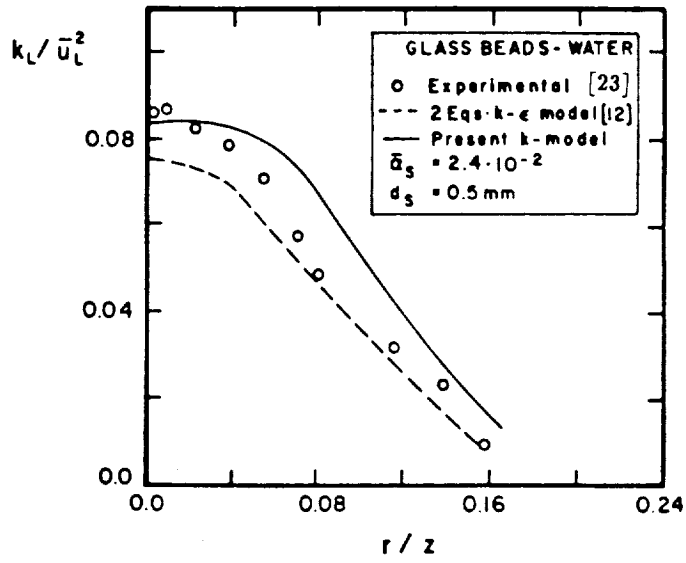

Figure 6. Predicted radial distribution of the turbulence intensity of water in water-solid jet flow.

suspension flows for which no set of comprehensive 2D data is available for comparison.

Case II: Turbulent Round Water Jet Laden with Uniform-size Solid Particles

Comparison between experimental data and numerical predictions of different turbulence closures are given in Figures 5 and 6.

The two-phase flow measurements on velocity, concentration and turbulence correlations used for comparisons are taken from Parthasarathy & Faeth (1987). Different axial locations within the round jet, between eight and fourty jet diameters from the injection nozzle are

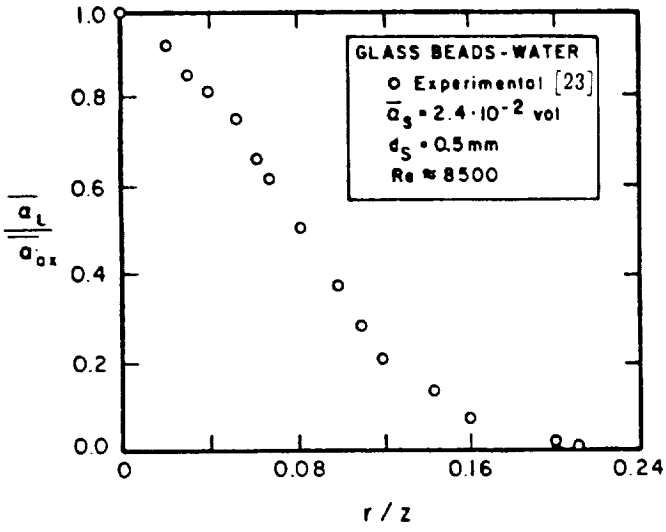

Figure 7. Radial distribution of solid phase concentration in water-solid jet flow.

considered. The radial distribution of solid concentration given in Figure 7 are at eight diameters from the nozzle.

The comparison shows that the two-equation two-phase k-ε model of Elghobashi and Abou-Arab (1983) describes both flows better than the one-equation mass/time averaged turbulence model. However, it is important to mention here that the presently developed closure uses only one transport equation and without adjusting any empirical coefficient. At the same time, the present closure is in its early stages and more refinements and validation tests are required, especially for coarse particles two-phase flows for which one would expect that the present k-formulation will provide improved predictions. The difference between the predictions of the mean and fluctuating flow velocity components as obtained by the present k-formulation and that of Ref. [12] depends on the particle size relative to its surrounding eddies. Figure 8 illustrates this difference at two different loading ratios for the pipe flow at a radial distance (R - r)/R equal 0.1.

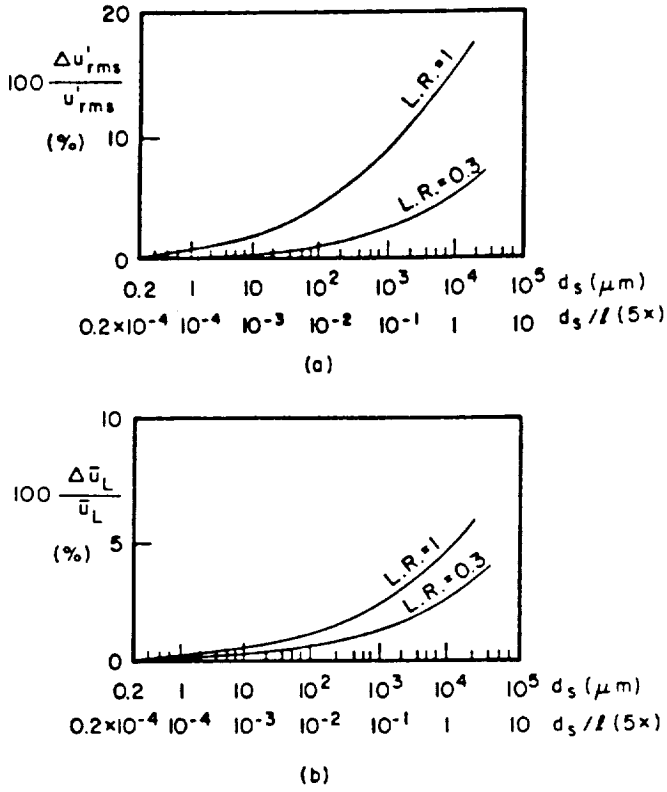

Figure 8. Differences between the present k-formulation and that of Ref. [12] for different mass loading ratios L.R.: (a) fluctuating and (b) mean axial velocity.

8. CONCLUDING REMARKS

The turbulence closure presented in this paper for dilute suspension flow is based on the fluid turbulence kinetic energy equation. The main features of this model are:

i) Two velocity scales are adopted in computation for large and medium size eddies, corresponding to the turbulence production and transfer range, respectively. They are expressed into the governing equations by a specific local mass/time averaging. On this basis the spatial and temporal transfer rates of the thermodynamic quantities and the particle-eddy interaction are better estimated.

ii) Spectral analysis of the interaction mechanism between particles and most energetic eddies provide analytical correlations for closure. The particle response and the modulation of turbulent eddying motion is given as a function of the particle-fluid density and size ratios.

iii) To keep the number of transport equations of the turbulence closure and the number of empirical constants as minimum as possible, the length scales l_p and l_T are described using algebraic expressions. Relations between these scales (Eqs. 40 and 47) are suggested.

iv) The model does not introduce additional empirical constants to the closure of the velocity scale equation.

REFERENCES

1. Abou-Arab, T.W., "Turbulence Models for Two-phase Flows". Encyclopedia of fluid mechanics, Vol. 3, Ed. N.P. Cheremisinoff, Gulf Publ., New Jersey (U.S.A.), pp. 863-907, 1987.

2. Abou-Arab, T.W. and Abou-Ellail, M.M.M., "Heat Transfer in Gas-solid Turbulent Pipe Flow". Proc. Int. Conf. on Numerical Methods for Transient and Coupled Problems, Italy, 1984.

3. Abou-Ellail, M.M.M. and Abou-Arab, T.W., "Prediction of Two-phase Flow and Heat Transfer in Vertical Pipes", 5th Int. Symp. Turbulent Shear Flows, pp. 8.1-8.9, 1985.

4. Al Taweel, A.M. and Landau, J. "Turbulence Modulation in Two-phase Jets", Int. Multiphase Flow, Vol. 3, pp. 341-351, 1977.

5. Buyevich, Yu. A., "Statistical Hydrodynamics of Disperse Systems". Part 4, Physical background and general equations", J. Fluid Mech., Vol.40, No. 3, pp. 340-507, 1971.

6. Chen, C.P., "Multiple-Scale Turbulence Model in Confined Swirling Jet Predictions", AIAA-J., Vol. 24, No. 10, 1986.

7. Crowder, R.S., Daily, J.W., and Humphrey, J.A.C., "Numerical Calculation of Particle Dispersion in a Turbulent Mixing Layer Flow", J. of Pipelines, Vol. 4, No. 3, pp. 159-170, 1984.

8. Crowe, C.T. and Sharma, M.P. "A Novel Physico-computational Model for Quasi One-dimensional Gas Particle Flows", Trans. ASME, J. of Fluids Engineering, Vol. 100, pp. 343-349, 1978.

9. Danon, H., Wolfshtein, M. and Hetsroni, G. "Numerical Calculations of Two-phase Turbulent Round Jets", Int. Multiphase Flow, Vol. 3, pp. 223-234, 1977.

10. Dingguo, X., "Turbulent Kinetic Energy of particle Phase in Solid-fluid Suspension Turbulence", Int. Symp. Multiphase Flow-China, pp. 396-401, 1987.

11. Elghobashi, S.E. and Abou-Arab, T.W., "A Second Order Turbulence Model for Two-phase Flows", Proc. of the 7th Int. Heat Transfer Conf., TF4, pp. 219, 1982.

12. Elghobashi, S.E. and Abou-Arab, T.W., "A Two-equation Turbulence Closure for Two-phase Flows", Phys. Fluids, Vol.26, No. 4, pp. 931-938, 1983.

13. Elghobashi, S.E., Abou-Arab, T.W., Rizk, M., Mostafa, A., "A Prediction of the Particle Laden Jet with a Two Equation Turbulence Model", Int. J. Multiphase Flow, Vol. 10, No. 6, pp. 697-710, 1984.

14. Genchiev Ah.D. and Karpuzov, D.S., "Effects of Motion of Dust Particles on Turbulence Transport Equations", J. Fluid Mech., Vol. 101, No.4, pp. 833-842, 1980.

15. Hanjalic', K. and Launder, B.E., "A Reynolds Stress Model of Turbulence and its Application to Thin Shear Flows, J. Fluid Mech., Vol. 52, No. 4, pp. 609-638 (1972).

16. Hanjalic', K., Launder, B.E. and Schiestel, R., "Multiple-time Scale Concepts in Turbulent Transport Modeling", Proc. of the 3rd Int. Symp. on Turbulent Shear Flow, pp. 10-31, 1979.

17. Hetsroni, G., "Handbook of Multiphase Flow", McGraw Hill, New York, 1982.

18. Hinze, J.O., "Turbulence", McGraw-Hill, New York, 1975.

19. Launder, B.E., "Heat and Mass Transport", In. Turbulence, Ed. P. Bradshaw, Springler-Verlag, Berlin, pp. 231-287, 1978.

20. Maeda, M., Hishida, K. and Furutani, T., "Optical Measurements of Local Gas and Particle Velocity in an Upward Flowing Dilute Gas-solids Suspension", Proc. Polyphase and Transport Technology-San Francisco, pp. 211-216, 1980.

21. Melville, W.K. and Bray, K.N.C., "A Model of the Two-phase Turbulent Jet", Int. J. Heat Mass Transfer, 22, pp. 647-656, 1979.

22. Michaelides, E.E., and Farmer, L.K., "A Model for Slurry Flows Based on the Equations of Turbulence", ASME-FED Vol. 13, "Liquid-solid Flows and Erosion Wear in Industrial Equipment", Ed. M.C. Roco, 1983, pp. 27-32.

23. Parthasarathy, R.N. and Faeth, G.M., "Structure of Particle-laden Turbulent Water Jets in Still Water", Int. J. Multiphase Flow, 13(5), pp. 699-716, 1987.

24. Peskin, R.L., "Stochastic Application to Turbulent-diffusion". In Int. Symp. on Stochastic Hydraulics, Ed. C.L. Chiu, Univ. of Pittsburg, PA, pp. 251-267, 1971.

25. Picart, A., Berlemont, A. and Gouesbet, G., "Modelling and Predicting Turbulent Fields and the Dispersion of Discrete Particles Transported by Turbulent Flows", Int. J. Multiphase Flow, 12(2), pp. 237-261, 1986.

26. Roco, M.C. and Balakrishnan, N., "Multi-Dimensional Flow Analysis of Solid-liquid Mixtures", J. of Rheology, Vol. 29, No. 4, pp. 431-456, 1985.

27. Roco, M.C. and Mahadevan, S., "Scale-up Technique of Slurry Pipelines-Part A: Turbulence Modeling", ASME-J. of Energy Resources Technology, Vol. 108, pp. 269-277, 1986.

28. Roco, M.C. and Shook C.A., "Modeling Slurry Flow: The Effect of Particle Size", Canadian J. Chem. Eng., Vol. 61, No. 4, pp. 494-503, 1983.

29. Roco, M.C. and Shook, C.A., "Turbulent Flow of Incompressible Mixtures", J. Fluids Engineering, Vol. 107, June 1985, pp. 224-231.

30. Shuen, J.S., Chen, L.D. and Faeth, G.M., "Prediction of the Structure of Turbulent Particle Laden in Round Jets", AIAA J., Vol. 21, pp. 1480-1483, 1983.

31. Soo, S.L., "Multiphase Fluid Dynamics", Revised Edition, S.L. Soo Assoc., 1983, also "Fluid Dynamic of Multiphase Systems", Blaidesll, Waltham, MA, 1967.

32. Spalding, D.B. "A General Computer Program for Two-Dimensional Parabolic Phenomena", Dept. of Mech. Engng., Report No. HTS/77/9, Imperial College, London, 1977.

33. Vernier, Ph., and Delhaye, J.H., "General Two-phase Flow Equations Applied to the Thermodynamics of Boiling Water Nuclear Reactors", Energie Primaire, Vol. 4, No. 1-2, p. 5, 1968.

34. Wang, C.S., Lyczkowski, R.W., and Berry, J.F., "Multiphase Hydrodynamic Modeling and Analysis of Non-Newtonian Coal/Water Slurry Rheology", Proc. Third Int. Symp. on Liquid-Solid Flows, Ed. M.C. Roco, ASME-FED, 1988.

APPENDIX - A

Mass/Time Averaged conservation Equations

Mass averaging the conservation equations of mass and momentum over a flow component (K) one obtains a new system of equations for mean velocity, concentration and kinetic energy of turbulence.

The point instantaneous conservation equation can be written for any flow component (K) or for the entire mixture in the folowing general form

$$\frac{\partial}{\partial t}(\rho\psi) + \nabla\cdot(\rho\psi\underline{u}) + \nabla\cdot\underline{J} - S = 0 \qquad (A1)$$

where: ρ = density
$\underline{u}$ = velocity vector
ψ = transported quantity
$\underline{J}$ = flux vector for ψ
S = source term

Let assume $\psi = u_{Ki}$. By splitting each flow property into mean and turbulent fluctuating component $(\bar{u}_{Ki} + u^t_{Ki})$ and mass/time or double time averaging the equation (A1), one obtains the following momentum equations in the i-th direction for an incompressible phase (K) without mass exchange with other flow components (see Roco and Shook (1985)):

$$\underbrace{\rho_K \frac{\partial}{\partial t}(\bar{\alpha}_K\bar{u}_{Ki} + \overline{\alpha^t_K u^t_{Ki}})}_{\text{Time Rate}} + \underbrace{\rho_K \frac{\partial}{\partial x_j}(\bar{\alpha}_K\bar{u}_{Ki}\bar{u}_{Kj})}_{\text{Mean Flow Convection}}$$

$$= \underbrace{\rho_K\bar{\alpha}_K\overline{b_{Ki}}}_{\text{Body Force}} - \underbrace{\frac{\partial}{\partial x_i}(\bar{\alpha}_K\bar{p}_K + \overline{\alpha^t_K p^t_K}) + \bar{p}_K\frac{\partial\bar{\alpha}_K}{\partial x_i} + \overline{p^t_K\frac{\partial\alpha^t_K}{\partial x_i}}}_{\text{Pressure Effect}}$$

$$+ \underbrace{\frac{\partial}{\partial x_j}[\bar{\alpha}_K\bar{\tau}_{K\Sigma ji}}_{\substack{\text{Frictional}\\ \text{Effect}}} \underbrace{-\rho_K\overline{\alpha_K\cdot u^t_{Ki}u^t_{Kj}}}_{\substack{\text{Inertial}\\ \text{Effect}}}$$

$$\underbrace{-\rho_K\overline{\alpha^t_K(u_{Ki}u_{Kj})^t + \overline{\alpha^t_K\tau^t_{K\Sigma ji}}}]}_{\text{Collisional Effect}} + \underbrace{(\overline{I_{Ki}})_{-K}}_{\substack{\text{Interactions}\\ \text{with } (-K)}} \qquad (A2)$$

where

K = phase (or generally a flow component)
$\bar{f}_K$ = mass/time average of f over K
i,j = 1,2,3 (Cartesian coordiantes)
b_{Ki} = body force in the i-th direction
$(\overline{I_{Ki}})_{-K}$ = projection in the i-th direction of the interaction vector $(\overline{\underline{I}_K})_{-K}$

The interaction term as it stands for solid/liquid drag is given by

$$(I_{Si})_L = (I_{Li})_S = 0.75\alpha_S\rho_L\frac{C_{DS}}{d_S}\frac{|u_{Ly}-u_{Sy}|(u_{Ly}-u_{Sy})}{(1-\alpha_S)^{1.7}} \qquad (A3)$$

This drag term takes a simple form for Reynolds numbers less than unity

$$(I_{Si})_L = -(I_{Li})_S = \alpha_S(18\mu_L/d_S^2)(u_{Li}-u_{Si}) \qquad (A4)$$

The transverse effects caused by the presence of other solid particles, Saffman force and Ho and Leal inertial force are neglected. Their importance is small in dilute suspension turbulent flows with fine particles.

Equation (A2) contains terms due to the unsteady flow, mean flow convection, diffusion, pressure, body force, as well as frictional, inertial and collisional effects. The mean form of the turbulence kinetic energy governing equation is obtained by subtracting from the steady state instantaneous momentum equation for a component K = L the corresponding mean flow equations, and then multiplying the resulting difference equation by $(u'_{Ki} + u''_{Ki})$. By averaging one obtain the kinetic energy equation for a flow component K = L. This equation reads

$$\rho_K\bar{\alpha}_K\bar{u}_{Kj}\left(\frac{\overline{\partial u'^2_{Ki}}/2}{\partial x_j} + \frac{\overline{\partial u''^2_{Ki}}/2}{\partial x_j}\right) + \frac{\partial}{\partial x_j}[\rho_K\bar{\alpha}_K(\overline{u'_{Kj}u'_{Ki}u'_{Ki}}$$

Group #1 (Convection) Group #2 (Velocity Diffusion)

$$+ \overline{u''_{Kj}u'_{Ki}u'_{Ki}} + \overline{u'_{Kj}u''_{Ki}u'_{Ki}} + \overline{u'_{Kj}u'_{Ki}u''_{Ki}} + \overline{u''_{Kj}u''_{Ki}u'_{Ki}}$$

$$+ \overline{u'_{Kj}u''_{Ki}u''_{Ki}} + \overline{u''_{Kj}u'_{Ki}u''_{Ki}} + \overline{u''_{Kj}u''_{Ki}u''_{Ki}})]$$

$$+ [\frac{\partial}{\partial x_j}(\rho_K\overline{\alpha'_K u'_{Ki}u'_{Ki}u'_{Kj}} + \overline{\alpha''_K u''_{Ki}u''_{Ki}u''_{Kj}})$$

Group #3 (Higher Order Correlations)

+ other 4th order and minor terms)]=

$$- \bar{\alpha}_K \frac{\partial}{\partial x_i} (\overline{u'_{Ki} P'_K} + \overline{u''_{Ki} P''_K} + \overline{u'_{Ki} P''_K} + \overline{u''_{Ki} P'_K})$$

Group #4 (Pressure Diffusion)

$$+ \bar{\alpha}_K (\overline{P'_K \frac{\partial u'_{Ki}}{\partial x_i}} + \overline{P''_K \frac{\partial u''_{Ki}}{\partial x_i}} + \overline{P'_K \frac{\partial u''_{Ki}}{\partial x_i}} + \overline{P''_K \frac{\partial u'_{Ki}}{\partial x_i}}$$

Group #5 (Extra Production and Transfer)

$$- (\overline{u''_{Ki} \alpha'_K \frac{\partial p''_K}{\partial x_i}} + \overline{u''_{Ki} \alpha''_K \frac{\partial p'_K}{\partial x_i}} + \overline{u''_{Ki} \alpha''_K \frac{\partial p''_K}{\partial x_i}}$$

$$+ \overline{\alpha''_K u'_{Ki} \frac{\partial p''_K}{\partial x_i}} + \overline{\alpha'_K u'_{Ki} \frac{\partial p''_K}{\partial x_i}})$$

$$- (\rho_K \bar{\alpha}_K \overline{u'_{Ki} u'_{Kj}} \frac{\partial \bar{u}_{Ki}}{\partial x_j} + \rho_K \bar{\alpha}_K \overline{u''_{Ki} u''_{Kj}} \frac{\partial \bar{u}_{Ki}}{\partial x_j})$$

Group #6 (Production)

$$- \left[\bar{u}_{Ki} \overline{\alpha'_K u'_{Kj}} \frac{\partial \bar{u}_{Ki}}{\partial x_j} + \bar{u}_{Kj} \overline{\alpha'_K u'_{Ki}} \frac{\partial \bar{u}_{Ki}}{\partial x_j} \right.$$

Group #7 (Extra Production)

$$+ \bar{u}_{Ki} \overline{\alpha''_K u''_{Kj}} \frac{\partial \bar{u}_{Ki}}{\partial x_j} + \bar{u}_{Kj} \overline{\alpha''_K u''_{Ki}} \frac{\partial \bar{u}_{Ki}}{\partial x_j}$$

$$\left. - (\overline{\alpha'_K u'_{Ki}} + \overline{\alpha''_K u''_{Ki}}) \frac{\partial \bar{P}_K}{\partial x_i} + \text{minor terms} \right]$$

$$+ \rho_K \bar{\alpha}_K \nu_K \overline{\frac{\partial u'_{Ki}}{\partial x_j} \frac{\partial u'_{Ki}}{\partial x_j}} + \rho_K \bar{\alpha}_K \nu_K \overline{\frac{\partial u''_{Ki}}{\partial x_j} \frac{\partial u''_{Ki}}{\partial x_j}}$$

Group #8 (Dissipation)

$$+ \rho_K \overline{\alpha'_K \nu_K \frac{\partial u'_{Ki}}{\partial x_j} \frac{\partial u'_{Ki}}{\partial x_j}} + \rho_K \overline{\alpha''_K \nu_K \frac{\partial u''_{Ki}}{\partial x_j} \frac{\partial u''_{Ki}}{\partial x_j}} + \text{mixed correlations}$$

Group #9 (Extra Dissipation & Diffusion)

$$+ \overline{u'_{Ki} (I'_{Ki})_{-K}} + \overline{u''_{Ki} (I''_{Ki})_{-K}} \qquad (A5)$$

Group #10 (Extra Dissipation)

APPENDIX B

The Modeled Form of the Turbulence Kinetic Energy Equation

The steady-state turbulence kinetic energy equation for the liquid phase (K = L) is:

$$\rho_L \bar{\alpha}_L \bar{u}_{Lj} \frac{\partial k_L}{\partial x_j} = \frac{\partial \bar{\alpha}_L}{\partial x_j} \frac{\mu_{Lt}}{\sigma_k} \frac{\partial k_L}{\partial x_j} + \alpha_L \mu_{Lt} (\frac{\partial \bar{u}_{Li}}{\partial x_j})^2$$

Convection Diffusion Production

$$+ \frac{\nu_{Lt}}{\sigma_{\alpha S}} \frac{\partial \bar{\alpha}_L}{\partial x_i} (\frac{\partial \bar{P}_L}{\partial x_i} + \bar{u}_{Lj} \frac{\partial \bar{u}_{Li}}{\partial x_j}) + \frac{\nu_{Lt}}{\sigma_{\alpha S}} \frac{\partial \bar{\alpha}_L}{\partial x_j} (\bar{u}_{Li} \frac{\partial \bar{u}_{Li}}{\partial x_j})$$

Extra Production

$$- \rho_L \bar{\alpha}_L \epsilon_L$$

Dissipation

$$+ \frac{18 \mu_L}{d_S^2} (\bar{u}_{Li} - \bar{u}_{Si}) \frac{\nu_{Lt}}{\sigma_{\alpha S}} \frac{\partial \bar{\alpha}_L}{\partial x_i}$$

Extra Dissipation

$$- \bar{\alpha}_S k_L (1 - \Gamma_{SL} + \Gamma_{RL}) - \frac{18 \mu_L}{d_S^2} (T1 + T2 - T3 - T4) \qquad (B1)$$

where the expressions for Γ_{SL}, Γ_{RL}, T1, T2, T3 and T4 are given in the text.

1. REPORT NO.	2. GOVERNMENT ACCESSION NO.	3. RECIPIENT'S CATALOG NO.
NASA CP-3047		

4. TITLE AND SUBTITLE	5. REPORT DATE
Constitutive Relationships and Models in Continuum Theories of Multiphase Flows	September 1989
	6. PERFORMING ORGANIZATION CODE ES42
7. AUTHOR(S) Edited by Rand Decker*	8. PERFORMING ORGANIZATION REPORT #
9. PERFORMING ORGANIZATION NAME AND ADDRESS George C. Marshall Space Flight Center Marshall Space Flight Center, AL 35812	10. WORK UNIT NO. M-616
	11. CONTRACT OR GRANT NO.
12. SPONSORING AGENCY NAME AND ADDRESS National Aeronautics and Space Administration Washington, D.C. 20546	13. TYPE OF REPORT & PERIOD COVERED Conference Publication
	14. SPONSORING AGENCY CODE

15. SUPPLEMENTARY NOTES

*National Research Council Associate.
Prepared by Space Science Laboratory, Science & Engineering Directorate.

16. ABSTRACT

During the first week of April 1989, a workshop, entitled "Constitutive Relationships and Models in Continuum Theories of Multiphase Flows," was convened at NASA's Marshall Space Flight Center. The purpose of this workshop was to open a dialogue on the topic of constitutive relationships for the partial or per phase stresses, including the concept of solid phase "pressure" and the models used for the exchange of mass, momentum, and energy between the phases in a multiphase flow. This volume is the result of the stated objective of the workshop. The program, abstracts, and text of the presentations made at the workshop are included.

17. KEY WORDS	18. DISTRIBUTION STATEMENT
Multiphase Flow, Two-Phase Flow Continuum Mechanics Turbulence, Rheology, Kinetic Theory Constitutive Equations	Unclassified--Unlimited Subject Category: 34

19. SECURITY CLASSIF. (of this report)	20. SECURITY CLASSIF. (of this page)	21. NO. OF PAGES	22. PRICE
Unclassified	Unclassified	172	A08

MSFC - Form 3292 (Rev. December 1972)

For sale by National Technical Information Service, Springfield, Virginia 22161

NASA-Langley, 1989

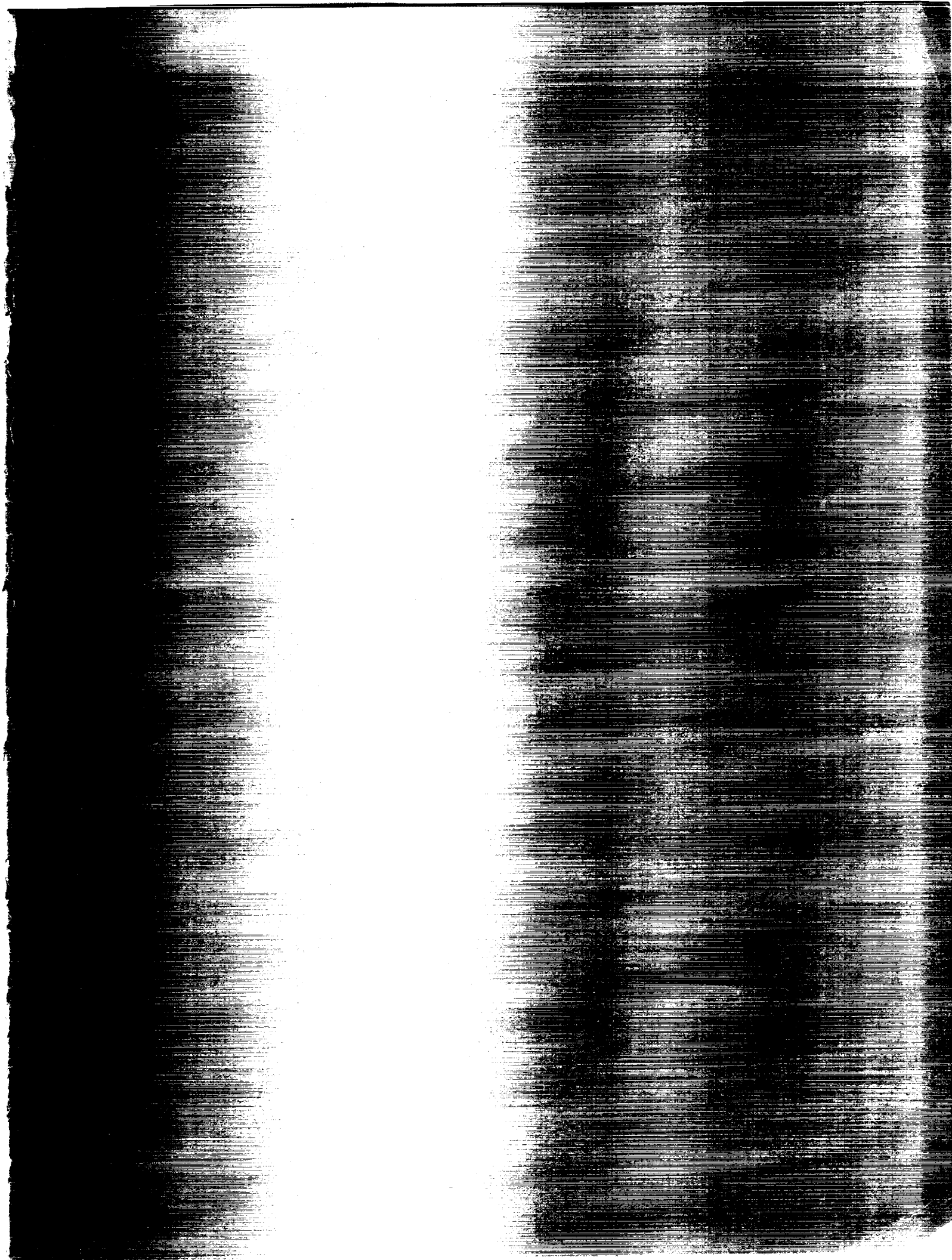

SPECIAL FOURTH-CLASS RATE
POSTAGE & FEES PAID
NASA
Permit No. G-27

D.C.

NASA

POSTMASTER: If Undeliverable (Section 158
Postal Manual) Do Not Return